Sedimentation of the Siluro-Devonian Clastic Wedge of Somerset Island, Arctic Canada

---

A thesis
presented to the
School of Graduate Studies
in partial fulfillment of the
requirements for the
Ph. D. degree in Geology

---

by
Martin R. Gibling

Ottawa, Canada. 1978

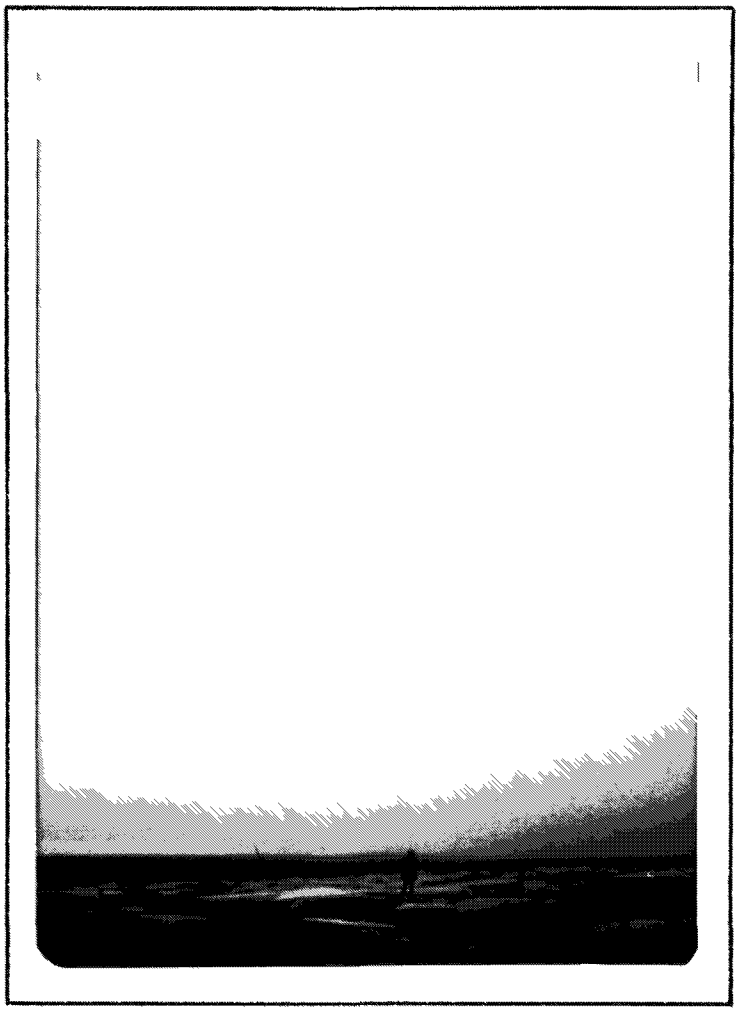

Where can I go from Thy Spirit?

Or where can I flee from Thy presence?

Psalm 139:7

ABSTRACT

The Siluro-Devonian clastic wedge of Somerset Island comprises two formations. The Somerset Island Formation is divided into a lower member of grey laminated dolosiltite and minor limestone, up to 130 m thick, and an upper member of red massive and grey laminated dolosiltite, up to 300 m thick. The overlying Peel Sound Formation, up to 600 m thick, and divided into four members, consists mainly of red sandstone and conglomerate.

Cycles in the Somerset Island Formation were shown by Markov analysis to contain the sequence: grey thin-bedded limestone, grey laminated dolosiltite, red massive dolosiltite. Structures representing algal mat types comparable to those of modern tidal flats indicate a repeated progression from shallow subtidal to terrestrial conditions during deposition of the cycles. The cyclicity reflects transgressive-regressive events, probably related to tectonism in the adjacent Boothia Uplift.

Peel Sound member 1 consists of red sandstone with less than 20% of siltstone and mudstone. Laterally extensive fining-upward cycles (3.9 m average thickness) were shown by Markov analysis to contain the sequence: erosion surface, large-scale trough and planar cross-stratified sandstone, small-scale cross-stratified or laminated sandstone, massive siltstone. The cycles represent accretion in braided river

systems, with bars and shallow (2 m) channels on low-gradient, distal plains. Rare non-cyclic sequences comprise laminated and trough cross-stratified sandstones, with current lineation and abundant cross-cutting erosion surfaces; deposition occurred in very shallow (less than 1 m) channels migrating rapidly on high-gradient, proximal surfaces.

Peel Sound members 2 and 4 consist of horizontally stratified framework conglomerate with minor sandstone. Current-parallel and -transverse orientation of clast A-axes indicates both suspension and bedload transport. Deposition took place on longitudinal bars in proximal braided rivers. Rare cross-stratified conglomerate and sandstone successions containing channels indicate deposition on foreset bars and large-scale bedforms in more distal braided rivers. Proximal-type conglomerates pass eastward into distal-type sandstones in the Cape Anne syncline, and these sediments constitute the bulk of the clastic wedge.

Peel Sound member 3 contains units of bright red, giant cross-stratified sandstone, intercalated with erosionally based units of grey pebbly sandstone with flute casts and current lineation. The strata represent eolian dune and flash flood deposits, respectively.

The succession of clast lithotypes in the Peel Sound conglomerates matches in reverse order the rock sequence presently exposed in the Boothia Uplift. Lateral facies changes and paleocurrent data indicate mainly easterly

transport, confirming that the Uplift was the main source of the detrital sediment. The clastic wedge contains abundant detrital dolomite of rudite to siltite grade, with some *in situ* penecontemporaneous and secondary dolomite. Petrography and analysis for Sr and Na suggests that the detrital dolomite was probably derived initially from erosion of contemporaneously formed dolomite and later from erosion of older dolostone formations. Comparable Siluro-Devonian regressive sequences on Prince of Wales and Cornwallis Islands were also derived from the Boothia Uplift. The Somerset Island succession coarsens upward gradually while the Prince of Wales Island succession contains abundant intercalated units of conglomerate, a result of local differences in tectonic style during uplift. The basal clastic units are upper Ludlovian or Pridolian in age on Somerset Island, but Gedinnian in age on Cornwallis Island, indicating that uplift advanced northward with time. The climate was semi-arid, probably with higher rainfall on the Uplift.

Analysis of size, shape and roundness of 558 clasts from the Peel Sound conglomerates suggests that internal texture exerted more influence on morphology than the rock type *per se*. Parameters of morphology and fabric generally show weak correlation, a reflection of short transport distance, intense flow and rapid deposition. Analysis of clast projection area indicates that these contact fabrics

fulfill the criteria proposed for hydrodynamic stability of isolate fabrics.

TABLE OF CONTENTS

TABLES

FIGURES

PHOTOGRAPHS

CHAPTER 1. INTRODUCTION AND STRATIGRAPHY

Location and access

Somerset Island, N.W.T., is located in the High Arctic between latitudes 72° and 74°N, and longitudes 90° and 96°W (Fig. 1). Relief is moderate, with the highest elevation (about 450 m) over the Precambrian terrain on the western part of the island. During the fleeting summer period of June to August, thaw exposes a surface cover of platy gravel (felsenmeer), with outcrop limited to river gorges and sea cliffs (Photos 1 and 2).

The island is uninhabited, and the nearest permanent settlement is at Resolute Bay on Cornwallis Island, accessible from the south by commercial flights. From Resolute, Somerset Island was reached by single- or twin-engined Otter, chartered by the government-sponsored Polar Continental Shelf Project. Landings were made by ski on the sea-ice, or with balloon tires on the tundra surface. Transport on the island was by foot, and by three-wheeled Honda 90 bikes. Aerial photos were used for location and geological mapping. The area lies within the zone of compass unreliability because of proximity to the North Magnetic Pole, and directional data were recorded by sighting on suitable landmarks.

Research programmes

The present thesis forms part of a research programme

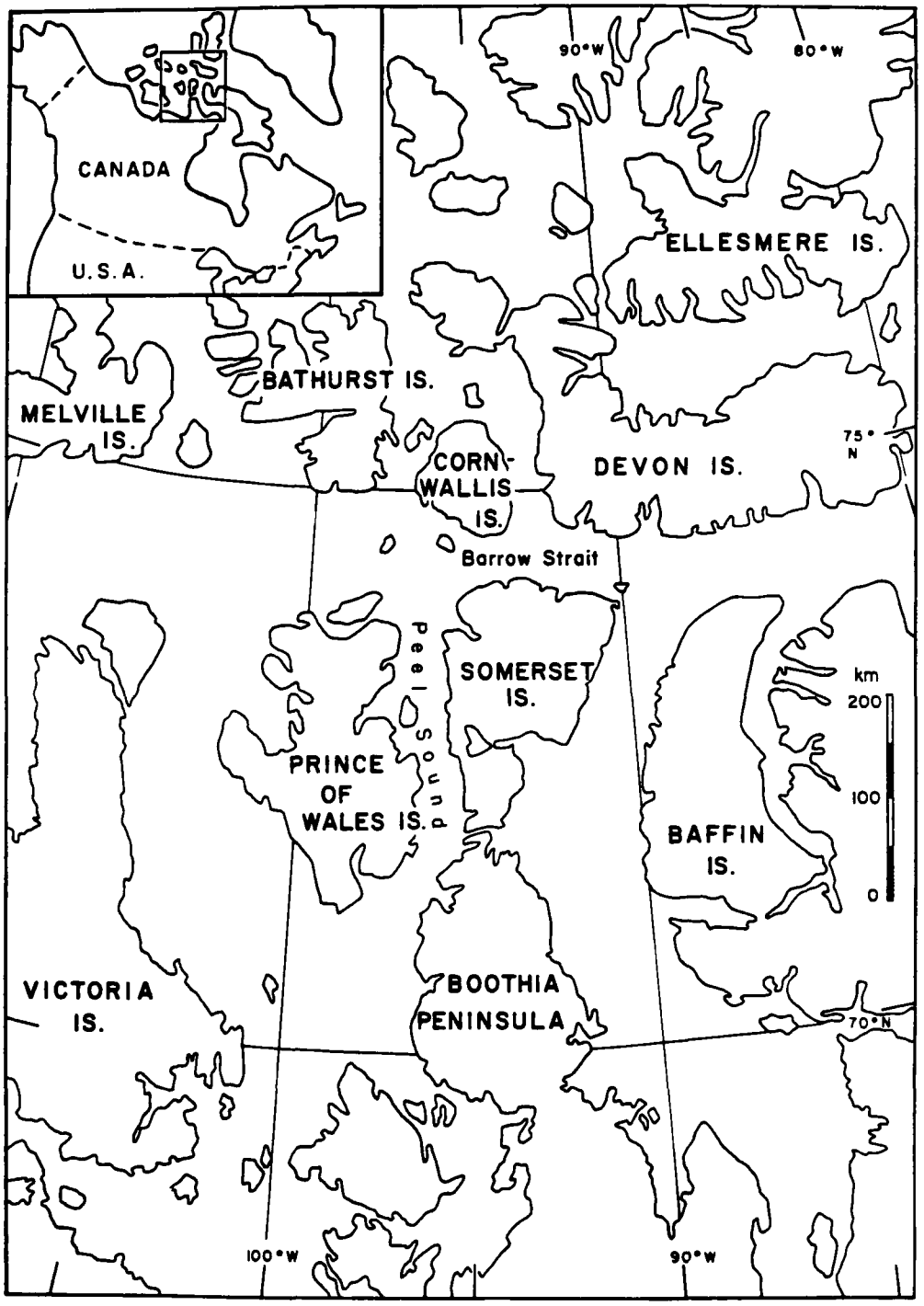

Fig. 1. Location map of Somerset Island, N.W.T.

in the south-central Arctic Islands that has been conducted by the University of Ottawa since 1964. Field work by the author was carried out during the summers of 1973, 1974 and 1976. In 1975, the Geological Survey of Canada commenced "Operation Boothia", a field mapping project on Somerset Island and the Boothia Peninsula under the direction of J. Wm. Kerr and G.E. Reinson (early work summarised by Reinson et al., 1976). Field work continued in 1976 (Miall and Kerr, 1977) with A.D. Miall replacing Reinson. Since there was considerable overlap between the two research programmes, publications have been prepared by members of the Geological Survey team in collaboration with the author (Miall, Kerr and Gibling, 1978 ; Miall and Gibling, in press). Reference will be made to data in these joint reports, emphasising the author's own contributions. Data from field work on Cornwallis Island with G.M. Narbonne (University of Ottawa), and on Prince of Wales Island with D.K. Elliott (Bristol University) in 1976 are also included.

General stratigraphy

The Phanerozoic part of the stratigraphic sequence on Somerset Island (Table 1) was described by Miall and Kerr (1977). Throughout most of the Lower Paleozoic, the stable northern margin of the North American continent was the site of shallow marine carbonate deposition (Thorsteinsson and Tozer, 1970). In Upper Silurian to Lower Devonian times,

TABLE 1. Stratigraphy of Somerset Island and northeastern Boothia Peninsula. Data from Dixon et al., 1971; Dixon, 1974; Miall and Kerr, 1977; Miall et al., 1978.

AGE	FORMATION		LITHOLOGY	THICKNESS (metres)
Cretaceous-Tertiary	Eureka Sound		Sandstone, siltstone, shale	300
Upper Silurian-Lower Devonian	Peel Sound	4.	Polymict conglomerate	120
		3.	Pebbly sandstone, conglomerate	240
		2.	Dolomitic conglomerate	280
		1.	Sandstone, siltstone	60-400
Upper Silurian	Somerset Island	2.	Siltstone, shale, dolomite	150-300
		1.	Dolostone, limestone	0-130
Upper Silurian	Read Bay		Limestone, (rubbly, argillaceous)	150-240
Lower-Upper Silurian	Cape Storm		Dolostone, (thin-bedded)	120-260
Silurian	Cape Crauford		Dolostone, evaporite	50+
Upper Ordovician-Lower Silurian	Allen Bay		Dolostone, (medium- to thick-bedded)	340-540
Upper Ordovician	Irene Bay		Limestone	0-97
Upper Cambrian-Upper Ordovician	Lang River		Dolostone, sandstone, shale, intraformational breccia	200-420
Proterozoic	Hunting		Dolostone, shale, sandstone	1160-1370
	Aston		Sandstone	800
Crystalline basement				

the emergence and erosion of the north-south trending Boothia Uplift in the area of Peel Sound resulted in the deposition of a wedge of clastic sediments at the margins of the Uplift (Brown et al., 1969). On Somerset Island, these later events are represented by the shallow marine Read Bay Formation (Upper Silurian), overlain conformably by the predominantly inter-supratidal Somerset Island Formation (Upper Silurian), and in turn by the fluvial Peel Sound Formation (probably mainly Lower Devonian). Broadly similar regressive sequences outcrop on Prince of Wales Island west of the Boothia Uplift (Miall, 1970b) and on Cornwallis Island (Fig. 1) north of Barrow Strait (Thorsteinsson, 1958; Gibling and Narbonne, 1977). The term "clastic wedge" will be used to refer to the deposits formed during emergence of the Boothia Uplift since the bulk of the sediments are detrital in origin.

The aims of the present study are as follows:

1) To investigate the sedimentology of the Siluro-Devonian clastic wedge on Somerset Island (the Somerset Island and Peel Sound Formations), and to interpret their environments of deposition.

2) To propose a model for the Upper Silurian to Lower Devonian paleogeography of the Boothia Uplift region.

Definition of units in the clastic wedge on Somerset Island

In early studies of the Siluro-Devonian strata of Somerset Island (Thorsteinsson and Tozer, 1963; Blackadar

and Christie, 1963), carbonate rocks were generally assigned to the Read Bay Formation, and clastic rocks to the Peel Sound Formation. Thorsteinsson and Tozer (1963, p. 122) drew the boundary in the transitional sequence at the lowest occurrence of red siltstone, a convenient mappable horizon. Following field work in 1973, the author felt that the transitional strata were sufficiently distinctive to justify formational status, a view substantiated by other workers (Reinson et al., 1976 ; Miall and Kerr, 1977). These strata are now assigned to the newly defined Somerset Island Formation (Miall, Kerr and Gibling, 1978).

Somerset Island Formation

The formation was examined in sections over a distance of 170 km north to south on the island (Fig. 2). At 100 m or more below the first red siltstone unit, the strata undergo a distinctive and persistent change, characterised by coincident changes in the following:

1) Lithology The typical grey nodular and wavy-bedded, mottled and argillaceous limestone of the Read Bay Formation is overlain by dolomitic and calcareous siltstone, grey or buff in colour. Typical Read Bay rock types recur only rarely at higher levels.

2) Stratification In the upper Read Bay Formation, stratification is wavy or indistinct, and recognisable units tend to be thick or very thick (30-100 cm and greater than 100 cm respectively). Thin to medium planar stratification (3-10 cm and 10-30 cm respectively)

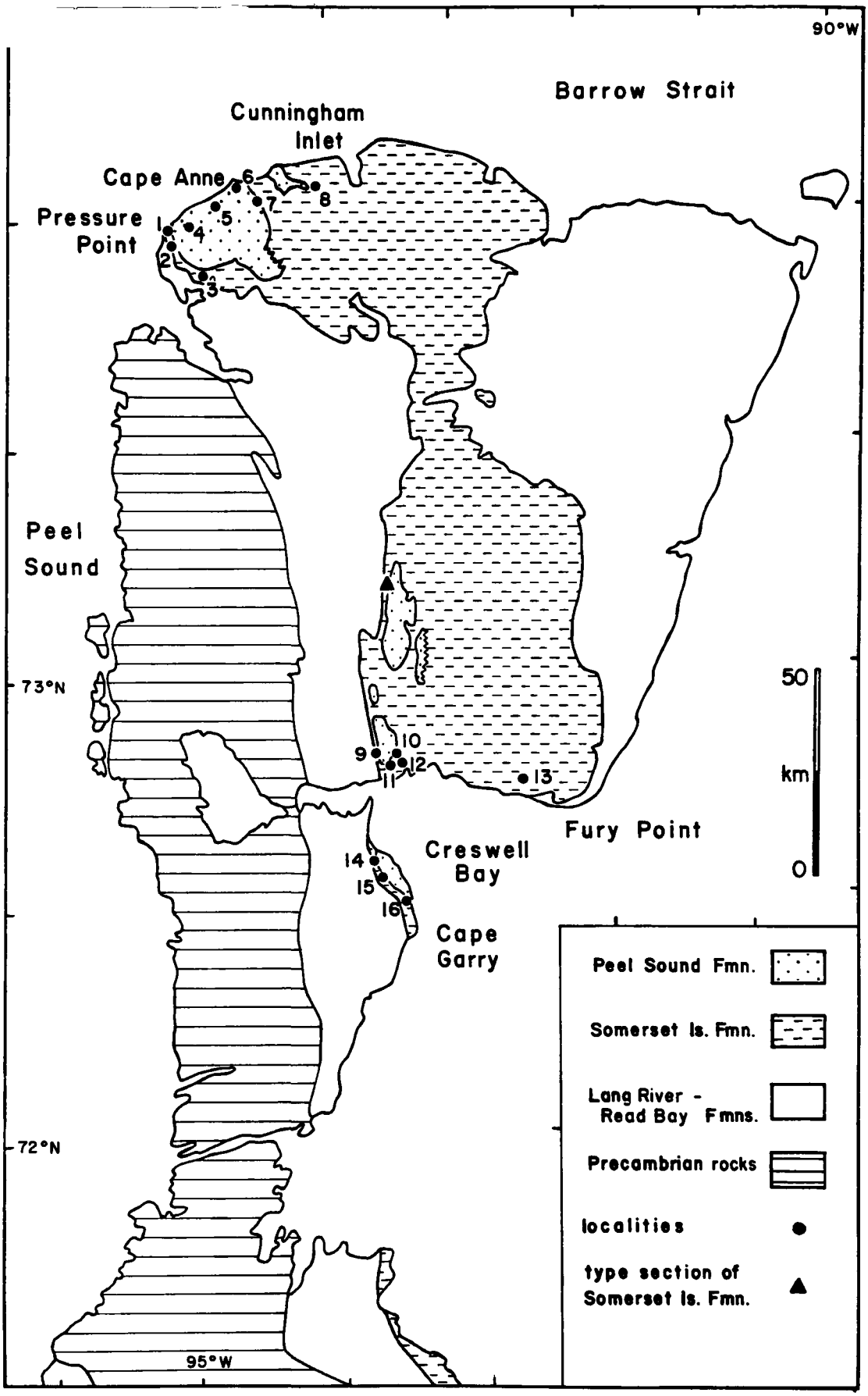

Fig. 2. Geological map of Somerset Island. Numbered localities show sites of principal measured sections. After Miall and Gibling (in press).

characterises the Somerset Island Formation.

3) Fauna The open marine Read Bay assemblages (including brachiopods, corals and stromatoporoids) are succeeded by a less diverse fauna in which ostracods predominate.

The unit chosen as basal to the Somerset Island Formation is the lowest planar stratified dolostone or limestone (Miall et al., 1978) in this transitional sequence. The more recessive nature of the Somerset Island Formation and the change in outcrop character from rubbly to platy weathering facilitates regional mapping. The incoming of abundant, laterally persistent units of red siltstone at higher levels in the formation, formerly taken to define the base of the Peel Sound Formation, was used to divide the Somerset Island Formation into an upper and a lower member. A few thin red or red/green-mottled siltstone beds are present in the lower member.

The lower member of the Somerset Island Formation is up to 130 m thick and consists predominantly of grey to buff dolomitic siltstone, with lesser amounts of calcareous siltstone, micritic and crystalline limestones and terrigenous siltstone. Ostracods, ostracoderms and gastropods are the predominant faunal elements, although an open marine invertebrate assemblage occurs in a few beds. The upper member is up to 300 m thick and consists predominantly of interbedded grey laminated and red massive dolomitic siltstones. Sandstone, terrigenous siltstone, and micritic limestone are also

present, with minor evaporites in the carbonate and finer-grained clastic units. The fauna consists mainly of ostracods and ostracoderms.

Peel Sound Formation

The Peel Sound Formation has been redefined so that the incoming of abundant cross-bedded units of red sandstone constitutes the base of the formation (Miall et al., 1978). Thin beds of sandstone, usually grey in colour, are common below this level, but the contact is generally readily mappable. The formation consists mainly of red sandstone and buff conglomerate with some siltstone and mudstone. Ostracoderms, the principal faunal element, are uncommon, and ostracods and gastropods very rare. The maximum thickness of about 600 m (Miall and Gibling, in press) is present in the Cape Anne syncline. Dineley (1966) and Brown et al. (1969) divided the succession in this area into four informal members (Table 1), the thicknesses of which were later determined accurately from regional mapping by Miall and Kerr (1977). Some members are in part lateral equivalents. Contacts between the units outlined above are fully gradational.

Criteria for subdivision are arbitrary and their utility lies in their correspondence to stages in the change of environments during regression. The Read Bay Formation is predominantly subtidal in origin (Jones and Dixon, 1977). The lower member of the Somerset Island Formation represents the incoming of inter-supratidal conditions, and the upper member a transition to

terrestrial sedimentation. The Peel Sound Formation is terrestrial, mainly fluvial, in origin. The succession on Somerset Island can thus be compared readily with successions elsewhere in the Boothia Uplift region (Chapter 7).

Regional distribution of stratigraphic units

The general location of sections through the two formations, examined by the author, is shown in Figure 2. Details of location and stratigraphic correlation of sections and geological structure are given in Appendix A, with information on type and reference sections for the formations; bed-by-bed section logs are available at the Department of Geology, University of Ottawa. A detailed stratigraphic section of the Somerset Island Formation and the basal Peel Sound Formation is shown in Figure 3; the Peel Sound Formation is generally poorly exposed, but incomplete sections are illustrated in Chapter 3.

The Somerset Island Formation thickens eastward away from the Uplift, due largely to the increasing thickness of the upper member (Fig. 4). In general, the two members are readily distinguishable, although some sections near the Uplift are anomalous in that the lower member consists largely of rather recessive dolomitic siltstones, similar to the upper member. Towards the east (Locality 13), the lower member is more calcareous and resistant, and contains interbedded units of nodular limestone of Read Bay type.

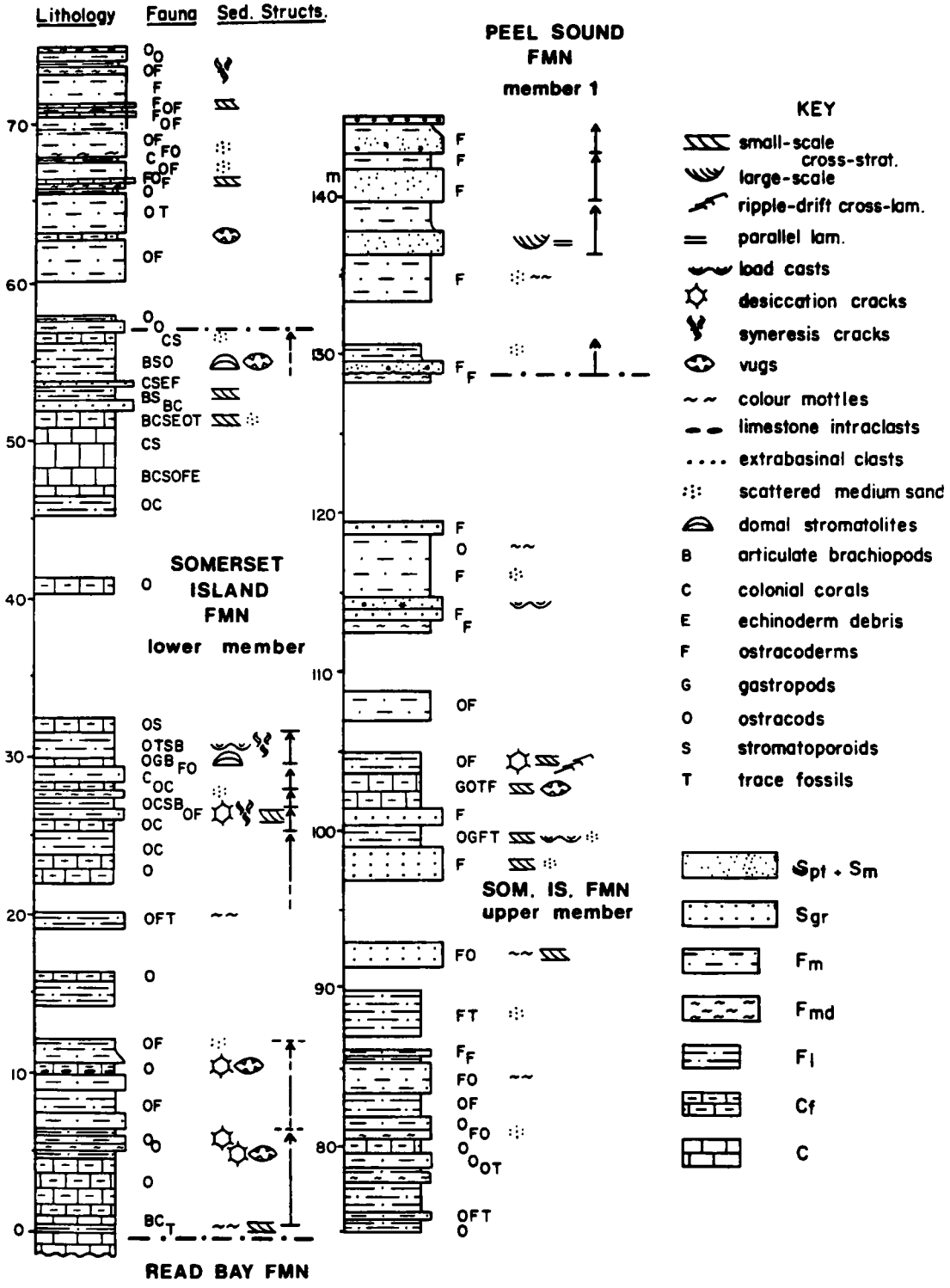

Fig. 3. Detailed section through the lower part of the clastic wedge in the Cape Anne syncline. Facies types described in Table 3. Cyclic facies successions are shown by arrows. Column width reflects grain size, as shown in the key. Section G74G at Loc. 2, Pressure Point.

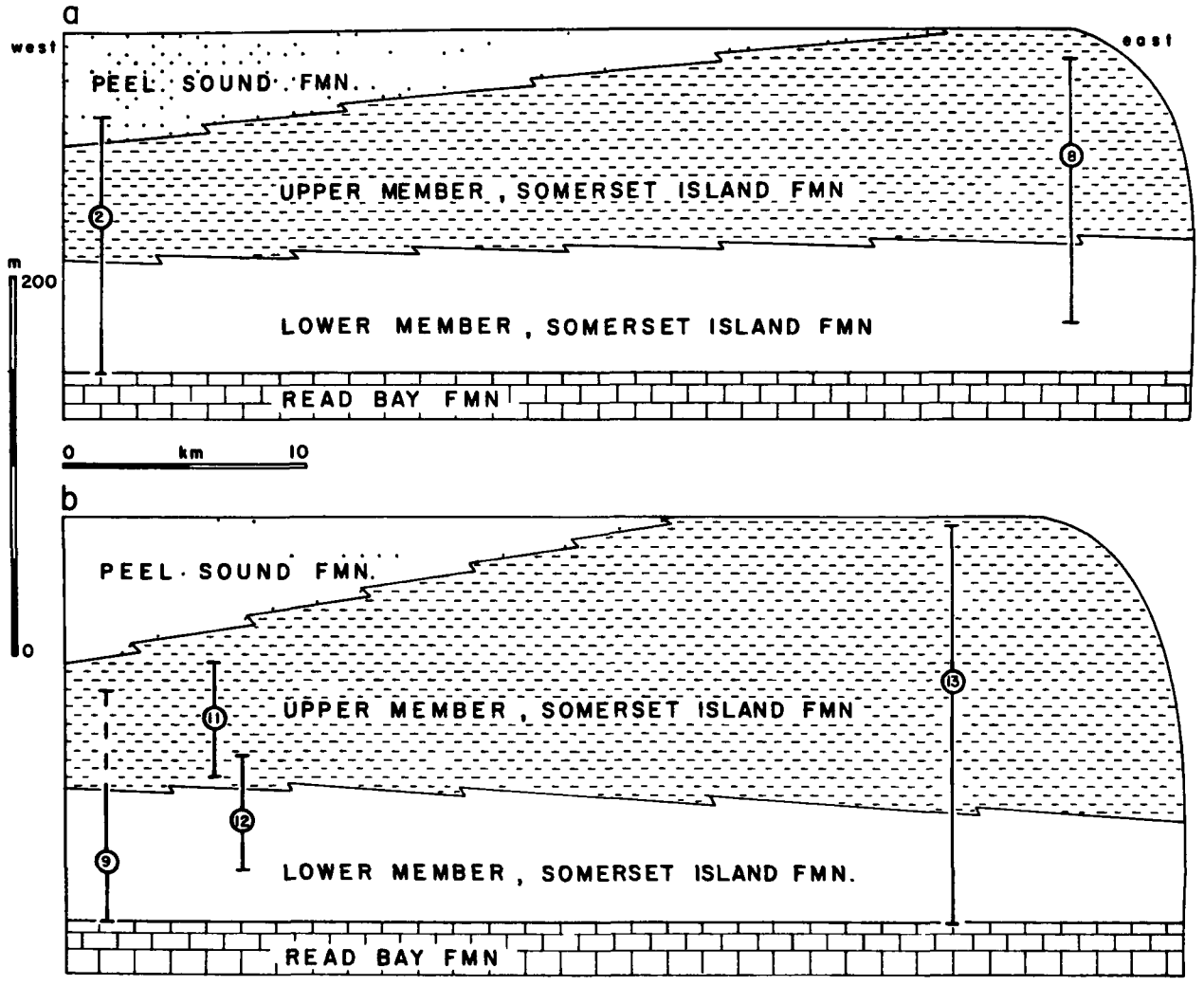

Fig. 4. Generalised cross-sections through the lower part of the clastic wedge in the Cape Anne (a) and Creswell Bay (b) synclines. Numbered localities shown in Fig. 2. Details of wedging between units are inferred. The top of the Read Bay Formation is used as a datum but is probably diachronous. After Miall et al. (1978), Fig. 5.

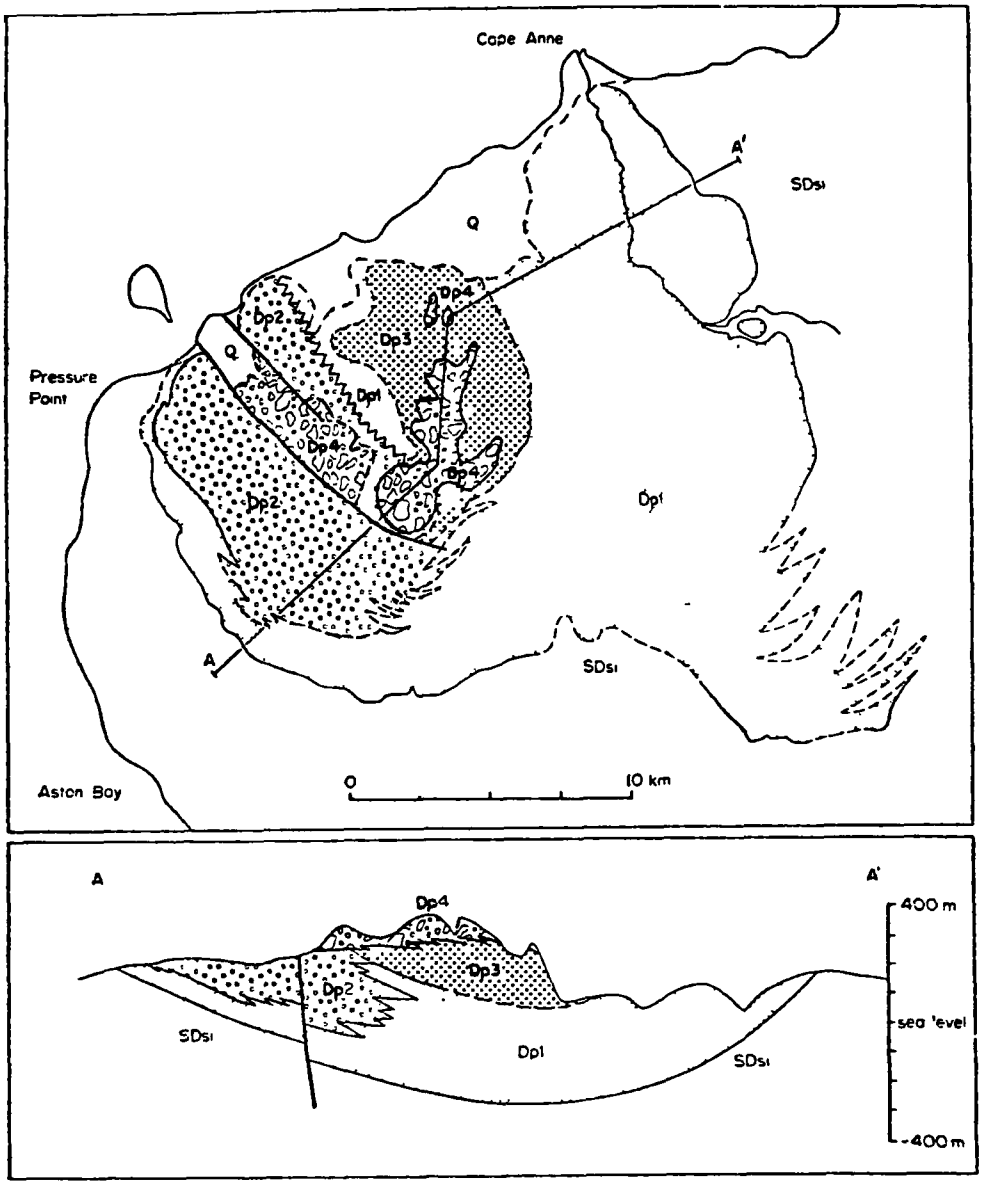

Fig. 5. Distribution of the four members of the Peel Sound Formation, northwestern Somerset Island. SD_{si} = Somerset Island Formation; D_{p1} to D_{p4} = members of the Peel Sound Formation; Q = Quaternary. After Miall and Kerr (1977), Fig. 22.4 .

The Peel Sound Formation outcrops in only a few isolated areas, having been largely removed by later erosion. Dineley (1966, p. 274) noted lateral facies changes within the formation in the Cape Anne syncline, and these have been mapped by Miall and Kerr (1977) as in Figure 5. The lower dolomitic conglomerate (member 2) passes laterally into thick sandstones of member 1 away from the Uplift. The upper polymict conglomerate (member 4) was observed to rest conformably on member 3 in the centre of the syncline, but shows an erosional contact with the lower conglomerate nearer the Uplift, indicating tectonism during deposition. Conglomerate is absent from the present outcrop of the Peel Sound Formation north of Creswell Bay, but polymict conglomerate (member 4) rests conformably on sandstones of member 1 near Cape Garry. The relationship between the conglomerate members in the Cape Anne syncline and the conglomerate at Cape Garry is uncertain.

Age of the formations

Determination of age relations in the clastic wedge is hampered by several factors: the lack of systematic study of many fossil groups; the difficulty of correlation in marine/non-marine transitional environments; and the proximity of the sequence to the Siluro-Devonian boundary with its difficulties of stratigraphic definition. Invertebrate groups present have generally proved non-diagnostic.

Conodonts from nineteen samples in the Somerset Island Formation were identified by Dr. T.T. Uyeno (unpublished report), and given Late Silurian (mid Ludlovian to Pridolian) ages. One sample from the top of the lower member at Locality 3 (G.S.C. Locality No. C-51855) gave a probable Ludlovian age on the basis of Ozarkodina n. sp. B of Klapper and Murphy, 1975. The occurrence of Ozarkodina confluens (Y morphotype of Klapper and Murphy) and Pelekysgnathus n. sp. at Locality 7 (G.S.C. Locality No. C-51856) may indicate an early Pridolian age.

Vertebrate faunas are abundant at several localities and have been assigned ages by comparison with the Ludlovian to Dittonian succession of the Welsh Borders, U.K. A tentative correlation of the British non-marine stages and ostracoderm zones with the marine stages of Europe is shown in Table 2. On Somerset Island, Hemicyclaspis murchisoni was described by Dineley (1968) from strata now correlated with the upper member of the Somerset Island Formation at Locality 1. An abundant traquairaspidid fauna occurs in both the Peel Sound and Somerset Island Formations in the same area (Dineley, 1968; pers. comm. D.K. Elliott, 1976). Protopteraspidids, which have been taken to indicate a Dittonian (probably Gedinnian) age (Table 2) have been collected from the upper member of the Somerset Island Formation, and are currently being studied by D.K. Elliott. These data suggest a Pridolian to Gedinnian age for the Somerset Island Formation.

Table 2. Marine and non-marine stages in the Siluro-Devonian of Europe. Ostracoderm zones and non-marine stages from the British (Welsh Borders) succession, marine stages from continental Europe. Modified from Table 1 of Broad and Dineley, 1973, who quote sources.

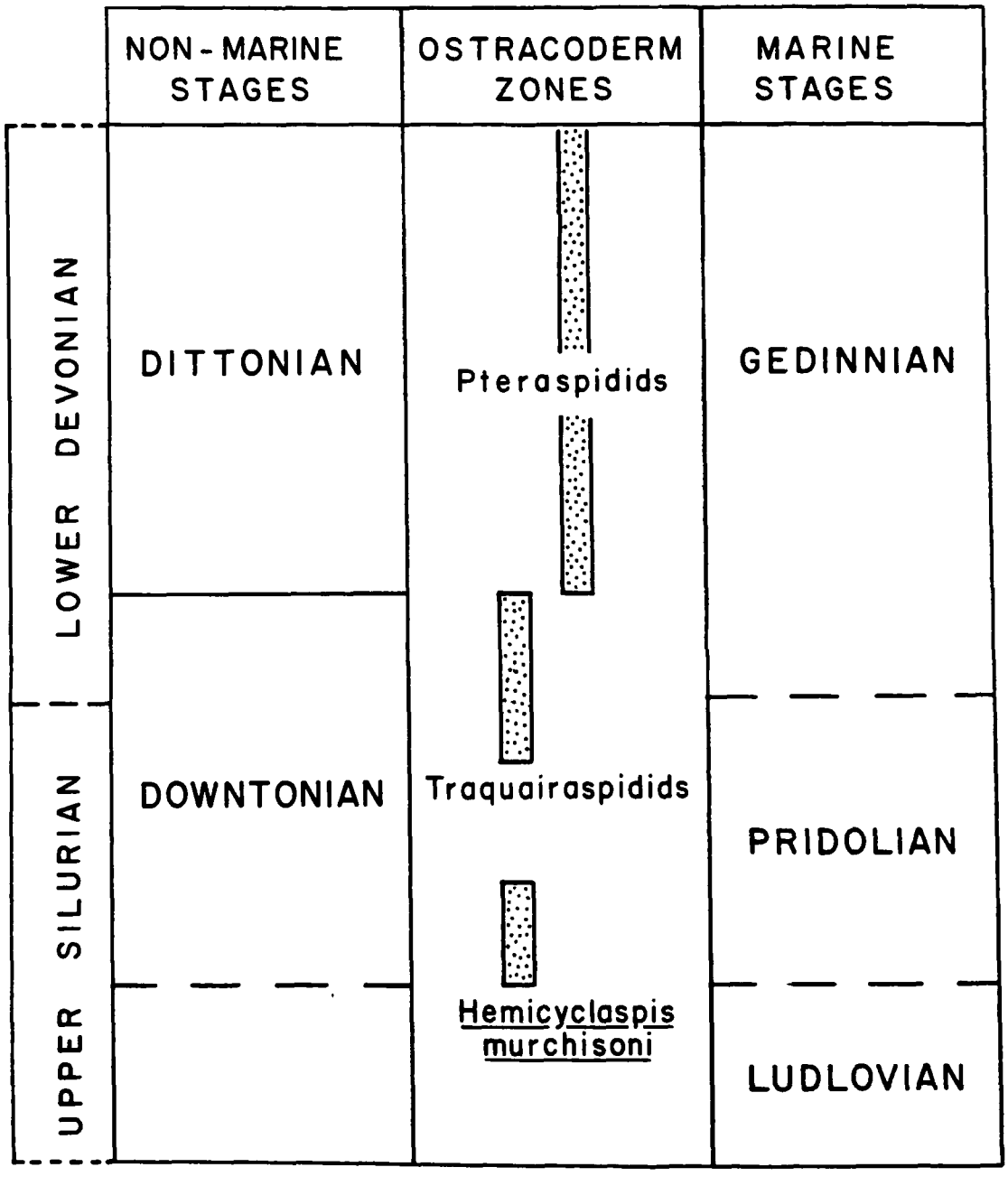

Conflict between age evidence from the vertebrates and from other faunal elements has been frequent, as noted by Miall (1969, Appendix I). The ostracoderms tend to indicate younger ages than the invertebrates and conodonts. There is now some evidence that the vertebrates may have flourished earlier in Arctic Canada than in the U.K. and elsewhere (Broad, 1973; Broad and Dineley, 1973; D.L. Dineley, pers. comm., 1977). Hence the Somerset Island Formation is considered to be Late Silurian in age on the basis of conodonts, and the ostracoderm faunas from adjacent strata may occur earlier in this region than elsewhere in the world. There is no definite evidence for an Early Devonian age for the Peel Sound Formation on Somerset Island, but the formation probably extends up into the Gedinnian.

As yet there are no definitive age data to prove or disprove diachroneity of sedimentary units across the area. However, it is probable that clastic sedimentation spread eastward with time away from the Boothia Uplift. This is suggested by the eastward thickening of the Somerset Island Formation (Fig. 4), the intercalation of limestones of Read Bay type in the lower member towards the east, and the general coarsening-upward nature of the clastic wedge.

Facies spectrum and summary of environments

The clastic wedge shows a complete gradation from shallow marine carbonates to coarse clastics of terrestrial

origin. To describe such a range of sediments, a facies scheme has been devised based on field data but also supplemented by detailed petrography. Reineck and Singh (1975, p. 4) defined a sedimentary facies as "...a sum of all the primary characteristics of a sedimentary unit." A facies name should be a descriptive rather than a genetic term, and lithology, fossils and sedimentary structures are the major characteristics that will be used in description.

Thirteen facies are recognised (Table 3), each designated by an upper case letter signifying the rock type, as in the following system used by Miall (1977) and Miall and Gibling (in press):

G conglomerate ("gravel")

S sandstone ("sand")

F siltstone and mudstone, often dolomitic ("fines")

C limestone and dolostone ("carbonate")

In addition, suffixes (lower case letters) indicate distinctive features of the facies, usually internal structure. The distribution of the facies through the stratigraphic units of the clastic wedge is shown in Figure 6.

The facies present in the two formations will be considered in terms of broad environmental setting, with coastal plain, alluvial plain and alluvial fan environments (Fig.7) discussed in separate chapters. These general environments correspond closely but not exactly with members or formations of the clastic wedge. Coastal plain deposits lie adjacent to sediments of the shallow marine tract, and comprise mainly inter-

TABLE 3. Major facies in the clastic wedge of Somerset Island. Abundance of fossils or structures shown by A (abundant), C (common), U (uncommon), R (rare). Lam.= horizontal lamination.

FACIES	LITHOLOGY	COLOUR	MAXIMUM THICKNESS(m)	FOSSILS	SEDIMENTARY STRUCTURES		ENVIRONMENTAL INTERPRETATION
					CURRENT	OTHER	
Limestone (C)	Micrite and allochems	Grey	5.5	Ostracods C Brachiopods U Corals U and other marine fauna	Lam.	?evaporite cavities	Sub-intertidal
Silty Limestone (C_f)	Micrite, dolosiltite and quartz-silt	Grey-green	6.0	Ostracods C Trace fossils U	Lam. Small-scale cross-strat. Graded beds Scours	Shrinkage cracks Vugs. Drapes Contorted lam.	Sub-supratidal
Laminated Siltstone/Fine Sandstone (P_l)	Siltstone - fine sandstone	Grey-green to red	3.0	Ostracods C Trace Fossils U Gastropods U Ostracoderms U	Lam. Scours Small-scale cross-strat. Ripple-drift cross-lam. Graded beds PCL (R)	Shrinkage cracks Vugs. Loads. Salt casts (R) Drapes. Contorted lam.	Inter-supratidal & terrestrial flooding
Massive Siltstone (P_m)	Siltstone, scattered medium sand	Red/purple/green, commonly mottled	15.0	Ostracoderms R-A Ostracods R-A Plants VR Trace fossils VR	Lam.	Vugs	Terrestrial flooding
Graded Sandstone (S_{gr})	Fine sandstone, scattered medium sand	Grey-green	0.3	Ostracoderms A	Low-angle cross-strat. Graded beds	Loads Drapes Shrinkage cracks	Terrestrial flooding
Interbedded Sandstone/ Siltstone (S_{lb})	Medium sandstone to siltstone	Red/purple/green	7.5		Lam. Small-scale cross-strat. Symmetric ripples	Loads Drapes	Lacustrine
Massive sandstone (S_m)	Fine to coarse sandstone, large pebbles	Red	3.0, ave. 0.1	Ostracoderms R-C Trace fossils R	Graded beds Lam. Small- and large-scale cross-strat.	Shrinkage cracks Vugs. Drapes Salt casts (R) Loads Contorted lam.	Fluvial or lacustrine
Small-Scale Cross-Stratified Sandstone (S_r)	Fine-medium sandstone	Red	3.2		Small-scale planar and trough cross-lam.	Drapes	Fluvial
Large-Scale Cross-Stratified Sandstone (S_{pt})	Fine-medium sandstone, small pebbles	Red/white	2.3	Ostracoderms R-C	Large-scale planar and trough cross-strat.	Contorted lam.	Fluvial
Laminated Sandstone (S_h)	Fine-coarse sandstone	Red	3.75	Ostracoderms R-C	Lam. PCL (R)		Fluvial
Erosion Surface (ES)	Intraclast lag, up to large pebble size		up to 20 cm amplitude				
Giant Cross-Stratified Sandstone (S_g)	Fine-coarse sandstone	Red	15.0		Giant planar and trough cross-strat.		Eolian
Massive Conglomerate (C_m)	Pebbles to boulders	Grey-yellow/red	30.0	Ostracoderms VR	Horizontal strat. Large-scale cross-strat.(R) Imbrication Scours		Fluvial

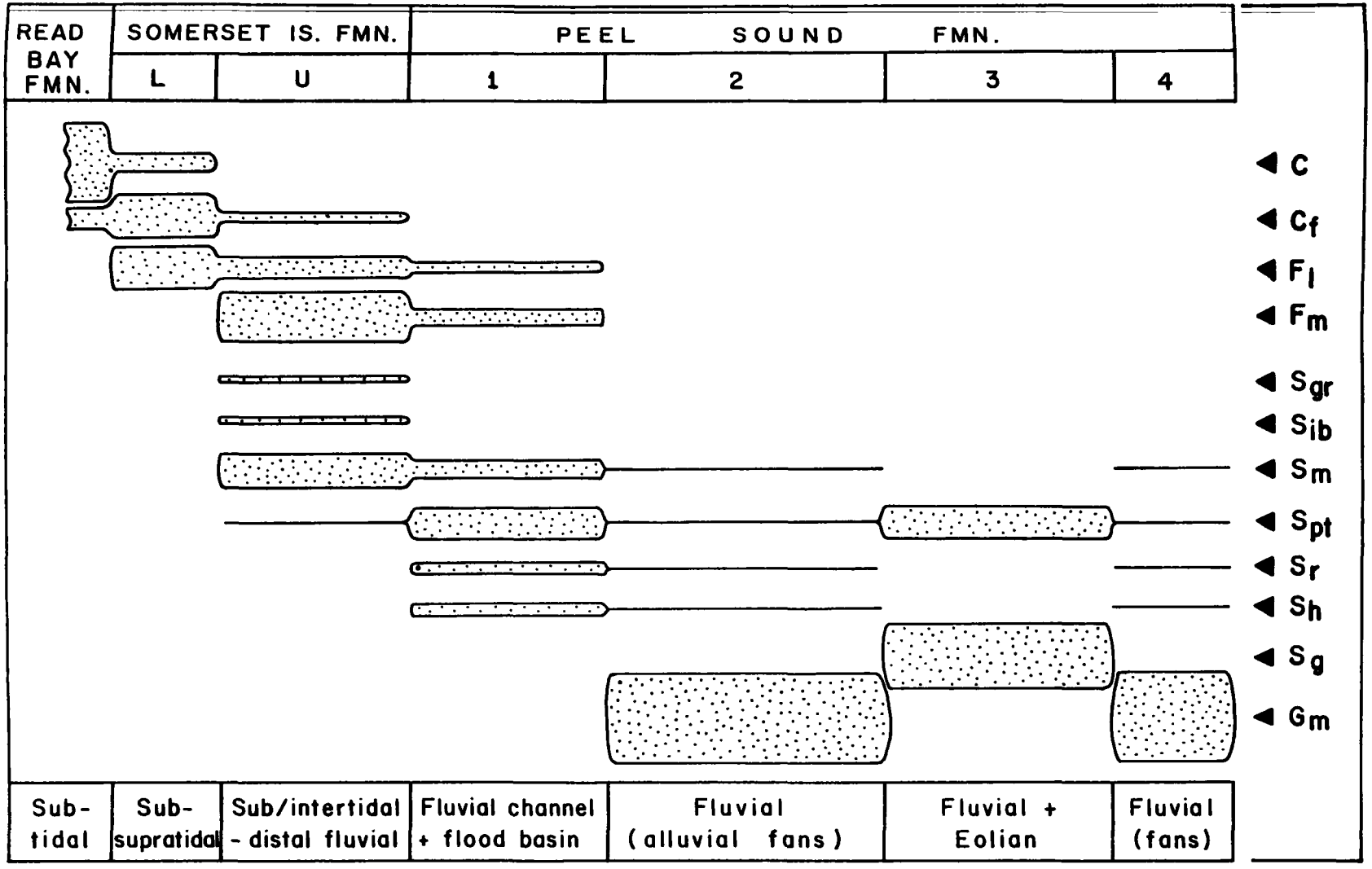

Fig. 6. Facies spectrum for the clastic wedge on Somerset Island. Width of bands indicates the relative proportion of the major facies in each stratigraphic unit. Facies code as in Table 3.

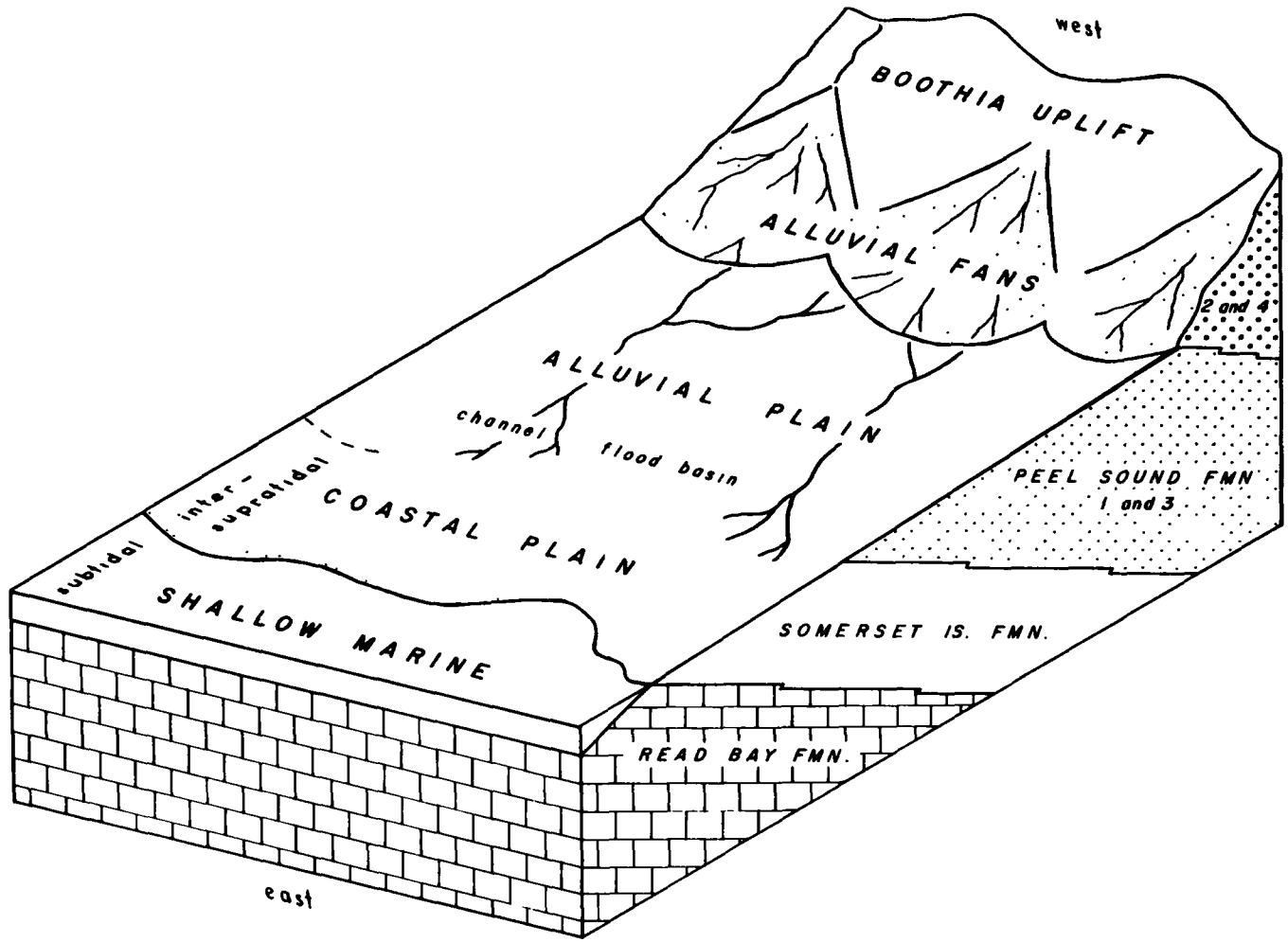

Fig. 7. Depositional environments of the clastic wedge on Somerset Island. See text for explanation of terms.

supratidal carbonates and clastics. Sediments of the alluvial plain consist of sandstones and siltstones deposited in fluvial channels and flood basins. They pass laterally into the coastal plain deposits through a zone of distal flood basin sediments in which both fluvial channel and tidal deposits are uncommon; this zone is considered an extension of the alluvial plain since the sediments were land-derived. Alluvial fan sediments at the mountain front consist of conglomerates deposited in braided stream systems.

1. Aerial view of northwestern Somerset Island, looking southeast. 1 and 2 = members of the Peel Sound Formation. Cliffs at Pressure Point in foreground 150 m high. Photo courtesy of B.R. Rust.

2. Panoramic view of the Cape Anne syncline, northwestern Somerset Island, looking west from Cape Anne. The Read Bay Formation (RB) dips 10° SE on Limestone Island. Peel Sound Formation (PS) members 3 and 4 form the hills (280 m elevation) in the centre of the syncline. Raised beach material in the foreground.

1

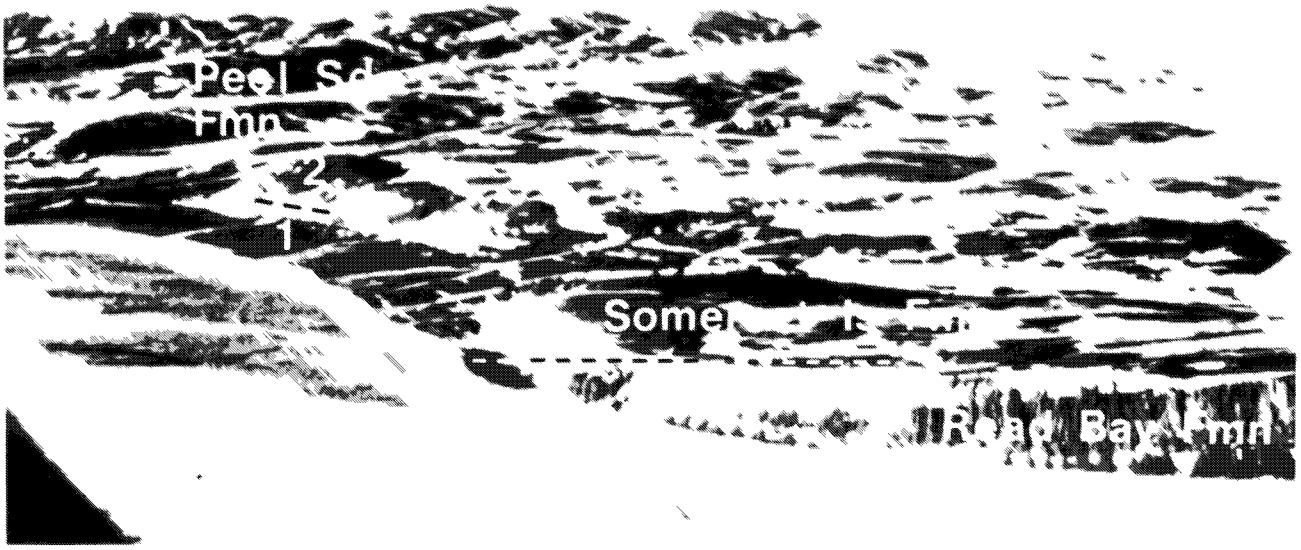

2

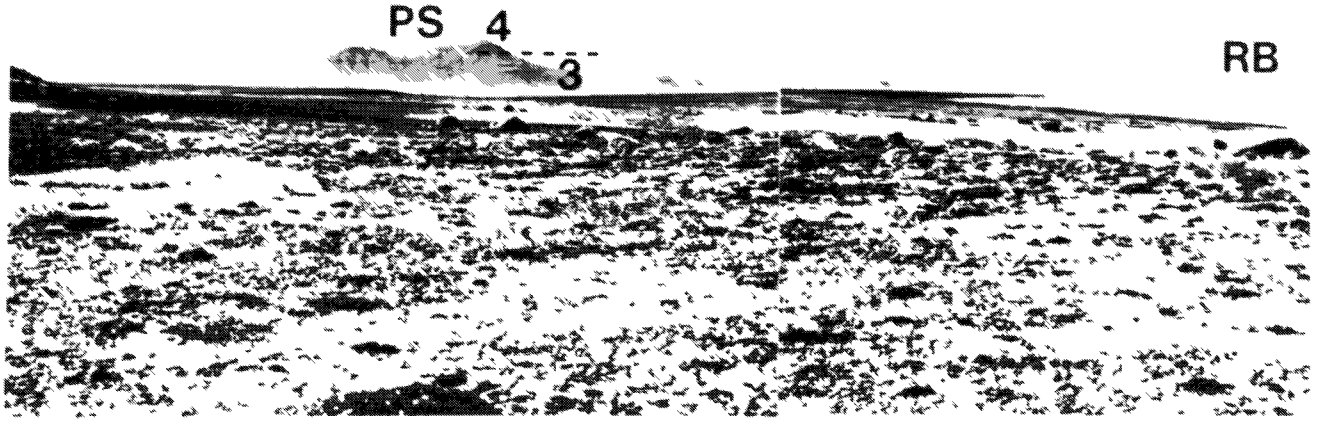

CHAPTER 2. COASTAL FLAT SEDIMENTATION

Introduction

Shallow subtidal to supratidal successions form most of the Somerset Island Formation. The following aspects of the successions will be discussed below:

1) Description of sedimentary facies.

2) Description of cyclic facies successions in vertical sections, using Markov chain analysis.

3) Identification of types of algal mat and their relationship to the cyclicity.

4) Interpretation of the facies and their cyclic relationships, using Shark Bay, Western Australia, as a Recent analogue.

Sections from both members of the Somerset Island Formation will be considered together because there is a continuum of facies in the two members (Fig. 8), and because it was difficult to distinguish the typical members in measured sections close to the Uplift. In general, the lower member shows less obvious cyclicity, and lacks the terrestrial intercalations of the upper member. Units of limestone and laminated siltstone (facies C, C_f and F_l) predominate in the lower member, and average between 0.75 m and 1.0 m in thickness (Fig. 8); units of massive siltstone (facies F_m) predominate in the upper member, and average more than 3.0 m in thickness.

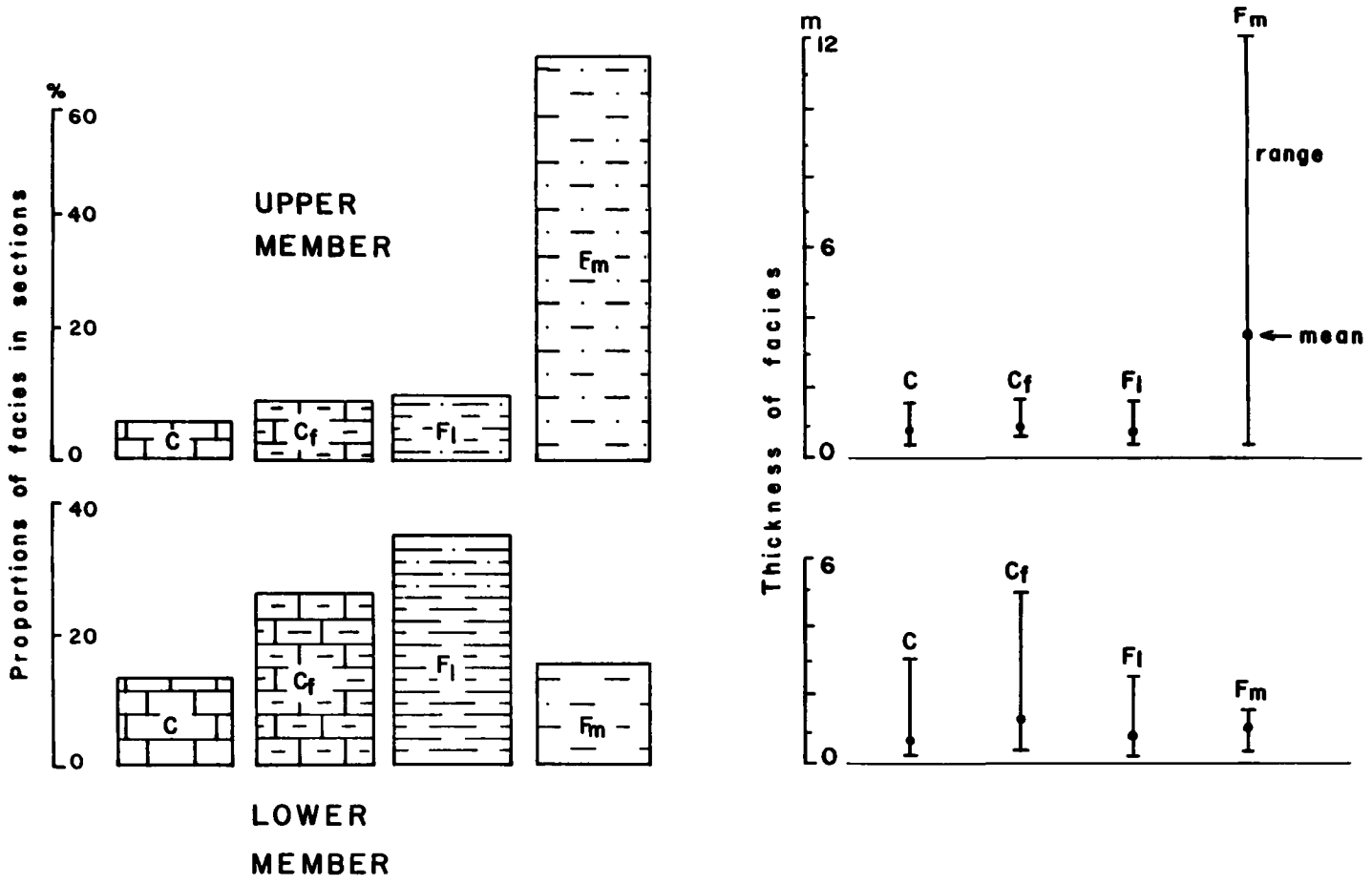

Fig. 8. Proportions and mean thickness of major facies in sections of the Somerset Island Formation. Lower member : section G74G, Loc. 2, 45 units. Upper member : section G74J, Loc. 13, 54 units. Facies code as in Table 3.

Nature of Facies

General scheme of description

The Somerset Island Formation includes a wide variety of rock types, from carbonate rocks (both dolomitic and calcareous) to terrigenous rocks and evaporites. The description of hundreds of samples eventually led to the recognition of a number of distinct facies. These commonly contain both carbonate and clastic constituents, and are believed to reflect distinct physical and chemical processes in the paleoenvironments. Hand specimens were cut and stained for calcite and dolomite with Alizarin Red S, as outlined by Friedman (1959) and Dickson (1966), and examined with a binocular microscope. This method has several advantages: many specimens may be prepared and examined rapidly; the relatively large areas cut and stained allow for more representative study; and sedimentary structures are well shown. To supplement this, about one hundred thin sections were examined after staining with Alizarin Red S and potassium ferricyanide (Dickson, 1966), and evaporite-bearing samples were analysed by X-Ray diffraction.

For general description of calcareous rocks, the main divisions of Folk's (1959) classification are used, in which allochems (pellets, intraclasts, fossils and ooliths) are distinguished from orthochems (micrite and sparite). Dolostones are described using the system shown in Table 4.

TABLE 4. Classification of dolomite.
After Hatch and Rastall, 1965, Fig. 41.

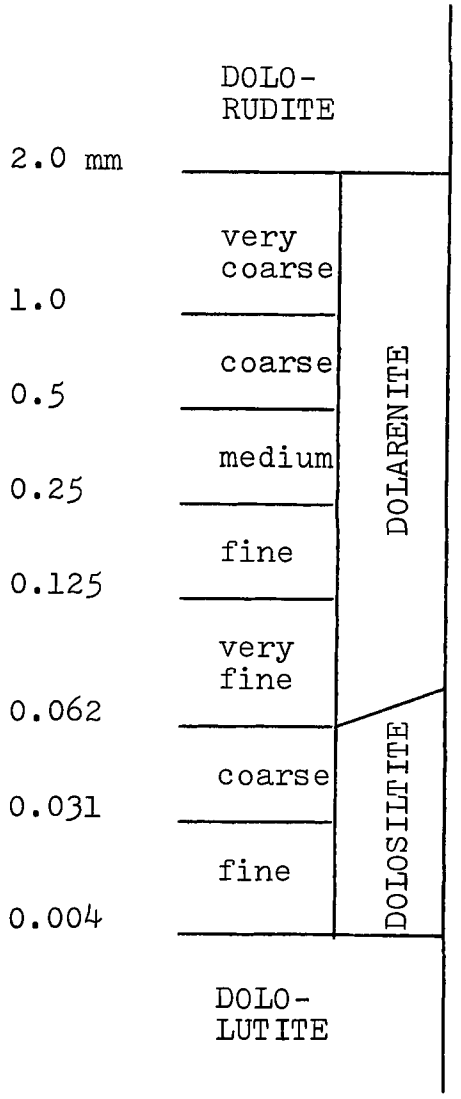

Leighton and Pendexter (1962, p. 57) noted that "In spite of attempts to avoid genetic implications in naming dolomites and dolomitic rocks, it is impossible to do so completely", and hence most descriptive systems imply either an allogenic or authigenic origin, or recognise that both types may be present in the same rock and require separate description (e.g. Folk, 1962). The system used here, taken from Hatch and Rastall (1965) and modified for dolostones, combines aspects of the allogenic classification of Grabau (1904) with Wentworth's (1922) scale of grain size. The system differs from the better known grain size classification of Folk (1962, Table II) in the use of the term "dolosiltite" for grains in the 4 - 62μ range, a major component of the rocks studied. It must be stressed that the system is used here strictly to describe the size of the dolomite crystals and has no genetic implications. Detrital silicate grains are described using Wentworth's scale of grain size. Facies containing both silicate grains and dolomite are named using the appropriate grain size terms ("siltstone", "fine sandstone").

Facies types

Limestone (C)

Most of the limestones are micritic, with variable quantities of allochems, pellets being the most abundant. Some pellets are probably fecal, and show consistent size

(about 0.2 mm diameter) and diffuse rounded margins. Others are up to 1 mm in diameter, with distinct angular margins, and may be fine intraclasts, or skeletal debris micritised by boring algae (Bathurst, 1966; Logan, 1974). Intraclasts are commonly subrounded, confined to discrete layers, and composed of micritic, bioclastic, pelletal and sandy limestones, and dololutite. The presence of intraclasts indicates that some early lithification took place during sedimentation. Recognisable fossils are common, and many of the indeterminate calcareous particles may be fragmented fossils. Algal activity is indicated by oncolites up to 2 cm in diameter, and probably also by micrite rims on intraclasts and skeletal fragments. No oolites were observed.

Non-calcareous components include quartz silt and dolosiltite (less than 20%), and diagenetic nodules and crystals of gypsum. Pink-staining sparite cement is restricted to a few beds rich in allochems. A blue-staining Fe-rich sparite, commonly late-stage (Dickson, 1966), fills fissures and cavities, and forms pseudomorphs after evaporites in many of the facies. Accumulation of dolomite and insoluble material such as iron oxides along stylolitic horizons is common.

Ostracods are the most abundant faunal element, but an open marine assemblage of complete and fragmented brachiopods, corals, stromatoporoids, pelmatozoans, trilobites, gastropods and ostracods also occurs in certain beds (Photo 3). Conodonts have been extracted from several samples.

Some units of this facies were open marine in origin, but the predominant ostracod fauna suggests a more restricted environment for much of the facies. Sedimentary features include lamination, and small circular pits which may be evaporite solution cavities.

Silty limestone (C_f)

Limestones containing more than about 20% of quartzose silt and dolosiltite appear distinctly granular on weathering and are arbitrarily grouped as silty limestones. The facies is intermediate in lithology between facies C and F_1 (see below), but differs from both in the variety of sedimentary structures that it contains (Photo 4). Small-scale symmetric and asymmetric ripples with siltstone "drapes" are common on bedding surfaces, with small-scale planar and ripple-drift cross-lamination and lenticular bedded cross-stratification (Reineck and Wunderlich, 1968) on vertical faces. Parallel to contorted lamination is common, and some laminae are graded on a 1 - 2 cm scale (percentage and size of silt decreases upward). Other structures include low domal stromatolites, lensoid shrinkage cracks, small scours and calcite-filled vugs (less than 1 cm diameter). The assemblage of structures indicates intermittent current action, fluctuating in strength, and variable rates of sedimentation. The low-diversity fauna, mainly of ostracods, is consistent with low intertidal conditions. Trace fossils include Chondrites and Paleophycus.

Laminated fine sandstone (F_1)

The facies consists of relatively coarse planar laminae, less than 1 mm thick, alternating with fine laminae from 0.1 mm to several mm thick. The coarser laminae are composed of very fine to fine dolarenite and quartz (average diameter 0.1 mm) in a matrix of micrite or dolosiltite; dolarenite usually constitutes about 75% of the coarser grains, and the proportion of matrix is variable. The finer laminae consist mainly of dolosiltite or micrite. Laminae either alternate abruptly, or are normally or reversely graded from dolarenite to dolosiltite on the scale of a few mm. Sedimentary structures include small-scale erosional features, load casts, contorted lamination, small-scale cross-lamination and shrinkage cracks (Photo 5). Ostracod fragments, commonly in current-stable orientation, are concentrated with medium-grained quartz at the base of some laminae. The structures indicate strong but intermittent current action in shallow water, probably in the intertidal zone. Sub-spherical vugs up to a few cm in diameter commonly contain gypsum nodules or rims of dog-tooth calcite (Photo 6).

A purely mechanical origin is probable for some of this facies, but the sediment-binding activity of filamentous algae may account for much of the lamination. These algae are important constituents of many modern tidal flats. The formation of cohesive mats is a discontinuous process, and layers of bound sediment alternate with thin layers of algal

filaments. The contrasting laminae reflect serial events such as fluctuations in moisture content, salinity, light (day and night), current velocity and sedimentation rate (Bathurst, 1975 p. 223). Davies (1970) listed the following criteria for the recognition of algal lamination:

1) Molds of algal filaments seen in thin section.

2) Organic films produced by massed algal filaments.

3) Evidence of cohesion (brecciation, overfolding and contortion).

4) Relationship to surface topography, e.g. algal laminae tend to thicken over surface relief.

5) General nature of sedimentary facies.

In facies F_1, the thin micritic or dolomitic layers may represent what were formerly layers of algal filaments between layers of bound grains. Contortion structures indicate that sediment in the laminae was cohesive, and the presence of low domes is also typical of algal lamination. The probable intertidal environment is consistent with an algal contribution.

Algal activity is further indicated by the presence of domal stromatolites interbedded with facies F_1 (Photos 7 and 8). They are usually calcareous rather than dolomitic, with alternate coarse and fine laminae. The coarse laminae consist of pelletal sparite with dolarenite, muscovite, sand-sized quartz and skeletal grains; the very thin finer laminae consist of dense, locally pelletal micrite, dololutite or dolosiltite (Photo 9). Lenses and irregular patches of

sparite are common, imparting a ragged microtexture. The domes are laterally-linked and isolate hemispheroids (LLH- and SH-C-types of Logan et al., 1964).

The variation in composition of the coarse laminae in flat-lying and domal growth forms reflects the material available for sediment-binding. Modern algae have been observed to bind even fine-grained quartz (Schwartz et al., 1975). As regards the finer laminae, Gebelein and Hoffman (1973) suggested that the Mg-rich sheaths of algal filaments are altered to thin dolomitic laminae during diagenesis. Inorganic/biochemical precipitation of aragonite has been noted in algal structures (Monty, 1967; Horodyski and Vonder Haar, 1975), and may account in part for the calcareous composition of domal stromatolites in the predominantly dolomitic sediment of the Somerset Island Formation. Stratiform algal growth predominates on low-gradient flats at present, with low domal structures (LLH-type) perpetuating local relief (Logan et al., 1974, p. 185-6).

Massive siltstone (F_m)

Facies F_m consists of thick beds of dolosiltite, with some dolarenite and a small percentage of micrite, quartz silt and medium-grained quartz. Units are usually thick (up to 15 m), conchoidally weathering and recessive, but some are well exposed in river bluffs (Fig. 9). Colour varies from red to grey-green, with colour mottling common. Units are internally massive, but sedimentary structures include

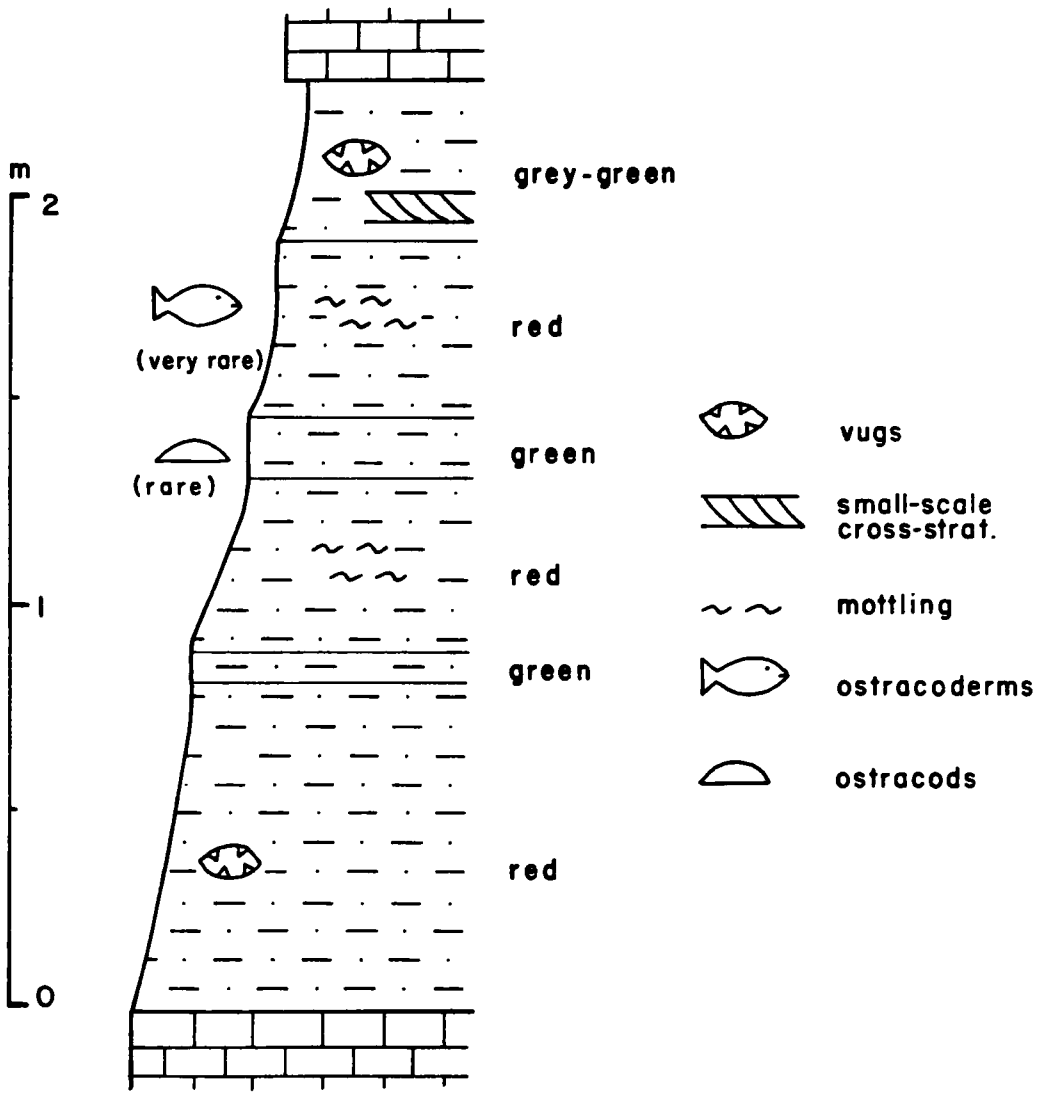

Fig. 9. Detailed section of a massive siltstone unit in the Somerset Island Formation. More resistant layers in profile contain higher concentrations of medium-grained quartz. All beds are conchoidally weathering. Unit G74J-4, Loc. 13.

rare parallel lamination, small-scale cross-lamination, and ferruginous laminae in the form of troughs a few mm deep, probably resulting from the migration of low amplitude bed forms. Fine fragments of ostracods and ostracoderms are concentrated locally or scattered in the sediment without preferred orientation, and medium-grained quartz varies from concentrated to scattered in distribution. Vugs are common, and in some units, shrinkage cracks are conspicuous where emphasised by lithological contrast.

Thick deposits of silt and clay are common in the flood basins of modern rivers (Reineck and Singh, 1975, p. 250-252), with fines deposited from shallow standing water after inundation of the flood plain. The deposits are internally laminated to poorly bedded, with mottling and bioturbation rather common. Massive siltstone is abundant in many ancient fluvial sequences, especially at the tops of fining-upward cycles (Allen, 1964a, 1970a). In the clastic wedge on Somerset Island, facies F_m in alluvial plain environments probably originated by overbank flooding (Chapter 3), but in coastal plain environments, the thick units of facies F_m which directly overlie inter-supratidal sediments are not associated with fluvial channel deposits, and a flood basin environment is unlikely. Deposition probably resulted from periodic flooding of coastal flats by ephemeral streams terminating on the alluvial plain, and from sheetwash following rain storms (Twidale, 1971, p. 97). Aivar Depers

(pers. comm., 1977) reported that alluvial fans bordering the Flinders Ranges in South Australia extend to the coast, and the fan deposits are slowly prograding over the supratidal deposits as the result of ephemeral sediment transport, especially during flash floods. In facies F_m, rare lamination, small-scale troughs, and shrinkage cracks suggest the influence of water during deposition.

The massive nature of facies F_m may have resulted from several processes. Bioturbation by plants and organisms is common in modern overbank sediments; however, plant remains are very rare in the clastic wedge, and vertical burrows rare in facies F_m (terrestrial burrowers may have been rare at that time). The commonly scattered distribution of fragmentary fossils and medium-grained quartz may suggest some bioturbation (Friend and Moody-Stuart, 1970, p. 182). Wind action may have reworked superficial sediment (e.g. Williams and Rust, 1969, p. 667-8; Twidale, 1971, p. 97), resulting in homogenisation.

Colour mottling is common in facies F_m, and is generally associated with oxidation/reduction effects. Mottling emphasises some original sedimentary features such as the wispy ferruginous laminae noted above, burrows, and <u>in situ</u> brecciation — probably by desiccation — of varicoloured mudstone and siltstone laminae. Reddening is present around gypsum nodules and fossils (ostracoderm, ostracod and rare probable plant fragments), and the pores in fish bone generally

contain crystalline hematite. Later fissures are associated with variability of colour. However, mottling is commonly diffuse and not obviously related to megascopic features, and much of it may result from soil-forming processes. Modern soils subjected to moisture fluctuation undergo alternate oxidation and reduction, resulting in redistribution of Fe and Mn, whose compounds show colours related to their oxidation state. The distribution of organic matter may greatly influence the site of precipitation and the oxidation state of these elements, and destruction of sedimentary structures by vegetation and burrowing is a common association. Such mottling is especially characteristic of the upper few feet of poorly drained hydromorphic soils, widespread in river plains, deltas, estuaries and lagoons (Buurman, 1975, p. 290), and around playa lakes in desert regions where the soils also contain salts (Hunt, 1972, p. 174). Buurman (1975) noted the occurrence of Tertiary hydromorphic soils, and figured samples with diffuse mottling, locally associated with bioturbation, which closely resemble mottled specimens from facies F_m in the Somerset Island clastic wedge. Vugs, resulting from solution of evaporites in facies F_m, indicate that hypersaline groundwaters were present.

Mottled siltstone (F_{md}), a distinctive variant of facies F_m, occurs as distinct beds averaging 30 cm in thickness, with abrupt basal contacts. Units contain dispersed quartz grains of medium sand size, ostracod fragments, and commonly

ostracoderm material in unusual abundance. Bright red/green diffuse mottling is a distinctive feature (Photo 10), also common in facies F_m; but in conjunction with abundant ostracoderm remains and quartz grains, it is considered diagnostic for facies F_{md}. The abrupt lower contact suggests that deposition was related to a distinct sedimentary event, possibly of relatively high energy in view of the fragmentary nature of the fossil material.

Quartz-sandstones (S_{gr} and S_m)

Rare, thin units of graded, medium-grained sandstone (S_{gr}) and massive sandstone (S_m), described in Chapter 3, are interbedded with the massive siltstones. They were probably formed by overbank floods or crevasse splays on an alluvial plain. However, scattered grains of medium to coarse grade are common in most of the facies previously described, and require comment.

The grains, composed exclusively of quartz, form a distinctive size population averaging 0.4-0.5 mm in diameter (range 0.2-1.0 mm), show excellent sorting and high sphericity, and are well rounded. The mineralogical and textural features of the grains probably reflect a source in an older sandstone such as the Proterozoic Aston Formation — a mature, shallow-marine quartzite (Dixon et al., 1971) — that is represented abundantly in clasts in the Peel Sound conglomerates. The common occurrence of the grains in fine-grained carbonate rocks (bimodal distribution) is difficult to explain as the

result of deposition by hydraulic processes which commonly separate components of such disparate grain size. Eolian transport, however, could result in the deposition of small amounts of relatively coarse grains in a variety of fine-grained sediment types, and much of the sand sized quartz in carbonate rocks of the Somerset Island Formation was probably derived from the deflation of local coastal dunes. The common dispersion of the grains in the carbonate matrix is consistent with eolian deposition, although this may also result from bioturbation (Friend and Moody-Stuart, 1970). In the Persian Gulf, Emery (1956, p. 2368) observed wind-blown "coarse" quartz grains in core samples up to 45 miles offshore, and Sugden (1963, p. 359 and Fig. 3) noted frosted, well-rounded eolian quartz of fine to very fine sand size in near-shore carbonates. Carbonate sediments in Card Sound, Florida, contain well-sorted quartz sand which has been transported into the area by waves and currents (Earley and Goodell, 1968); however, the sorting action of hydraulic processes has brought together quartz and carbonate grains of similar size (ibid., Figs. 2 and 3), in contrast to the commonly bimodal size distribution of the two components in carbonate rocks of the Somerset Island Formation.

Dololutite

Beds of white dololutite constitute less than 1% of the Somerset Island Formation. The beds are a few cm thick,

lensoid and show abrupt contacts, with irregular tops penetrated by wedge-shaped fissures (Photo 11). Lamination is weak or absent; fragmental ostracods are the only fauna. Medium-grained quartz is concentrated in hollows and fissures on the ancient erosion surfaces, and angular intraclasts of dololutite are common in overlying units. In one instance, thin bioclastic beds show incipient brecciation along bedding planes, with dololutite both as thin laminae between the fragments (Photo 12), and as superficial zones of alteration on micritic intraclasts.

Dolomitisation was clearly penecontemporaneous, with lithification at the sediment surface; the facies resembles dolomitic crusts recorded in modern supratidal environments (Illing et al., 1965; Shinn, 1968), resulting from dolomitisation following evaporative concentration of groundwater. Germann (1969) related brecciation of ancient crusts to storm action.

Evaporites

Although constituting less than 1% of the Somerset Island Formation, evaporites are important as indicators of the presence of hypersaline fluids. Gypsum was identified by X-Ray diffraction in eight samples. Nodules of gypsum occur in several facies, and gypsum locally fills desiccation cracks (Photo 13); the nodules were present before compaction, since sedimentary laminae are deformed around them (or around vugs

resulting from their dissolution, Photo 6), and the presence of euhedral gypsum crystals, or their pseudomorphs, enclosing ostracod fragments suggests a diagenetic origin. Elsewhere, thin beds contain tabular cavities, indicative of the former presence of gypsum or anhydrite (Photo 14). Diagenetic anhydrite nodules and gypsum crystals commonly form from hypersaline groundwaters in modern tidal flat environments such as the sabkha of Abu Dhabi Persian Gulf (Evans et al., 1969) and at Shark Bay, Western Australia (Logan, 1974: gypsum crystals only). The gypsiferous nodules of the Somerset Island Formation probably were composed of anhydrite originally.

Bedded evaporites are less common in the Somerset Island Formation. A few bedding planes show halite casts preserved in fine sandstone (Photo 15). One bed of gypsum 80 cm thick is enclosed in facies F_m and extends laterally for 120 m (Photo 16); bands of fibrous selenite less than 0.5 cm thick alternate with lenses and laminae of grey-brown crystalline gypsum, dolosiltite and quartz, indicating that precipitation of gypsum alternated with influxes of fine clastic sediment. In modern environments, bedded evaporites can precipitate in both marine and non-marine situations. On flats adjacent to the Colorado River delta, some depressions near the landward margin of the supratidal zone retain water after tidal flooding, resulting in halite and gypsum precipitation (Thompson, 1968, p. 26-7). In many desert basins, ephemeral or semi-permanent

lakes (inland sabkhas) result from groundwater seepage and inflow from wadis, with precipitation of gypsum, halite and other salts consequent upon intense evaporation (Jones, 1965; Hardie, 1968; Glennie, 1970).

Coquina

Only three units of coquina were observed in the Somerset Island Formation. The facies is largely composed of whole or fragmentary high-spired gastropods in micrite or sparite (Photo 17). A few rounded intraclasts of dololutite and laminated dolosiltite are present, with about 15% medium-grained quartz, and a few ostracods. The well-sorted nature of the deposit indicates high energy. Gastropods are often associated with algal structures in adjacent strata. At Shark Bay, coquina occurs in subtidal environments where fine material is winnowed away, and in beach ridge and dune deposits where skeletal grains are concentrated by storm action (e.g. Hagan and Logan, 1974).

Vertical distribution of facies

Markov chain analysis

If a cyclic repetition of facies is present, environmental interpretation is greatly facilitated because data can be summarised readily and because many types of cycle are indicative of certain environments. Such successions have often been described by comparison with an idealised cycle,

but this involves the danger of forcing the sequence into a predetermined framework. Markov chain analysis provides an objective statistical method for analysing cyclicity, as summarised by Miall (1973). Each unit in the stratigraphic sequence is assigned to one of a small number of "states", preferably four to six. The number of vertical transitions from each state to each of the other states is tabulated in a transition count matrix. In the embedded Markov chain method (Krumbein and Dacey, 1969) used here, counts are made only at a change in state in the section, regardless of the thickness of the units (i.e. no A to A type transitions). Matrices are then constructed to calculate the probability of a given transition occurring randomly (independent trials probability matrix), and the actual probability of occurrence (transition probability matrix). The difference matrix compares the two and indicates which transitions have occurred with a greater than random frequency. The X^2 test is applied to assess the significance of the result, as outlined by Gingerich (1969) and Harbaugh and Bonham-Carter (1970, p. 121). Since Gingerich's test is recommended only where each value of the transition count matrix is greater than 5 (Miall, 1973, p. 352), the latter test was used in this study. Analysis employed a version of the computer programme of Miall (1973), modified by Dr. B. Jones.

The method is subject to various limitations. The condensation of sections into a few states is highly subjective

and may involve gross over-simplification, and one state may have several modes of origin, generating "randomness". Significant but rare states must be combined with others. Intervals of no exposure break the sequences, and it is unwise to count a transition across such a break. Local variation is often masked by combining sections. Analysis is aimed at identifying the "typical", not at distinguishing the "atypical".

An ordered vertical sequence of facies nearly always implies an ordered arrangement of environments in space, because lateral migration of the environments results in vertical accumulation of a facies sequence (Walther, 1894). In some cases, the ordering is more strongly time-related (e.g. deposition of graded beds from waning currents to give the Bouma sequence). Likewise, a disordered vertical sequence may reflect an irregular pattern of environments ("crazy quilt" of Potter and Blakeley, 1968) or unpredictable events such as storms or floods (e.g. Jones and Dixon, 1976). "Randomness" may also result from poor judgement in the definition of states.

Analysis of coastal flat cyclicity

Field measurement showed the presence of carbonate-clastic cyclicity (Gibling, 1977) in several sections of the Somerset Island Formation (Fig. 10); the cycles are commonly conspicuous in cliff exposures (Photo 18), with the carbonate facies standing out as scarps separated by scree slopes of

massive siltstone. These observations were confirmed by Markov analysis, combining data from five sections in the Somerset Island Formation, totalling 396 m. Transition matrices (Table 5) are based on 198 transitions between the six major facies, and the X^2 test showed significance at the 99.9% level. The path diagram derived from Markov analysis (Fig. 11) may be used to construct a generalised cycle (Fig. 12), showing the following distinctive features:

1) Carbonate (micritic) rocks in the lower part grade up into clastic rocks containing both detrital silicate and dolomitic material.

2) Facies C, C_f, F_l and F_m follow in sequence, suggesting a regular spatial arrangement of these facies.

3) Facies F_{md} and S_{gr}/S_m show relationship only to facies F_m, and are abruptly based. They are interpreted as the product of random events which interrupted deposition of the massive siltstone.

4) Thin-bedded and laminated units predominate in the lower part of the cycle, passing into thick-bedded or unbedded units above.

5) Ostracods and gastropods are common in the lower part but rare above, while fragments of ostracoderms are characteristic of the upper part.

6) Colour changes from grey below to predominantly red above.

7) The mean thickness of 27 complete cycles in four

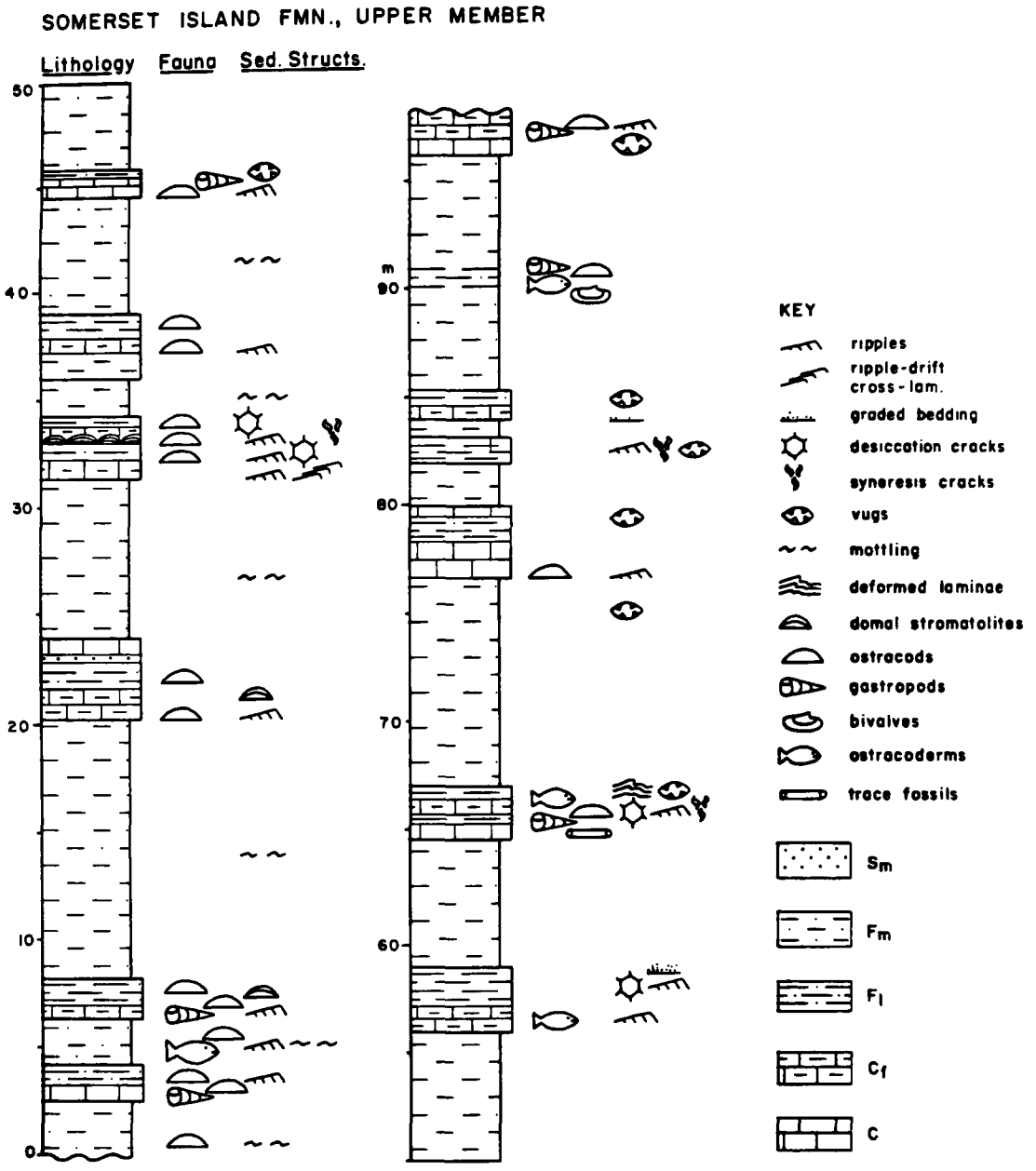

Fig. 10. Detailed section showing carbonate-clastic cyclicity in the upper member of the Somerset Island Formation. Section profile shows relative resistance of units. Section G74J, Loc. 13. Facies code as in Table 3.

TABLE 5. Markov chain analysis: data for the Somerset Island Formation. Sections G73J, G74D, F, G and J. Symbols for facies as in Table 3.

TRANSITION COUNT MATRIX:

	C	C_f	F_l	F_m	F_{md}	$S_{gr} + S_m$
C	0	12	12	3	0	0
C_f	4	0	29	8	1	0
F_l	10	18	0	21	5	3
F_m	11	7	14	0	8	7
F_{md}	0	2	1	10	0	1
$S_{gr} + S_m$	1	2	3	4	1	0

DIFFERENCE MATRIX:

	C	C_f	F_l	F_m	F_{md}	$S_{gr} + S_m$
C	.00	.20	.11	-.16	-.08	-.06
C_f	-.08	.00	.33	-.11	-.07	-.07
F_l	-.02	.02	.00	.04	-.01	-.03
F_m	.06	-.13	-.08	.00	.08	.08
F_{md}	-.15	-.09	-.24	.46	.00	.01
$S_{gr} + S_m$	-.05	-.04	-.03	.11	.02	.00

No. of Transitions: 198

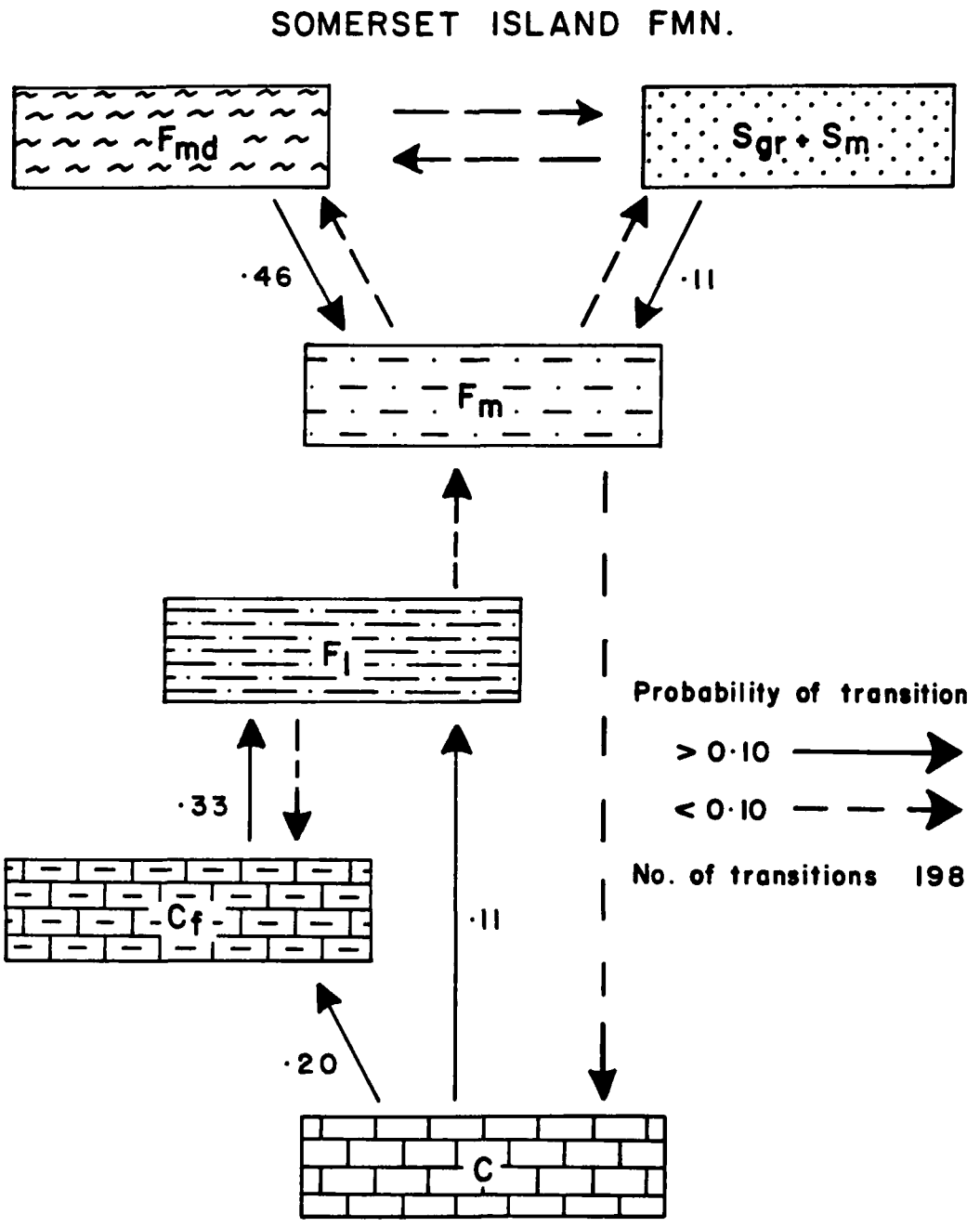

Fig. 11. Markov chain analysis : Path diagram for sections in the Somerset Island Formation. Facies code as in Table 3.

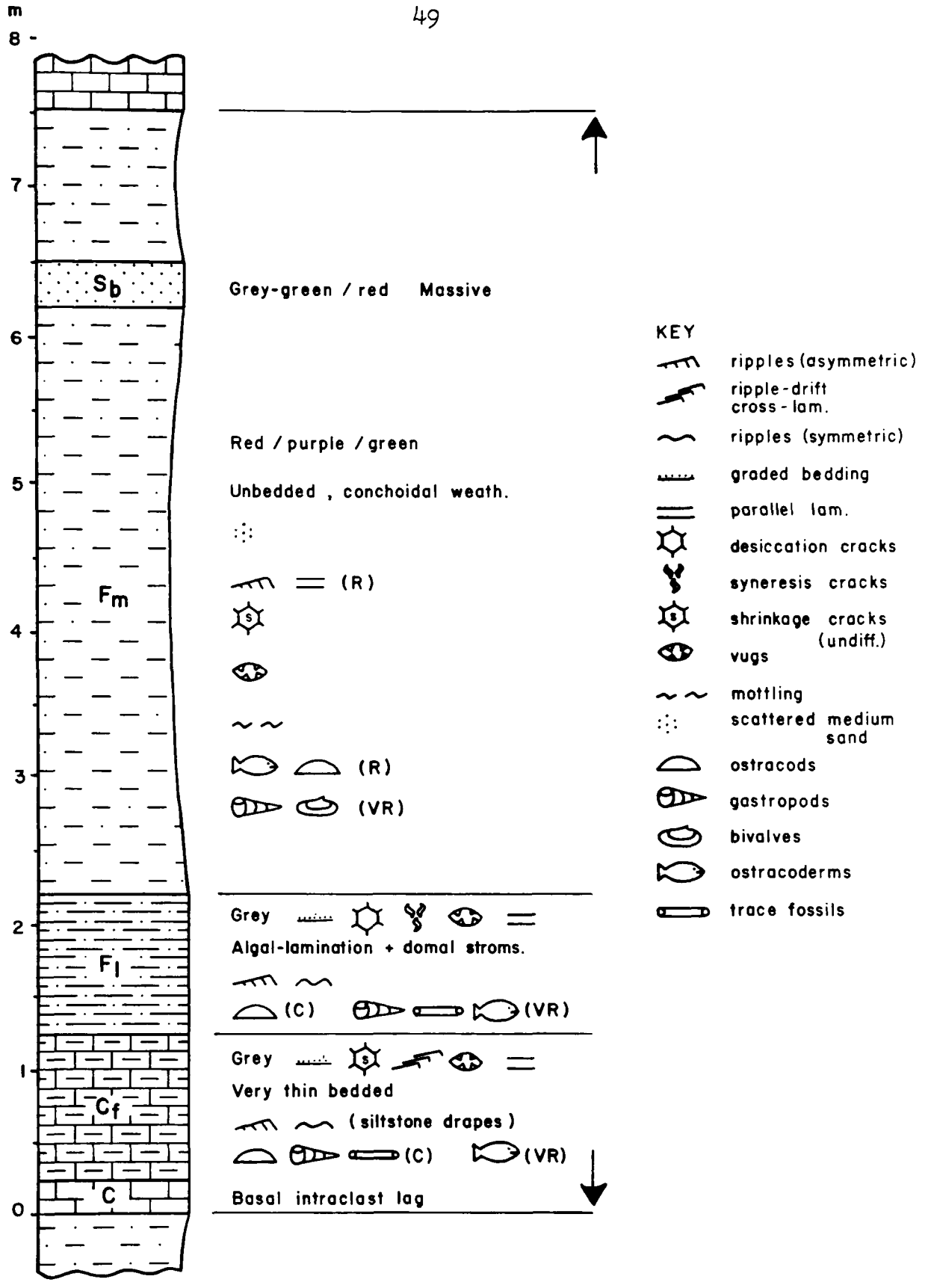

Fig. 12. Generalised carbonate-clastic cycle, Somerset Island Formation. Facies code as in Table 3; and facies proportions as in Fig. 8 (upper member, section G74J). Section profile shows relative resistance of units.

TABLE 6. Mean thickness of complete cycles in sections in the Somerset Island Formation.

SECTION	NO. OF COMPLETE CYCLES	MEAN THICKNESS (m)	STANDARD DEVIATION
G 73J	6	5.09	1.98
G 74G	6	2.23	1.39
G 74D	4	5.33	1.70
G 74J	11	7.44	4.59
ALL SECTIONS	27	5.45	3.70

sections is 5.45 m, though the variation between sections is considerable (Table 6).

Algal lamination as an environmental indicator

At Hamelin Pool, Shark Bay, Western Australia, Logan et al. (1974) distinguished seven types of algal mat, characteristic of both sheet and domal growth forms, on the basis of colour and surface texture. The mat types reflect biological factors, such as algal species present, and the mechanism of sediment binding. They show an environmentally related sequence across the shallow subtidal to supratidal flats. Characteristics and zonation of the four main types of mat (colloform, smooth, pustular and film) are listed in Table 7. In vertical section, they can be distinguished by the nature of the lamination and the type of cavities (fenestrae)present. Their distribution reflects a desiccation gradient related to the frequency of tidal flooding, and flats of uniform gradient exhibit good zonation, modified locally due to irregular relief. Three other mat types (gelatinous, tufted and blister) occur in areas of poor drainage or with a shallow tidal-groundwater table. Distribution of mats can be modified further by wave- and tidal-current scour, sediment influx, and browsing by organisms. For a fuller discussion of the biological and environmental factors concerned, see Logan et al. (1974) and Gebelein (1974).

The recognition of mat types provides a valuable tool in facies interpretation, provided that the mats have occupied the same environmental niches both in space and time. Algal mats on Andros Island, Bahamas, are virtually restricted to supratidal environments (Shinn et al., 1969), probably due to the suitability of the intertidal zone for destructive grazers, burrowers and root systems under humid climatic conditions. However, there is close similarity between the facies assemblages in the coastal plain sediments of the Somerset Island Formation and the Holocene sediments at Hamelin Pool (see below), and both contain evaporites, suggesting that climatic conditions were similar. Stromatolite distribution is closely related to grazing activity (Garrett, 1970); subtidal stromatolites are common in many Precambrian strata deposited before the advent of grazing organisms (Hoffman, 1974). However, grazing organisms were in existence by Cambrian times (Edhorn, 1977), so that a balance between algal growth and destruction by grazing was probably established by the Silurian.

Stromatolitic lamination produced by the four main types of mat is present in the Somerset Island Formation (Photos 19. 21. 22 and 23). The stromatolitic structures show a clear relationship to the cyclicity (Fig. 13). The lower parts of some cycles contain colloform mat structures, suggestive of subtidal conditions (Table 7), and the presence of oncolites (Photo 20) suggests shallow subtidal to lower inter-

TABLE 7. Characteristics and environmental zonation of the main algal mat types at Hamelin Pool, W. Australia. Data from Logan et al. (1974). Classification and origin of fenestration discussed by Logan (1974).

MAT TYPE	ZONE	DOMINANT TYPES OF ALGAE	SURFACE APPEARANCE	FABRIC
FILM	Supratidal/ Upper Intertidal	Coccoid	Thin films on indurated substrates	Thin pelletoid rind with faint lamination
PUSTULAR	Middle-Upper Intertidal	Coccoid	Rough pustular surface	Lamination weak or absent; medium fenestrae
SMOOTH	Lower Intertidal	Filamentous	Smooth surface	Finely laminated; fenestrae fine or or absent
COLLOFORM	Subtidal	Filamentous/ Coccoid	Colloform surface (hollow, linked convexities)	Laminae separated by coarse fenestrae 1-3 cm long

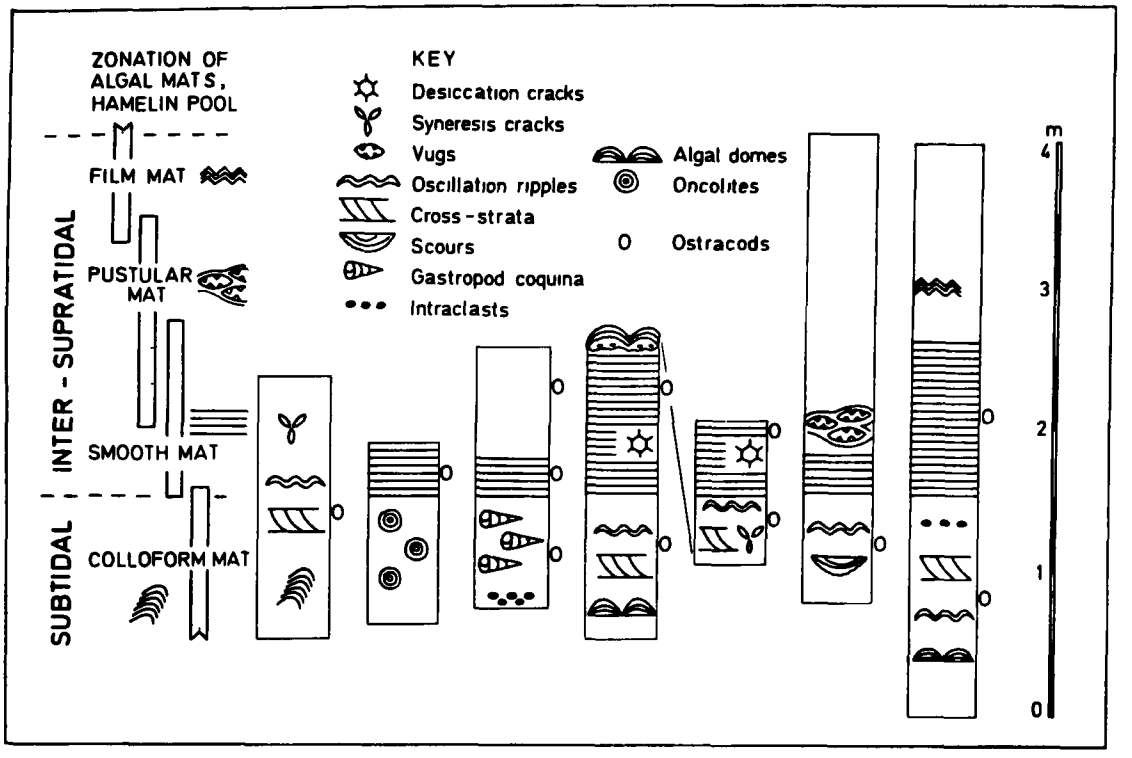

Fig. 13. Distribution of algal mat types in seven cycles from the upper member of the Somerset Island Formation. Zonation of mat types at Hamelin Pool from Logan et al. (1974). Cycles include facies C, C_f and F_l; F_m above is not shown. Cycles are correlated at the incoming of smooth mats (probable base of intertidal zone).

tidal conditions (Logan et al., 1964, p. 81). Stromatolitic lamination representing smooth mats is very common, forming thick units with desiccation cracks (facies F_1), and suggests lower intertidal environments for facies F_1 in the cycles. Pustular mat structures indicate middle to upper intertidal conditions. Film mat structures (upper intertidal to supratidal) are inconspicuous in vertical sections, but occur as crusts on brecciated surfaces observed in scree from the uppermost resistant units in the cycles. Gelatinous and blister mat structures were also identified (Photos 24 and 25), but in sections with poor exposure or no obvious cyclicity.

In summary, algal structures suggest that the lower better-cemented parts of the cycles were deposited in subtidal/intertidal to supratidal environments. The overlying recessive siltstones lack algal features and carbonate cement, and are interpreted as the deposits of terrestrial flats beyond the landward limit of tidal flooding.

Cycles of the Devonian Pillara Formation of Western Australia have also been interpreted by means of algal structures (Read, 1973). Subtidal bioclastic limestones pass up into limestones with fine laminoid fenestral fabrics (representing smooth mats, lower intertidal), irregular fenestral fabrics (representing pustular mats, middle to upper intertidal), and tubular fenestral fabrics (associated with halophytic plants in upper intertidal-supratidal environments at Shark Bay).

Interpretation of the Upper Silurian coastal flat sequences

Analogous Recent environments and cyclic sequences

Interpretation of the Somerset Island Formation is aided by comparison with a modern analogue in which the distribution of facies has been studied in three dimensions. Recent carbonates of Shark Bay, Western Australia, have been described in detail in Memoirs 13 and 22 of the American Association of Petroleum Geologists. The general setting of the area was outlined by Logan and Cebulski (1970). Within Shark Bay (Fig. 14) lies the area of the Hutchison Embayment at Hamelin Pool (Hagan and Logan, 1974). The embayment is 5 km from north to south, with beach ridges along the western margin, and a subtidal pool 0.5 m deep, connected to the Hamelin Basin by a narrow tidal channel and bordered by extensive inter-supratidal flats up to 2.5 km wide. Hypersaline tidal waters (salinity about 65‰) enter the embayment, and increase in salinity to 84-90‰ in the tidal pond; concentrations up to 289‰ have been recorded in near-surface groundwaters on the flats. Although partially protected, the area is exposed to wave action from northerly wind systems, resulting in beach ridges at the landward margin of the flats. The climate is semi-arid. Definitions for the intertidal and supratidal boundaries in this area are given by Hagan and Logan (1974, p. 285-7).

Hagan and Logan (1974) described the sedimentary facies

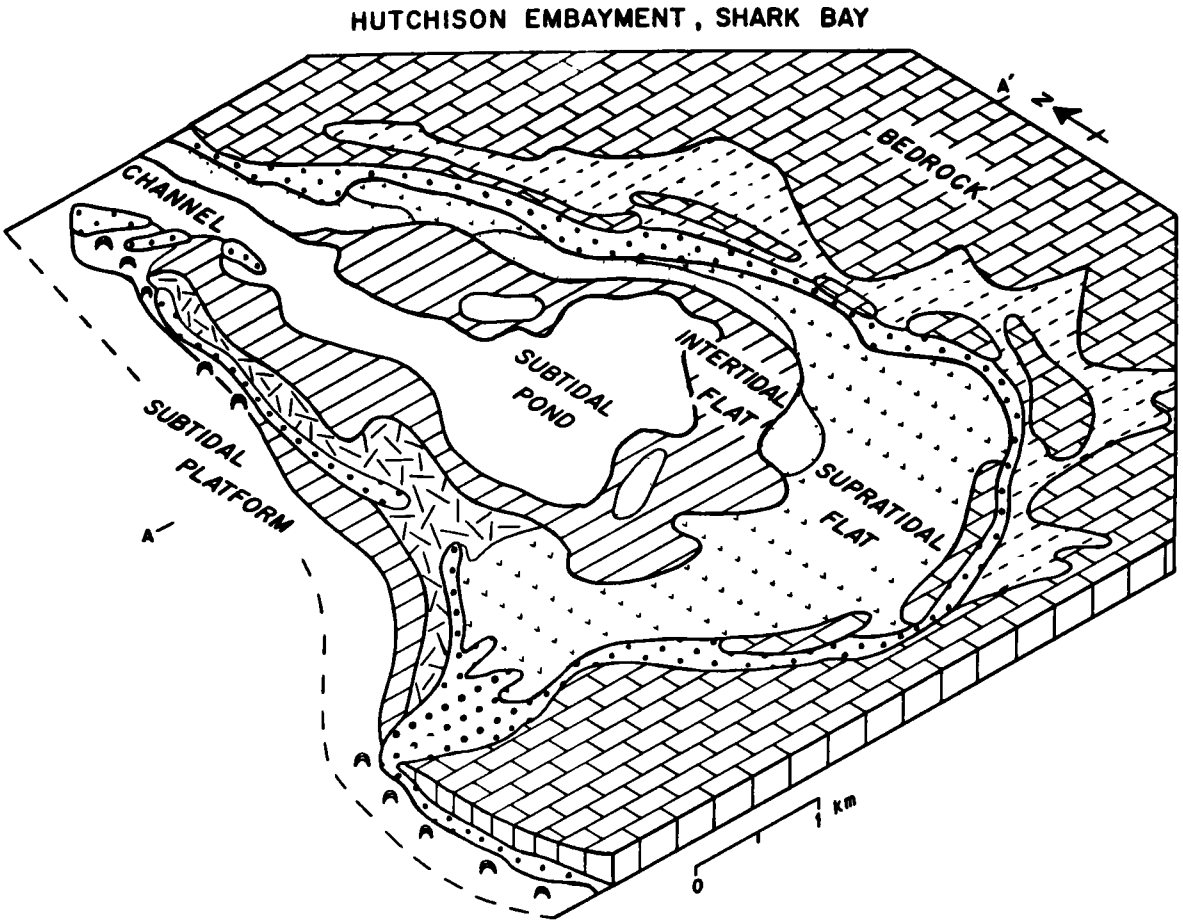

LITHOLOGY	MAT TYPES	ENVIRONMENT
Limestone		Pleistocene bedrock
Coquina and skeletal grainstone		Beach ridge + dunes / Alluvium } Subaerial
Red-brown silt and clay		
Evaporitic packstone	Blister + film	Supratidal
Aragonite crusts and coquina		
Intraclast grainstone		
Algal-laminated packstone	Smooth + pustular	Intertidal
Columnar and ellipsoidal stromatolites		
Skeletal grainstone and digitate stroms.	Colloform	Subtidal

Fig. 14. Facies map of Hutchison Embayment, W. Australia. Thick lines represent major environmental subdivisions. Line A - A' indicates line of section for Fig. 15. From Figs. 3, 4 and 10 of Hagan and Logan (1974).

using the classification of Dunham (1962). Sediments of the tidal pool comprise skeletal grainstones transported from the subtidal area outside the embayment. Digitate stromatolites of colloform type occupy large areas. In the intertidal zone, pellet packstones are bound by smooth and pustular algal mats. In the supratidal zone, the packstones contain diagenetic gypsum crystals, and thin surface sheets of halite; local aragonitic crusts are brecciated to form intraclast pavements by desiccation and evaporite growth pressure, and are associated with film mats. Although dolomite was not noted, it occurs locally as lithified pavements and intraclasts elsewhere in the Shark Bay area (Logan, 1974, p. 225-6). Damper areas support gelatinous, tufted and blister mats, the last being extensively developed in the supratidal region. Behind the coquinas of the beach ridges and dunes lies a zone of red-brown silty alluvium.

The sediments of the Somerset Island Formation differ petrographically from those in the Hutchison Embayment. The former are mudstones or wackestones, in Dunham's classification, composed largely of micrite with dolomitic and terrigenous grains, and subordinate amounts of skeletal and pelletal material. However, the distribution of the facies enables a close comparison to be made between the two deposits (Table 8). Wilson (1975, p. 302) noted that micritic textures are characteristic of many shallow marine-tidal flat sequences in the geological column.

TABLE 8. Comparison of facies at Hutchison Embayment, W. Australia with those of the Somerset Island Formation.

HUTCHISON EMBAYMENT (QUATERNARY)	ENVIRONMENT	SOMERSET ISLAND FORMATION (U.SIL.)
Terrigenous silt and clay	Alluvial Flats	Massive siltstone (F_m), with mottled siltstone (F_{md}), sandstone (S_{gr} and S_m) and evaporites.
Coquina and skeletal grainstone	Beach Ridges and Dunes	Coquina
Pellet packstone with intraclast breccia, aragonitic crusts and evaporites. Blister and Film mats.	Supratidal	Silty limestone (C_f) and laminated siltstone (F_l), with dololutite crusts and intraclasts, and evaporites.
Pellet packstone with algal lamination. Smooth and Pustular mats.	Intertidal	Smooth, pustular and film mat structures.
Skeletal grainstone and digitate stromatolites. Colloform mats.	Subtidal	Limestone (C) and silty limestone (C_f). Colloform mat structures.

Coring in Holocene sediments at Hutchison Embayment has shown that the surface facies can be recognised in vertical section (Fig. 15). Up to 5 m of sediment rest on older limestones ("bedrock"), and the history of the area was interpreted by Hagan and Logan (1974) as follows:

1) About 5000 B.C., a Holocene rise in sea level (eventually to 2 m above the present level) caused transgression, with the establishment of marine sedimentation in Hutchison Embayment. A basal sheet of skeletal packstone and wackestone up to 2.5 m thick was deposited across the area. No onlapping facies relations were observed in the cores, transgression being represented only by a layer of lithoclasts and rolled fossils.

2) After 2500 B.C., sea level fell 2 m to the present level. Outbuilding of the flats produced a regressive sequence, with seaward progradation of facies.

Core sections across Hutchison Embayment are shown in Figure 15. On the eastern margin of the embayment, facies belts were established across the "bedrock" surface and prograded westwards into the tidal pond. Subtidal sediments covered the western area until, with construction of the barrier beach-ridge, the embayment was isolated from the subtidal area of Hamelin Pool, enabling flats to build out eastwards into the tidal pond. The pond was thus progressively filled by progradation from all margins. A three dimensional model of events at the eastern margin of the embayment is shown in

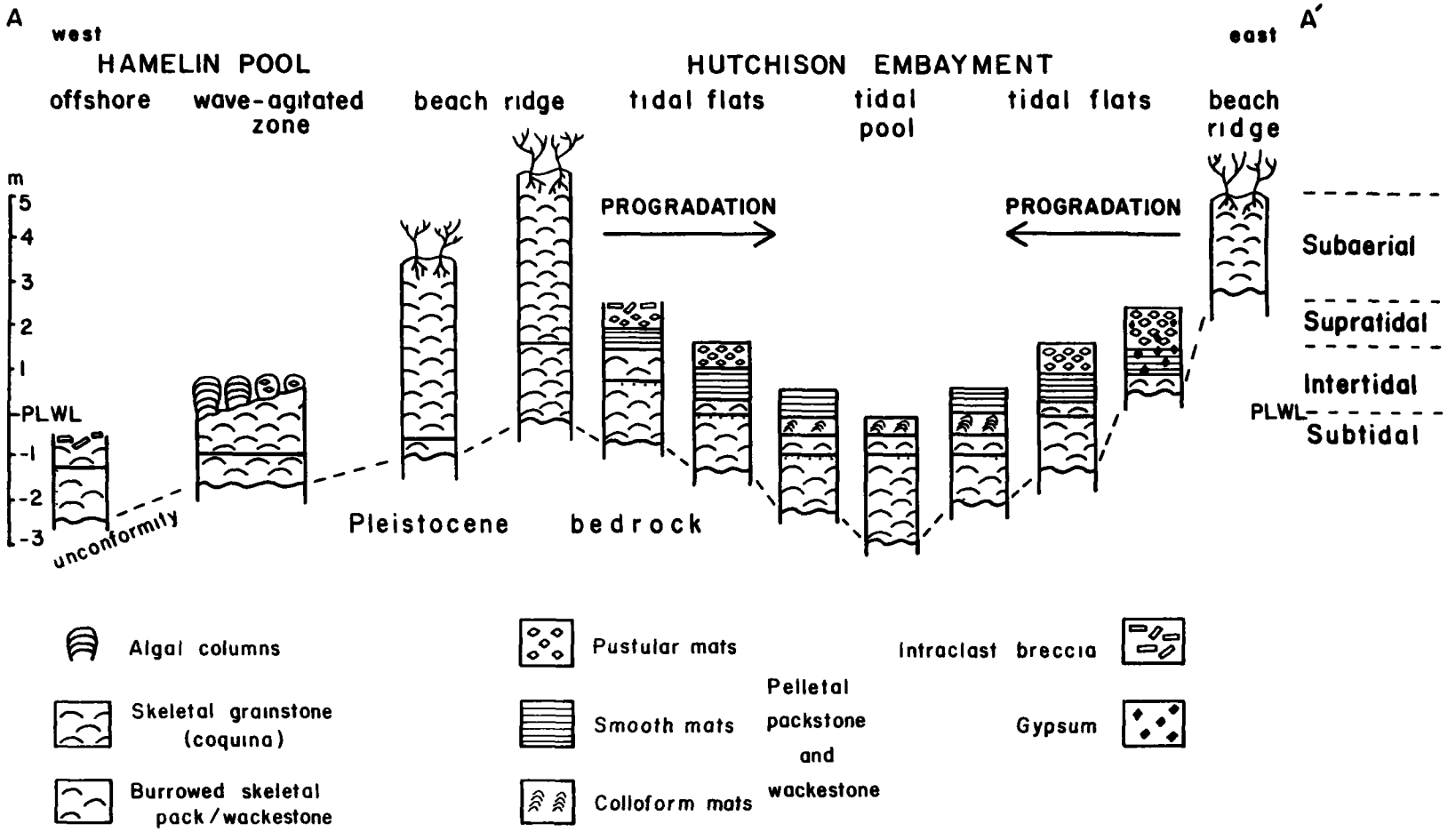

Fig. 15. Generalised cross-section of Holocene sediments at Hutchison Embayment. Line of section shown by A - A' in Fig. 14. From Figs. 16 to 18 of Hagan and Logan (1974).

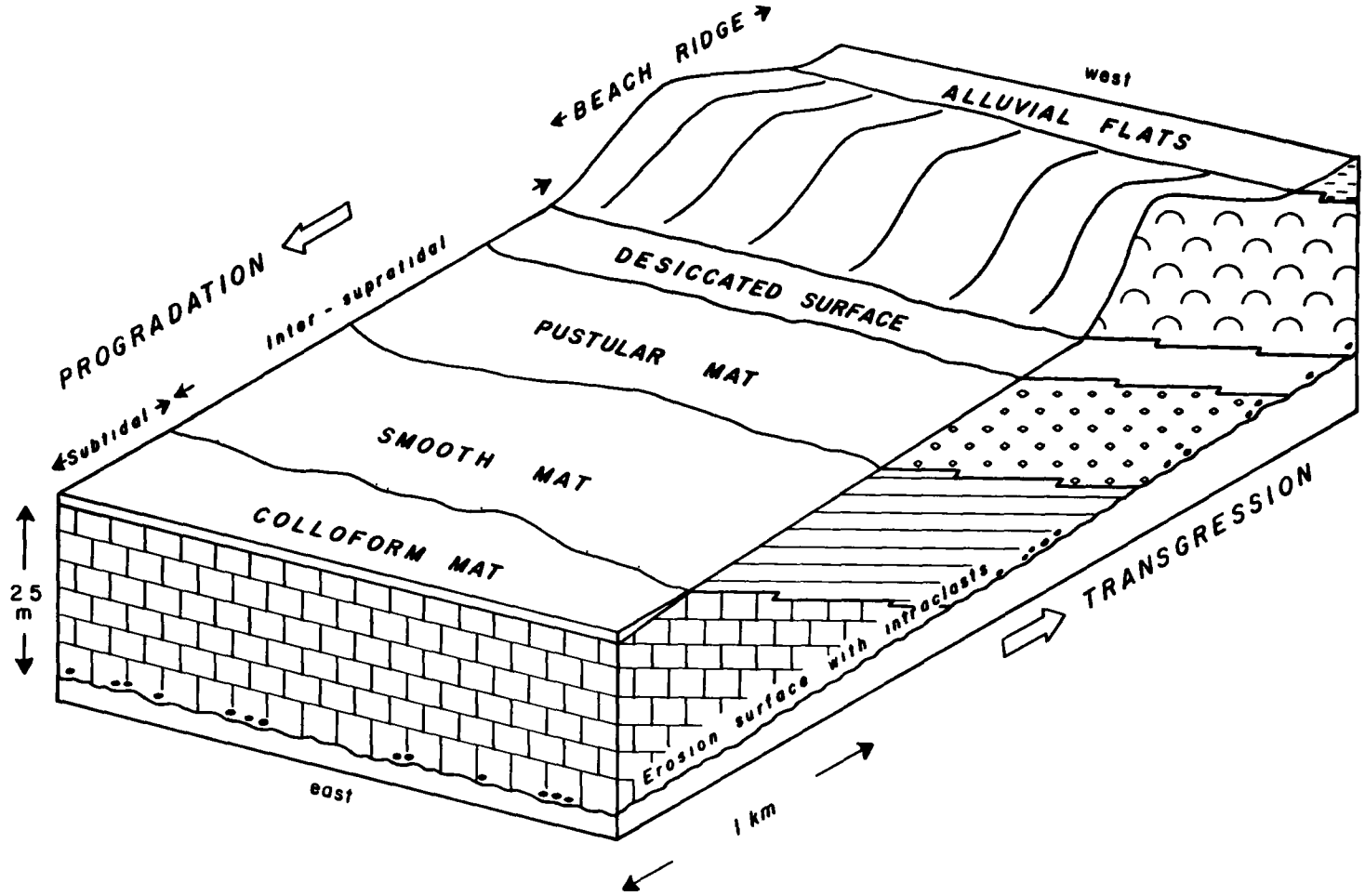

Fig. 16. Vertical succession of facies resulting from Holocene sea-level changes in the Hutchison Embayment. Constructed from Figs. 16 to 18 of Hagan and Logan (1974).

Figure 16. At Shark Bay, the transgressive-regressive sequence of events resulted from fluctuations in relative sea level related to glaciation. Both eustatic and isostatic activity may have been involved.

Similar vertical sequences underlie many modern tidal flats. A Quaternary progradational tidal flat sequence proved by coring at Abu Dhabi also resulted from marine transgression followed by progradation under conditions of stable or falling sea level (Evans et al., 1969). A regressive sequence probably also underlies tidal flats on Andros Island, Bahamas (Shinn et al., 1969, p. 1225).

Origin of coastal flat cyclicity in the Somerset Island Formation

Cycles similar to those in the Somerset Island Formation and interpreted as representing subtidal to supratidal transitions have commonly been described from the geological record(Wilson, 1967; Wood and Wolfe, 1969; Schenk, 1969; Chuber and Pusey, 1972; Lucia, 1972; Bosellini and Hardie, 1973; Read, 1973). Thick units of supratidal evaporite cap the cycles in several formations, but were not observed in the cycles on Somerset Island. The cycles in the Somerset Island Formation (Fig. 12) closely resemble the sequences described from cores in the Hutchison Embayment, and are interpreted as resulting from tidal flat progradation. The cycles are planar or erosively based, but show little indication of transgression other

than a thin lag of intraclasts and quartz grains, or thin layers of gastropod coquina (?beach deposits). The main phase of sedimentation was regressive, with subtidal carbonates passing up into laminated detrital sediment of the inter-supratidal flats, and into thick-bedded terrestrial siltstones above. Binding of sediment by algae may have been a major factor in the outbuilding of the Upper Silurian flats. Wave- and tidal-current structures are common in the silty limestone facies, and sediment was probably transported by longshore drift, as proposed for Upper Devonian clastic regressive cycles by Walker (1971). Eventually, terrestrial sediments of fluvial derivation spread across the area.

Migration of tidal channels and inlets is also known to produce vertical sequences of facies in shallow marine sediments. As the channel migrates laterally, a progressively shallowing sequence accumulates above the lagged erosion surface at the channel base. The production of a widespread cyclic sequence may be geologically instantaneous: Van Straaten (cited in Klein and Sanders, 1964) observed 10 m of lateral migration in 118 days for channels on the Wadden Sea flats, and Kumar and Sanders (1974) calculated 64 m/year migration for the Fire Island tidal inlet on Long Island, N.Y. over 115 years. Smith (1968) interpreted a Silurian cyclic sequence as the product of tidal channel migration. However, it is unlikely that the cycles in the Somerset Island Formation originated from channel migration. Only facies C

and C_f could have been deposited within the channels, which would have been less than 1 m deep. Since the overlying facies (F_l and F_m) are typical of deposition on inter-supratidal and terrestrial surfaces, the major part of the cycles would have resulted from progradation. Also, no channel structures were observed.

The cause of progradational cyclicity during deposition of the Somerset Island Formation is uncertain. By analogy with Shark Bay, an isostatic or eustatic mechanism is probable, and in view of the association of sedimentation with the rise of the Boothia Uplift, a series of tectonic events is the probable cause. Cycles resulting from such events of regional significance should be traceable over wide areas: one unit (G74J-9) near Fury Point has been traced unchanged for 20 km away from the Boothia Uplift, but outcrop is generally discontinuous. Tidal flat cyclicity is known to result from regional events — cycles in the Upper Devonian Duperow Formation can be traced for several hundred miles across the Williston Basin (Wilson, 1967), perhaps reflecting sea level fluctuations, abrupt periodic subsidence, or climatic rhythms influencing reef growth and basin restriction. Berry and Boucot (1973) interpreted a worldwide regressive-transgressive event of Late Ordovician to Early Silurian age as glacio-eustatic, but it is not known if it produced small-scale cycles, and it is unlikely that major ice sheets existed during the Upper Silurian to Lower Devonian (Blatt et al., 1972, p. 590).

Cyclicity on tidal flats may also result from a balance between subsidence and sedimentation. Thompson (1968) noted that the rate of sediment supply by longshore drift to tidal flats at the mouth of the Colorado River was drastically reduced following the building of the Hoover Dam in 1935, resulting in the erosion of the flats, and the accumulation of a lag of shell gravel mantling the surface. Presumably, continued subsidence would cause transgression, while a later increase in the sedimentation rate would lead to progradation of the flats. This mechanism could operate in conjunction with eustatic and isostatic activity. However, no evidence of deltaic deposits or tributary river systems has been found in the tidal flat sequences of the Somerset Island Formation.

The incoming of facies F_1, containing smooth mat structures, in the cycles defines the base of the intertidal zone and provides a sea level datum. The thickness of the inter-supratidal parts of the cycles should provide an estimate of tidal range, assuming that the rate of subsidence was low compared to that of progradation. Facies F_1, however, is not always present, but the thickness of the lower cemented parts of the cycles enables an approximate estimate of tidal range. Since the cemented parts may represent subtidal to topmost supratidal environments, the estimate will be a maximum. In the section at Locality 13 where the hard bands are clearly visible (Photo 18), their mean thickness in

twelve cycles is 2.15 m (± 1.02 m). At Carnarvon in the northern part of Shark Bay, tidal range at maximum spring tide is 1.7 m (Logan and Cebulski, 1970), a comparable value.

Summary

The Somerset Island Formation contains cyclic sequences which have been analysed statistically by Markov chain analysis. The cycles are abruptly based, and show an upward gradation from grey, thin-bedded carbonates with an ostracod-gastropod fauna, through grey, laminated, dolomitic siltstones with ostracods, to poorly cemented, red, dolomitic and terrigenous siltstones, massive in texture and containing rare ostracods and ostracoderms. Cycles average 5.5 m in thickness.

Distinctive types of stromatolitic lamination occur in the cycles and are closely comparable to Recent algal lamination at Shark Bay, Western Australia. The lower carbonate-rich parts of the Upper Silurian cycles contain algal mat structures restricted to shallow subtidal to supratidal environments at Shark Bay, while the upper more terrigenous parts of the cycles lack algal features and were probably deposited beyond the landward limit of tidal flooding.

The cycles in the Somerset Island Formation represent progradation of tidal flats, resulting in a repeated vertical succession of facies from subtidal to distal fluvial environ-

ments. Tectonism associated with the rise of the Boothia Uplift probably caused changes in relative sea level and hence lateral migration of the facies.

3. Limestone (facies C) containing stromatoporoids (s) and corals (c). Pen 15 cm long. Unit G74G-33, Loc. 2.

4. Silty limestone (facies C_f). Unit contains symmetric and asymmetric ripples, siltstone drapes, and brecciation (probably related to evaporites). Pen 15 cm long. Unit G74J-7, Loc. 13.

3

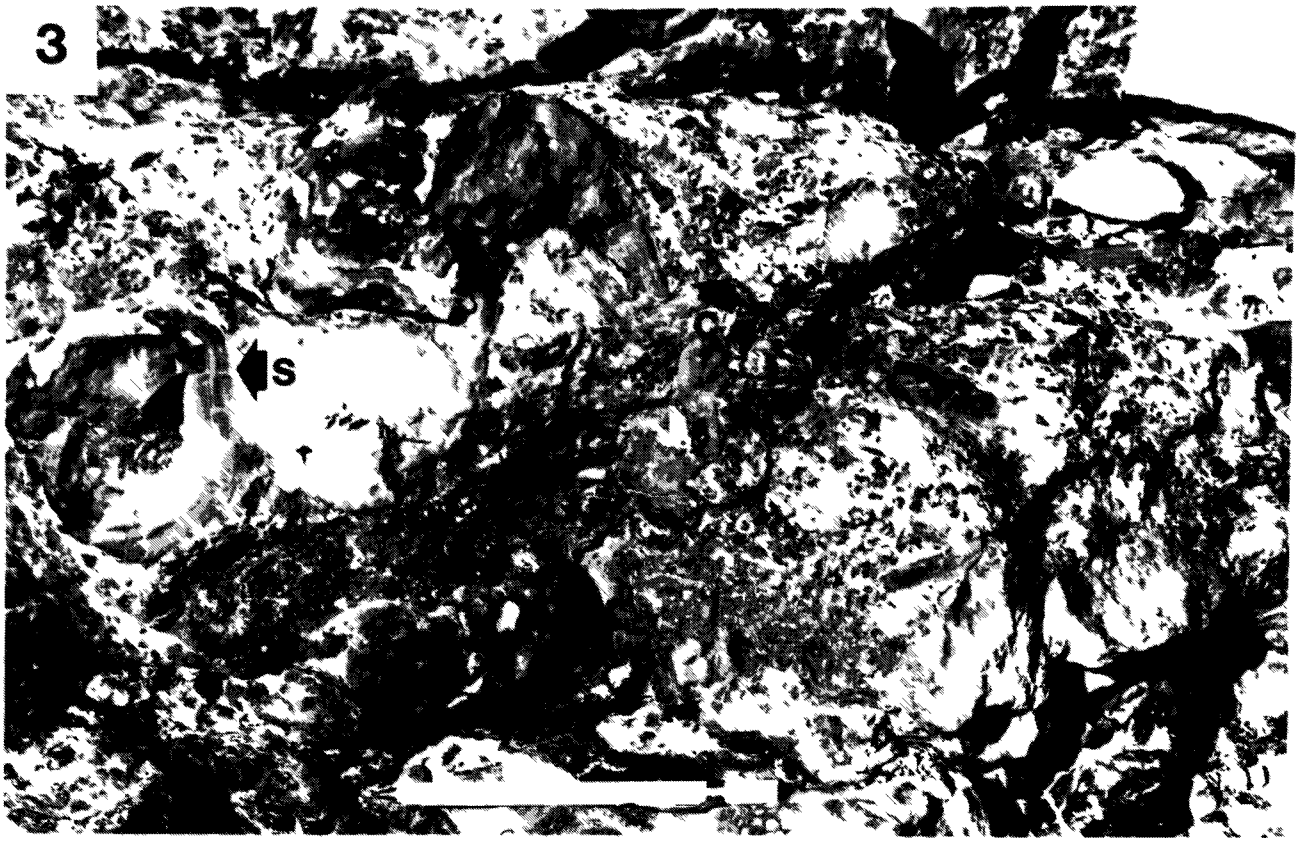

4

5. Photomicrograph of laminated fine sandstone (facies F_1), showing alternate coarser and finer laminae, graded laminae, scours at bases of coarser laminae, and desiccation fissures. Plane polarised light. Unit G74J-9f, Loc. 13 (see Photos 45 and 46).

6. Laminated fine sandstone (facies F_1) containing vugs. Vugs are lined by calcite crystals (probably gypsum nodules originally), and are pre-compactional since the laminae are deformed around them. Hammer 30 cm long. Unit G73F-3, Loc. 16.

5

6

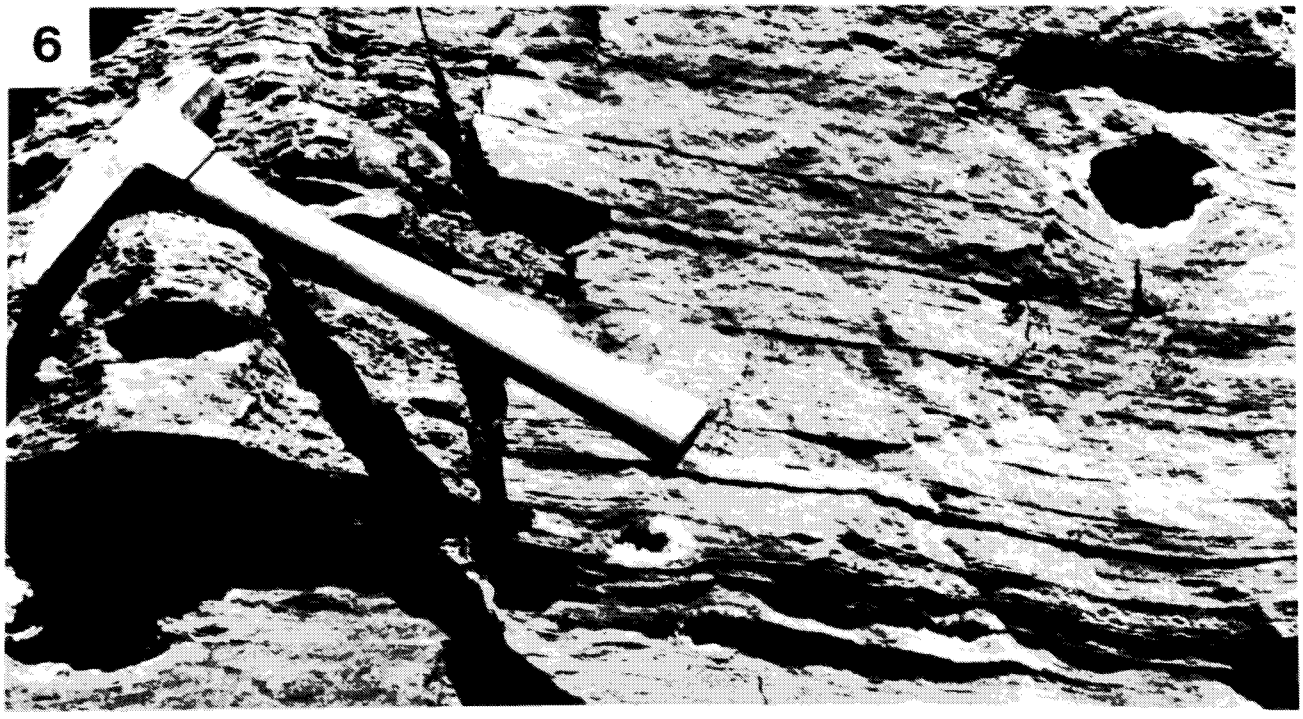

7. Domal stromatolites of smooth mat type, underlain by thin intraclast bed and algal-laminated siltstone (facies F_1). Unit G74J-9, Loc. 13.

8. Cut section of domal stromatolite shown in Photo. 7. Note thickening of laminae over underlying irregularities. Stromatolite calcareous, vuggy dololutite beneath.

9. Photomicrograph of stromatolite of colloform type. Coarser laminae contain fine dolarenite and quartz sand with ostracod valves; finer laminae composed of dololutite. Unit G73M-2, Loc. 10.

7

8

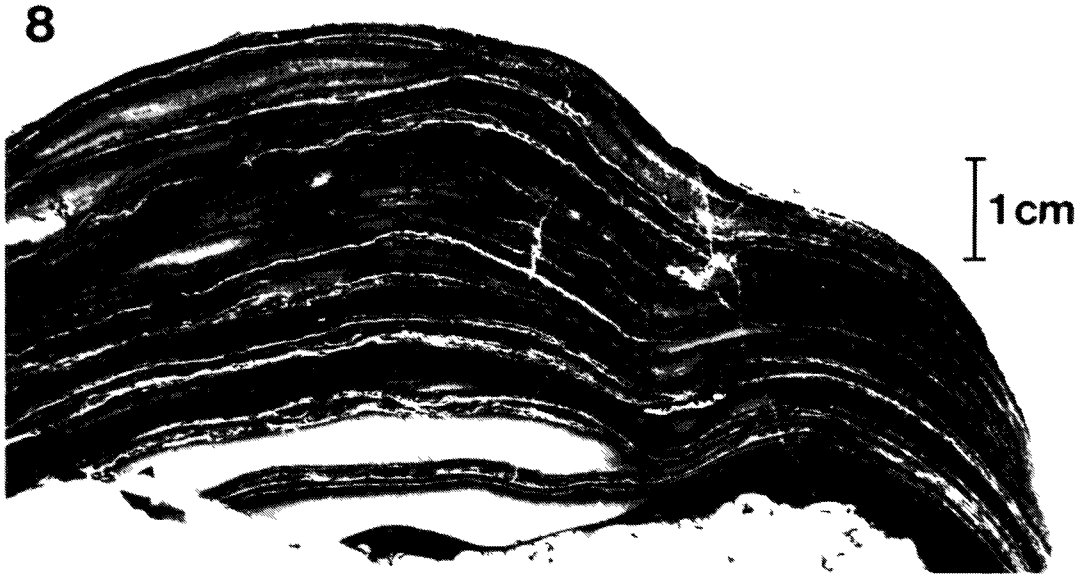

9

10. Mottled siltstone (facies F_{md}), showing distinctive red/green mottling (dark/pale areas) and ostracoderm fagments (o). Unit G74G-54a, Loc. 2.

11. Lensoid bed of white dololutite, showing weak lamination, fissures infilled with quartz grains (f), and derived intraclasts (i). Unit G73J-22, Loc. 9.

12. Dololutite showing evidence of penecontemporaneous origin. Laminated micritic limestone (m) shows incipient and complete brecciation. Dololutite (d) forms paler material between fragments and along bedding surfaces, and rims the fragments. Unit G73K-4b, Loc. 11.


10
O
1cm

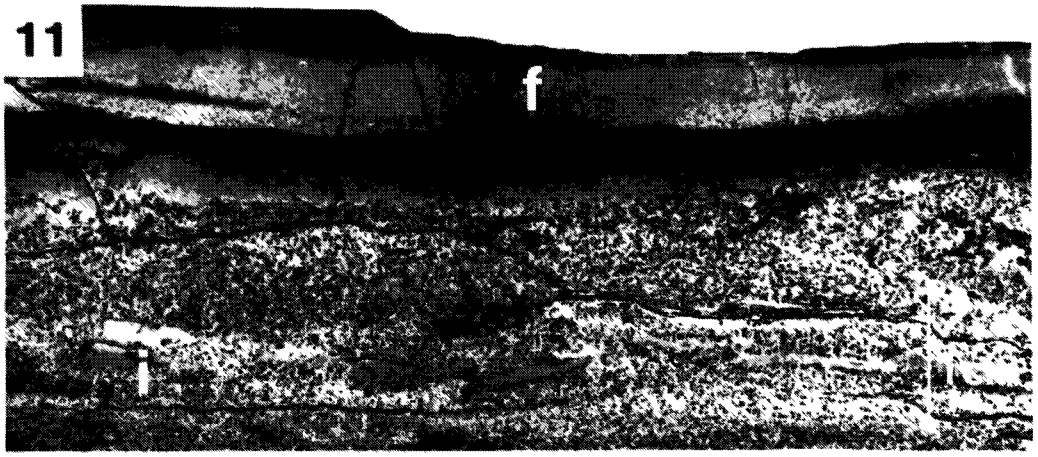
11
f


12
m
1cm

13. Desiccation cracks containing gypsum nodules. Pen 16.5 cm long. Loc. 13.

14. Tabular cavities formed by solution of ?gypsum crystals, enclosed in dololutite. Unit G73K-28, Loc. 12.

15. Halite casts. Casts are preserved on the lower surface of a bed of fine sandstone. Unit G74J-32, Loc. 13.

13

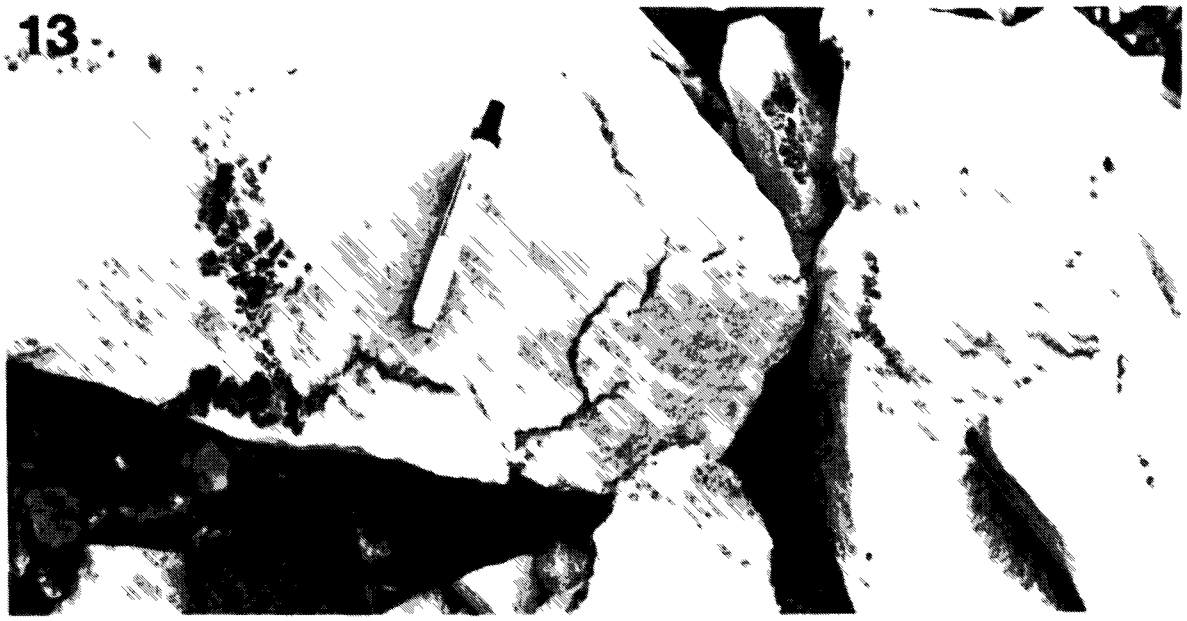

14

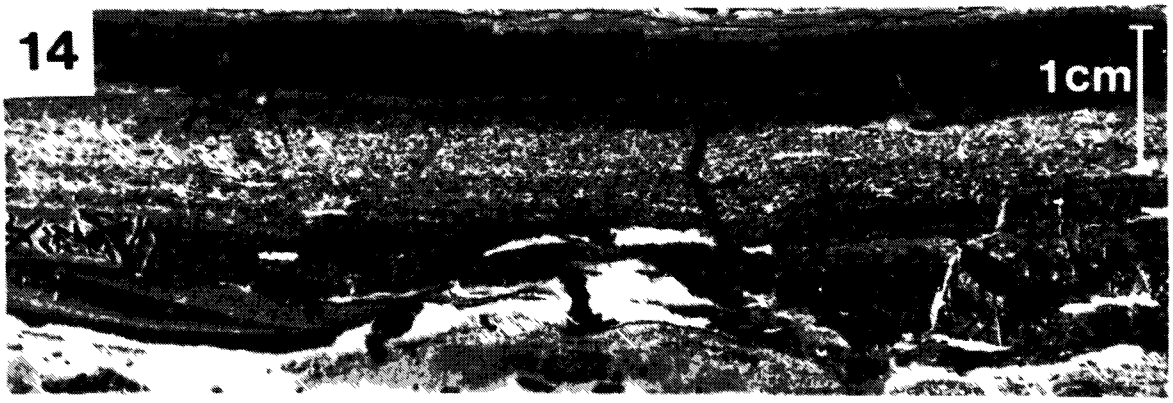

15

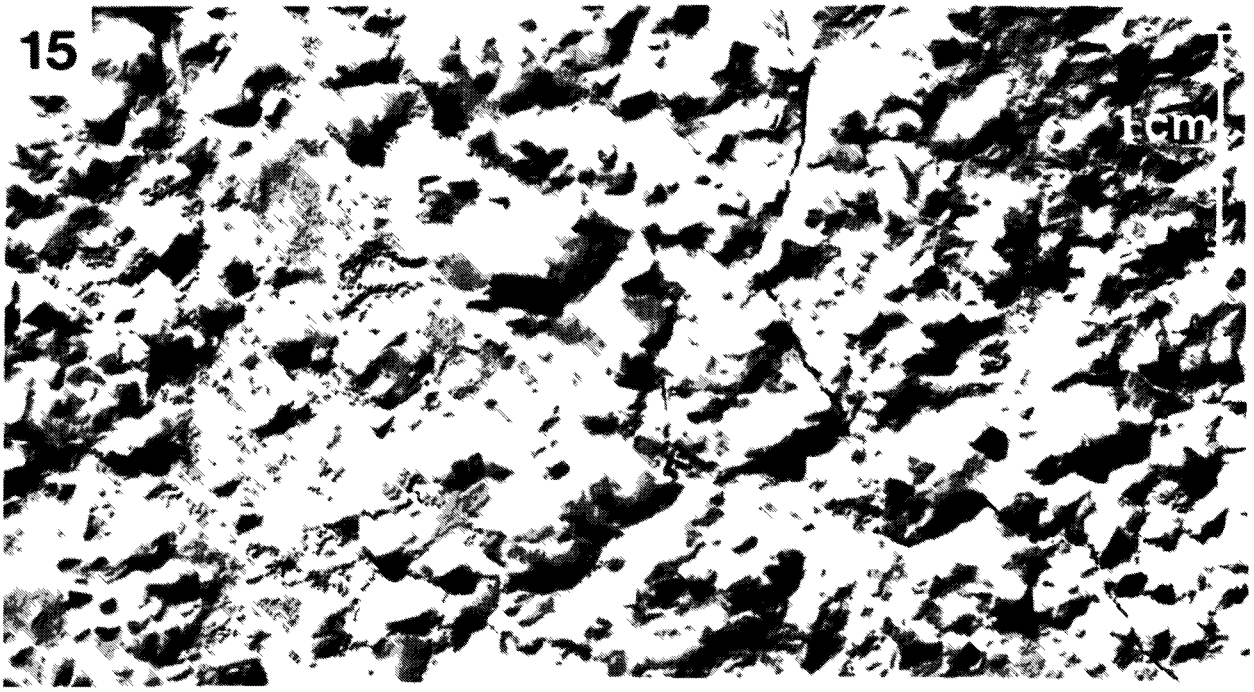

16. Interbedded selenite and dolosiltite, occurring as a lens in facies F_m. Pen 15 cm long. Unit G74J-19, Loc. 13.

17. Gastropod coquina, with some intraclasts and a micrite matrix. White patches are sparite, and abundant small cavities in lower part are probably due to solution of evaporites. Unit G74J-5, Loc. 13.

16

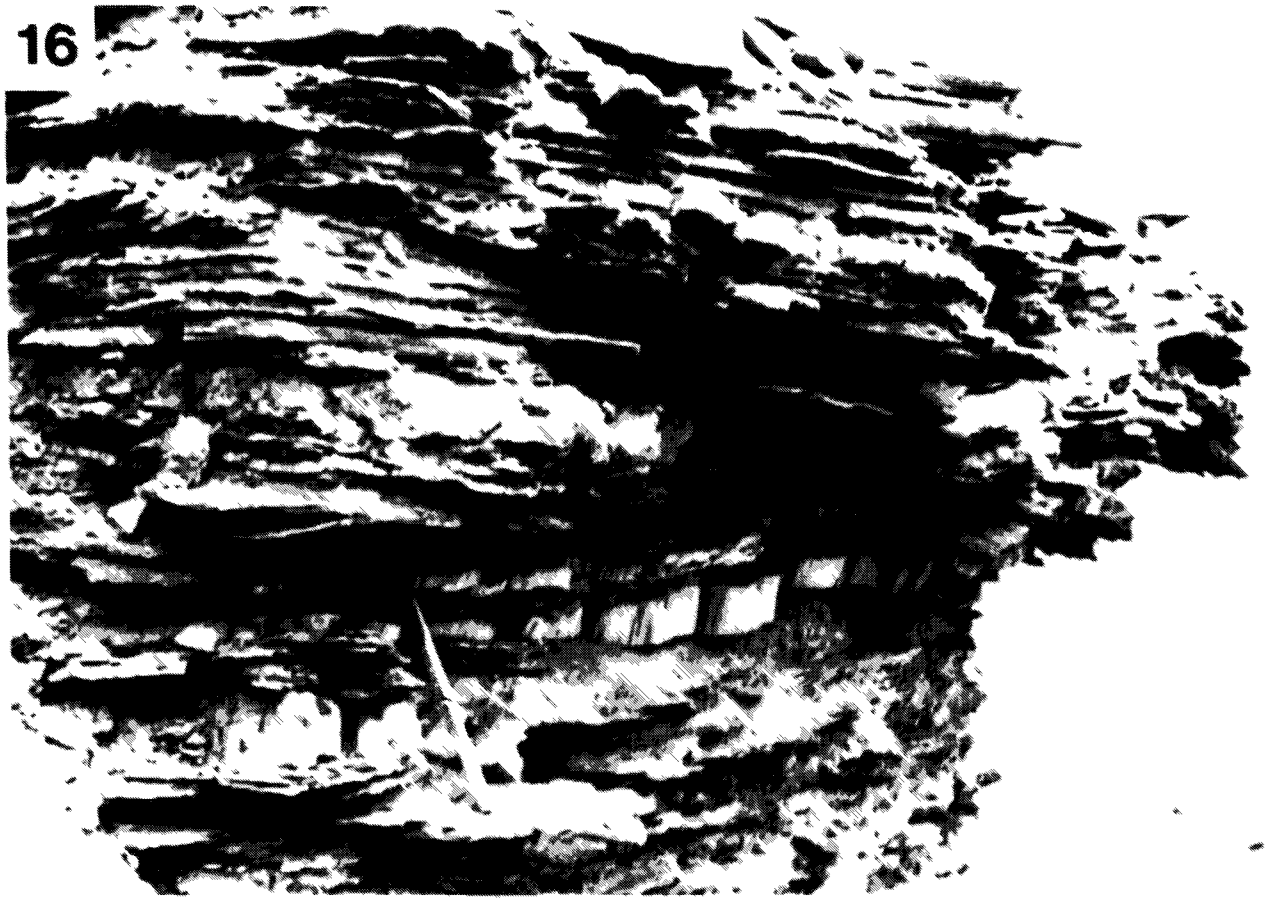

17

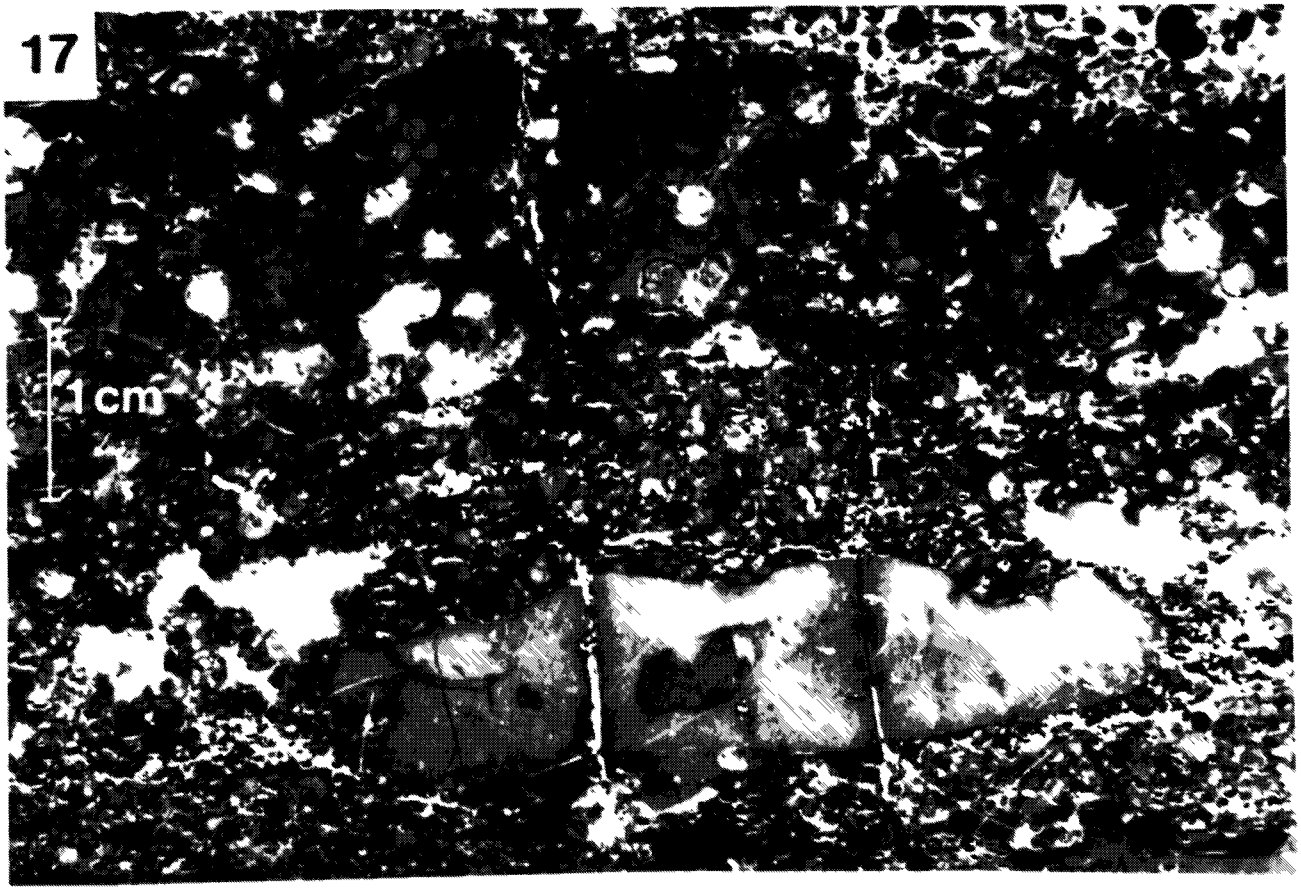

18. Carbonate-clastic cycles in the upper member of the Somerset Island Formation. Resistant scarps formed by carbonates in the lower part of the cycles, with recessive siltstones above. Section G74J, Loc. 13.

18

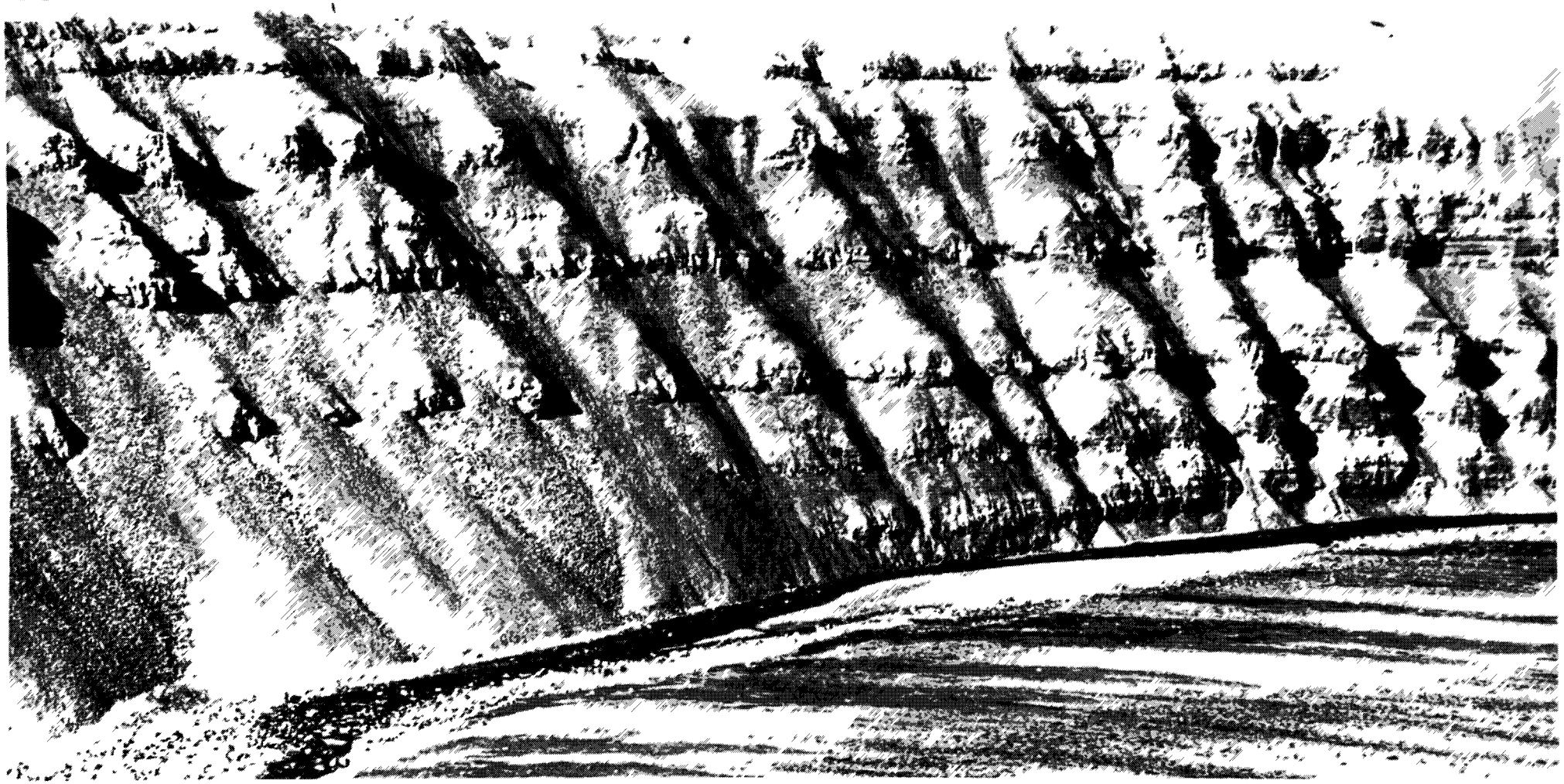

19. Colloform mat structures, showing coarse laminoid fenestration (f), and associated with convex-up ostracods (o) and evaporite pseudomorphs (e). Unit G73M-2, Loc. 10.

20. Oncolites in silty limestone. Matchbox 4 cm wide. Near Loc. 7, Cape Anne syncline.

19

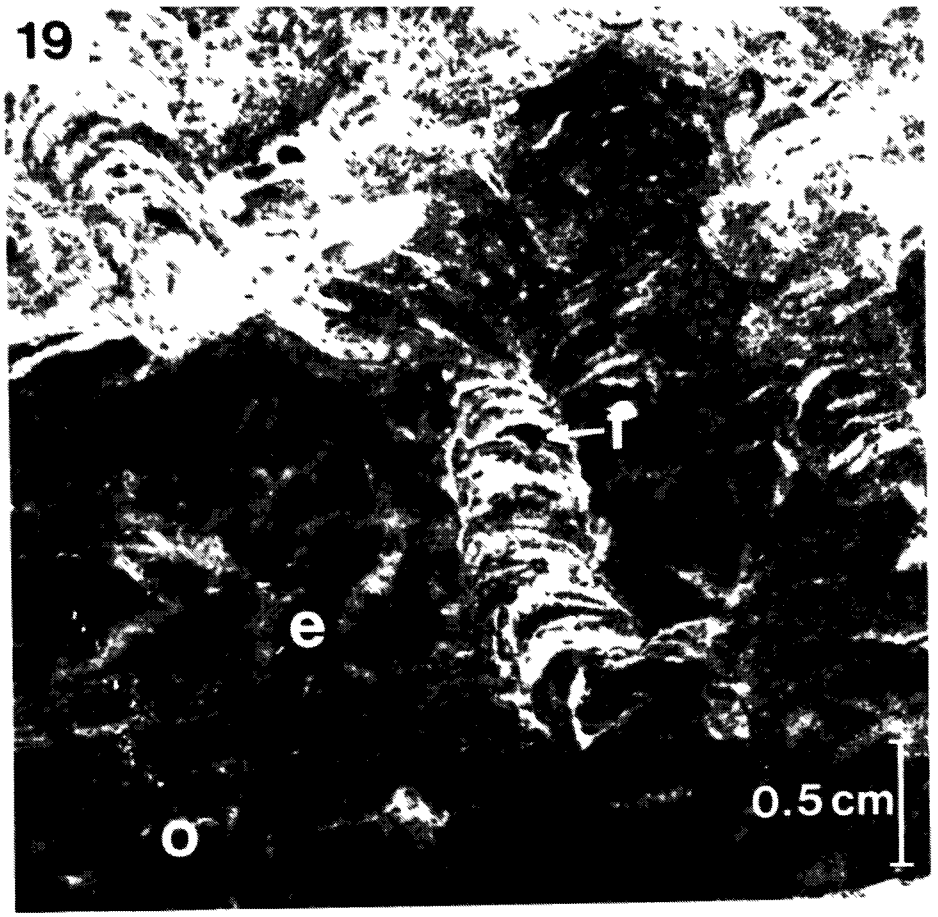

20

21. Smooth mat structures, laminated and unfenestrated, with small-scale doming, contortion and brecciation of laminae. Unit G74J-3b, Loc. 13.

22. Pustular mat structures, showing irregular fenestration (f) and weak lamination. Unit G74K-4, Loc. 11.

23. Film mat structures, forming thin crust over irregular surface of quartz sandstone. Note thickening over irregularities. Unit G74J-7, Loc. 13.

21

22

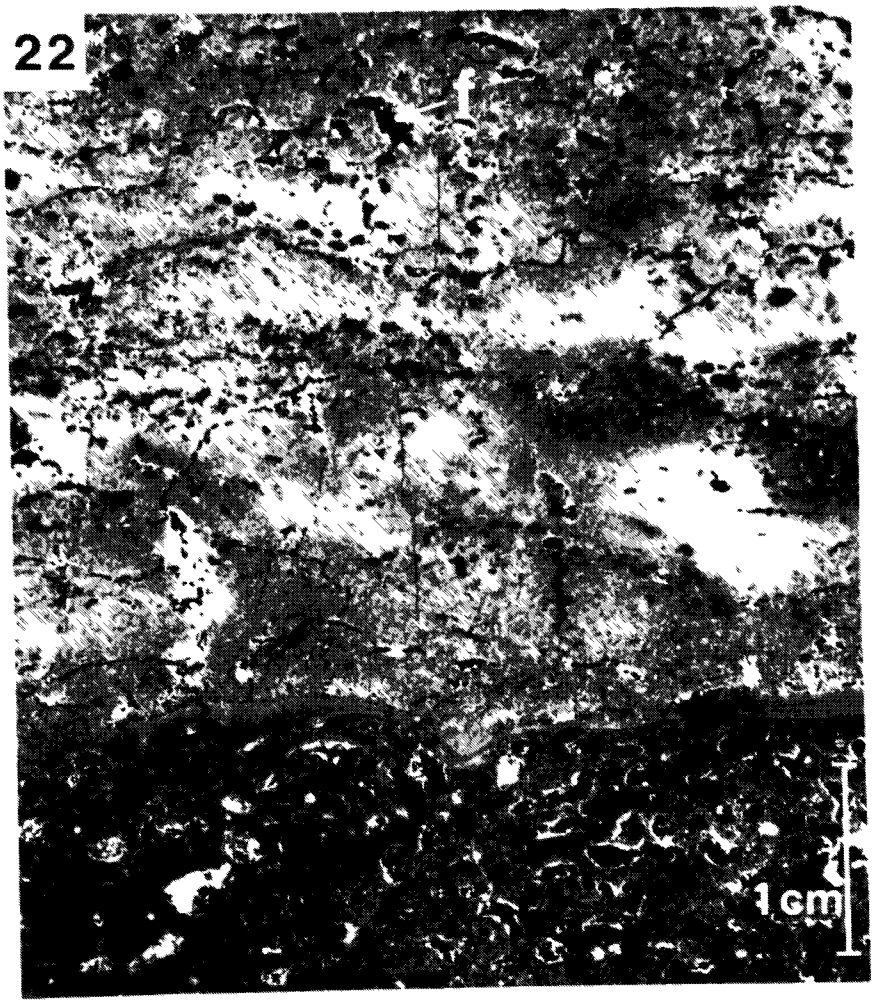

23

24. Gelatinous mat structures. Thin algal laminae, brown in colour, bind intraclasts and medium-grained quartz. Unit G73G-15, Loc. 14.

25. Blister mat structure, showing convoluted surface on the bedding plane. Unit G73K-9. Loc. 11.

24

25

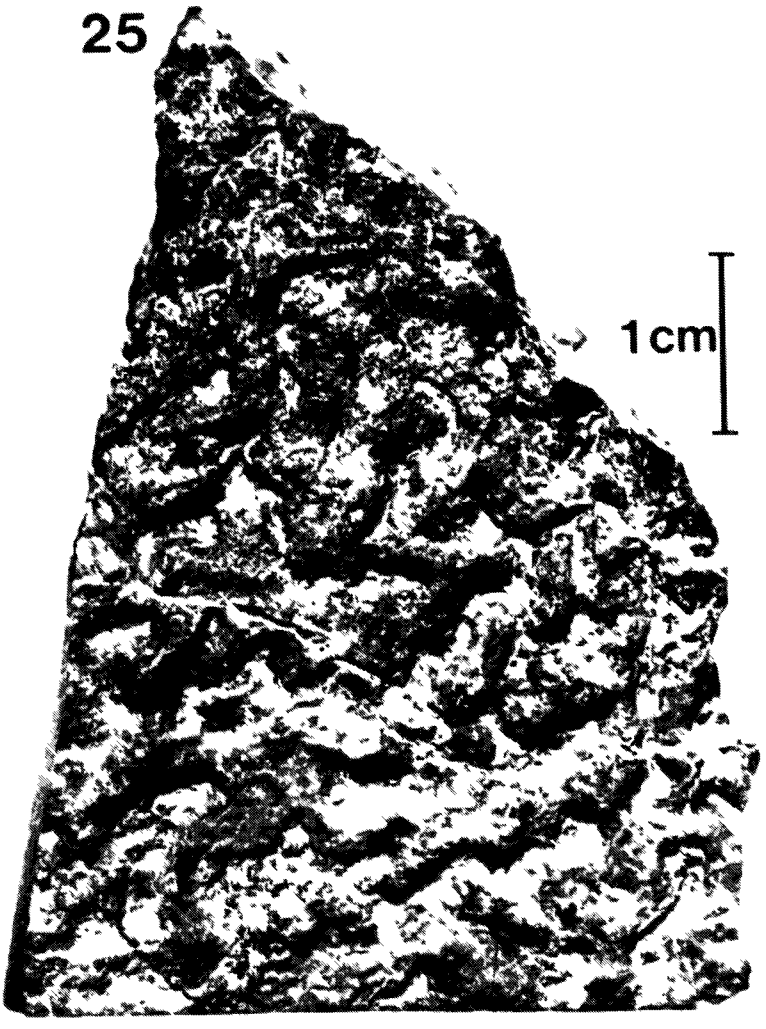

CHAPTER 3. ALLUVIAL PLAIN SEDIMENTATION

Introduction

The base of the upper member of the Somerset Island Formation is defined by the incoming of abundant red siltstone, commonly interbedded with limestone and dolostone in cycles resulting from the progradation of tidal flats (Chapter 2). In some sections of the upper member, thick sequences dominated by red siltstones pass up into the red sandstones of members 1 and 3 of the Peel Sound Formation. The red siltstone/sandstone successions of the two formations will be considered together since they result from extensive alluvial plain sedimentation landward of the tidal flats (Fig. 7). Sediments of the alluvial plain include fluvial channel and flood basin deposits.

Petrography

Thirteen facies, distinguished mainly on lithology, sedimentary structures and contacts between units, were identified during field work; detailed petrography was not a major focus of study. The siltstones consist of dolosiltite with some quartz silt (the origin of the dolomite is discussed in Chapter 6). The sandstones are mainly litharenites of the calclithite group in the classification of Folk (1968, p. 129),

i.e. sand-sized sedimentary rock fragments, predominantly carbonates, are a significant component. The rock fragments are mainly dolostone, with some chert and sandstone; metamorphic fragments are locally common, but igneous fragments are rare. Clast types in the Peel Sound conglomerates show similar relative abundances (Chapter 4). Quartz grains are strained or unstrained, and in medium- to coarse-grained sandstones are usually well rounded. Other minerals include plagioclase, alkali-feldspar (in some cases with authigenic overgrowths), muscovite, biotite, chlorite, altered ferromagnesian minerals, and a few grains of zircon, tourmaline, epidote, rutile and apatite. Petrographic data is consistent with derivation from the sedimentary Paleozoic and Proterozoic formations of the Boothia Uplift, with the underlying igneous and metamorphic basement also contributing detritus.

Nature of facies (Table 3, stratigraphic distribution in Fig. 6)

Laminated siltstone/fine sandstone (F_1)

Parallel lamination is the characteristic internal structure, and is associated with other current structures, and desiccation and syneresis cracks. Ostracods are common. As in the tidal cycles, some units give clear evidence of an algal origin, with small-scale domal stromatolites, contortion and brecciation. Most units, however, do not show these features and the structures suggest shallow water conditions

with current action. A distinctive sub-facies, pale pink in colour, consists of current or algal laminated sediment with shrinkage cracks, ripple marks and bioturbation (Chondrites). Facies F_1 may indicate occasional tidal incursions across the alluvial plain, but in most cases, the sedimentary context usually suggests deposition from shallow water in flood basins.

Interbedded sandstone/siltstone (S_{ib})

The facies is characterised by abrupt alternations, on the scale of a few cm, of varicoloured sandstone and siltstone (Photo 26). Layers contain parallel- to wavy-lamination and small-scale cross-lamination, and coarser layers are commonly loaded. Shrinkage cracks were not observed. The interbedding indicates periodic influxes of sediment into standing water.

Several interpretations are possible for facies S_{ib}. The variation in grain size (Photo 26) may be attributed to the changes in energy level characteristic of tidal environments. Allen (1974) in a study of the Upper Silurian Downton Castle Formation of the Welsh Borders described a facies of trough cross-bedded sandstone interbedded with rippled siltstone and laminated mudstone (his facies C), and containing lingulid brachiopods, modiolopsidid bivalves, ostracods and plant remains, which he interpreted as shallow marine. However, no fossils have been found in facies S_{ib}, and since open marine conditions are invariably represented by carbonates in the

clastic wedge, S_{ib} is unlikely to be marine. Fluvial environments, especially in or near levees, contain facies with interbedding (Reineck and Singh, 1975, p. 246), and in ancient sediments "alternating" facies commonly occur above channel sandstones in fining-upward cycles (e.g. facies F of Cant and Walker, 1976; facies association 4 of this study). However, at Localities 9-11, the facies is not associated with fining-upward cycles, and one unit is more than 7 m thick. A third possibility is a fluvio-lacustrine origin. Daley (1973) described a facies with alternation of siltstone and mudstone layers and lenses, associated graded bedding and erosional internal contacts from the Oligocene Bembridge Marls of southern England. The facies forms the basal part of fining-upward cycles up to 3.3 m thick, interpreted as the result of the infilling of shallow lakes by pulses of river-borne sediment. Facies S_{ib} is not closely similar to this facies, but the mechanism of sedimentation may be analogous. The "lakes" would have been shallow, temporary pools, perhaps oxbow lakes or local swamps in some cases.

Wavy-laminated sandstone (S_{wl}) is a variant of facies S_{ib}, consisting of 1-2 m units of thin-bedded yellow or white sandstone. Bioturbation is common, but no body fossils were observed. Abundant symmetric ripples produce a wavy-laminated appearance, especially where draped by thin siltstone laminae. The presence of secondary ("ladder") ripples in primary ripple troughs and oriented at right angles to the primary ripples

suggests the action of wind on bodies of very shallow water (cf. Rust, 1972a, Fig. 6). Desiccation cracks indicate periodic subaerial exposure. The facies may be of marine origin (tidal flats or lagoons) or non-marine origin (shallow pools).

Graded sandstone (S_{gr})

Discrete beds of grey-green sandstone, up to 30 cm in thickness (Photo 27), show abrupt (often loaded) basal contacts. A basal lag of siltstone intraclasts and quartz grains of medium sand size locally infills desiccation cracks in the underlying bed. Low-angle small-scale cross-lamination is common, and siltstone drapes occur on parting surfaces. Ostracoderm shields and fragments are sufficiently abundant locally to form "pavements" of closely spaced bone material (Photo 28), and shields show parallel and convex-up (current stable) orientation as a result of current action. Sedimentary structures indicate rapid deposition from shallow water.

Massive sandstone (S_m)

The facies is termed "massive" because internal structures generally are not apparent, although sub-planar bedding is present locally; bounding surfaces, however, are commonly distinct. The three following types of sandstone are grouped as one facies since they are difficult to distinguish from each other in weathered sections:

1) In sections with sandstone predominant, units of massive sandstone up to 50 cm thick overlie discrete or

graded lags of extrabasinal pebbles (commonly imbricated) and intraclasts. The units rest on planar or irregular surfaces.

2) Sections dominated by siltstone contain interspersed units of erosionally based massive sandstone. They average 10 cm in thickness, and a few contain large- or small-scale cross-beds, or parallel to contorted laminae. Ostracoderm fragments are common. The erosion surfaces underlying the units, and their commonly massive appearance suggest rapid deposition from flows of relatively high velocity, probably resulting from overbank flooding or crevasse splay, in view of their abrupt intercalation with other facies.

3) Fine- or medium-grained sandstone units, medium-bedded and several metres in thickness constitute a third type. Green siltstone laminae define bedding planes and irregular parting surfaces. Horizontal burrows and ostracoderm material are uncommon. These units are difficult to interpret, but may represent sedimentation in shallow standing water, producing well-defined planar beds draped by siltstone settling out between sedimentation events.

Small-scale cross-stratified sandstone (S_r)

Small-scale cross-lamination (sets less than 5 cm thick: Allen, 1963) forms one of a series of sedimentary structures in thick fluvial sandstone successions. Where the structure

occurs in facies previously defined, it is not considered to define a separate facies. Cosets are of trough type (nu-cross-stratification of Allen, 1963) and are commonly associated with parallel lamination lacking primary current lineation. Small-scale cross-stratification results from the migration of ripples (Harms et al., 1963), and indicates flow in the lower regime (Harms and Fahnestock, 1965).

Large-scale cross-stratified sandstone (S_{pt})

Large-scale planar and trough cross-strata are considered as one facies because they could not always be distinguished from each other reliably in poorly exposed or weathered sections. Grouped troughs are the dominant type, with isolated trough and planar cross-beds less common (pi-, theta-, and alpha-cross-stratification, respectively, of Allen, 1963). Cross-bed thickness ranges from 6 to 38 cm (mean of 16 cm in 28 examples). Dip of the laminae varies laterally from 6° to 32° (mean of 16°). Successive cross-laminae often show variation in grain size, and in more uniform sandstone can be identified by the presence of siltstone intraclasts. The sandstones are fine to medium grained.

In the Peel Sound Formation, many troughs infilled by cross-strata show irregular (erosional) bases (Photos 29 and 30). In some cases, scour and fill may have been part of the same hydraulic event (e.g. migrating dune systems), but in other cases, they were probably separate events (Allen, 1963,

p. 105). In a study of the Middle Devonian Battery Point Formation of Gaspé, Cant and Walker (1976) distinguished trough cross-strata from ellipsoidal scours infilled by layers parallel to the lower bounding surface. However, Augustinus and Riezebos (1971) observed that inclined foreset and parallel-layered fills of troughs and scours are commonly intergradational, depending on trough asymmetry and direction of fill, and both are considered as one facies in the present study since it often proved difficult to make the distinction. Broad shallow scours infilled by layers of siltstone and cross-bedded sandstone were also observed locally (e.g. Fig. 17).

A sub-facies of white, medium- to coarse-grained sandstone was observed in the Peel Sound Formation to the north of Creswell Bay (Localities 9 and 11). The sandstone is well sorted and contains pebbles and intraclasts. Large-scale planar and trough cross-strata are the dominant sedimentary structures. Ostracoderm shields are notably abundant and show parallel orientation. The well-sorted nature and mature composition of the sandstone may reflect a distinctive source, and the abundance of ostracoderms suggests an unusual environmental setting.

Large-scale cross-stratification commonly results from the migration of dunes (Williams, 1968), with flow conditions in the upper part of the lower regime (Harms and Fahnestock, 1965). It also results from migration of bar avalanche faces

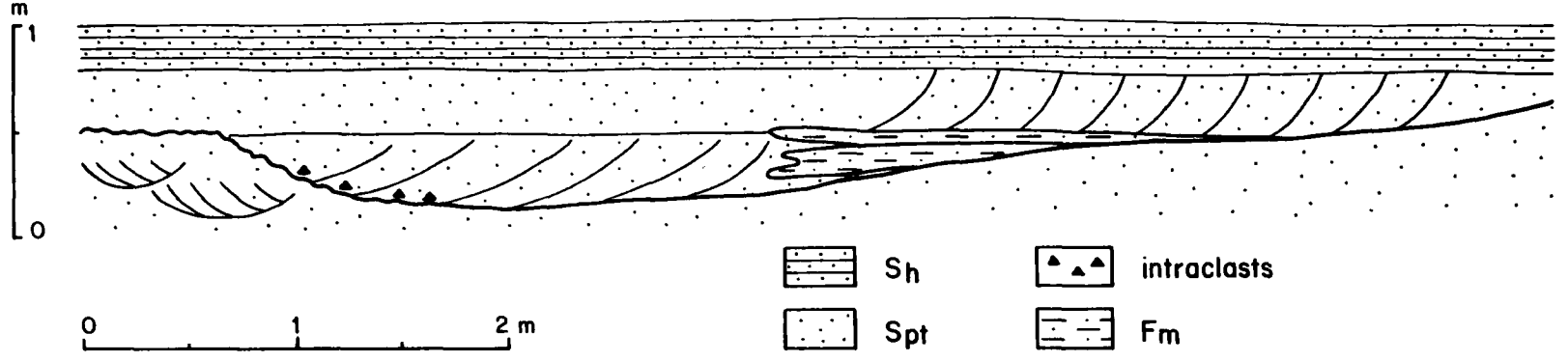

Fig. 17. Field sketch of a complex channel fill in Peel Sound member 1. Channel occurs in cycle 4, Fig. 26. Section G76A, Loc. 6. Facies code as in Table 3.

(Smith, 1972). Giant cross-beds (greater than 3 m set thickness) form a special category of facies S_{pt}, and are described later in the chapter as facies S_g.

Laminated sandstone (S_h)

Facies S_h resembles S_m in commonly containing planar bedding but differs in containing well-developed parallel lamination which produces a distinctive weathering character. The following two types of S_h, not always readily distinguishable, are present in the Peel Sound Formation:

1) Laminated sandstone lacking primary current lineation and closely associated with facies S_r, suggesting deposition under plane bed conditions in the lower flow regime (Harms and Fahnestock, 1965).

2) Laminated sandstone showing primary current lineation, and groove and tool marks, suggestive of plane bed conditions in the upper flow regime (Allen, 1964b).

Plane beds are common in modern rivers, and in fluvial systems showing lateral deposition plane beds of the upper flow regime should be less closely related to stream power than bedforms such as ripples and dunes (experimental and theoretical work discussed by Allen, 1970b). Leflef (1973) observed that in Upper Devonian fining-upward fluvial cycles, parallel lamination shows less relationship to grain size and position than does high-angle cross-stratification. Lamination

forms in a variety of environmental situations due to local increase in velocity, commonly associated with shallowing. Parallel laminae showing distinct lithological contrast can result from the migration of low amplitude bedforms (Smith, 1971a; McBride et al., 1975).

Erosion surfaces (ES)

Scoured horizons (e.g. Photo 30) are considered as a distinct facies for the purposes of Markov chain analysis, and were included by Cant and Walker (1976) in their analysis of part of the Battery Point Formation. The surfaces are usually laterally extensive, with less than 20 cm of relief, but locally also outline shallow channels up to 7 m wide and 0.7 m deep(Fig. 17). Some erosion surfaces consist of smoothly based troughs infilled by cross-strata, and may have resulted from erosion in the scour hollows of advancing dunes. A thin lag of siltstone intraclasts usually overlies the surface, with extrabasinal clasts abundant locally.

Association of facies in vertical sections

The sedimentary facies of the alluvial plain (Fig. 7) can be grouped into a number of distinctive associations in vertical sections, each association containing different facies types and proportions (Fig. 18). The associations represent several environmental settings, the probable geographic rela-

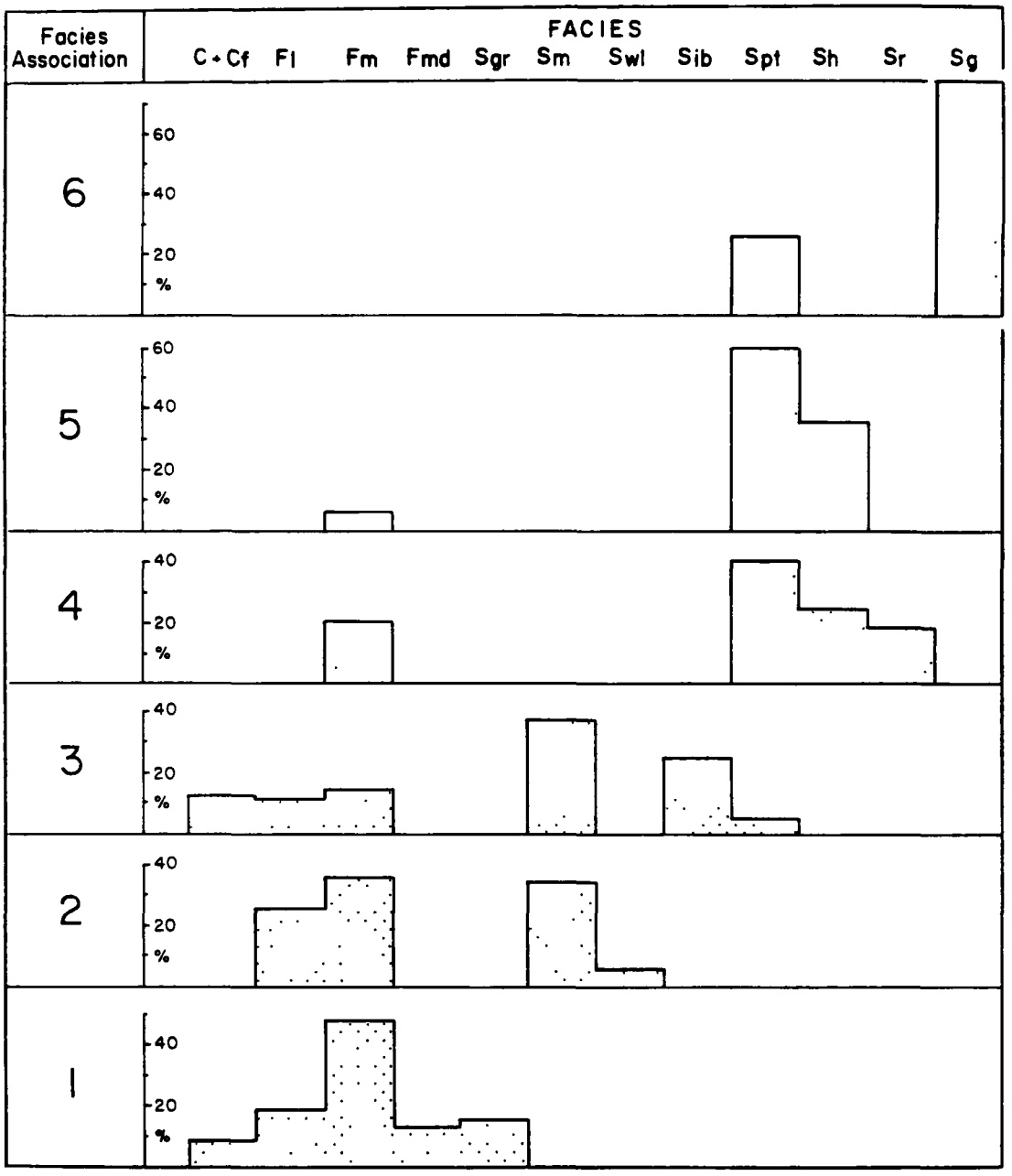

Fig. 18. Facies types and proportions in facies associations 1 to 6. Facies code as in Table 3.

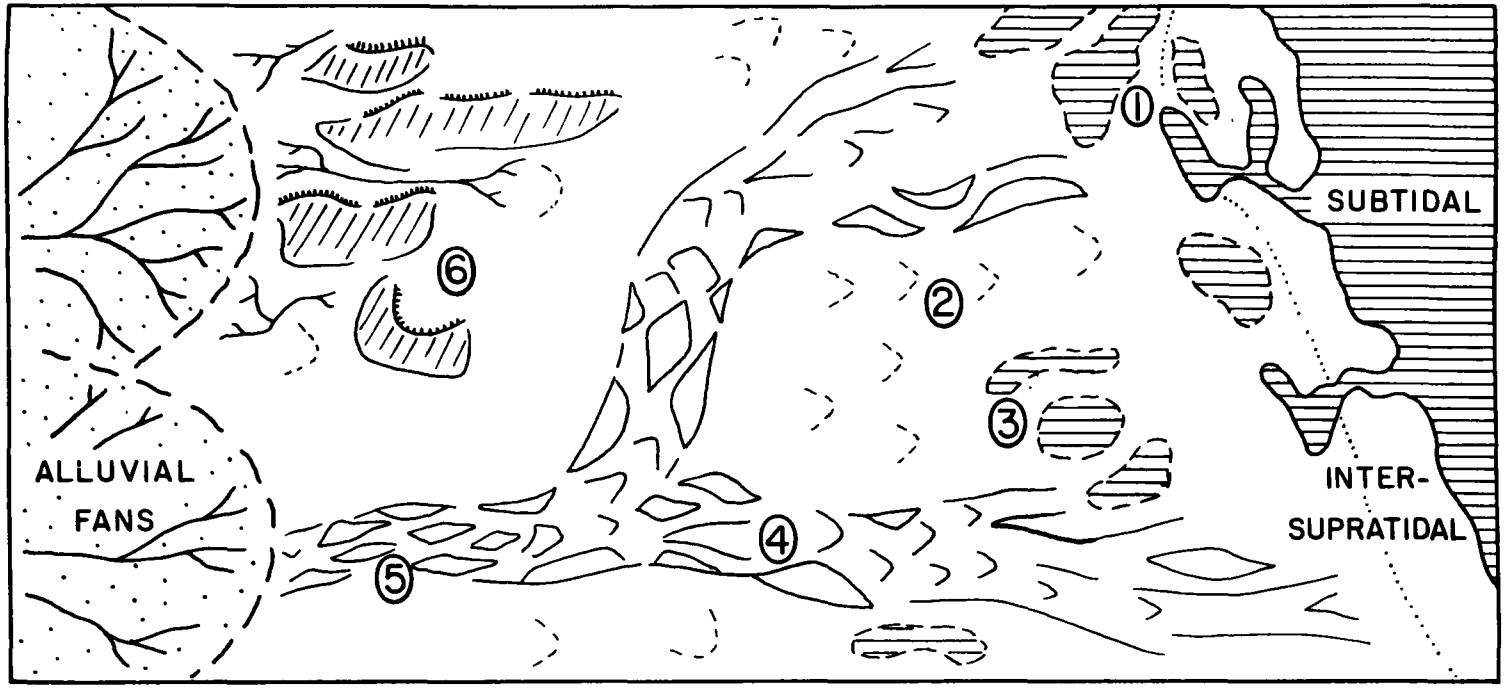

Fig. 19. Depositional environments for facies associations (numbered 1 to 6) of the alluvial plain. 1 = coastal flood basins, with limited marine influence; 2 = inland flood basins; 3 = shallow freshwater ponds filled by fluvial deposition, with limited marine influence; 4 = distal braided streams; 5 = proximal braided streams; 6 = eolian dunes and flash flood deposits. Associations are shown as lateral equivalents, but not all have been recognised at each locality. Also, associations 1 to 5 occur in the upper member of the Somerset Island Formation and member 1 of the Peel Sound Formation, while association 6 occurs in member 3 of the latter.

tionships of which are shown schematically in Figure 19.

Facies association 1

The association is well seen in the Upper Member of the Somerset Island Formation at Locality 2, Pressure Point (Fig. 20). The sediments overlie inter/supratidal and subtidal deposits (Chapter 2), and the restricted fauna (rich in ostracods), in addition to a few limestone units, indicates a limited marine influence during deposition. The facies present suggest deposition in calm waters of coastal basins with occasional crevasse splay events.

Massive and laminated siltstones, commonly red in colour, form 66% of the sections (Fig. 18). Desiccation cracks are common in these facies. Some beds show algal lamination. Facies F_m is interpreted as sediment deposited from stagnant overbank floodwaters, with subsequent homogenisation by bioturbation, whereas the intercalated units of F_l suggest deposition from flowing water with little subsequent bioturbation.

Discrete beds of facies F_{md} and S_{gr} (Fig. 20) make up 25% of the association. Both facies are rich in ostracoderm shields and fragments. Their abrupt contacts with the siltstones, the relative abundance of sand-sized quartz in both facies, and the internal structures in S_{gr} suggest sedimentation events of relatively high energy, and the facies are interpreted as the result of energetic overbank flooding or

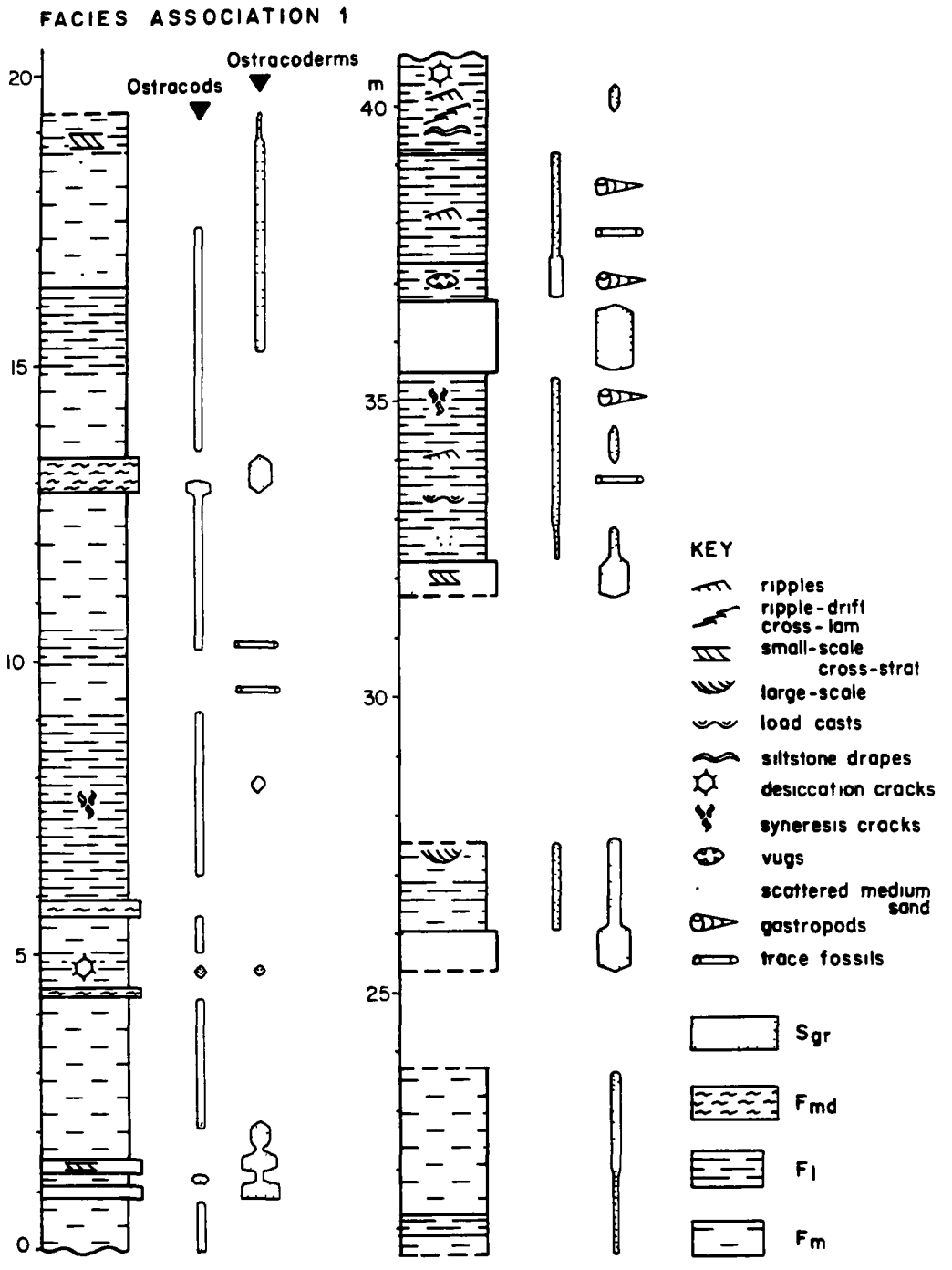

Fig. 20. Detailed section in facies association 1. Upper member of Somerset Island Formation, section G74G at Loc. 2. Column width reflects grain size, as shown in key. Facies code as in Table 3.

crevasse splay across the subaerial flood basin surface. The mottling in facies F_{md} may reflect subsequent drying and movement of moisture in the fine sediment. The presence of a few beds of unfossiliferous micritic limestone suggests occasional marine incursions.

The distribution of ostracoderms and ostracods in facies association 1 is strongly antipathetic as shown in Figure 20. Fragmental ostracods are abundant in the massive and laminated siltstones, while ostracoderm fragments are most abundant in facies S_{gr} and F_{md}, although present in other facies. The ostracods include several species of leperditiids (M.J.C. Copeland, pers. comm., 1975). Berdan (1968) observed that Paleozoic leperditiids are commonly associated with a restricted fauna in fine limestones and dolostones, some showing desiccation cracks, and concluded that they were adapted to environments subject to temporary subaerial exposure, such as tidal flats. These conclusions are supported by the results of the present study. A normal marine fauna is absent from facies association 1, but from sedimentary evidence alone, it is difficult to decide whether the ostracods were living under hypersaline or brackish conditions. Indeed, some modern ostracods can tolerate a wide range of salinity (Whittaker, in Gramann, 1971, p. 97). However, the rarity of evaporites in facies association 1 at Locality 2 suggests that hypersaline conditions were unusual, and that the ostracods were living under brackish conditions, with intermittent freshwater inflow

and limited connection to the open sea. The ostracods are commonly present in great abundance, a feature typical of many modern "opportunistic" species adapted to restricted environments. The extreme rarity of ostracods in the overlying fluvial sediments of the Peel Sound Formation suggests a low tolerance to freshwater. In contrast, the interpretation advanced above for facies F_{md} and S_{gr} as the deposits of freshwater floods suggests that the ostracoderms which they contain were transported into the area from freshwater habitats. Neither ostracoderms nor ostracods were found *in situ*, and, since both groups are readily transportable (Denison, 1956, p. 365; Kilenyi, 1971), mixing of the faunas would be expected. In facies association 1, the vertebrate fragments tend to occur rarely with ostracods in facies F_m and F_l, whereas ostracods were not observed with the fish in facies S_{gr}. This evidence is consistent with the transport of vertebrate fragments into ostracod habitats. De Windt (1972, p. 130) observed a similar antipathetic relationship between cyathaspidid ostracoderms and leperditiid ostracods in the Upper Silurian of Pennsylvania.

No cyclicity was observed either in the field or by means of Markov chain analysis of the section at Locality 2, and most contacts are gradational. Facies F_{md} and S_{gr} are abruptly based, and represent statistically random events during continuous deposition of siltstone (Chapter 2). Closely adjacent sections are difficult to correlate, suggesting that the areal

distribution of facies was disordered ("crazy quilt") in contrast to the regular zonation of the facies of tidal origin.

Sections in the upper member of the Somerset Island Formation at Locality 13 near Fury Point contain thick siltstone units (F_m and F_l) with evaporites in the terrestrial parts of carbonate-clastic cycles. A salina deposit of stratified gypsum is enclosed in red massive siltstone (Photo 16); salt casts occur on several bedding surfaces (Photo 15); and the siltstone also contains early diagenetic gypsum (Photo 13). Facies F_{md} and S_{gr} were not observed. Thin beds of laminated siltstone contain abundant ostracods, with a few vertebrate fragments and bivalves. Periodic rainfall may have produced pools of fresh or brackish water, providing favourable conditions for the organisms. Crystalline gypsum also outcrops in a fault-block near Cunningham Inlet (Locality 8), well to the east of the Boothia Uplift. It is probable that as continental sedimentation spread eastward away from the rising mountain belt, the alluvial plain adjacent to the tidal flats developed hypersaline tendencies and was less influcenced by meteoric waters.

Facies association 2

The association occurs towards the top of the upper member of the Somerset Island Formation in sections near Cape Anne and Cunningham Inlet (Localities 7 and 8). As in facies association

1, thin beds of sandstone are interspersed with thick siltstone successions (Fig. 21), but in association 2, limestone is absent, ostracods rare, and as regards the coarser units, facies S_m replaces facies S_{gr} and F_{md}. The association suggests sedimentation in flood basins with crevasse splay events, but little or no marine influence.

Facies F_m forms the "background" lithology, constituting nearly 40% of the sections (Fig. 18). The facies is devoid of fauna apart from rare fragments of ostracoderms. Facies F_m represents flood basin environments receiving fines from overbank flooding, and the rarity of colour mottling in facies F_m in facies associations 2 to 5 suggests that soils were well drained, the water table was low, and surface pools were absent. Abruptly based units of facies S_m, about 10 cm thick, total 35% of the sections. They contain abundant ostracoderm shields and fragments but few ostracods, and are attributed to crevasse splays or high energy overbank floods. In the Upper Old Red Sandstone of the Scottish Borders, similar interbeds of sandstone and pebbly sandstone were described by Leeder (1973a) and interpreted as flood deposits of overbank or crevasse splay type. Laminated siltstone (F_l), some of algal origin, and wavy-laminated sandstone (S_{wl}) form 25% and 3% of sections, respectively. Desiccation cracks are common, and vugs resulting from dissolution of evaporite nodules suggest hypersalinity during deposition or early diagenesis. Neither facies contains body fossils, but trace fossils

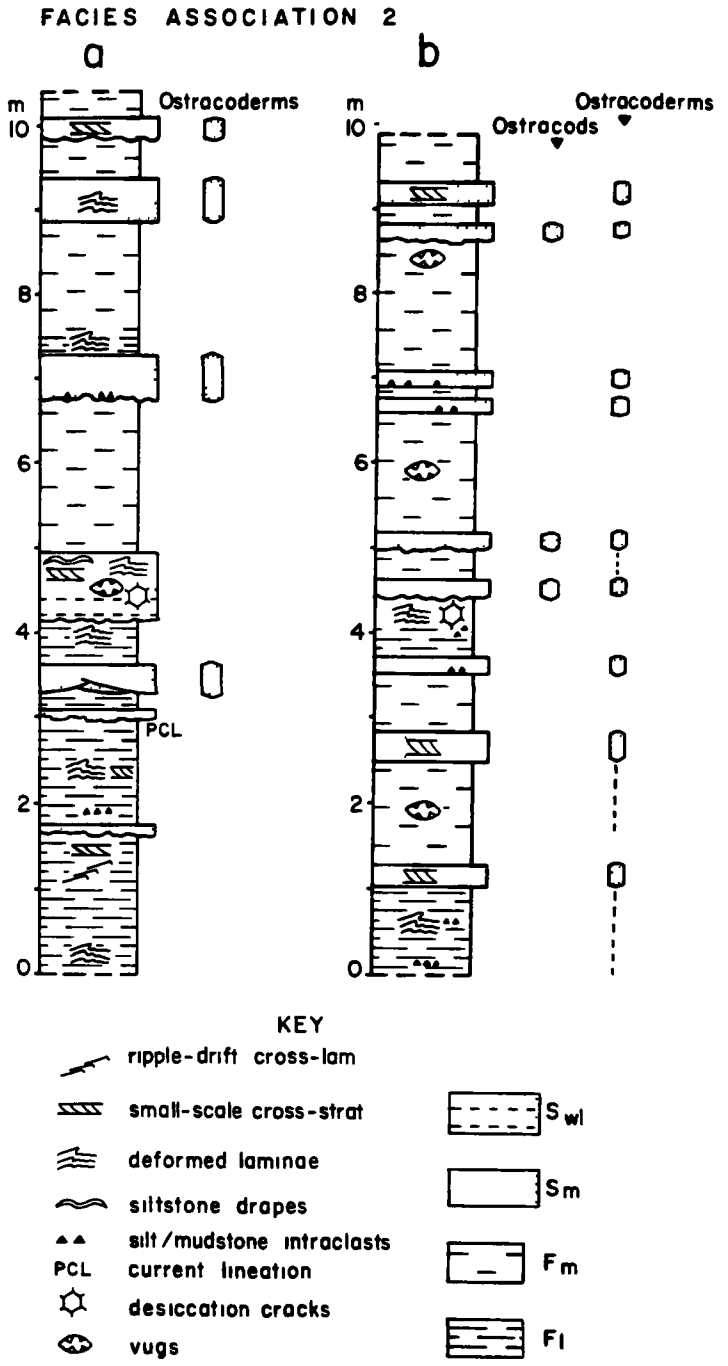

Fig. 21. Detailed sections in facies association 2. Representative sections in upper member of Somerset Island Formation ; a) at Loc. 8 (G76D). b) at Loc. 7 (G76C-1). Proportions and thicknesses of facies are accurate, although bed-by-bed log was not drawn up. Column width reflects grain size, as shown in key.

including Chondrites are common. Facies F_l and S_{wl} suggest the presence of shallow saline pools on the flood plain, or shallow marine embayments. It should be noted that Chondrites is very common in marine Phanerozoic sediments (e.g. Kennedy, 1975), but has not been reported from non-marine environments.

As in facies association 1, ostracoderms are abundant in the coarser units, in association with a few ostracods, and were probably transported from river channels during flooding as described by Smith (1945, p. 28) in the central plain of Thailand. The absence of ostracods from the siltstones, in contrast to association 1, suggests that flood waters infiltrated or dried up rapidly, so that ephemeral pools were uncommon; alternatively, the ostracods may have been less tolerant of freshwater than of brackish conditions, although they do occur rarely in fluvial channel and crevasse splay sediments of the clastic wedge.

Facies association 3

This association constitutes most of the upper member of the Somerset Island Formation at Localities 9-11 in the Creswell Bay area (Fig. 2), sections G73J, L and M. In contrast to the previous associations, association 3 consists predominantly of red sandstone, with facies F_m a relatively minor constituent (Fig. 18), although in view of its recessive weathering character, the facies may be scree covered in some sections.

A few limestone units indicate that the site of deposition was close to the sea, but ostracods are very rare, and the facies principally suggest the infilling of shallow fresh-water ponds by fluvial sedimentation.

Interbedded sandstone and siltstone (facies S_{ib}) and thick units of medium-bedded sandstone (S_m, second and third types) constitute 25% and 37%, respectively, of the sections. Other facies constitute 10% or less (Fig. 18). Resistant beds of wavy-laminated sandstone (S_{wl}) were observed in one poorly exposed section but could not be estimated quantitatively. As noted under facies descriptions, facies S_{ib} and S_m may represent deposition during fluvial flooding of shallow pools, while facies S_{wl} suggests deposition in shallow standing water under marine or non-marine conditions. Facies S_{pt} is rare in facies association 3 (Fig. 22a). The facies is characteristic of deposition in fluvial channels in other facies associations of the clastic wedge. At several localities, facies S_{pt} is unusual in being white (high quartz percentage), well sorted, and in containing abundant shields of Torpedaspis. In sections of the lower member of the Peel Sound Formation north of Transition Bay, Prince of Wales Island, units of well sorted sandstone and conglomerate which contain abundant Torpedaspis directly overlie limestones with marine invertebrates, and are interpreted as marine shoreline deposits. The white sandstones of facies S_{pt} on Somerset Island may be of similar origin. The site of deposition was certainly never far distant from the

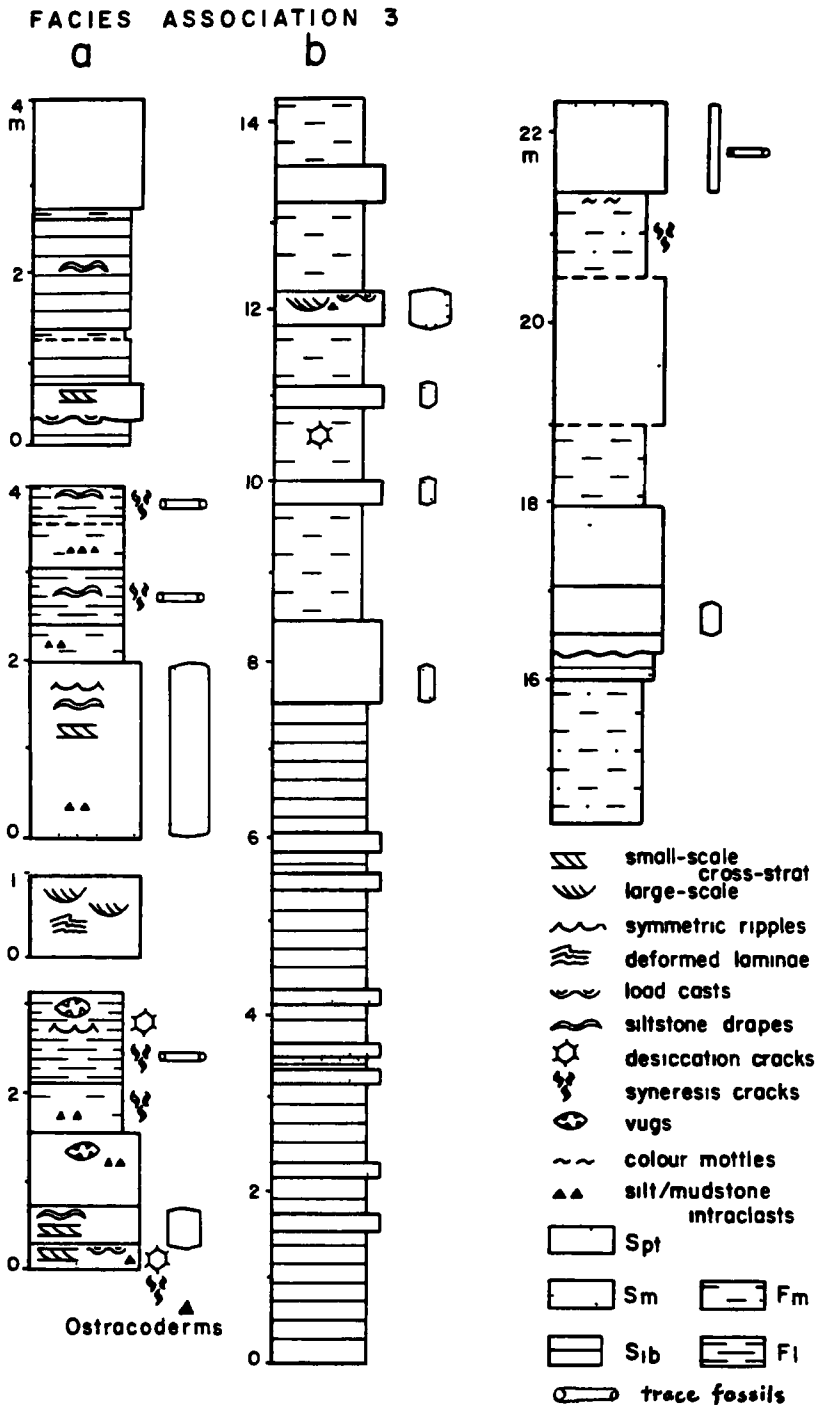

Fig. 22. Detailed sections in facies association 3.
Sections in upper member of Somerset Island Formation :
a) at Loc. 9, with discontinuous outcrop (G73J).
b) at Loc. 11 (G73L).
Column width reflects grain size, as shown in key.
Facies code as in Table 3.

sea, since several sections contain undoubted marine intercalations. At Localities 10 and 11, three limestone units up to 3 m thick are intercalated with redbeds. One unit contains digitate colloform stromatolites of probable subtidal origin (left hand cycle of Fig. 13), and the presence of ostracods, gastropods, lingulid brachiopods and conodont fragments in other units also supports a marine environment, albeit somewhat restricted. One unit commences with a basal intraclast lag, probably representing transgression (Chapter 2), and is overlain by a progradational sequence of tidal flat type.

In discontinuous sections of the Peel Sound Formation at Locality 9, four clastic-carbonate cycles, about 3 to 4 m thick, were observed, (two are illustrated in Fig. 22a). Red medium-bedded sandstone (S_m) is overlain by pale pink laminated siltstone, highly dolomitic, and containing vugs, algal laminae, Chondrites and desiccation features. In comparison with other Peel Sound Formation samples analysed for trace elements (Chapter 6), the Sr/Ca ratio is relatively low and the Mn content relatively high (statistically significant at the greater than 95% level). These results are consistent either with inversion of original aragonite to calcite under meteoric influence prior to dolomitisation (Veizer et al., in press), or possibly with deposition of detrital dolomite, low in Sr. The cycles may represent progradational tidal sequences or

the drying up of shallow pools on a flood plain. Ostracoderm shields and fragments, abundant in facies S_m in the lower parts of the cycles, are of genera typical of fluvial environments elsewhere in the Peel Sound Formation, and include articulated protopteraspidids which cannot have been transported far from their original habitat. Similar cyclic bedded marlstones were described by Friend and Moody-Stuart (1970) from Devonian sediments in Spitsbergen interpreted as flood plain deposits, and the cycles in facies association 3 are interpreted as resulting from deposition in flood plain pools.

The section at Locality 11 (Fig. 22b) shows a sequence of facies associations. The lower part consists of facies S_{ib} with thin units of facies S_m, interpreted as the infilling of shallow pools in the flood basin by pulses of coarse sediment and crevasse splay events of higher energy. The upper part resembles facies association 2, with thin units of facies S_m (crevasse splays) interbedded with thick units of massive siltstone. The lower strata of fluviolacustrine type are devoid of fauna, but in the upper part, ostracoderms are abundant in many of the coarser crevasse splay units and absent from other facies (except facies S_{pt}, white cross-bedded sandstone). The significance of the upward change in facies association cannot be assessed since the discontinuous nature of outcrop in the area renders correlation difficult.

Sandy braided and meandering river deposits

Previous studies

Sedimentation in modern and ancient meandering streams has been investigated by numerous authors (e.g. Harms et al., 1963; Allen, 1965, 1970b; Jackson 1975, 1976a and b). In contrast, sandy braided stream deposits are poorly known, although Walker (1976), Miall (1977) and Rust (in press) have recently reviewed these sediments. Before considering facies associations 4 to 6, the characteristics of the two types of river system will be discussed, and criteria presented for distinguishing their deposits.

Definition of channel systems

Rust (in press) has drawn attention to the confusion surrounding the definition of modern fluvial systems. The two most common types of stream, meandering and braided, are defined by different criteria, which are, respectively, sinuosity and the number of channels. Single channels are referred to as meandering if their sinuosity (ratio of channel length to down-valley distance) exceeds 1.5 (Leopold et al., 1964, p. 281), although other authors have used a different critical sinuosity (1.3 in Moody-Stuart, 1966; 1.7 in Leeder, 1973b). Single channels of lower sinuosity are termed straight. A braided stream is defined as one that is divided into more than one channel, with successive junction and division; individual

channels are of low sinuosity. Anastomosing streams also consist of several channels but these are of high sinuosity (Schumm, 1972). To rectify this confusion, Rust (in press) defined a braiding parameter on the basis of the number of channel divisions per mean meander wavelength of the fluvial system. Fluvial systems with a braiding parameter of less than 1.0 are termed single-channel systems, and those with a braiding parameter greater than 1.0 are termed multi-channel systems. "Meandering" and "braided" systems are the most common subtypes of these two categories, meandering systems being high-sinuosity single-channel subtypes, and braided systems being low-sinuosity multiple-channel subtypes (Table 9). Straight and anastomosing streams are uncommon, and will not be considered further in this study. Morphology, bedforms and sedimentary structures of generalised braided and meandering rivers are illustrated in Figure 23, taken from Walker (1976).

Lithology

The nature of the sediment load has a major influence on channel morphology (Schumm, 1972, p. 99) and hence on the preservation potential of fine sediment (Rust, in press). Schumm (1968, 1972) distinguished types of stable alluvial channel (i.e. not subject to progressive aggradation or degradation) on the basis of the suspended load/bedload ratio. Rivers with a high proportion of suspended load, such as most

TABLE 9. Classification of fluvial channel systems.
After Rust, in press, Table 1.

	Single-channel system (Braiding Parameter < 1)	Multi-channel system (B.P. > 1)
Low sinuosity (< 1.5)	Straight	BRAIDED
High sinuosity (> 1.5)	MEANDERING	Anastomosing

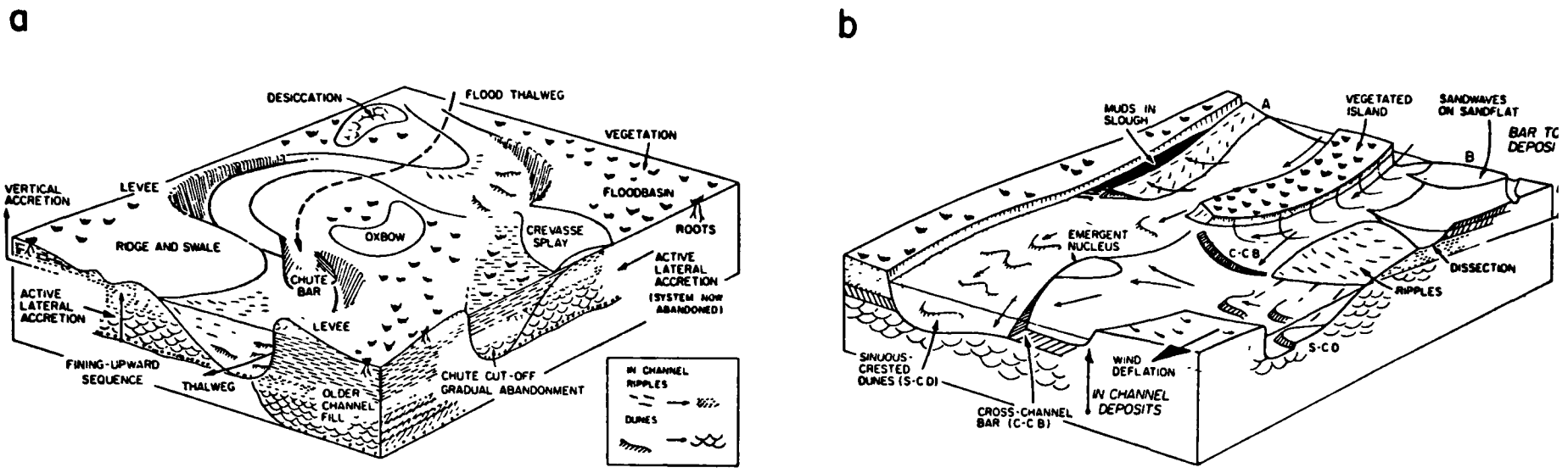

Fig. 23. Major morphological elements of river systems (after Walker, 1976, Figs. 1 and 9).

a) A meandering river system. Erosion on the outside bend of meander loops leads to lateral accretion on the opposite point bar - the dunes and ripples in the channel give rise to trough cross-bedding and ripple cross-lamination, respectively, (inset, lower right), which are preserved in a fining-upward sequence.

b) A braided river system based on the South Saskatchewan. Stippled areas exposed, all other features under water. Bar A is being driven laterally toward the far bank and is forming a slough in which mud is being deposited. Sandflat B is complex, with dissection features and flood-stage sandwaves. Fining-upward sequences may result.

meandering streams, have banks of cohesive, fine-grained sediment which inhibit lateral erosion by the channel, so that the river becomes "entrained" in a meander belt of resistant silt and clay (Walker, 1976, p. 104 and Fig. 8a). Marginal levees built up by deposition at the channel margin during flooding further confine the channel flow. At high discharge, the river overflows its banks or breaches the levees to deposit extensive sheets of fine-grained sediment in the flood basin. Vertically accreted deposits thus have a high preservation potential, and are commonly thick. In contrast, rivers with a high proportion of bedload sediment, including most braided streams, have banks composed of coarser, less cohesive material; rapid lateral migration of channels during high discharge erodes fine sediment deposited temporarily in inter-channel areas. Vertically accreted deposits have a low preservation potential (Walker, 1976. p. 105) and consist of thin veneers, intraclasts, and fills of abandoned channels, such as those observed by Williams and Rust (1969) on a relatively inactive tract of the braided Donjek River.

Channel sediments in braided systems tend to be coarser grained than those of meandering systems, and may contain abundant framework gravel as in the proximal Donjek River (Rust, 1972 a). Availability of sediment is evidently a limiting factor, and braiding may develop in river systems transporting silt, such as the Yellow River of China (Chien, 1961) and the distal reaches of the Slims River, Yukon (Fahnestock, 1969). However,

abundant framework gravel has not been reported from meandering channels , and in general, coarse-grained alluvial sequences lacking primary siltstone or mudstone beds are likely to be of braided origin. For a discussion of variables influencing the development of braided rather than meandering systems, see Miall (1977).

Sedimentary structures

In some meandering streams, point bar deposits consist of large-scale low-angle cross-beds, the epsilon type of Allen (1963), which represent the original depositional surface of the bar. They have been described in the sedimentary record by Moody-Stuart (1966), Beutner et al. (1967), Cotter (1971), Leeder (1973a) and others, and are diagnostic of point bar deposition. However, such accretion surfaces are commonly obscured by down-channel migration of smaller scale structures, principally dunes and ripples. Leeder (1973b) pointed out that of 231 meandering river cycles described from ancient sequences by Allen (1970a), only eleven contain epsilon cross-stratification. Another factor working against their recognition in ancient deposits is that in modern rivers, their lateral slope is less than 4°, except in very small channels (Allen, 1970a).

Large-scale trough cross-beds are the predominant sedimentary structure both on point bars and in many sandy braided channels, resulting principally from the migration of sinuous-

crested dunes (Jackson, 1976b; Walker, 1976). In distal, sandy braided systems, the migration of avalanche faces of transverse bars commonly generates large-scale planar cross-stratification (Smith, 1972), and planar sets are also produced by sand waves (Cant, 1977). Large-scale planar cross-sets are less common in meandering river deposits, where they are formed during the migration of transverse bars, scroll bars, and probably sand waves superimposed on point bar surfaces, or in channels (Jackson, 1976a).

Vertical successions

Stream power decreases systematically from the base to the margins of stream channels, but this decrease is particularly regular from the lower to the upper part of the point bar in meandering streams. This results in an upward decrease in grain size and in the magnitude of bedforms on the gently sloping depositional surface of the point bar (Allen, 1970b). The bedforms are likely to be preserved as a vertical (cyclic) succession of sedimentary structures by lateral accretion of the point bar (Fig. 23a). The type of succession observed is related to the nature of flow in different parts of the meander belt (Jackson, 1976b), and not all sections through point bars in the lower Wabash river showed fining-upward sequences with cyclic successions of sedimentary structures. Ancient, fining-upward alluvial sequences have been described by Allen (1964a, 1965, 1970a and b).

In braided stream systems, point bars are uncommon and usually form by the coalescence of smaller scale bedforms (Collinson, 1970, Fig. 3 and p. 38; Miall, 1977, p. 16). Most braided streams contain complexes of within-channel bars, the classification of which is discussed by Miall (1977) and Rust (in press). Longitudinal bars, elongate in the direction of flow, predominate in proximal reaches with gravel bedload (Rust, 1972a; Boothroyd and Ashley, 1975). "Sandy foreset bars" — a term used by Miall (1977, p. 16) to include linguoid, transverse and other types of bar predominantly transver to flow — are common in sandy, more distal reaches (e.g. Collinson, 1970; Smith, 1970; Cant, 1975). The sandy foreset bars tend to show complex bedform sequences, and bar top and low stage deposits are often eroded at high stage. Sequences of sandy braided alluvium are thus unlikely to show the regularity common in cyclic meandering successions. Walker (1976, p. 107) outlined a possible stratification sequence from studies of the braided South Saskatchewan River (Fig. 23b), with trough cross-strata (deposits of sinuous-crested dunes in channels) overlain by planar cross-sets (foresets of in-channel bars), capped by smaller scale cross-sets (bedforms on the bar tops). Comparable sequences were observed in the Battery Point Formation (Cant, 1977). Miall (1977, p. 38) suggested that cyclicity in braided stream deposits could also result from flow deceleration during flood cycles, from lateral accretion of bars attached to river margins, and from

infilling of abandoned channels; vertical sequences reconstructed by Miall, using data from modern braided systems and inferred ancient analogues, are notable for their variability in scale and stratification sequence. Thus regular vertical sequences are more characteristic of meandering systems but can also occur in braided stream deposits.

Lateral continuity of strata

The rapid growth and destruction of bars in braided channel systems (e.g. Smith, 1974; Hein and Walker, 1977) typically produces sets of elongate bodies of sediment, parallel and transverse to flow, with erosive, cross-cutting relations. These include aggradational sequences in active channels, abandoned channel fills and bar remnants. Strata wedge out laterally, as opposed to the steady lateral accretion of meander belts, which results in units that are relatively continuous over wide areas (Fig. 23). The degree of continuity observed in ancient strata may depend in part upon the orientation of sections, and on the degree of exposure.

Paleocurrents

The low sinuosity of braided channels results in a relatively low directional variance of many structures in channel-bar systems, and the paleocurrent vector magnitude (a measure of the degree of uniformity of orientation: Curray, 1956) is correspondingly high. The more sinuous channels of

meandering streams generally result in more variable orientation, with vector magnitudes lower for comparable structures. However, many other factors can influence vector magnitude, notably the rank of the structure studied (Miall, 1974). Bars are sufficiently large to influence flow, and the orientation of bar foresets is commonly oblique to flow (Smith, 1972). In view of the abundance of bars in braided streams, such a paleocurrent distribution in ancient sediments may be indicative of a braided stream origin. The oblique orientation of bar foresets in the braided South Saskatchewan River was used by Cant (1977) as one criterion for assigning a braided stream origin to part of the Middle Devonian Battery Point Formation of Gaspé, in which the paleocurrent direction of planar sets is at a high angle to that of associated trough cross-strata. Divergent orientation of planar sets has also been observed in point bars of the meandering lower Wabash River of Illinois by Jackson (1976b).

Types of braided river deposit

A facies model for meandering river deposits is well established, but braided rivers are more complex in morphology and produce more variable deposits (Walker, 1976). Rust (in press) has grouped sandy braided alluvium into three types (Fig. 24) — proximal high and low slope, and distal types. The distal type is transitional into the deposits of meandering rivers . The fluvial sediments of the Peel Sound Formation

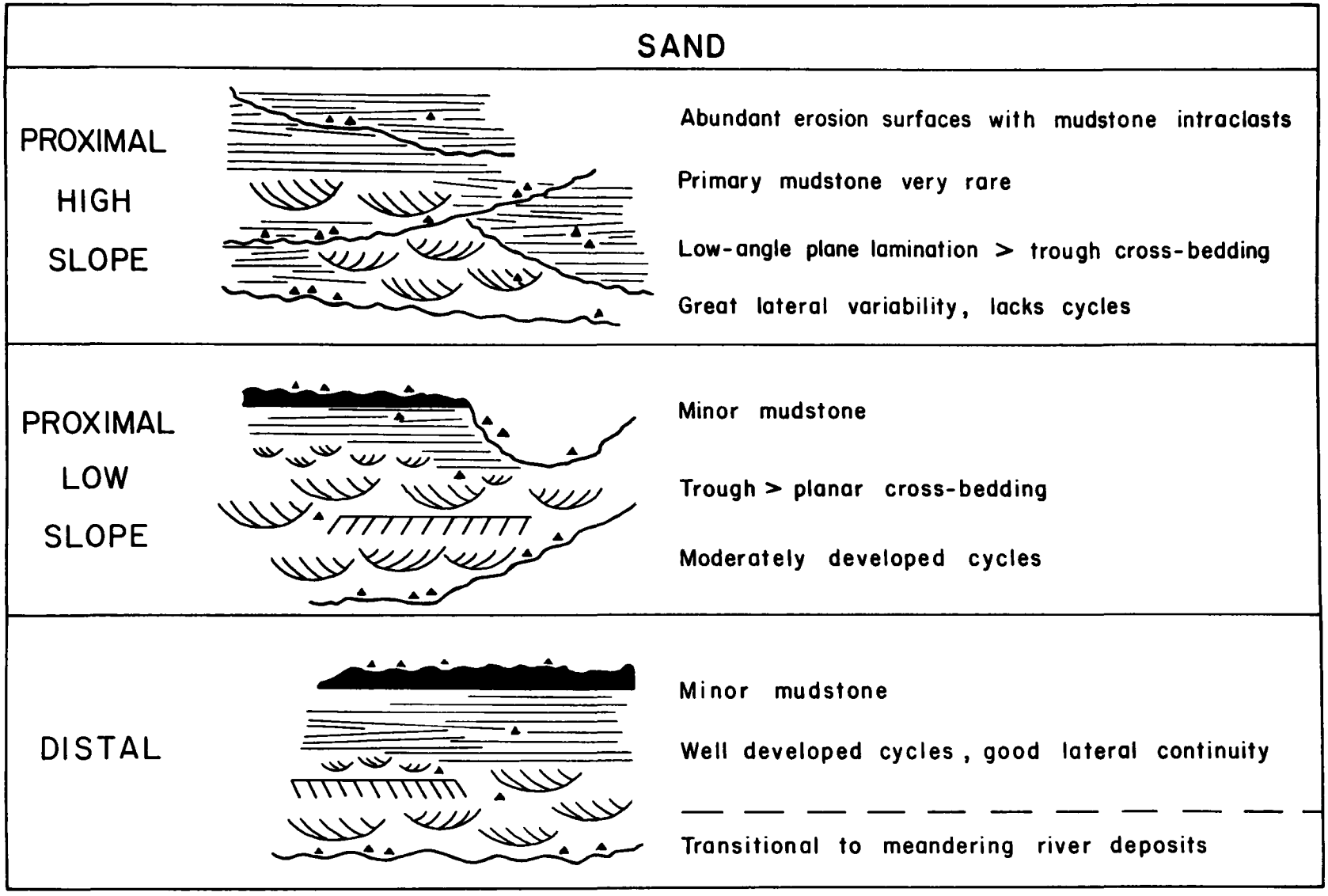

Fig. 24. Depositional model for braided fluvial sands. Adapted from Rust (in press), Table 2.

114

will be compared with these general types. Of the four types of braided river deposit defined by Miall (1977), none are closely applicable to facies associations 4-6, although the Donjek and Platte types show some comparable features.

Facies association 4

General features

At Cape Anne, Pressure Point and Cape Garry (Localities 1, 6, 14 and 15), sections in member 1 of the Peel Sound Formation contain thick red sandstones with some siltstones, and show an obviously cyclic sequence of facies. The predominance of large-scale cross-stratified sandstone is striking (39% , Fig. 18) in view of its scarcity (less than 3%) in the previous associations, whereas facies F_m constitutes only 20% of the succession. The stratigraphic setting, the red colouration, the evidence of channelling and the fining-upward nature of the cycles suggest that the sediments are fluvial in origin.

Ostracoderm fragments are common in the lowermost sandstones, but are rare higher in the succession. The general scarcity of ostracoderm material in these fluvial sequences is in strong contrast to their abundance in several facies in the previous three associations. Ostracods, bivalves, and horizontal and vertical burrows are very rare. One sandstone bed contains articulated bivalves in close association with

ostracoderm shields and burrows. Plant remains or rootlet beds have not been observed in the Peel Sound Formation on Somerset Island.

Fluvial cyclicity

Markov chain analysis is a useful aid to facies analysis in sections showing cyclicity (see Chapter 2). Facies sequences from four sections in member 1 were combined to give 75 transitions between the six facies recognised, and transition count and difference matrices are presented in Table 10. The X^2 test showed significance at the 99.9% confidence level, and the statistically derived path diagram is illustrated in Figure 25. Photo 31 shows a cycle consisting of a 2 m unit of facies S_{pt}, overlain by 1.7 m of facies S_r and S_h in thin beds with siltstone laminae; beneath the resistant base of the next cycle, thin units of facies S_m are interspersed in massive siltstone. Thirteen cycles from sections in member 1, illustrated in Figure 26, can be divided into the deposits of three sub-environments, by analogy with modern fluvial systems.

1) Channel deposits

Most cycles commence with an irregular erosional surface, sub-planar and with less than 20 cm relief, covered by a thin basal layer of intraclasts. In the overlying beds, minor erosional surfaces outline shallow scours averaging

TABLE 10. Markov chain analysis: data for facies association 4, Peel Sound Formation. Symbols for facies as in Table 3.

TRANSITION COUNT MATRIX:

	ES	S_m	S_{pt}	S_r	S_h	F_m
ES	0	2	8	1	1	0
S_m	0	0	1	0	3	2
S_{pt}	2	0	0	5	8	4
S_r	0	0	0	0	3	5
S_h	5	1	4	2	0	4
F_m	4	3	4	0	3	0

DIFFERENCE MATRIX:

	ES	S_m	S_{pt}	S_r	S_h	F_m
ES	0.00	.07	.37	-.04	-.17	-.22
S_m	-.17	0.00	-.11	-.12	.27	.13
S_{pt}	-.11	-.11	0.00	.12	.14	-.04
S_r	-.18	-.09	-.28	0.00	.14	.42
S_h	.11	-.04	-.07	-.01	0.00	.01
F_m	.09	.12	-.03	-.13	-.05	0.00

No. of Transitions: 75

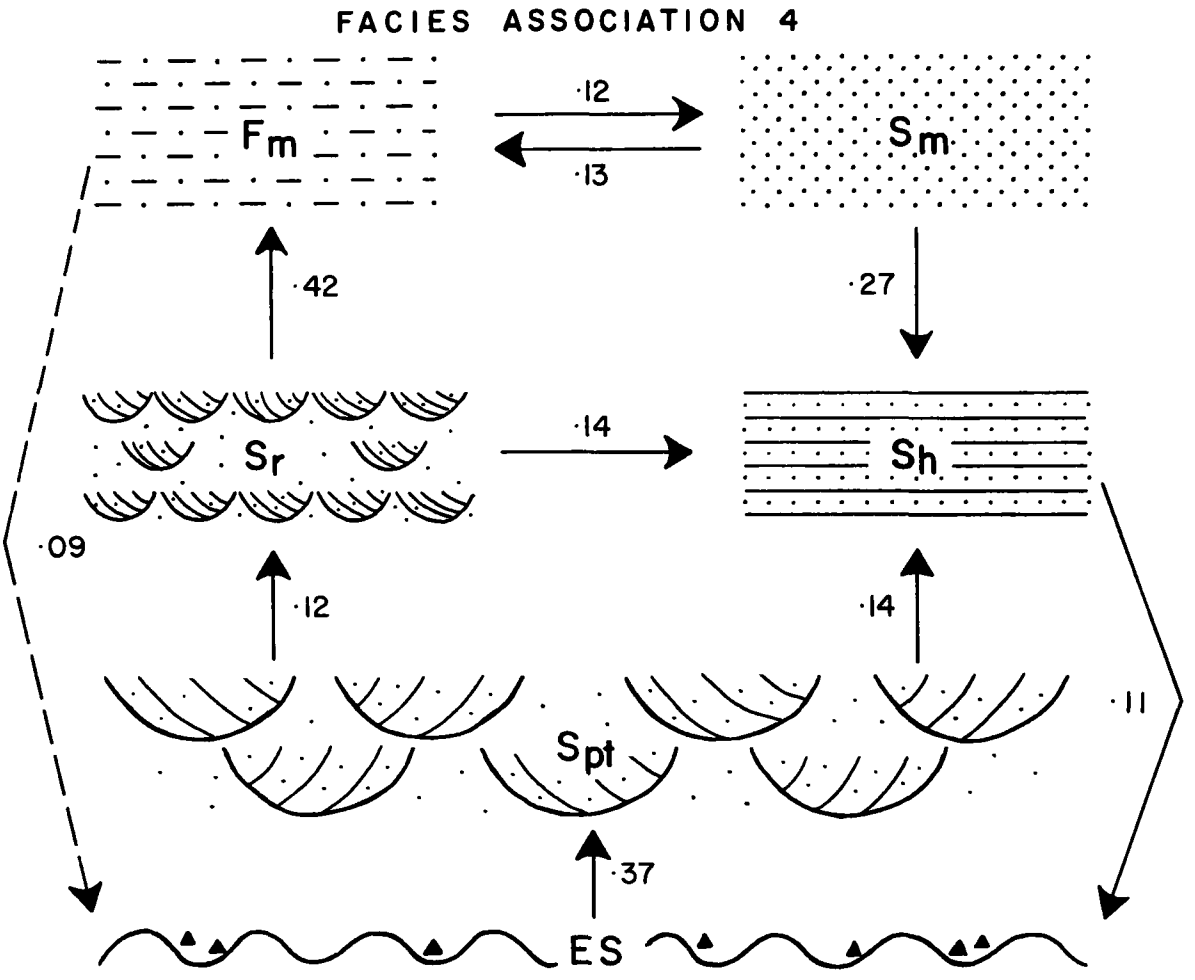

Fig. 25. Markov chain analysis : Path diagram for facies association 4, Peel Sound member 1. Facies code as in Table 3.

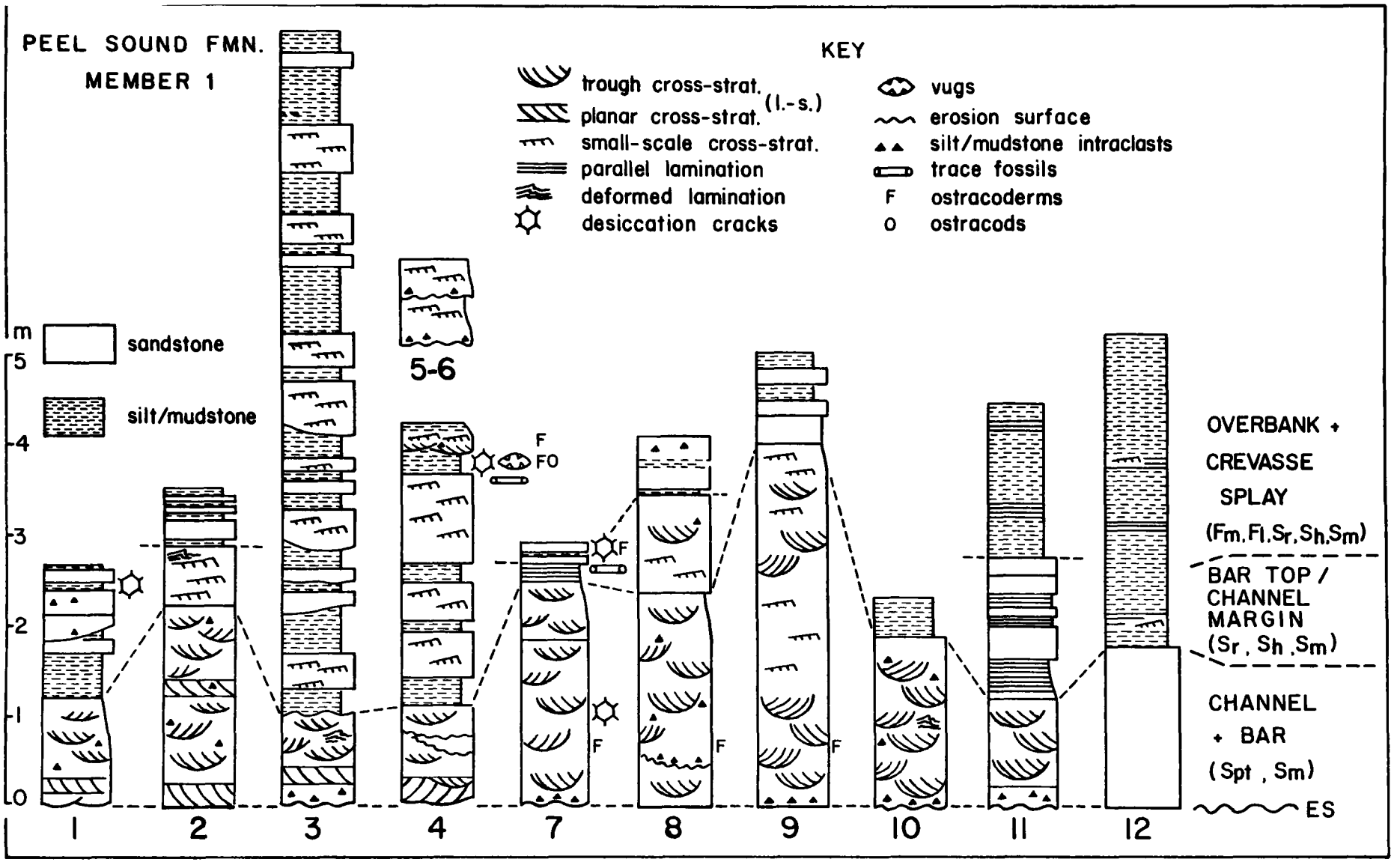

Fig. 26. Fluvial cycles in facies association 4. Cycles 1-7 from section G76A, Loc. 6; cycles 8-10 from G76B, Loc. 6; cycle 11 from G73C, Loc. 15; cycle 12 from G76C, Loc. 7. Column width reflects grain size, as shown in key. Facies code as in Table 3.

10-20 cm depth, infilled with cross-strata. The cycles are dominated by facies S_{pt}, with trough cross-stratification abundant, but several cycles contain sets of planar cross-stratatraceable laterally for 8 m or more (e.g. cycles 2-4, Fig. 26).

The close association of facies S_{pt} with scoured surfaces suggests deposition within major channels, and distinct channel structures on a smaller scale occur in some cycles. One such channel (Fig. 17) is 7 m wide and 0.7 m deep, asymmetric in cross section , and filled from one side by cross-bedded grey sandstone with tongues of red, finer grained sandstone; laminated sandstone completes the sequence. In cycle 4, small scours cut into the top of a planar cross-set.

2) Bar top or channel margin deposits

A distinct unit of finer grain-size and often of considerable thickness commonly occurs between the channel deposits and the topmost fines (e.g. cycles 2, 7, 8, 9 and 11, Fig. 26). Facies S_r and S_h predominate, commonly closely interbedded, while primary current lineation and other evidence for upper regime flow were not observed. Large-scale cross-beds and desiccation cracks are present. The finer grain size, the smaller scale of sedimentary structures and the evidence of desiccation suggest deposition in topographically higher parts of the fluvial system, such as the tops of bars or the margins of major channels (levees).

3) Overbank deposits

The lower units are usually overlain abruptly (erosionally in cycle 3) by red siltstone of facies F_m, containing desiccation cracks. Intercalated thin units of sandstone, abruptly or erosionally based, comprise facies S_m (cycle 1), and S_h and S_r (cycles 2 to 4). This assemblage of facies resembles facies association 2, and is similarly interpreted as the product of vertical accretion, with calm overbank and higher energy crevasse splay sedimentation in flood basins. Sections which show well-defined cyclicity contain a low proportion of overbank siltstone (20%).

A few fining-upward cycles at Locality 6 (section G76A) are unusually thin, averaging 0.5 m, but show good facies sequences:

top of cycle 4 $\quad ES \longrightarrow S_{pt} \longrightarrow S_r + S_h \longrightarrow F_m$

cycles 5 + 6 $\quad ES \longrightarrow S_h \longrightarrow S_r \longrightarrow F_m$

In a section at Locality 2 (section G74G), thicker, erosionally based units of S_m and S_{pt} are interbedded with massive siltstone which constitutes 70% of the succession (Fig. 27). The coarse units differ from those of facies association 2 (Fig. 21) in their greater thickness and the facies sequences which they contain. The units described above are intermediate in character between fluvial channel sandstones and the flood basin crevasse splay deposits typical of association 2, and

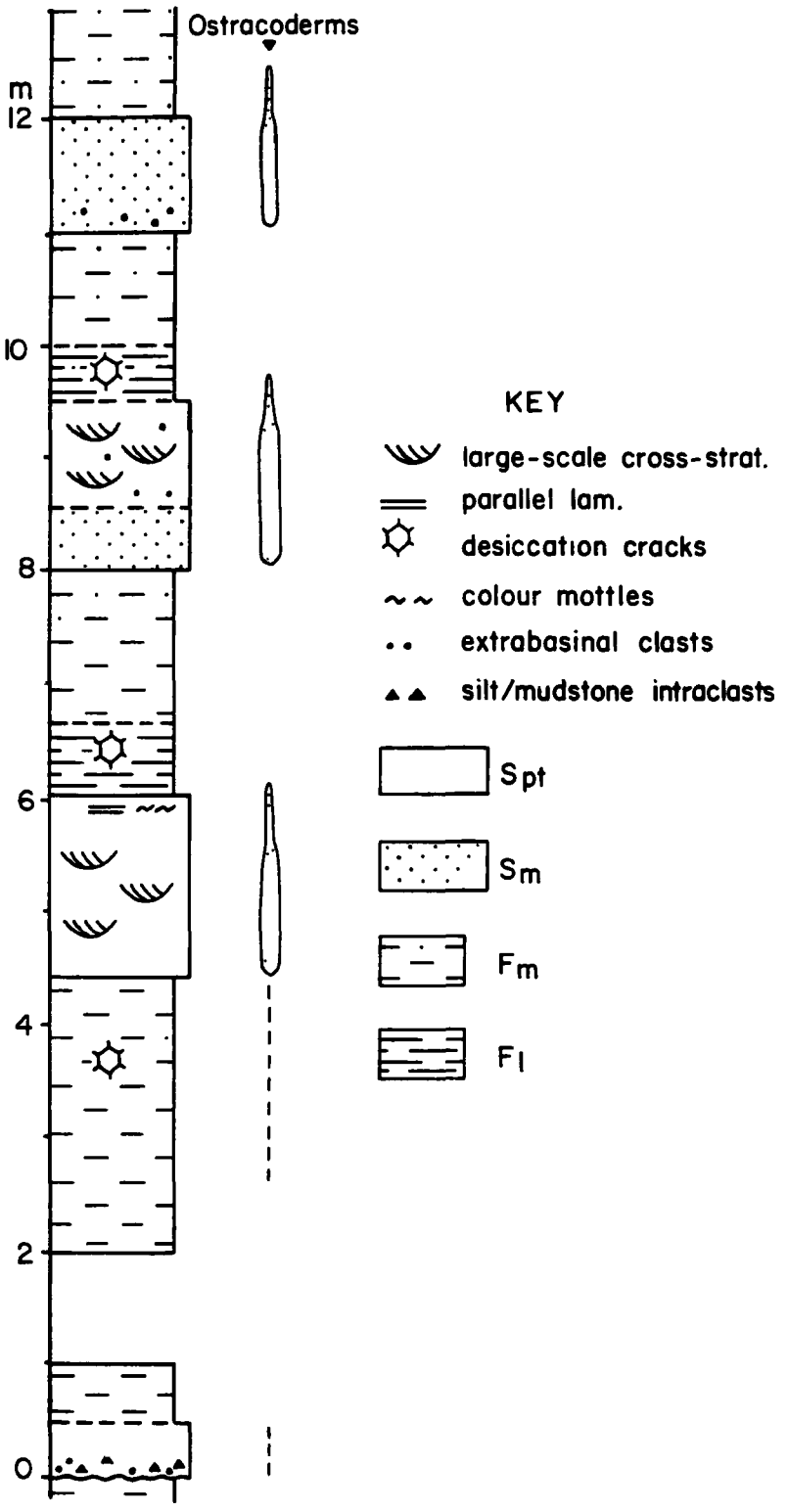

Fig. 27. Detailed section in facies association 4. Column width reflects grain size, as shown in key. Section G74G, Loc. 2. Facies code as in Table 3.

the sediments are interpreted as more proximal crevasse splay deposits with facies sequences resulting from decelerating flow. Leeder (1973a) has described similar sequences from the Old Red Sandstone of the Scottish Borders, with his Type B and Type E beds resembling, respectively, the thinner and thicker units described above.

4) Characteristics of the cycles

1) Cycles are of fining-upward type, with a well-defined succession of facies.

2) Twenty-nine cycles average 3.43 m in thickness, with cycle thickness reasonably constant in different areas of outcrop:

Cape Anne Syncline (Localities 2,6 and 7)	17 cycles	3.51 m average
Cape Garry (Locality 14)	7 cycles	3.84 m
(Locality 15)	5 cycles	2.56 m

The tops of some cycles are truncated by the overlying cycle as indicated by superimposition of channel sandstones (facies S_{pt}), with erosional contacts (e.g. cycle 7, Fig. 26), and these cycles were excluded from thickness calculations, as were the thinner avulsive cycles (less than 0.75 m).

3) Many cycles contain a distinct lower "coarse member", comprising channel and bar top/channel margin

deposits, with a mean thickness (11 units, excluding crevasse splays) of 2.13 m. The upper "fine members" of overbank sediment average 1.79 m in thickness.

4) Cycles show good lateral continuity (Photo 32).

Interpretation of cycles

The predominant lithology of facies association 4 is fine- to medium-grained sandstone. Primary mudstone and siltstone (F_m) constitute only 20% of the sections, with intraclasts abundant on major and minor erosion surfaces and on foresets. In comparison, 231 typical meandering cycles average 43% primary fines (calculated from Table 4 of Allen, 1970a), while cycles in the Battery Point Formation, interpreted as braided, average about 10% fines (Cant and Walker, 1976, Fig. 16). The relatively low percentage of fines in facies association 4 suggests comparison with sandy braided alluvium. Sedimentary structures in the channel deposits are consistent with this interpretation. The trough cross-sets and laterally continuous planar cross-sets are interpreted as the deposits of sinuous-crested dunes and sandy foreset bars respectively, both typical of braided rivers, and laminated sandstone is scarce in the channel deposits. The presence of smaller channels within the cycles (Fig. 17) also supports a braided origin, with channels of bedload type. Scours which cut into the tops of planar sets (Cycle 4, Fig. 26) may be similar to small channels formed at

low stage on the tops of bars in the Platte River (Smith, 1971b, p. 3414). Epsilon cross-stratification was not observed.

Paleocurrent data for the trough-sets from several localities in the Cape Anne syncline show unidirectional flow across the area (Fig. 28 ; Appendix B), with a vector magnitude of 48% (significant at the 97% confidence level), indicating moderate variation in flow direction. Data for the planar sets are insufficient to determine their relationship to the trough sets, but observation of inaccessible cliff faces suggests that the dip directions of the two types are commonly at a high angle, consistent with a bar foreset origin for the planar sets.

Fluvial cyclicity is best developed in meandering rivers, and the Peel Sound Formation cycles resemble those of meandering rivers in their broadly fining-upward nature, their good lateral continuity, and their sequence of channel to channel margin/bar top to overbank deposits, with coarse and fine members. However, similar channel to bar top sequences can also occur in braided alluvium (Fig. 23b), and in modern braided rivers, overbank sediments can be deposited extensively on alluvial islands and low-lying inactive areas (Williams and Rust, 1969, p. 651). The thickness of the coarse member gives an approximation of channel depth (Leeder, 1973b); coarse members of the Peel Sound cycles average only 2.13 m, which indicates that the channels were relatively shallow, a feature

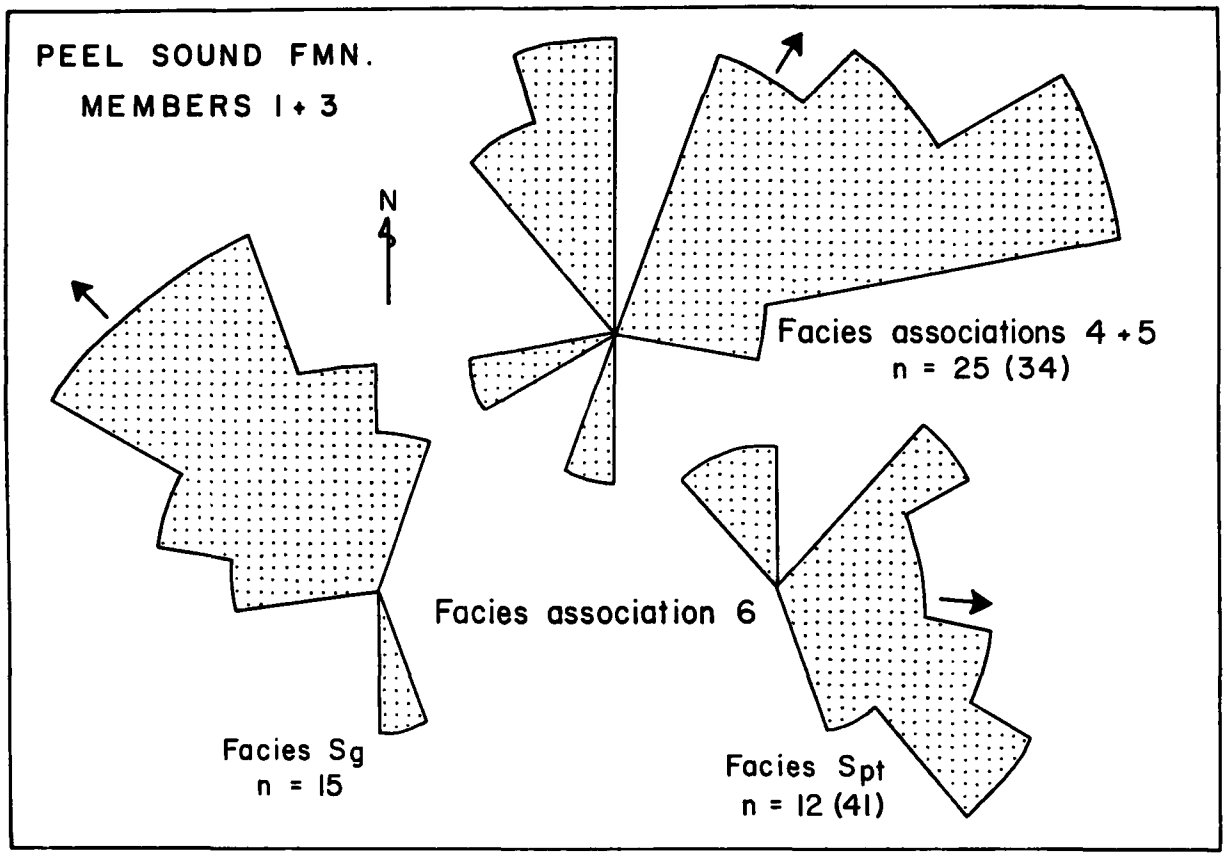

Fig. 28. Paleocurrent data from Peel Sound members 1 and 3 in the Cape Anne syncline. Solid arrows indicate statistical vector means. Data collected from large-scale sets of trough and planar cross-stratification at Locs. 1, 5, 6 and 7. In most cases, several trough sets were measured from one coset, and their mean orientation calculated; figures in brackets indicate total number of measurements. Facies code as in Table 3.

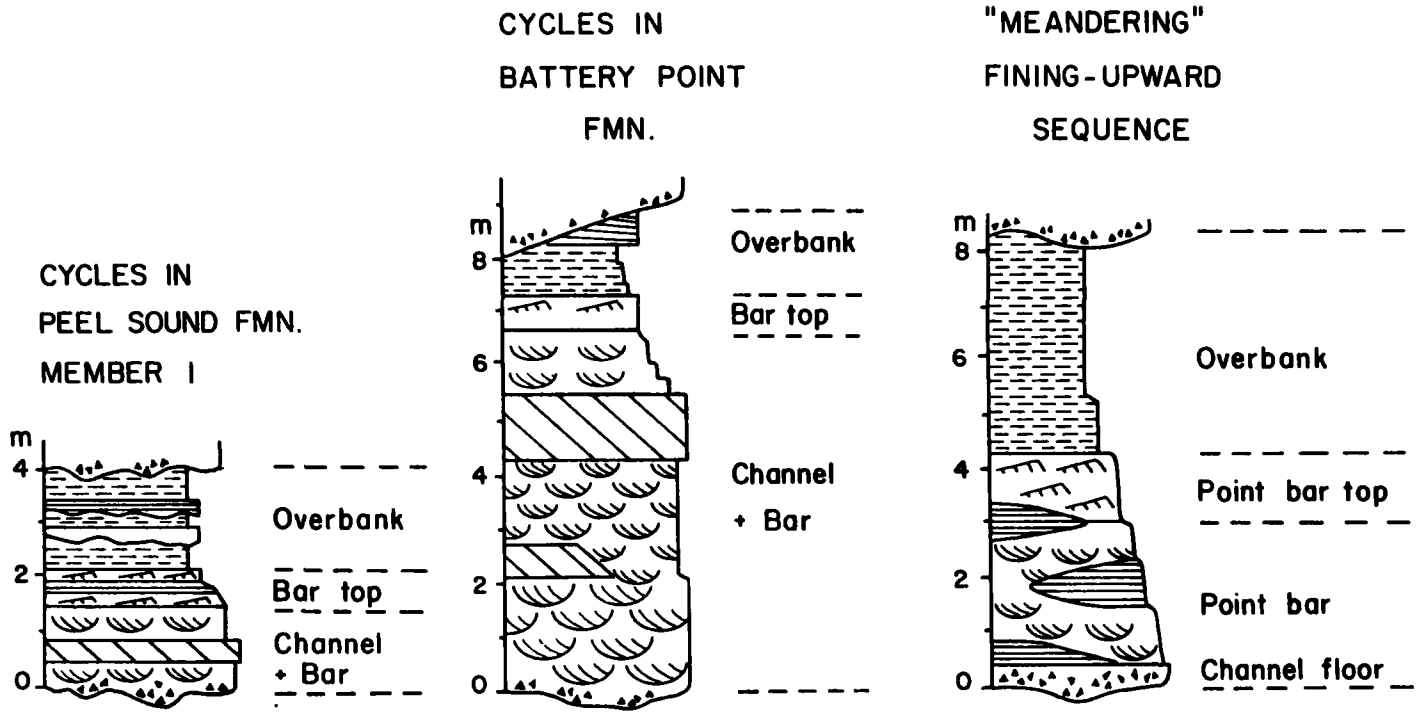

Fig. 29. Comparison of generalised fluvial cycles in Peel Sound member 1, the Battery Point Formation, and a modern meandering river. Facies code from this study is used for similar facies in the three cycles. Adapted from Cant and Walker (1976), Fig. 16.

127

characteristic of bedload channels in braided systems.

Comparison of generalised cycles from the Peel Sound Formation, the Battery Point Formation (interpreted as braided by Cant and Walker, 1976), and meandering sequences (Fig. 29) shows that the Peel Sound cycles are intermediate between the other two types in the percentage of primary fines, and are only about half as thick. The cycles compare most closely with the distal braided type (Fig. 24) of Rust (in press), transitional to the meandering type, and were probably deposited in systems of shallow channels with stable alluvial islands. Cyclic sequences with generally similar characteristics have been described from the Devonian Wood Bay Formation of Spitsbergen (Moody-Stuart, 1966), the Stubdal Formation of Norway which contains only about 5% of fines (Turner, 1974), and the Upper Old Red Sandstone of the Scottish Borders with about 30% fines (facies association 2, Fig. 5, of Leeder, 1973a).

Facies association 5

Sandstones in the basal 12 m of Peel Sound member 1 near Cape Anne (Locality 7) contain an association of facies very different from the cyclic association described above (comparison in Table 11). The section consists of medium-grained sandstone containing abundant erosion surfaces (ES) which underlie shallow channels up to 30 cm deep. Facies S_{pt}

predominates (Fig. 18) with trough sets much more common than planar sets. Less common laminated sandstone (S_h: low-angled or plane-laminated) shows primary current lineation and groove casts, rare in the cyclic successions at Cape Anne, and resembles facies G of the Battery Point Formation (Cant and Walker, 1976). Ripple-drift cross-lamination and desiccation cracks are also present. Siltstone and mudstone beds are very rare, but intraclasts of these lithotypes are abundant. Ostracoderm fragments are much more common than in the overlying cyclic association. The section is composed essentially of cross-cutting lenses of sandstone, apparently lacking prevailing cyclicity, although rare cycles in the lower part consist of fining-upward sequences less than 1 m thick:

$$ES \longrightarrow S_{pt} \longrightarrow S_h/F_m$$

Figure 30 shows the general (non-statistical) relationships of the facies.

The low percentage (less than 5%) of primary siltstone and mudstone is consistent with deposition in sandy braided systems, and the facies association, the abundance of scours, the cross-cutting relationships of many units, and the lack of cyclicity are indicative of proximal high slope deposits (Fig. 24). The shallow multi-channel system was characterised by rapid erosion and aggradation in channels, and lacked

TABLE 11. Comparison of cyclic and non-cyclic fluvial facies associations (4 and 5).

	CYCLIC ASSOCIATION 4	NON-CYCLIC ASSOCIATION 5
Predominant grain size	Fine sand	Medium sand
Primary siltstone %	20	< 5
Intraclasts	Common	Abundant
Erosional surfaces	Common, sub-planar	Abundant, channelled and sub-planar
Cyclicity	Fining-upward sequences	Rare fining-upward
Continuity of strata	Laterally continuous	Commonly lensoid
Predominant facies	S_{pt}	S_{pt} + S_h
Type of cross-bed	Trough; planar uncommon	
PCL and groove casts	Rare	Common
Ripple-drift cross-lamination	Rare	Common in finer units

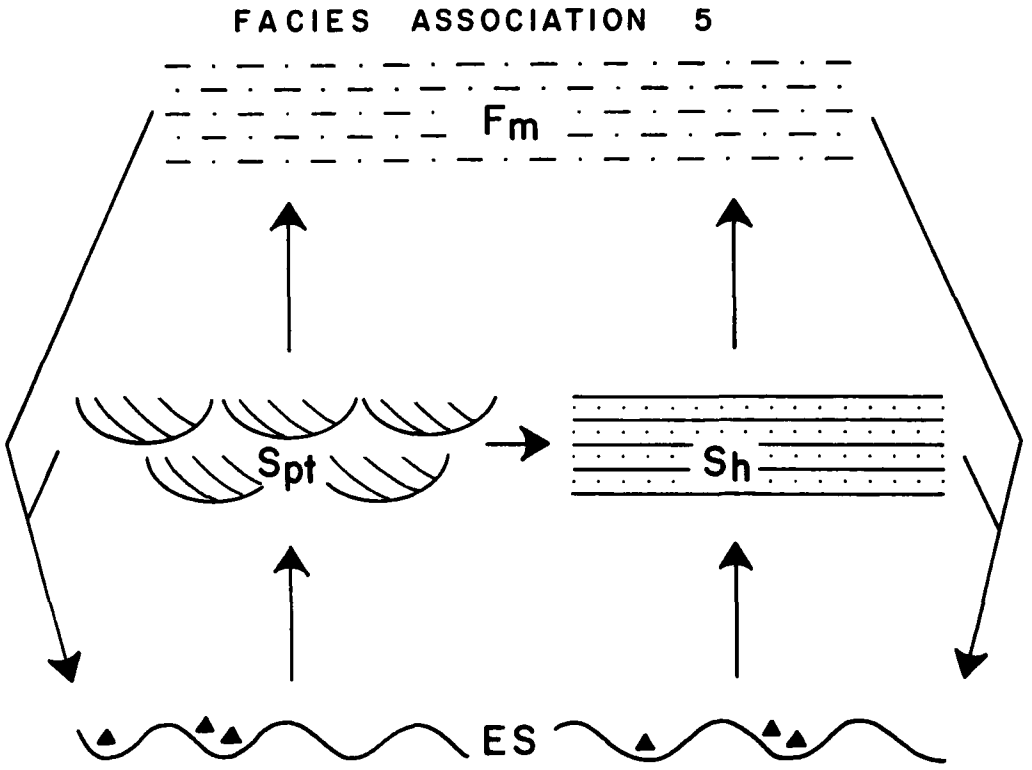

Fig. 30. Facies relationships in facies association 5. Derived by inspection of strata at Loc. 7. Facies code as in Table 3.

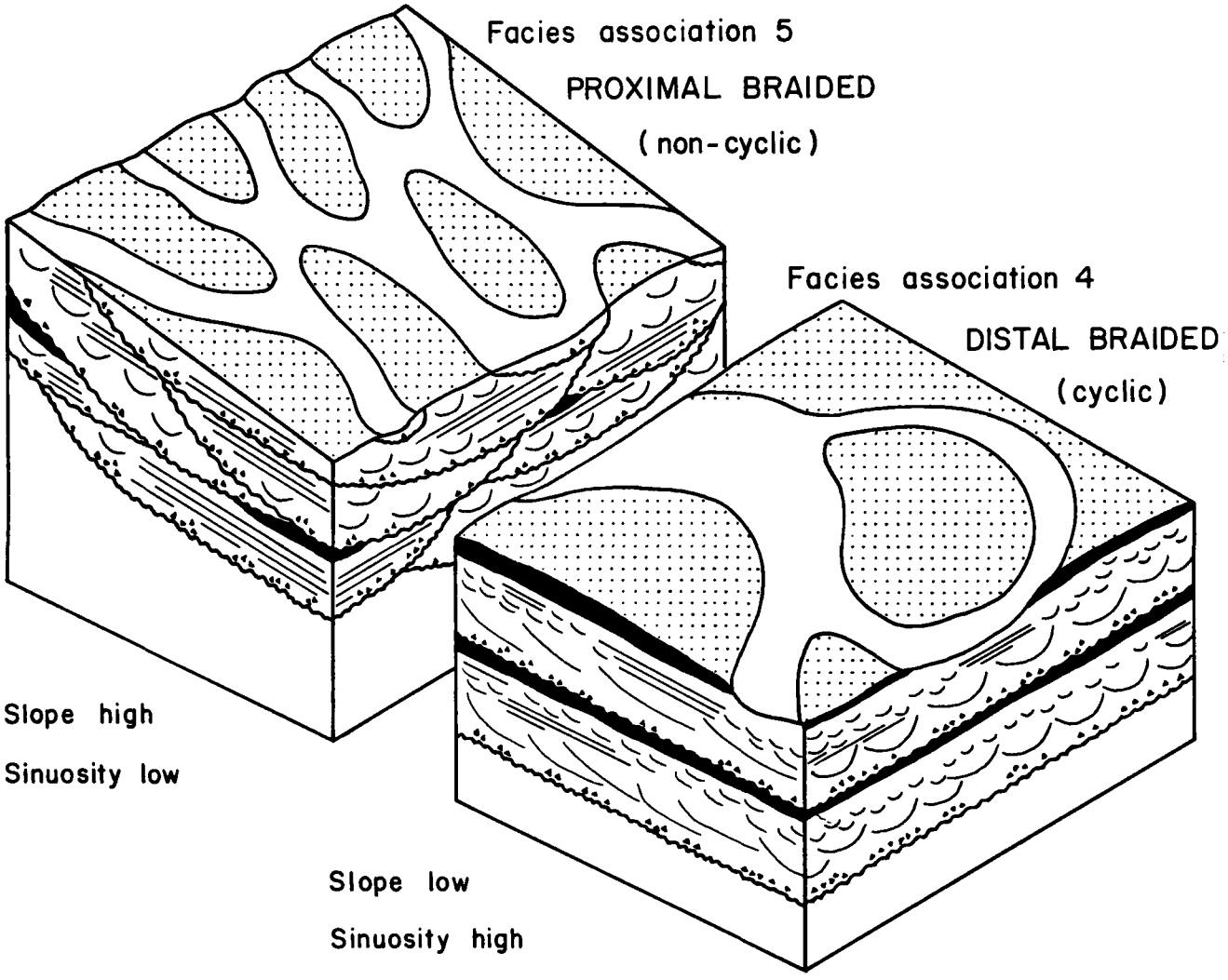

Fig. 31. Relationship between cyclic and non-cyclic fluvial facies associations (4 and 5).

extensive areas of overbank sedimentation. Trough cross-strata represent the migration of dunes, with facies S_h resulting from higher velocity flow, possibly in shallower reaches or on the tops of bars. The facies association is similar to that observed in sandstones of the Malbaie Formation of Gaspé, also interpreted as proximal high slope deposits (Gibling and Rust, 1977). Figure 31 illustrates the probable relationship between the cyclic and non-cyclic fluvial associations.

Facies association 6

In the western limb of the Cape Anne syncline, Peel Sound member 3 consists of alluvial plain sediments, with 240 m of sandstone and pebbly sandstone overlying the conglomerate of member 2 (Photo 2). Sandstones of member 1 pass up into those of member 3 on the eastern limb where member 2 is absent (see cross-section, Fig. 5). The member consists of an intimate alternation of two facies (Fig. 18): trough cross-bedded pebbly sandstone with thin units of conglomerate (S_{pt}), and giant cross-bedded sandstone (S_g). No organic remains (not even ostracoderm fragments) were found in either facies.

Facies S_{pt} consists predominantly of medium-to coarse-grained sandstone showing moderate sorting, with extrabasinal, commonly imbricate clasts. up to 10 cm in diameter (Photo 33),

and intraclasts of green siltstone. The sandstone is grey to dull red in colour. Units average 2 m in thickness (maximum 3 m). are relatively well cemented, and can be traced laterally for at least two kilometres (Photo 2). They are erosionally based (Photo 34), with flute casts, current crescents, primary current lineation and groove casts on the basal surfaces (Photo 35). Large-scale trough cross-stratification is the predominant structure, with cross-laminae in some cases overturned, and cross-strata commonly infilling irregularly based scours. There is no obvious vertical succession of sedimentary structures, although this may in part be a function of poor exposure.

The facies closely resembles the flood deposits of modern ephemeral streams, although most of the structures are not confined to this environment. Sixty percent of the sediments laid down during a flood event in the Lake Eyre basin, central Australia, consists of trough cross-stratified sands deposited by migrating dunes (Williams, 1971). A further 25% is composed of planar sets resulting from growth of channel bars. Lower regime flow prevailed during deposition for the majority of the sediments studied. The presence of flute casts indicates flow under highly turbulent conditions (Dzulynski and Walton, 1965, p. 201), and flat-bedded sandstone (less than 5%) with parting lineation suggests periods of flow in the upper regime (Allen, 1964b). Similar flood deposits in southern Israel, mainly of gravel with a

sandy veneer, contain a variety of structures (Karcz, 1972), including flow-aligned ridge and trough systems (harrow marks) and obstacle marks such as sand shadows and current crescents, while dunes are abundant as bedforms. Karcz noted that fluctuations in flow regime led to poor hierarchical ordering of sedimentary structures, and hence cyclicity would not be expected in sequences formed in such an environment. In both cases , sedimentation resulted from flash flooding through low-sinuosity braided channel systems under relatively arid climatic conditions. The absence of ostracoderm material in facies S_{pt} of this facies association may be explained by the ephemeral nature of the flows.

Facies S_g consists of medium- to coarse-grained, well-sorted sandstone, with very rare pebbles. The uniformly bright red colour is in strong contrast to the duller shades of facies S_{pt}. Units commonly exceed 15 m in thickness (Photos 2 and 36), but exposure is limited on account of their weakly cemented, friable nature. Large-scale cross-bedding is the predominant sedimentary structure, with sets up to 6 m thick (Fig. 32). McCabe (1977, p. 275) used the term "giant" for sets over 3 m thick. Planar cross-sets predominate (10 out of 13 sets measured), although some of the thicker ones could be trough sets with a large radius of curvature. Cosets of planar cross-strata are tabular or wedge-shaped in sections parallel to foreset dip (Photo 37), while trough sets are mainly solitary, and foreset dip ranges

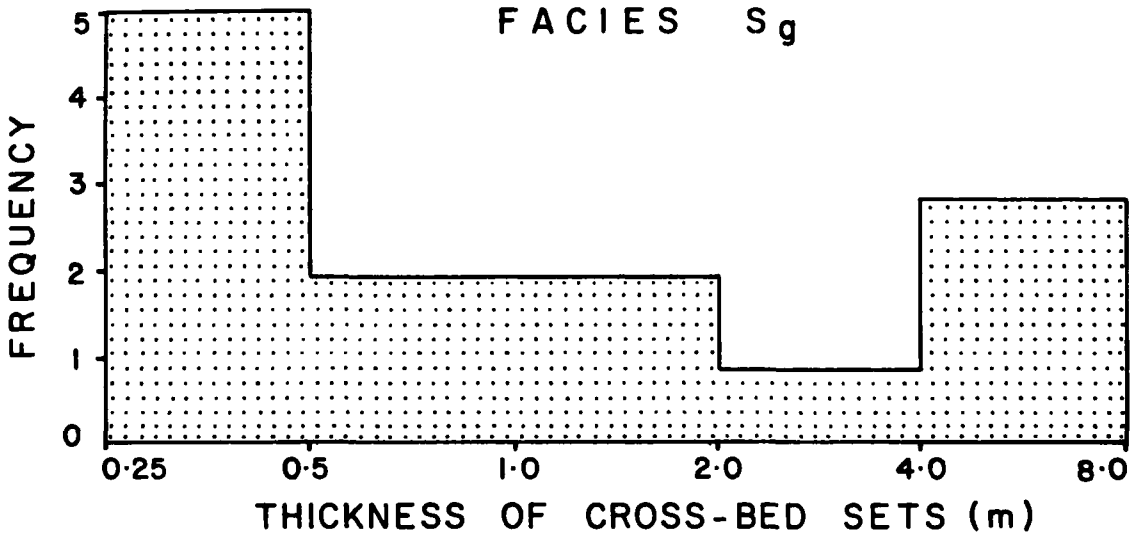

Fig. 32. Cross-bed thickness in facies S_g , Loc. 5.

from 10-33° with a mean of 22.5° (12 measurements). The cross-beds are interspersed with rare thin units of laminated mudstone (Photo 38), but no cyclicity was observed, and the irregular erosion surfaces with intraclast lags, characteristic of the Peel Sound fluvial associations, are apparently absent. An important feature of the facies is the anomalous northwestward paleocurrent orientation, approximately at right angles to the paleoflow data from other units of the clastic wedge (Fig. 28; Appendix B).

Giant cross-beds have been described from modern eolian dunes (e.g. McKee, 1966), and large-scale bedforms which may produce giant cross-beds have been noted in rivers such as the Brahmaputra (Coleman, 1969), and in subtidal environments (e.g. Stride, 1970). Large-scale sloping depositional surfaces are also characteristic of small deltas and fluvial point bars, but in both cases, surfaces tend to be obscured by superimposed smaller bedforms, and where the large-scale (epsilon) cross-beds of point bars are recognisable, they are low-angle and occur in fining-upward sequences (e.g. Cotter, 1971). In the present case, all environments except eolian and large-scale braided rivers may be eliminated in view of the overall terrestrial aspect of Peel Sound sedimentation, and the interbedding of giant cross-beds in member 3 with undoubted fluvial units (S_{pt}). Facies S_g was interpreted as the deposit of a large trunk river by Miall and Kerr (1977, p. 103-4). There is some precedent in the literature for

such an interpretation. The Brahmaputra contains sand waves up to fifty feet high (Coleman, 1969, p. 190), although figured cross sections show preserved sets of cross-strata less than four feet thick. Conaghan and Jones (1975) described cosets of cross-strata up to 5 m thick from the Triassic Hawkesbury Sandstone of Australia, and used the Brahmaputra as a modern analogue. (Ashley and Duncan, 1977, in a discussion of their paper, disputed a fluvial origin for the giant cross-strata, and tentatively suggested eolian action on a barrier bar-tidal delta complex for their formation). Giant cross-bed sets up to 40 m thick which occur within channels in the Upper Carboniferous of northern England were interpreted as the deposits of alternate, side-attached bars in distributaries cut into delta slope deposits (McCabe, 1977).

The weight of evidence, however, favours an eolian origin for facies S_g. Firstly, the general petrographic character of the facies is significant. Facies S_g is well sorted and is almost devoid of pebbles, both features typical of modern dunes (Glennie, 1970, p. 11). The extreme scarcity of pebbles is virtually inexplicable if the facies is fluvial, for pebbles are abundant in the interbedded facies S_{pt} (Photo 33), and if facies S_{pt} represents the deposits of streams tributary to the trunk river (Miall and Kerr, 1977), pebbles transported into the trunk river should at least have accumulated locally in scours or bedform troughs, even if not transported

by flows capable of producing the 6 m cross-bed sets. The sandstone is also relatively uncemented, which accords with Glennie's (1970, p. 12) observation that water-lain sediments in deserts are commonly cemented as the result of evaporation, in contrast to eolian sediments which remain relatively uncemented. The bright red colour of facies S_g is not in itself diagnostic of eolian deposition, but the contrast with the water-lain facies S_{pt} — grey to dull red in colour — is striking, and militates against a subaqueous origin for the bright red units; the more consistent saturation of sediments in a major river system with a high water table should lead to less oxidised (duller) sediments than those of ephemeral tributaries, while the reverse is seen in member 3.

Secondly, the cross-stratification shows features more in common with known eolian deposits. The large size and the variability in size of sets in facies S_g are both typical of eolian deposits (Reineck and Singh, 1975, p. 199). McKee (1966) observed that tabular sets were the predominant form in recent dunes at White Sands, New Mexico, with rarer wedge-shaped sets resulting from changing wind directions. Similarly, planar-tabular sets predominate in facies S_g, while the wedge-shaped sets figured by McKee (1966, Plate VIII C, D and E) are geometrically similar to the sets in Photo 37, with the cross-strata parallel to the inclined lower bounding surface — a type not mentioned by Allen (1963) in a study of fifteen commonly occurring types of cross-stratification. Rain prints,

rippled foreset surfaces, lag grains (Steidtmann, 1974; Walker and Harms, 1976), and avalanche lobes (Hunter, 1976) have all been reported from modern dunes, but were not observed in facies S_g. Their apparent absence may in part reflect the paucity of exposed foreset surfaces. The rarity of deformational structures characteristic of eolian dunes (McKee and Bigarella, 1972) is less easily explained, but is also a serious problem for a fluvial hypothesis. Avalanche faces of modern dunes are commonly close to the angle of repose (30-34°) and this has sometimes been used as a criterion for eolian origin. However, foreset dip depends on the type of dune, the amount of moisture and the location of the foreset within the dune complex (McKee, 1966; Steidtmann, 1974), and the steep upper part of the avalanche face tends to be removed by erosion. Thus the relatively low mean dip (22.5°) of cross-beds in facies S_g is not unusual for an eolian deposit.

Thirdly, many features typical of large-scale fluvial sedimentation are absent from facies S_g. Deposition in the Brahmaputra, for example, takes place as flow wanes and large-scale structures commonly contain evidence of rapid deposition (e.g. ripple-drift cross-lamination), not observed in facies S_g. Large-scale structures are also partly destroyed by lower stage flow. The scarcity of deformation structures is an even greater problem for a fluvial than for an eolian interpretation, considering Coleman's (1969, p. 217) remark

that "In every outcrop examined, some type of primary or secondary distortion was observed." At low stage in the Brahmaputra, scour pockets in the channel are filled with laminated silty clay, and foresets are commonly draped. In facies S_g, however, erosion surfaces and intraclasts are lacking, and fine sediment is confined to rare horizontal laminae of mudstone (Photo 38), with foresets consisting entirely of sandstone.

Finally, alternation of fluvial (wadi) sediments and eolian sands, with facies showing abrupt contacts and different transport directions , is typical of basin margin deposits in modern deserts (Reineck and Singh, 1975, p. 211-212). Norris and Norris (1961) and Sharp (1966) described eolian dunes closely associated with ephemeral fluvial systems in California, and Sellards (1923) noted the occurrence of localised dunes on the Red River flood plain. Large-scale cross-stratified red sandstones of probable eolian origin in the Devonian of southwest Ireland (Horne, 1975), are laterally equivalent to conglomeratic alluvial fan deposits and interbedded with fluviatile sediments of ephemeral stream type. While such evidence is circumstantial, it lends credence to the interpretation of eolian deposits in member 3, since the red sandstone is abruptly interbedded with undoubted fluvial pebbly sandstone (S_{pt}) and in part is laterally equivalent to the fan conglomerates of members 2 and 4 (Fig. 5).

In summary, the sedimentological evidence collectively

is most easily reconciled with an eolian origin for the giant cross-beds, whereas there are serious problems with a fluvial interpretation.

Summary

In the clastic wedge on Somerset Island, sedimentary facies (siltstone and sandstone) of alluvial plain environments can be grouped into six facies associations, the first five of which consititute most of the upper member of the Somerset Island Formation and member 1 of the Peel Sound Formation. Associations 1-3, with siltstone predominant, were deposited in coastal flood basin environments with limited marine connections; ephemeral pools and more persistent bodies of standing water were present locally. The overlying associations 4-5 consist mainly of sandy braided channel alluvium with minor flood basin sediment, with facies sequences non-cyclic (proximal high slope type) or cyclic (distal type). In sections adjacent to the Boothia Uplift, the sandstones of member 1 of the Peel Sound Formation are overlain abruptly by conglomerates of member 2, but further east in the Cape Anne syncline, member 1 passes up into ephemeral braided stream deposits interbedded with thick units of eolian sandstone (association 6, member 3). Facies associations show some localisation (Fig. 33), but their geographic relationships cannot accurately be reconstructed. The rise of the Boothia Uplift

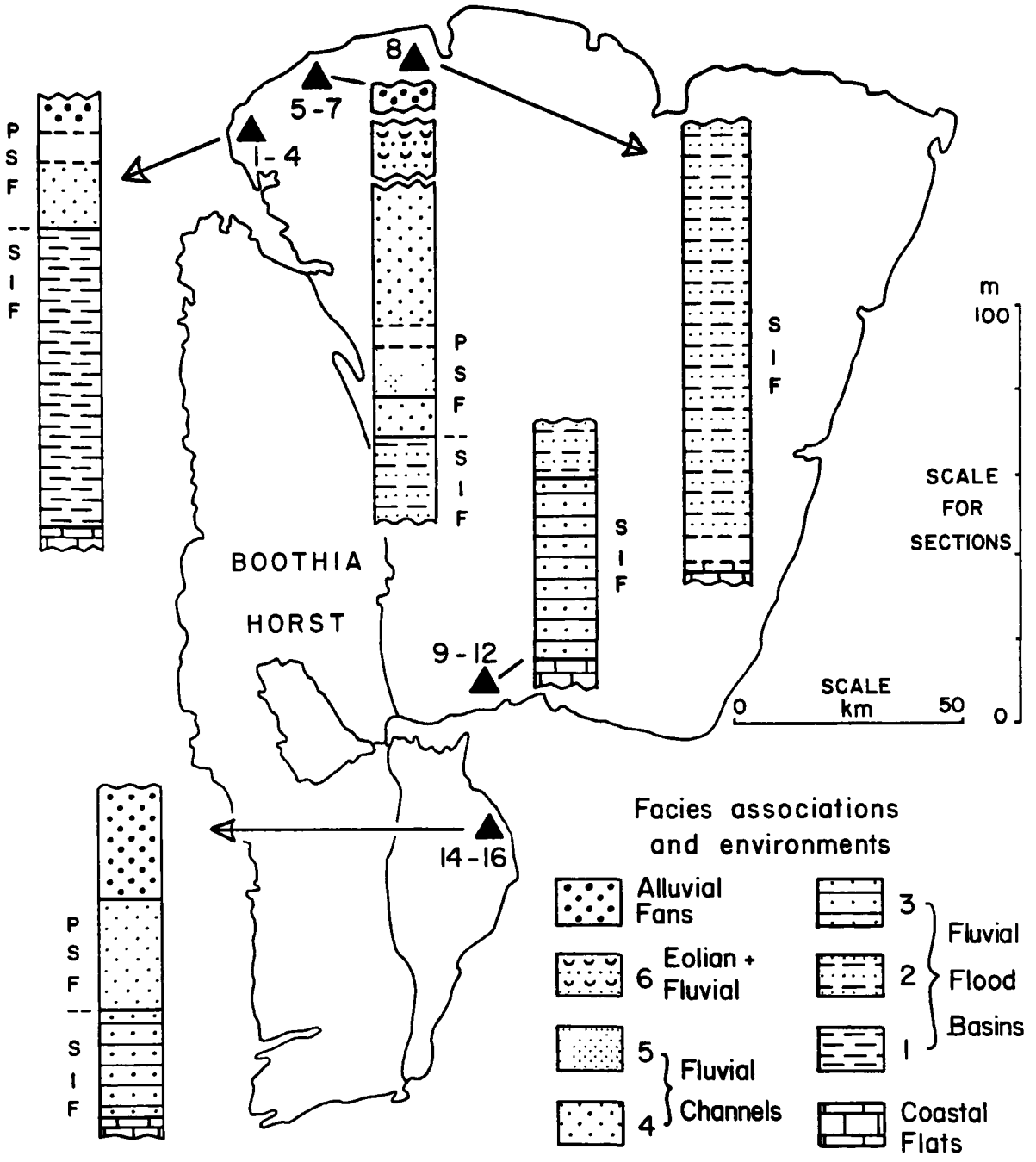

Fig. 33. Sequence of facies associations in alluvial plain sediments on Somerset Island.
Columns to scale but covered intervals condensed.
SIF and PSF = Somerset Island and Peel Sound Formations.

resulted in a general coarsening upward of successive associations as the alluvial plain advanced eastward. Paleocurrent data indicate consistent derivation of sandstones from the uplift (Fig. 28) with the exception of the eolian dunes which show a northward direction of transport.

26. Interbedded sandstone and siltstone (facies S_{ib}), with load structures (l) and lenticular layers. Unit G73J-51, Loc. 9.

27. Graded sandstone (facies S_{gr}). Layers of medium-grained sandstone, commonly lenticular, show low-angle cross-lamination (c) and erosional bases (e). Pen 15 cm long. Unit G74G-45, Loc. 2.

28. Ostracoderm material in graded sandstone (facies S_{gr}). Bedding plane shows convex-up shields of traquairaspidids (t), a large cyathaspidid (c) and heterostracan fragments. Matchbox 4.5 cm long. Section G74G, Loc. 2.

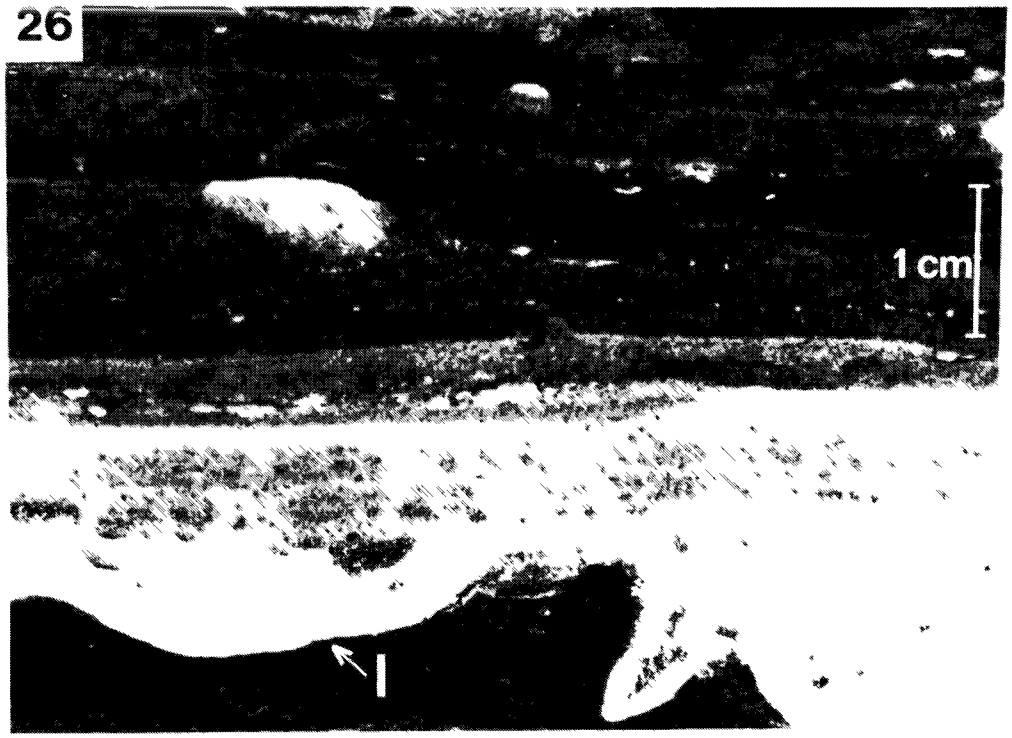
26
1 cm
l

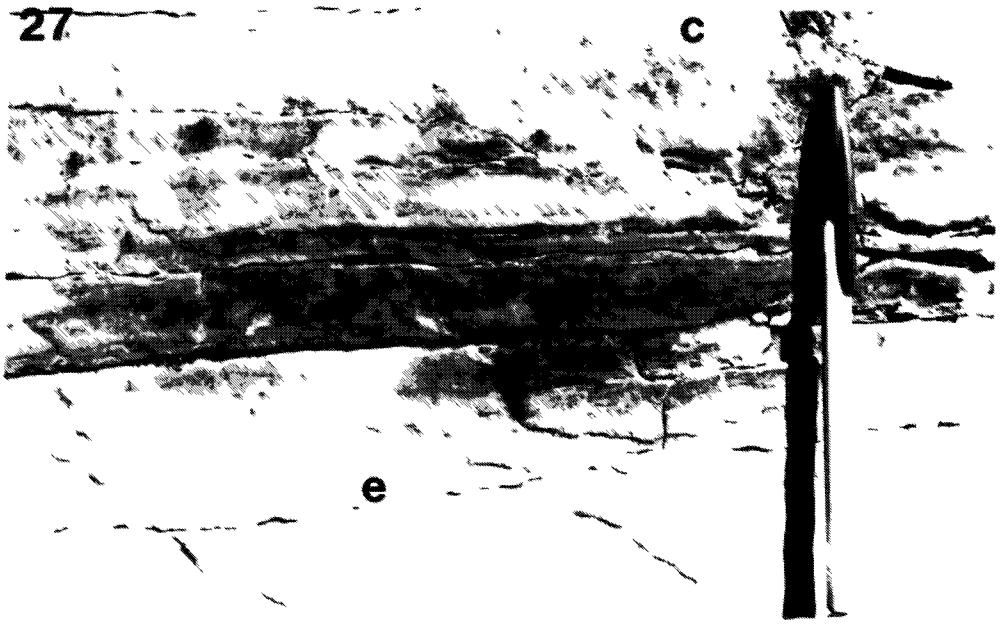
27
c
e

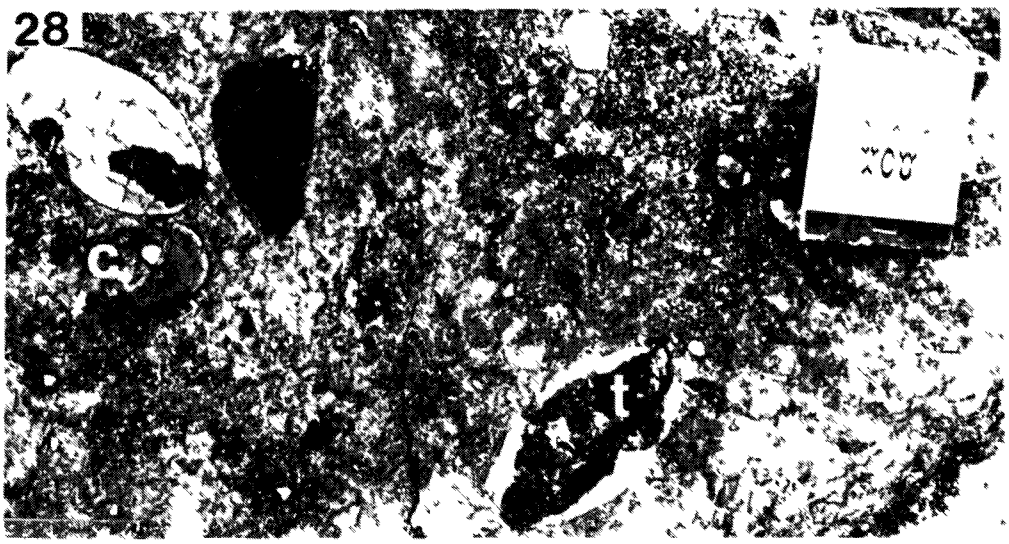
28
c
t

29. Large-scale trough cross-stratified sandstone (facies S_{pt}), showing foresets, with variable dip, commonly outlined by weathered-out intraclasts. Troughs are erosionally based and die out laterally. Facies S_h above. Notebook 25 cm long in upper left. Unit G76B-9, Loc. 6.

30. Shallow scours in facies S_{pt}. Cliff section is parallel to paleoflow direction. Scours contain cross-strata. Andrew Miall for scale. Section G76B, Loc. 6.

29

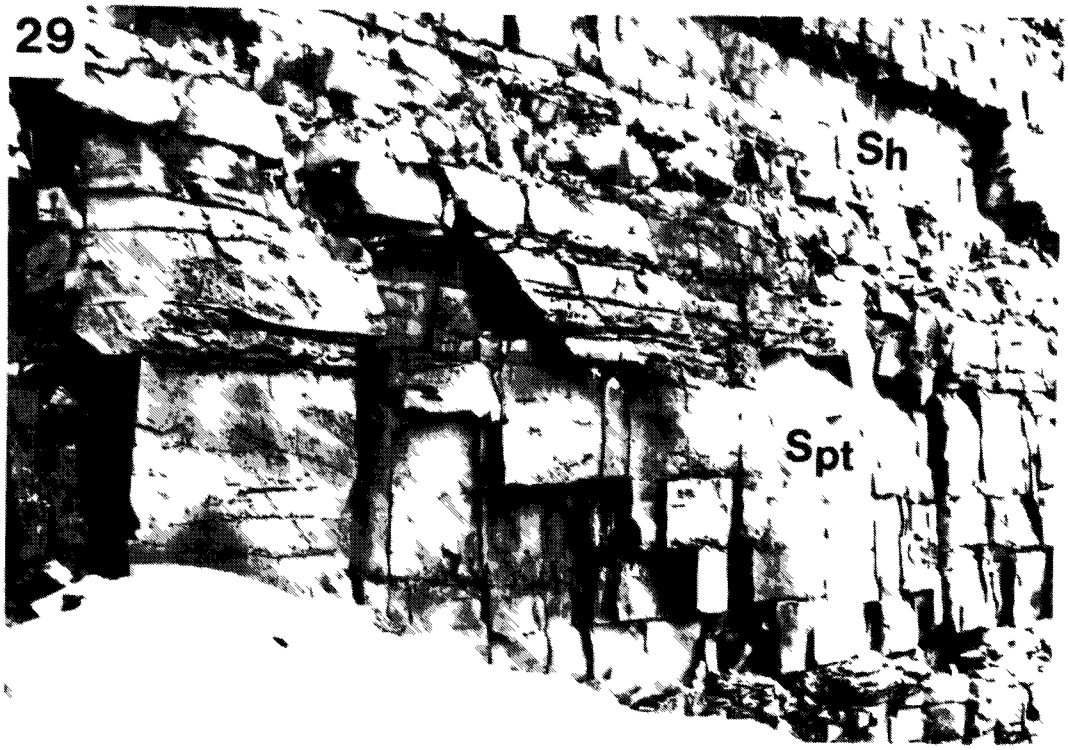

30

31. Fining-upward cycles in Peel Sound Formation member 1. Cycle A is shown with facies codes (see Table 3). Section G73B, Loc. 15.

32. Lateral continuity of units in fluvial cycles. Cycles do not weather distinctively due to low F_m%. Section G76B, Loc. 6.

31

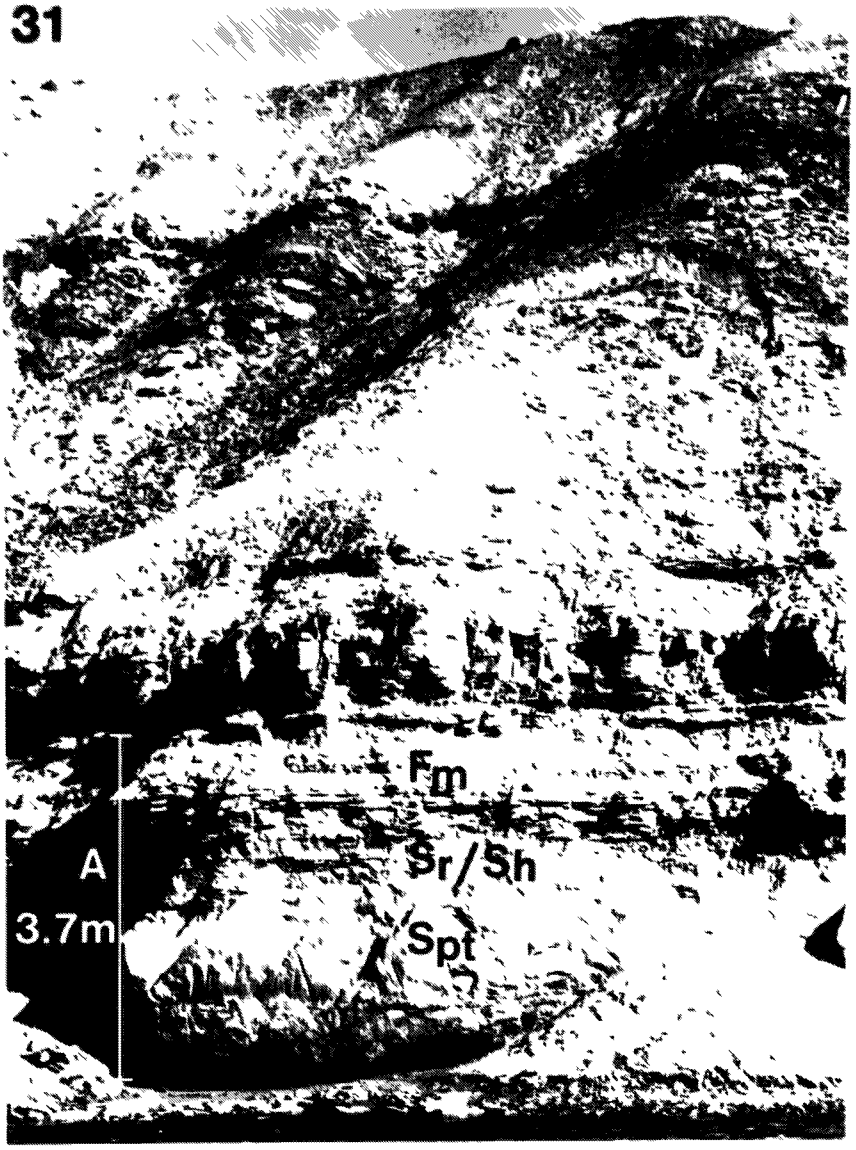

32

33. Facies S_{pt} overlying giant cross-stratified sandstone (S_g). Note erosional contact and pebbles in facies S_{pt}. Brian Rust for scale. Peel Sound member 3, Loc. 5.

34. Erosional contact between facies S_{pt} and S_g in Peel Sound member 3, Loc. 5. Hammer 28 cm long.

35. Current crescent (C) and primary current lineation (L) in facies S_{pt}. Crescents infilled with pebbles. Scale is 30 cm long. Loc. 5.


33

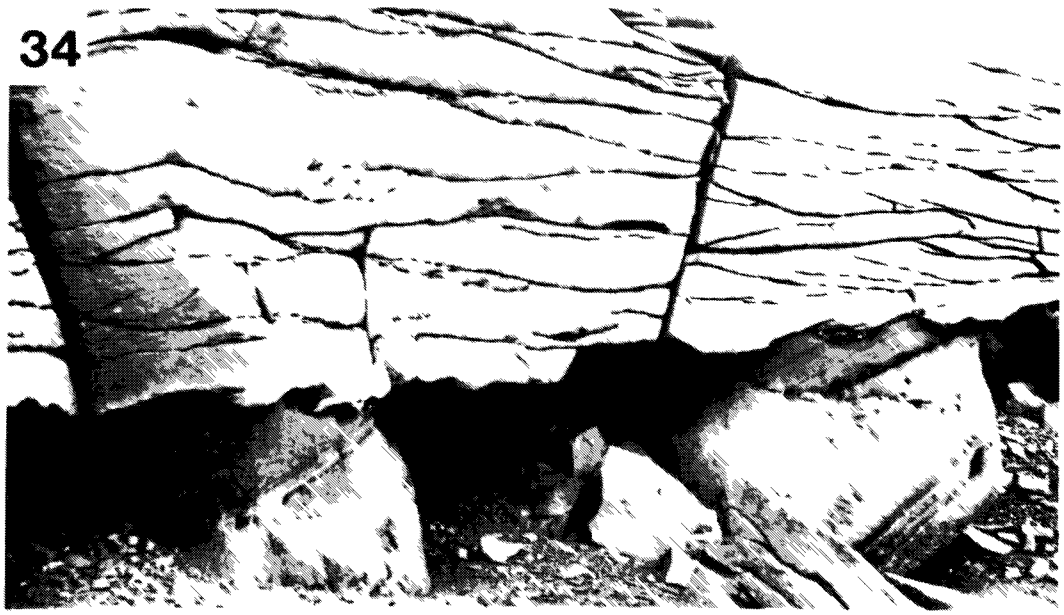
34

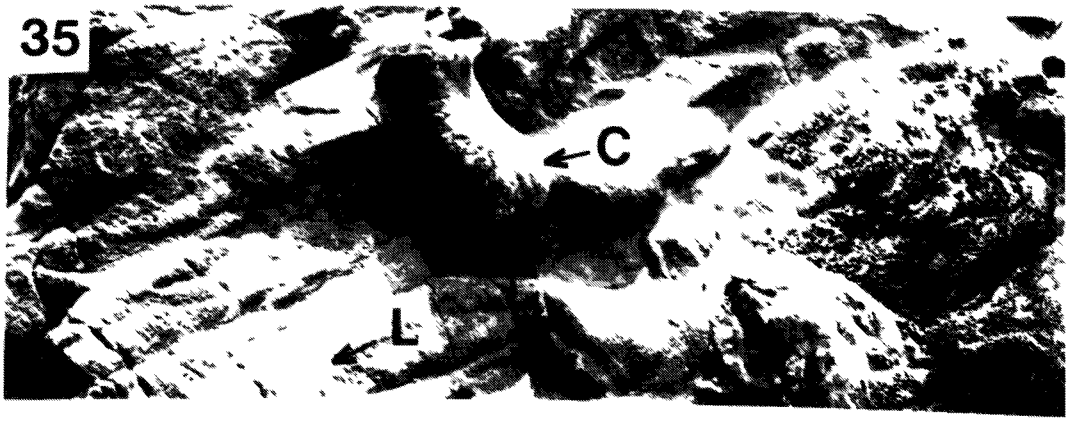
35
C
L

36. Crags formed in facies S_g. Peel Sound member 3, Loc. 5.

37. Large-scale planar cross-stratification in facies S_g, Loc. 5. Basal contact of sets is planar, erosional and inclined, with cross-strata (lithologically homogeneous) parallel to lower bounding surface of set. Hammer 28 cm long.

38. Planar cross-stratified red sandstone interbedded with laminated white mudstone in facies S_g. Hammer 30 cm long. Loc. 5.

36

37

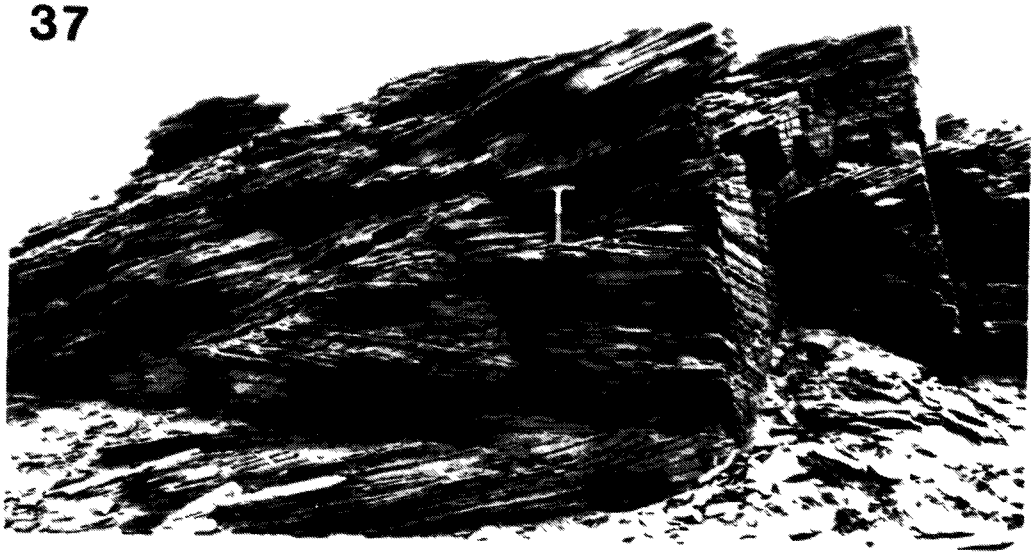

38

CHAPTER 4. ALLUVIAL FAN SEDIMENTATION

Stratigraphy and general setting

Members 2 and 4 of the Peel Sound Formation in the Cape Anne syncline (Table 1) were examined at Localities 1, 4 and 5 (Fig. 2), and are composed mainly of buff conglomerate. The conglomerate of member 2 consists largely of buff-weathering dolostone and red quartzite clasts in a matrix of sand-sized dolomite and quartz. It is better cemented and paler in colour than the conglomerate of member 4, which also contains igneous and metamorphic clasts in a matrix of sand-sized quartz. At Cape Garry (Localities 14 and 15), conglomerate lithologically similar to member 4 in the Cape Anne syncline rests conformably on sandstones of member 1. The conglomerate members are very uniform lithologically, averaging 90% massive conglomerate and 10% sandstone in the five sections measured.

Coarse gravel occurs in present-day alluvial fans, braided rivers, beaches, and in deep sea and glacial environments. On Somerset Island, the conglomerates lie adjacent to the Boothia Uplift, and in the Cape Anne syncline, they pass laterally eastward into the alluvial plain sediments of members 1 and 3 (Fig. 5). In vertical sections through the clastic wedge, the conglomerates overlie a succession which generally coarsens upwards from tidal carbonates to fluvial

sandstones (Chapters 2 and 3). Thus the sedimentary context suggests alluvial fan or near-source braided stream deposition. On Prince of Wales Island, conglomerates of the Peel Sound Formation showing similar stratigraphic relationships were interpreted as alluvial fan deposits by Miall (1970a).

Deposition of modern alluvial gravel

The stratigraphic relationships of the conglomerate members indicate deposition on alluvial fans or in gravel bedload rivers. Studies of modern terrestrial gravels have concentrated on those of arid and semi-arid climatic regions such as the southwestern U.S.A. (Bull, 1964; Bluck, 1964; Denny, 1965; Hooke, 1967), and on those of humid regions associated with fluvioglacial activity such as the northern Rockies (Rust, 1972a; Gustavson, 1974; Smith, 1974; Boothroyd and Ashley, 1975; Hein and Walker, 1977).

On the fans of the southwestern U.S.A., active or abandoned braided channels ("washes") are the main geomorphic features, being commonly less than 1 m deep and 100 m wide. Near the fan apex, channels as much as 15 m deep are incised into the fan surface (Denny, 1965, p. 7-8). The deposits of the channel systems comprise gravel, sand and silt (Bull, 1972, p. 68). Debris-flows are important agents of transport and deposition, especially on the proximal parts of many fans (Hooke, 1967; Bull, 1972). The flows are of high

density (up to 2500 Kg/m^3: Curry, 1966), and exhibit laminar flow with dispersed particles supported by the strength of the matrix rather than by turbulence (Johnson, 1970; Fisher, 1971; Middleton and Hampton, 1973; Enos, 1977). The quasi-plastic behaviour of the flows prevents adjustment of the load by selective deposition, so that the flow "freezes" when frictional forces outweigh the effect of momentum (usually due to decreased slope or loss of water by infiltration). The sieve deposits described by Hooke (1967), although abruptly based and lobate in form, contrast with those of debris-flows in consisting of well-sorted framework gravel. They are water-laid deposits which form on fans poor in silt and clay, so that infiltration results in rapid deposition. Most debris-flow deposits consist of abruptly based sheets of unstratified, poorly sorted gravel with the clasts supported by the matrix (Walker, 1975a, p. 155). Clasts usually show random or sub-horizontal orientation of maximum projection planes, but commonly show vertical orientation where flows are viscous (Bull, 1972, p. 70-71), or in the later stages of flow, as noted in distal lobes of debris-flows in the Donjek valley, and in finer flows in the Carboniferous Cannes de Roche Formation of Gaspé by Rust (in press). Discharge on fans in arid climates is extremely ephemeral. Rather than feeding permanent streams beyond the fan, most flows lose water rapidly by infiltration, and channel systems on the fan surface tend to die out at the distal fringes of

the fan. The fan gravels commonly interfinger with finer sediments of the valley-floor (Bull, 1972, p. 77-8), although they may pass laterally into coarser valley gravels.

In contrast to the southwestern U.S.A., discharge variation in the northern Rockies is seasonal, due to heavy summer rains on the mountains and meltwater from winter snow and permanent ice-fields (Gustavson, 1974). Diurnal fluctuation due to melting of ice on warm, sunny days is important in rivers such as the Kicking Horse (Hein and Walker, 1977). In consequence, many channel systems exhibit semi-permanent flow. Braided systems in these areas contain abundant longitudinal bars, described by Rust (1972a) from the Donjek river of the Yukon, and by Gustavson (1974) and Boothroyd and Ashley (1975) from rivers in Alaska. Longitudinal bars consist of poorly sorted framework gravel with weak horizontal stratification, and the imbricated clasts show A-axes predominantly transverse to flow. Rust (in press) suggests that the bars are probably large-scale bedforms in equilibrium with peak flow conditions, in contrast to the view of Leopold and Wolman (1957) that longitudinal bars form by deposition of coarse bedload material in mid-channel at falling stage. Sand accumulates in minor channels and as wedges at bar margins (Rust, 1972a). Transverse or linguoid bars, generating planar cross-bed sets by migration of avalanche faces, are more important in finer grained, more distal outwash sediments. Debris-flows are common (Winder,

1965). Ryder (1971) observed that debris-flow deposits are most abundant in the proximal parts of fans (now virtually inactive) in British Columbia.

A general depositional model for modern terrestrial framework gravels and their ancient equivalents has been outlined by Rust (in press), using criteria such as the dominant internal structure of the beds, imbrication, cyclicity, and the presence of fines and debris-flow deposits (Fig. 34). The proximal high slope setting is typical of the near-source parts of the alluvial fans described above, with debris-flow deposits interbedded with sheets of poorly stratified water-laid deposits. The proximal low slope group includes deposits of the lower parts of fans and the upstream reaches of braided rivers such as the Donjek, and apart from the rarity of debris-flow deposits, resembles the high slope group. The "Scott" type of braided river deposit (Miall, 1977) resembles these two groups. Distal low slope deposits such as those of the downstream reaches of the Donjek are characterised by trough cross-stratified framework gravel of finer grain-size, more ordered facies sequences (cyclicity) and some primary mudstone in overbank areas. These deposits resemble the "Donjek" type of Miall (1977). The Upper Paleozoic Cannes de Roche and Malbaie Formations of Gaspé were used by Rust as ancient examples of these three types of framework conglomerate.

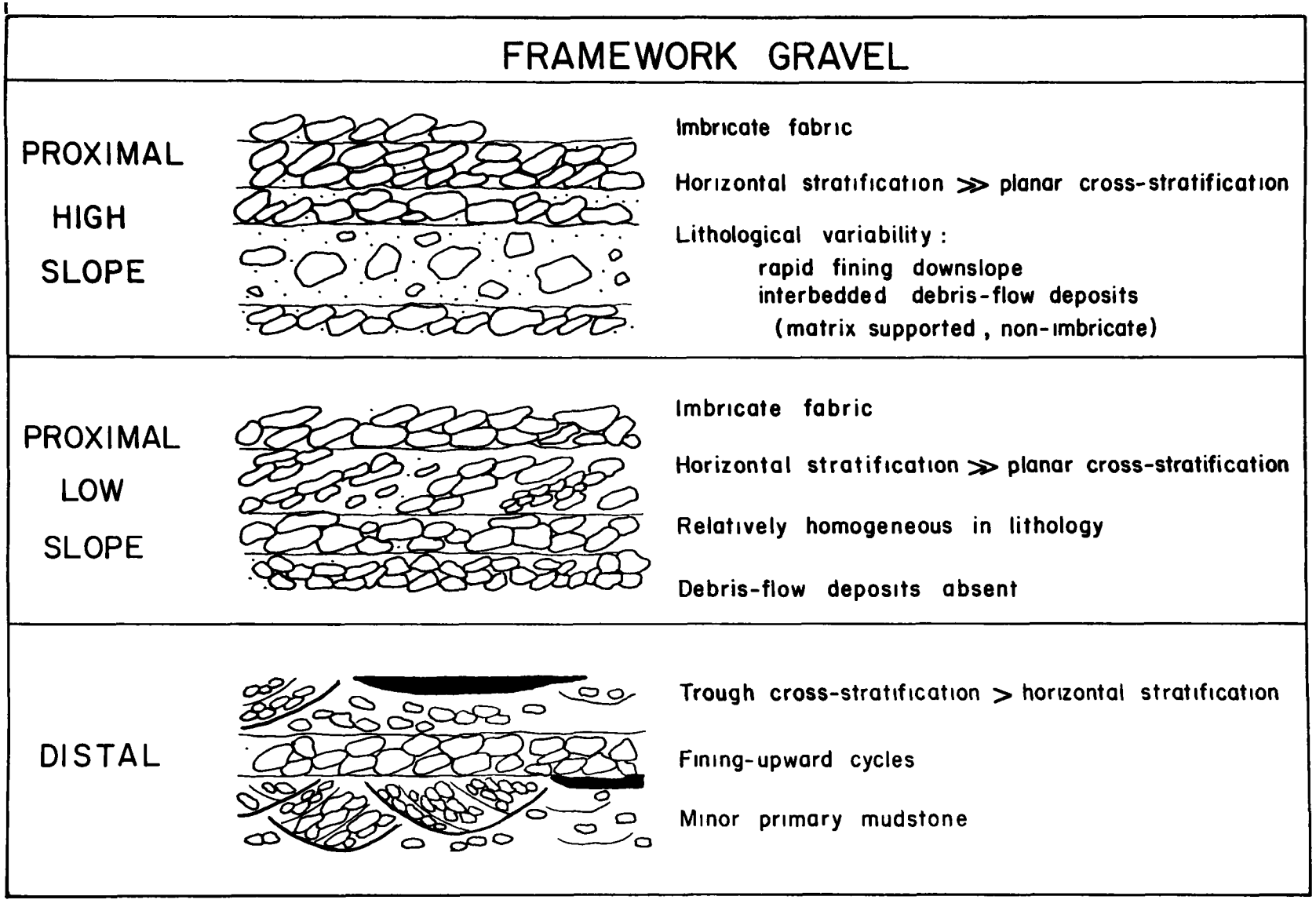

Fig. 34. Depositional model for alluvial framework gravel. Adapted from Rust (in press), Table 2.

Facies description of Peel Sound members 2 and 4

Massive conglomerate (G_m)

Photo 39 shows a typical unit of the facies. The poorly sorted framework conglomerate is composed of pebble- and cobble-sized clasts of massive and laminated dolostone, quartzite, and subordinate igneous and metamorphic rock types and chert. Clasts are rounded and of moderate sphericity. The sandstone matrix consists of dolarenite and quartz. The following three types of conglomerate are present:

1) Coarse conglomerate (73% of sections), with clasts averaging 5-10 cm in long axis, maximum 35 cm, and with quartzite forming more than 25% of the clasts (dolostone less than 75%) in a matrix of dolarenite and quartz sandstone (Photo 39).

2) Fine conglomerate (17% of sections), with clasts averaging 2-3 cm, maximum 10 cm, and with dolostone forming more than 90% of the clasts in a dolarenite matrix (Photo 40).

3) Openwork conglomerate (less than 1%), well sorted, with clasts averaging 1-2 cm.

Bedding is usually defined by variation in clast size and composition, and by changes in the proportion and nature of the matrix. Horizontal stratification is predominant but

poorly developed, so that subdivision of sections into units is often arbitrary, although, where recognisable, the units are commonly continuous laterally for several hundred metres. Sets of large-scale cross-strata (Photos 41 and 42) are rare and cannot be traced for more than 2 m laterally. A few erosionally based troughs about 50 cm deep are infilled with layers of conglomerate and sandstone. Photo 43 shows one large channel, about 4 m deep and 15 m wide, containing a basal layer of coarse, pebbly sandstone with a ?planar cross-bed set more than 1 m thick. The sandstone, containing numerous ostracoderm fragments, is overlain by coarse conglomerate with weak horizontal stratification.

The moderate degree of sphericity of the clasts hinders recognition of internal fabric, but imbrication of both isolate and contact types (Laming, 1966) is common. A few ostracoderm fragments are present in the lowermost units and in the isolated channel noted above, the only fauna observed.

Sandstone (S_m, S_{pt}, S_r and S_h)

In the Cape Anne syncline, thin lenses of sandstone, abruptly or in some cases gradationally based, separate thick units of conglomerate (Photos 40 and 44). The sandstones are internally massive, laminated (with primary current lineation) or cross-bedded. In member 4 at Cape Garry, thicker units of pebbly sandstone are present (facies S_{pt} and S_m).

Sedimentation of conglomerate in the Cape Anne syncline

In a general discussion of conglomerates, Walker (1975a) listed sorting and size distribution, fabric, stratification and grading as major descriptive features with significance in terms of depositional processes. These aspects of the Peel Sound conglomerates will be discussed below.

Sorting and size distribution

The importance of a clast-supported or matrix-supported texture in interpreting processes of transport has been emphasised by Walker (1975a, p. 135-6). Clast support (framework) indicates that the current was transporting a gravel bedload with finer sediment in suspension above the bed, while matrix support implies transport of a mixed load of gravel and fines. In the present study, the term "clasts" is used for particles larger than granule size (greater than 4 mm).

What percentage of clasts is necessary to form a framework? A consideration of the packing of equal-sized spheres shows that they occupy 52-74% by volume, depending on the tightness of the packing (Pettijohn, 1975, p. 73). More angular or inequidimensional grains will tend to pack better, so that the volume percentage of grains necessary to form a framework will be greater. Since most grain-size data is derived from sieving, clast content has usually been expressed

in terms of weight percentage. Plumley (1948) used the above volume percentages to calculate corresponding weight percentages for large spheres in a matrix of small spheres, finding that if the spaces between the small spheres are not infilled by still finer sediment, the spheres are in contact at 68-78% by weight. He concluded that sixteen samples of terrace gravel from the Black Hills, which averaged 80% of clasts by weight, were framework gravels with a matrix derived by infiltration between the clasts. In the Lafayette gravel of the south-central U.S.A. studied by Potter (1955), a group of nineteen analyses averaged 70.9% clasts by weight (range 59.6-81.4%), and by comparison with Plumley's data, Potter suggested simultaneous deposition of clasts and matrix (matrix support). Folk and Ward (1957, p. 7) considered 70% as the critical weight percentage (most of their samples from the Brazos River, Texas, lay in the 45-70% range and hence were probably matrix supported), and Dyer (1970) showed that grain-size parameters in samples from the Solent favoured 75% as a reasonable value for framework conditions. In general, volume percentage compares the volume of clasts to the total volume of sediment, while weight percentage compares the weight of the clasts to the weight of clasts and the matrix grains which occupy part of the remaining space. The volume percentage of clasts is thus lower than the weight percentage due to matrix porosity.

Grain size analysis is not possible for the indurated

conglomerate of the Peel Sound Formation, so that weight percentages are not readily obtainable. Instead, an estimate of clast percentage by area was obtained using a grid system of 100 points at 10 cm intervals, drawn up on the rock face by means of a measured length of string and a marker pen. One hundred points were found to be adequate for consistent results. Since clasts have relatively high sphericity (not strongly inequidimensional), areal percentage gives a reasonable estimate of volume percentage. The generally high sphericity and roundness of the clasts (Chapter 5) suggests that Plumley's volume estimate of 52-74% clasts is a reasonable indication of a framework, since the clasts do not tend to pack closely.

Fifty-five "point counts" on rock faces gave a range of clast percentage from 40-73% with a mean of 61.3% (standard deviation ± 7.5%). The conglomerates are interpreted as being predominantly clast supported, and excavation of several beds confirmed this (Photo 39). The matrix therefore filtered into spaces in the framework either as a result of deposition from steady flow in the wake of upstanding clasts (Einstein, 1968), or during deposition from fluctuating or waning flow when the clasts were no longer in motion. Beds in the lower range of clast percentage may have formed by simultaneous deposition of clasts and matrix, although Bluck (1967, p. 147-8) noted that backwash eddying on beaches may generate a matrix-supported texture by removing framework

clasts and replacing them with finer material. Clasts were thus transported mainly as bedload, and there is no evidence that debris-flows were a major agent of transport.

Walker (1975a and b) compared the size of clasts transported on the bed with the diameter of sand grains maintained in suspension by the same flow (Fig. 35). If matrix and clasts in a clast-supported conglomerate were not originally in hydraulic equilibrium, they will show misfit on the graph. Unfortunately, the poorly sorted nature of the conglomerates studied and the lack of grain-size analysis prevent identification of the largest suspended grain. In general, the coarse sand to fine granule nature of the matrix suggests hydraulic equilibrium with the pebble to small cobble grade of the clasts.

Fabric

Fabric is discussed in detail in Chapter 5. The terms used in describing the clasts are shown in Figure 36. Fabric data have a 360° distribution and cannot usually be analysed by ordinary linear techniques such as calculation of means and standard deviations. Curray (1956) outlined a method for the statistical treatment of such data. The mean direction of orientation of the elements is known as the vector mean, and the degree of preferred orientation is given by the vector magnitude, dependant on the spread of the data and the size of the sample. The significance level of the vector

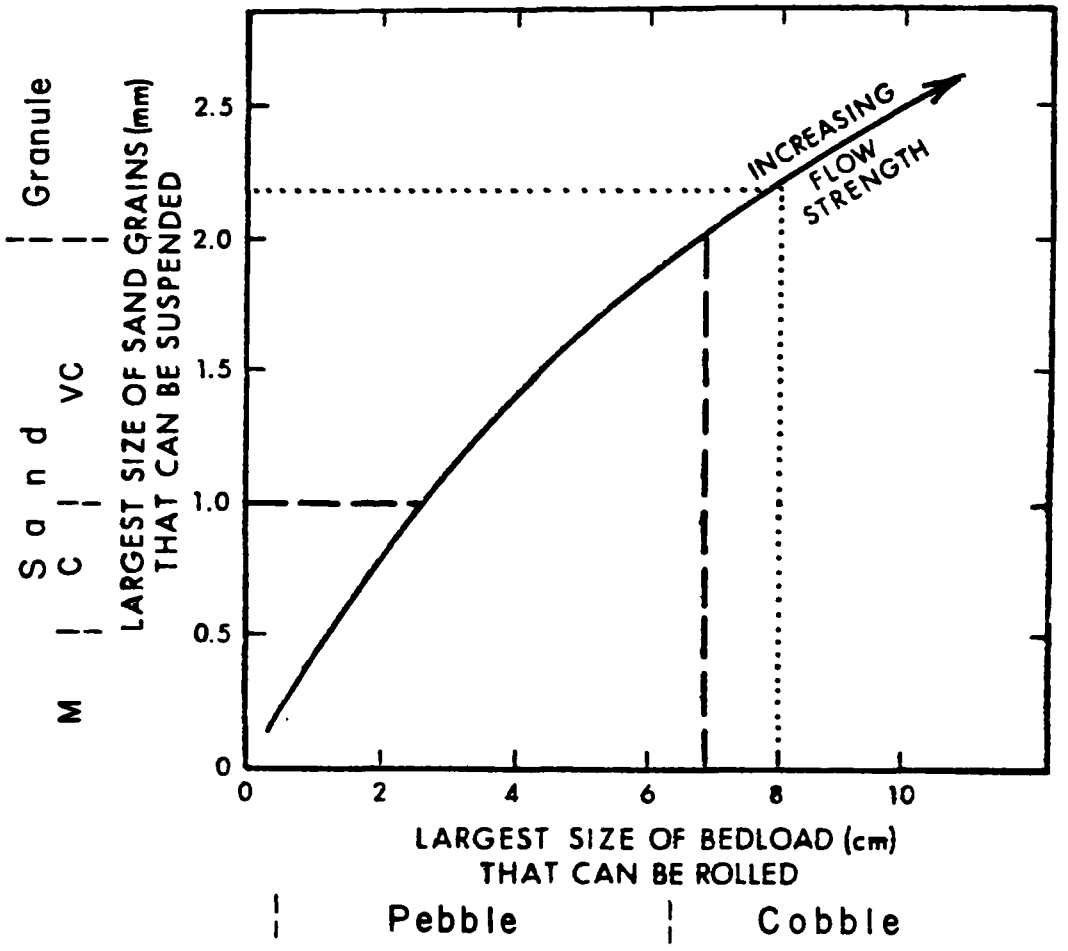

Fig. 35. Curve relating size of clasts transported by rolling to size of sand suspended by the same flow. For example, the dotted lines show simultaneous rolling of 8 cm cobbles and suspension of 2.2 mm granules. The dashed lines indicate a misfit between bedload and rolling of 7 cm cobbles, followed by a decrease in flow strength and subsequent infiltration of pore spaces by 1.0 mm sand. After Walker (1975a), Fig. 7-3.

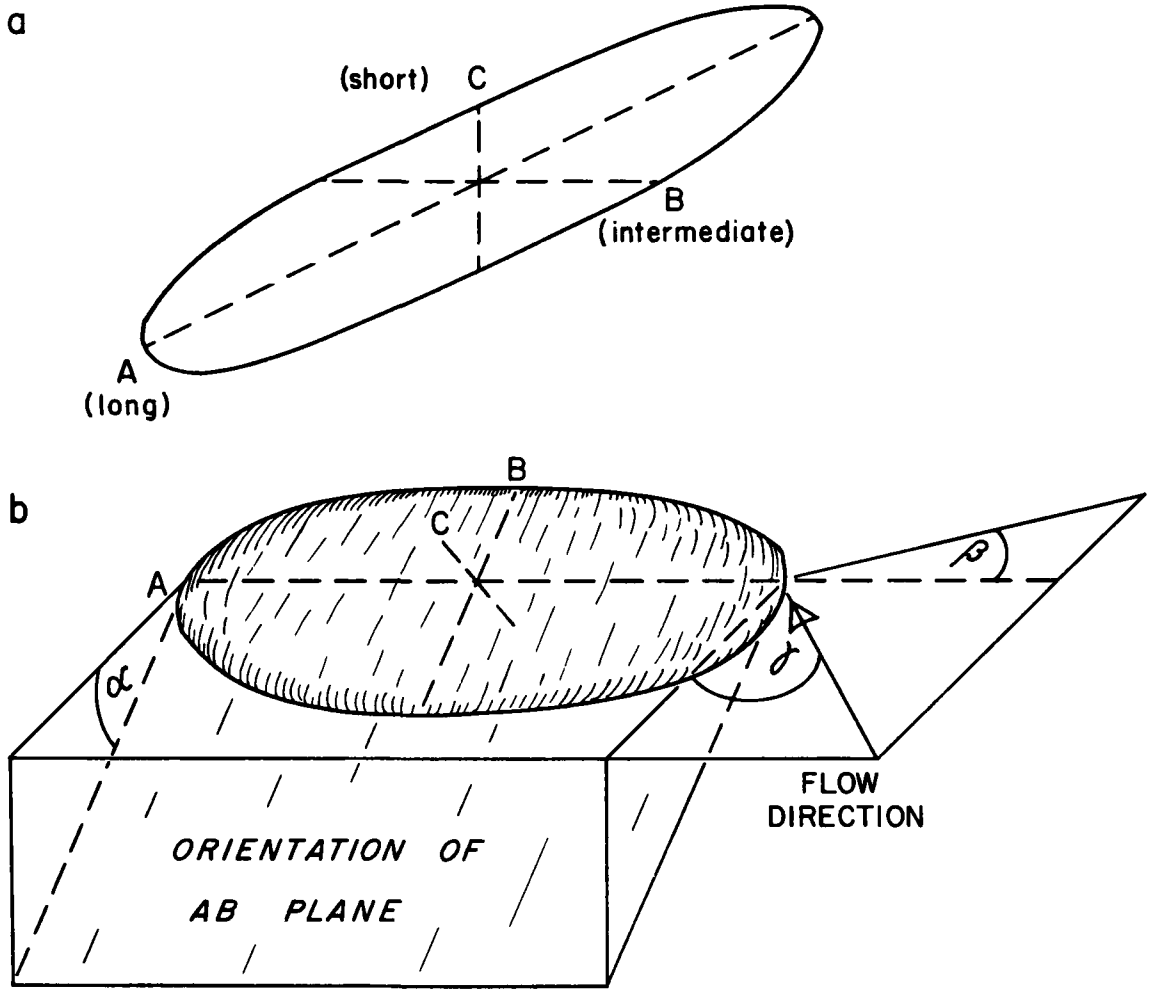

Fig. 36. Clast geometry (a) and orientation parameters (b)

magnitude is determined from the Rayleigh test, as described in Curray (1956). Different methods are necessary to analyse unipolar data, such as the AB dip direction, and bipolar data, such as the A-axis orientation. Computer programmes were used in analysis.

In general, studies of modern framework gravel suggest that current-normal orientation of the long axes of clasts results from bedload transport, while current-parallel orientation may be produced by saltation or suspension(Chapter 5). Many framework gravels, however, show little preferred orientation. In modern streams, the maximum projection (AB) planes of the clasts tend to dip upstream, resulting in imbrication, and this feature is well developed in many units of the Peel Sound Formation conglomerates (Photo 39). Figure 37 compares foreset dips of cross-strata in sandstone units of members 2 and 4 with the vector mean for AB dip direction of clast samples from conglomerate units. It is evident that clasts are dipping predominantly upstream, so that the orientation of mean AB dip of each sample may be used as an indication of flow direction for describing the A-axis orientation.

Fabric was studied in detail in eleven units of the Peel Sound Formation. The clast content of the beds studied ranges from 57-68% with a mean of 65%, suggesting that all are of framework conglomerate. A-axis orientation, although poorly defined, shows current-parallel, current-normal and oblique

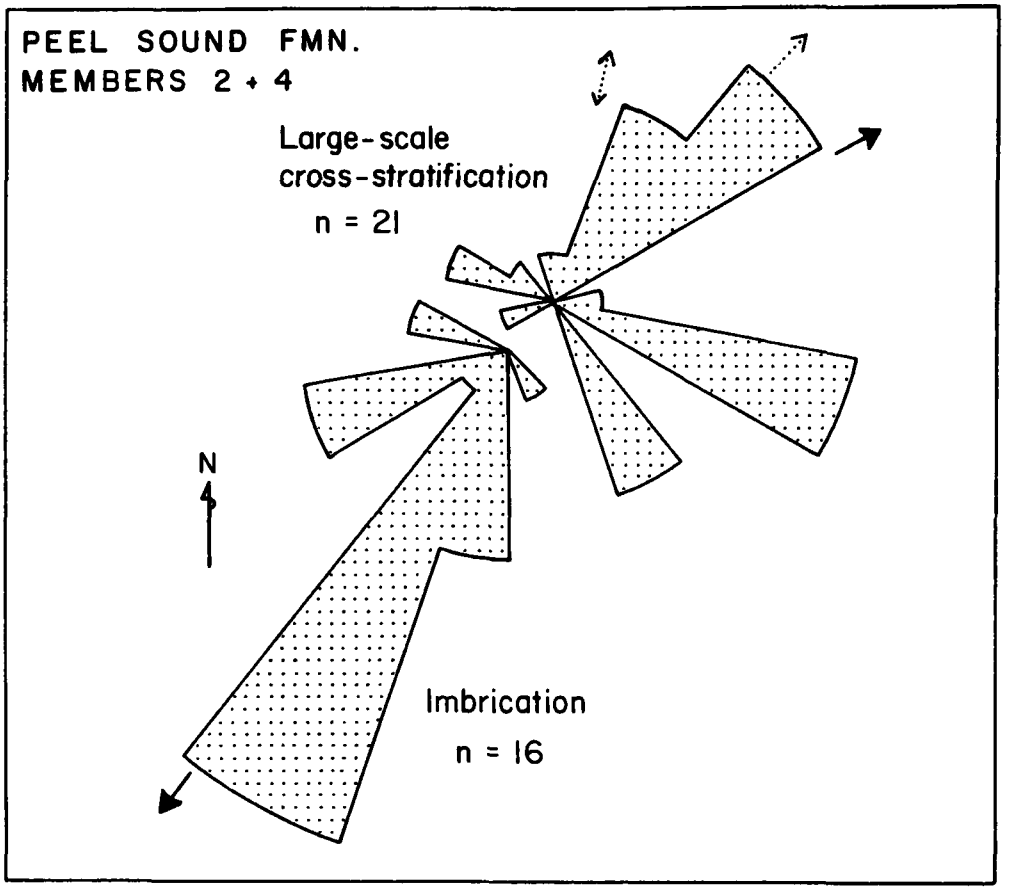

Fig. 37. Paleocurrent data from Peel Sound members 2 and 4 in the Cape Anne syncline. Large solid arrows show statistical vector means. Imbrication: mean AB dip direction of 16 clast samples (dip in opposite sense to flow). Cross-beds: foreset dip directions of large-scale ?planar cross-beds. Primary current lineation (one): two-headed arrow. Channel (one, Photo 48): single-headed arrow indicates plunge of channel axis.

orientations predominating in different samples (Appendix C1). High-energy flow with both bedload and suspension transport is implied.

Stratification and grading

Poorly developed horizontal bedding with imbricate clast fabric is the main type of stratification observed in the conglomerate (Photo 40). Such stratification is typical of longitudinal gravel bars in modern proximal high and low slope settings (e.g. Rust, 1972a; Gustavson, 1974). Hein and Walker (1977) observed that longitudinal bars in the Kicking Horse river formed under conditions of high fluid and sediment discharge. In a few units of member 2, horizontally stratified coarse conglomerate passes laterally into large-scale cross-strata including cross-beds of open-work conglomerate (Photos 41 and 42). The cross-strata closely resemble the deposits of small avalanche faces which develop at the downstream and lateral margins of longitudinal bars in proximal outwash, and consist of finer grained sediment than the bars (a sand wedge at a lateral bar margin is shown in Fig. 4 of Rust, 1972a). Similar cross-strata in the proximal low slope conglomerate of the Malbaie Formation of Gaspé were interpreted by Rust (in press) as deposited on the avalanche faces of longitudinal bars. In the Malbaie, the facies constitutes less than 20% of the total conglomerate, and the individual cross-bed sets occupy a relatively small

volume (averaging 125 m^3), passing laterally into horizontally stratified conglomerate, the main facies. Foreset dip directions of the Malbaie cross-strata show high directional variance, consistent with deposition on the lateral margins of bars.

The cross-strata of the Malbaie conglomerates commonly contain openwork conglomerate (pers. comm. B.R. Rust, 1977). Potter (1955, p. 12-13) observed thin cross-beds of fine openwork gravel in the Lafayette gravel, interpreted as fluvial, and openwork gravel occurs in modern braided river deposits (McDonald and Banerjee, 1971; Martini and Ostler, 1973; Smith, 1974). Smith (1974, p. 221) interpreted the texture as the result of deposition of gravel during high flow when most fines are in suspension. Eynon and Walker (1974, p. 61-2) noted that bar-front gravels in a Pleistocene braid bar in southern Ontario contain less sand than most other parts of the bar, and this may be explained in part by the tendency for sand to be swept downstream from the bar crest rather than contributing to the foresets. Although the origin of openwork texture is poorly understood, the presence of openwork in cross-strata of the Peel Sound conglomerates is consistent with bar-face deposition in a proximal braided system.

Channels are not common in the conglomerates of the Peel Sound Formation. In view of the extensively channelled nature of proximal braided systems, this might seem to be at variance with the previous interpretation of a proximal high

or low slope setting. However, the longitudinal bars described by Boothroyd and Ashley (1975) in Alaskan outwash are 30-100 m long, while those of the proximal Donjek are 150-450 m long (Rust, 1972a); at the scale of outcrop usually observable in ancient conglomerates distinct channels would probably be less evident than the more continuous units of horizontally stratified conglomerate, especially where lithological contrast is poor. In the Peel Sound Formation, the large channel shown in Photo 43 may have been a major distributary, possibly incised as a fan-head trench on the upper part of an alluvial fan.

Sedimentation units are often difficult to recognise in the poorly stratified conglomerate, and consistent changes in grain size are not obvious, although both coarsening- and fining-upward tendencies were observed. Some conglomerate beds grade up into sandstone, which was probably deposited from waning flow in small hollows on the bar surfaces and contains structures typical of bedforms of the lower flow regime or the transition to the upper flow regime (lineated plane beds, dunes and ripples). Intraclasts and beds of siltstone were not observed, suggesting that overbank areas and channel fill sequences were absent from the depositional area. The degree of preferred orientation (vector magnitude) of conglomerate and sandstone paleocurrent data is strikingly different. Grouping the vector means of AB dip direction (imbrication) for the clast samples shown in Figure 37 gives a

vector magnitude of 80% at a significance level of less than 10^{-4}. This relatively low directional variance for the conglomerate fabric suggests formation at high stage with minimal deflection of the flow from the downslope direction (Bluck, 1974; Rust, in press). In contrast, the sandstone cross-beds give a vector magnitude of only 43% at a significance level of less than 0.02, and probably formed at lower stage, when flow diverged around emergent structures.

In summary, the stratigraphic context of the conglomerates indicates the deposition of coarse detrital wedges adjacent to the mountain front of the Boothia Uplift, probably as a series of alluvial fans. The sedimentology suggests deposition in a proximal low slope setting, where braided channel systems constructed longitudinal bars of imbricate framework gravel. Debris-flow deposits have not been observed. The deposits closely resemble those of braided outwash systems of the northern Rockies, and further resemble them by passing distally into sandy braided alluvium (facies association 4, Chapter 3). Distal low slope deposits were not observed in the Cape Anne syncline.

Sedimentation of conglomerate at Cape Garry

Polymict conglomerate of Peel Sound member 4 constitutes the top 30 m of section at Locality 14, Cape Garry. Framework pebble conglomerate (G_m) is present, but the section

consists mainly of medium to coarse sandstone with pebbles isolate or in thin bands. Facies S_m consists of massive sandstone and pebbly sandstone, while facies S_{pt} (unlike previous associations) is mainly planar cross-stratified, with some sets extending laterally for more than 10 m. Erosion surfaces strewn with intraclasts and pebbles outline channels as much as 1 m deep (Fig. 38a), which contain units of framework conglomerate. Lateral variability on a smaller scale is shown in Figure 38b, in which thin beds and lenses of large- and small-scale cross-stratified sandstone, laminated sandstone and framework conglomerate are interbedded. Sigmoidal cross-bed sets and ripple-drift cross-lamination indicate periods of rapid deposition. Facies similar in lithology and lateral variability were described from sediments of the Donjek River (facies F of Williams and Rust, 1969. p. 668 and Fig. 19), and interpreted as the deposits of very small-scale channel and bar systems. The only vertical sequences observed are of the type:

$$ES \longrightarrow S_m/S_{pt}$$

Ostracoderm material was not observed.

The section shows characteristics intermediate between the proximal and distal low slope types for framework conglomerate (Fig. 34). Facies S_m probably resulted from deposition of sand and gravel in longitudinal bars, while planar cross-stratified sandstone of facies S_{pt} suggests deposition in sandy foreset bars.

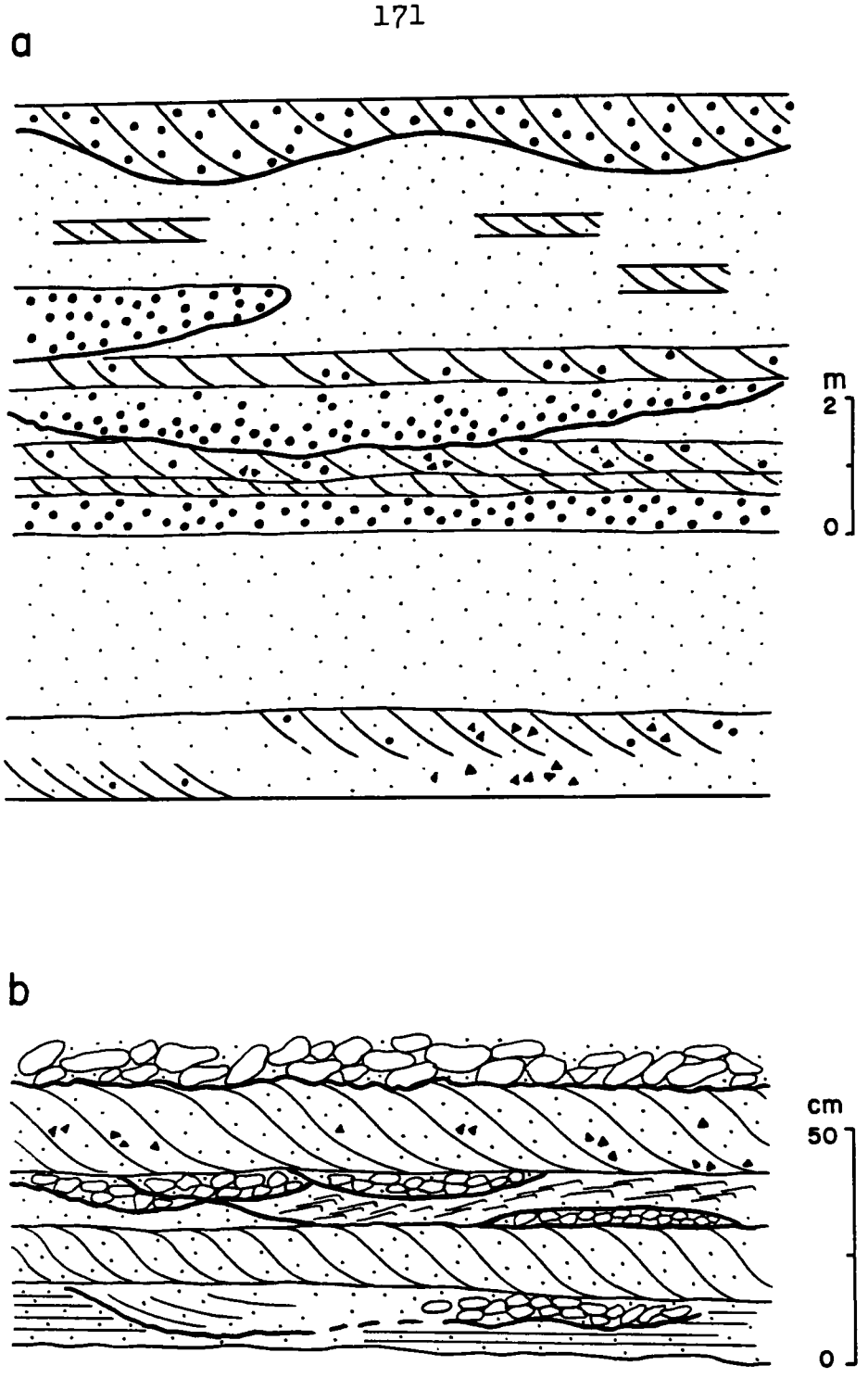

Fig. 38. Field sketches of channels in Peel Sound member 4. Sections G73G and H, Loc. 14. Dots = sandstone; ellipsoids and solid circles = extrabasinal clasts; solid triangles = intraclasts; sedimentary structures described in the text.

Source of the conglomerate wedge

Sediment dispersal and lateral facies changes

Paleocurrent data from both the conglomerate and sandstone units of members 2 and 4 indicate derivation from the Boothia Uplift to the southwest (Fig. 37), in accord with the evidence of lateral facies change from conglomerate to sandstone eastward (Fig. 5). Lateral changes of clast size in the conglomerates also support this hypothesis, despite the fact that the sections measured in member 2 at Locality 4 are discontinuous and difficult to relate stratigraphically. Section G74A, which includes the basal beds of the member is overlain by section G74C, while section G74B to the northeast is separated from the previous sections by a northwesterly-trending graben containing downfaulted strata of member 4 (Fig. 5 and Appendix A). G74B is probably laterally equivalent to G74C. Figure 39 shows a stratigraphic reconstruction of the sections, with pie diagrams to illustrate the percentage of coarse conglomerate, fine conglomerate and sandstone in each section. Fine conglomerate is particularly abundant in the lowermost strata of the member and in G74B, further from the Uplift. The pie diagrams give an approximate measure of the size distribution of clastic particles in the sections, and indicate a general fining of the wedge eastward. Since the paleocurrent data indicate a similar direction of transport for each section,

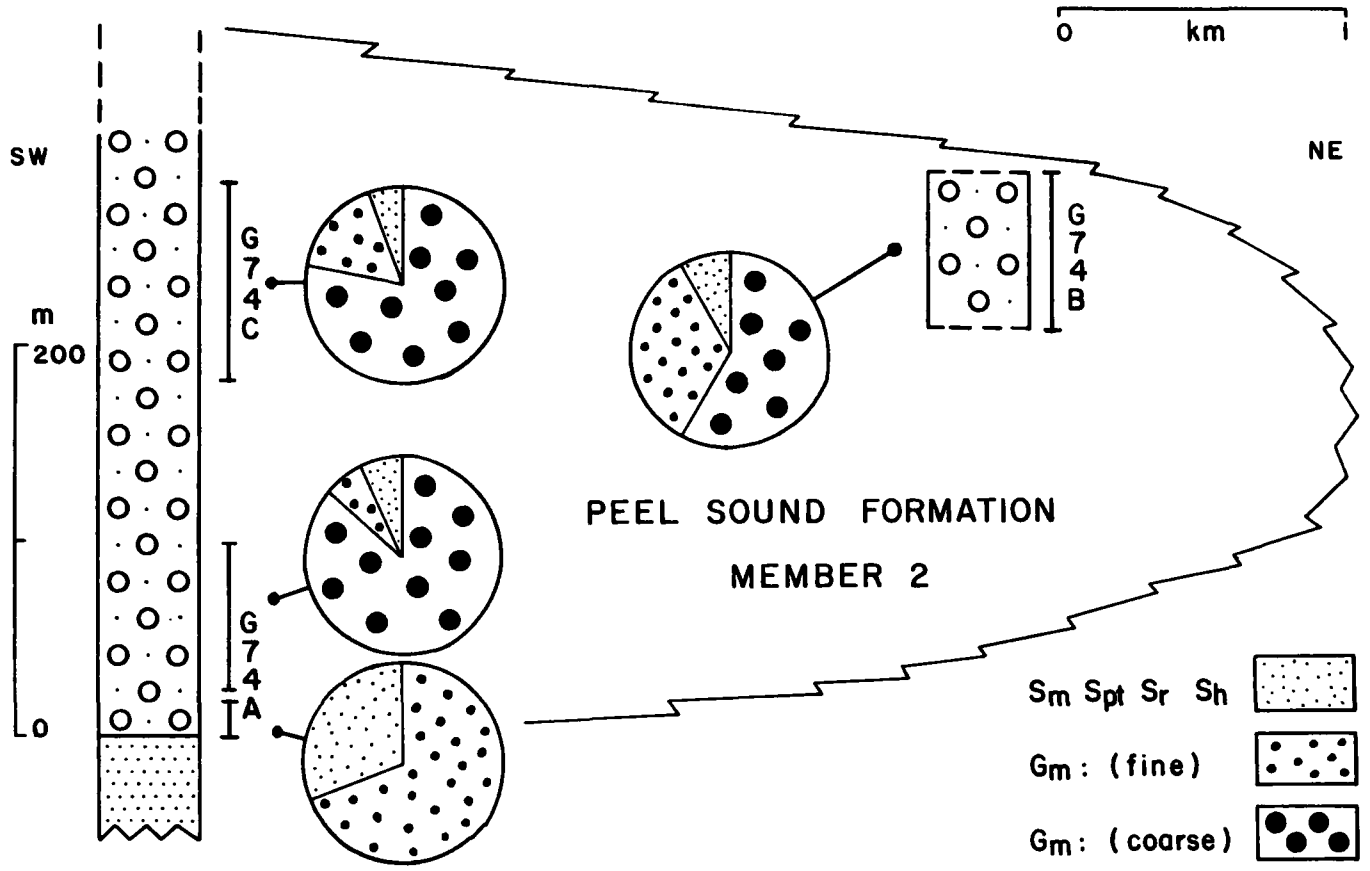

Fig. 39. Facies proportions in sections in Peel Sound member 2, Loc. 4. Facies code as in Table 3.

173

it is unlikely that the fine dolomitic conglomerate was derived from a separate source area on the Uplift.

The rather sharp distinction in size and composition between the coarse and fine conglomerate requires explanation. On Shadow Mountain fan in Death Valley, California, the coarse debris of the upper fan is derived directly from the mountain front, while the finer gravel on the lower fan comes from erosion of material on the upper fan (Denny, 1965, p. 56). In this way, there is selective sorting of finer material across the fan surface, and many fans show a down-slope decrease in mean grain size (Blissenbach, 1954; Bluck, 1964). Similarly, it is probable that the fine conglomerate in the Peel Sound Formation represents a distal facies reworked from material deposited nearer to the source. The abundance of fine conglomerate in the lowermost strata and the general coarsening-upward trend suggests migration of proximal over distal facies during the initial stages of outbuilding of the conglomerate wedge to the northeast. The mountains may also have been lower during the early stages and hence supplying finer debris. Coarse and fine conglomerates very similar to those on Somerset Island were noted by Miall (1969, p. 60-61) in the upper member of the Peel Sound Formation near Transition Bay, Prince of Wales Island, where the fine conglomerate becomes less abundant upwards in the section.

Vertical changes in clast type

Using the grid system described above, the relative abundance of different clast lithotypes was determined for 55 units in the two members (Appendix C3). Sample size for each unit was about 60 clasts. The data was subjected to regression analysis, correlating the relative abundance of the major lithotypes with stratigraphic height. Clast lithotype abundance shows a marked correlation with stratigraphic height (Fig. 40). The basal 20 m of member 2 consists of fine conglomerate (Fig. 39), composed almost entirely of dolostone clasts derived from the Lower Paleozoic formations and from the Proterozoic Hunting Formation. Above this level, clasts of red and grey quartzose sandstone derived from the Proterozoic Aston Formation become abundant, with coarse conglomerate as the major facies type. The proportion of sandstone clasts increases progressively through member 2. Minor lithotypes include chert and silicified oolite (Lower Paleozoic or Hunting Formation), black quartzite (?Aston Formation), and rare coarse-grained igneous rocks of intermediate composition (Precambrian basement). Rare silicified fossils in clasts, about 150 m above the base, were probably derived from the upper Lang River Formation on Somerset Island, of Upper Ordovician age, and include the nautiloid Armenoceras, and corals tentatively identified as Tollina, Streptelasma and Paleophyllum (pers. comm. O.A. Dixon, 1975). Member 4 contains a more diverse assemblage of clasts. Igneous clasts

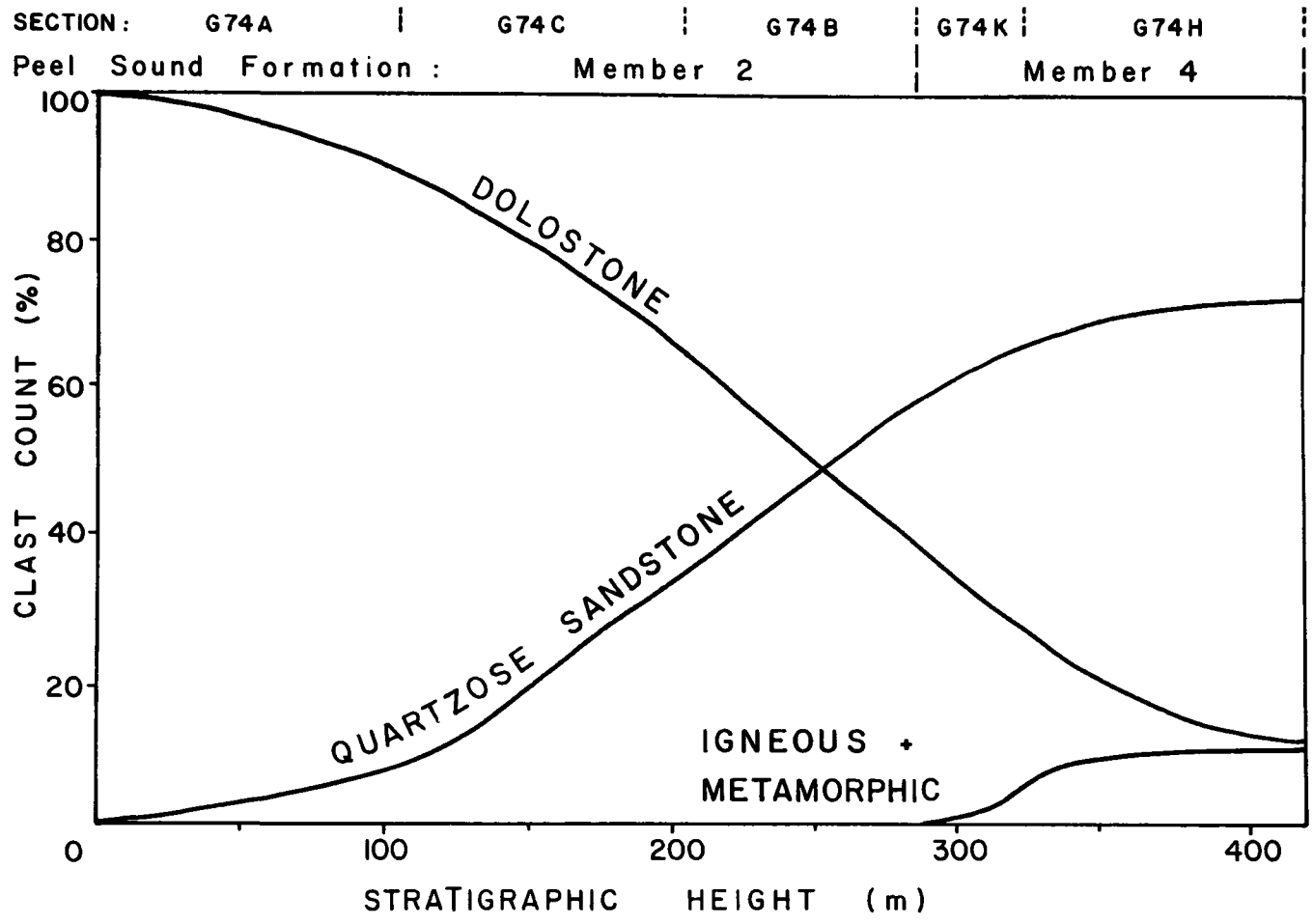

Fig. 40. Stratigraphic variation in clast composition in Peel Sound members 2 and 4. Sections placed in inferred sequence. Data from 55 clast counts (Appendix C3).

176

(intermediate and basic plutonic rocks and porphyries) and metamorphic clasts (quartzo-feldspathic gneisses) average 15% of the total, with a few clasts of black and green quartzite. Rare clasts of red dolostone containing columnar stromatolites resemble a distinctive lithology described from the Aston Formation by Dixon et al. (1971), and were also observed as clasts in the Peel Sound Formation on Prince of Wales Island by Miall (1969. p. 51). The composition of the sandstone matrix parallels that of the clasts. being composed of dolomite and quartz in member 2 (relatively well cemented), but mainly of quartz in member 4 (poorly cemented).

The conglomerate members show "reverse stratigraphy", first noted in the clastic wedge by Miall (1970a) on Prince of Wales Island. As the Boothia Uplift rose, the younger rocks (Lower Paleozoic) were eroded, contributing to the lowermost conglomerate units, and as uplift continued, erosion penetrated more deeply with progressively older rocks being exposed in the sequence: Hunting Formation, Aston Formation, Precambrian basement. These lithological units contributed clasts to progressively younger beds of the conglomerate wedge.

Reconnaissance of member 4 at Cape Garry suggests a similar "reverse stratigraphy", although the lowest conglomerate unit contains clasts derived from all the lithological units noted above (member 2 is absent). As in the Cape Anne syncline, the conglomerate consists of poorly sorted clasts, well rounded and of moderate sphericity, embedded in a friable sandstone

matrix. In the basal units at Locality 14, dolostone clasts form 58% of the large to very large pebble size (530 clasts), but 25 m higher in the section, dolostone composes only 10% of the large pebble size. The remaining clasts are quartzose sandstone (Aston Formation) and basement rocks in about equal proportions. A few clasts of micritic limestone (?Read Bay Formation) are also present, in contrast to the Cape Anne syncline where none were observed, and vein quartz is especially abundant in thin conglomerate lenses in the underlying sandstones. The outcrop pattern of the source area was evidently complex.

Summary

The conglomerate of members 2 and 4 of the Peel Sound Formation formed as a wedge at the eastern margin of the Boothia Uplift, with clast size decreasing away from the Uplift, and the conglomerate passing laterally eastward into fluvial and eolian sandstones of members 1 and 3. Paleocurrent data confirms that the Boothia Uplift to the southwest was the major source of the sediment, and the progressively deeper erosion of the source area with time is shown by the "reverse stratigraphy" of the predominant clast types. The framework conglomerate in the Cape Anne syncline shows both current-normal and current-parallel A-axis orientation, indicating that the clasts were transported both as bedload and in

suspension. Stratification is mainly horizontal and poorly defined, with minor cross-stratification, features observed in longitudinal bars in proximal low slope braided rivers. The conglomerate member at Cape Garry contains a higher proportion of sandstone and pebbly sandstone, with planar cross-stratification and channels, and was probably deposited both in longitudinal and sandy foreset bars in a more distal braided environment. The braided stream deposits formed alluvial fans adjacent to the mountain front.

39. Coarse framework conglomerate (G_m) in Peel Sound member 4. Conglomerate shows poor sorting of rounded and sub-spherical clasts. Sandstone lens at top of outcrop indicates bedding, and clasts are imbricated, dipping to the left with a component towards the observer. Section G74H, Loc. 5. Photo courtesy of B.R. Rust.

40. Resistant bed of fine conglomerate overlain by coarse conglomerate in member 2. Note poorly defined horizontal stratification, and sandstone lenses (Photo 44) at lower right. Unit G74B-17, Loc. 4.

41. Cross-beds of coarse and fine conglomerate and sandstone in member 2. Imbrication in the underlying coarse conglomerate indicates flow direction opposite to that indicated by the cross-beds. Hammer 30 cm long. Unit G74C-4, Loc. 4.

39

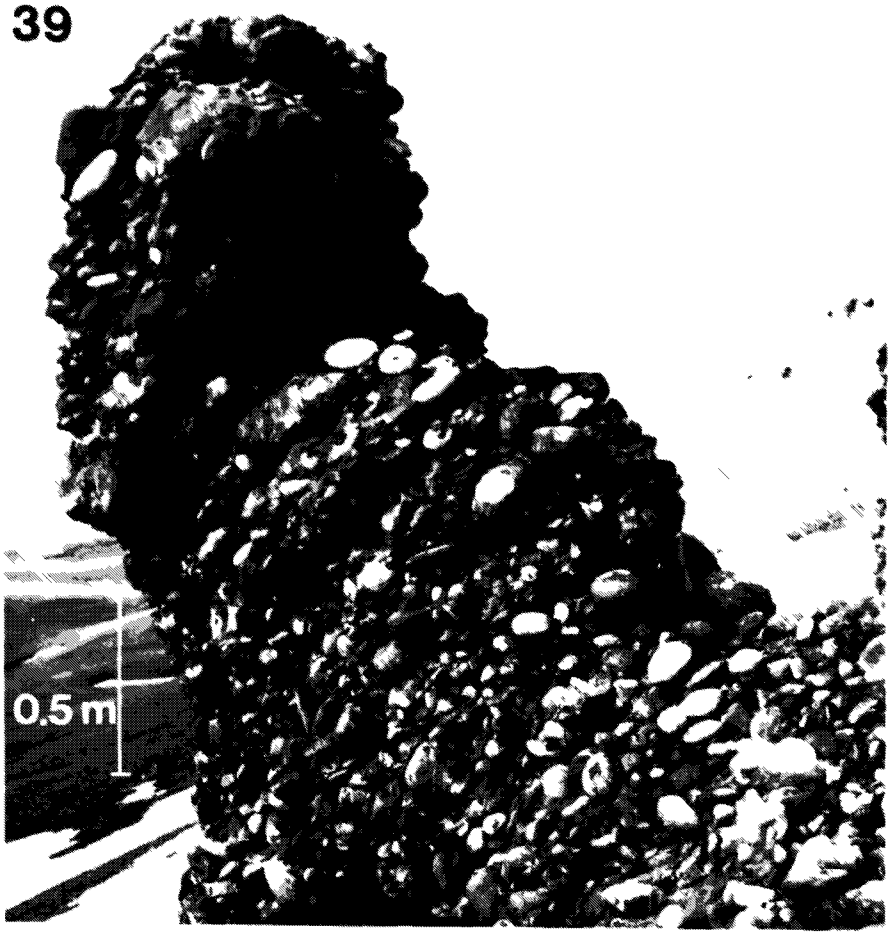

40

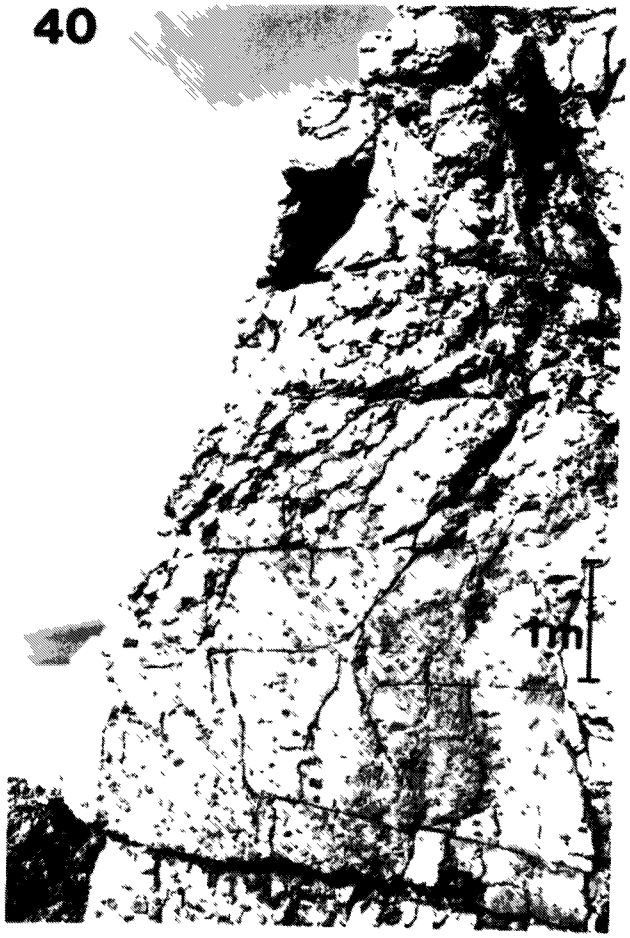

41

42. Cross-beds with fine, openwork conglomerate in member 2. Hammer 30 cm long. Unit G74C-30, Loc. 4.

43. Channel cut into coarse conglomerate in member 2. Erosional base of channel is inclined to the left, with channel axis perpendicular to cliff face. Within the channel, large-scale cross-bedded sandstone (dip direction oblique to channel axis) is overlain by horizontally bedded coarse conglomerate. Loc. 4.

44. Sandstone lenses at the base of a fine conglomerate unit in member 2 (Photo 40). Hammer 30 cm long. Unit G74B-17, Loc. 4.

42

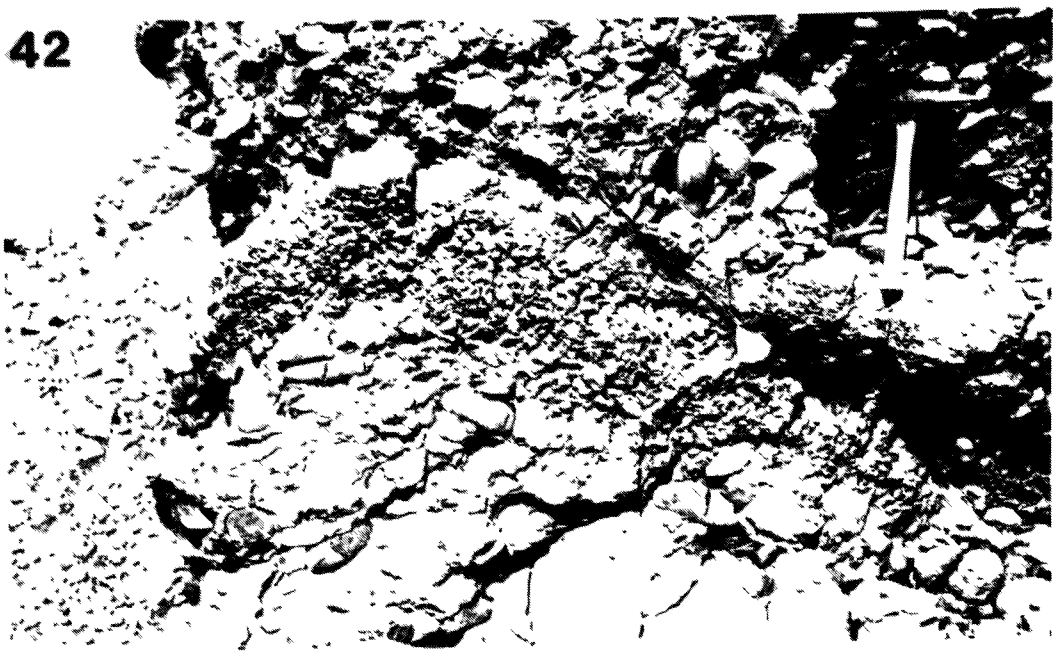

43

44

CHAPTER 5. ANALYSIS OF CONGLOMERATE FABRIC

Introduction

One of the first observations of coarse clast fabric was that of Jamieson (1860, p. 349-350) who compared the orientation of clasts in Scottish Pleistocene gravels with the fabric which he observed in stream gravels, in which the clasts dipped upstream. The study of fabric necessitates describing the geometry of individual clasts, and defining their orientation in space (Fig. 36). Clasts may be considered to be triaxial ellipsoids (Krumbein, 1941, p. 71-2) with three reference axes ($A \geqslant B \geqslant C$) at right angles to each other. The orientation of a clast in space may be defined by describing the orientation of the AB plane and the A-axis. The AB plane, that containing the A- and B-axes, is the maximum projection plane of the clast, and the angle of dip of the plane will be referred to as α. Groups of overlapping clasts with AB planes inclined in the same direction are said to be "imbricated" (Becker, 1893, p. 54), from the Latin imbrex: a tile (superimposed dipping slabs). Photos 39 and 41 show clasts dipping consistently to the left of the photos (upstream). The dip direction of the AB plane is not always precisely into the flow, and the angular deviation of dip direction from the direction of flow is designated γ. The angular deviation of the A (long) axis from a position

transverse to flow is designated β.

Method of study and parameters used

In sections in the Cape Anne syncline, eleven beds of imbricated coarse conglomerate were selected for detailed study of fabric. Sampling was restricted to an area about 2 m long and 0.5 m high within a sedimentation unit on a well-exposed vertical face. After the clasts had been cleared of the overlying matrix with hammer and chisel, the angle of AB dip, the direction of dip, and the orientation of the A-axis and its direction of plunge were measured with a Brunton compass. Since compass readings are not reliable in this area, azimuths were measured with respect to the rock face, the orientation of which could be determined from aerial photos, with accuracy estimated to be $\pm$ 10°. Each clast was then removed and the A-, B- and C-axes measured to the nearest mm (A-axes measured range from 1.5 to 23.2 cm, i.e. pebble to cobble grade). Roundness of the clasts was estimated visually. If on extraction the clast proved to be irregular in form, it was replaced in the mould and fabric measurements were repeated. Rust (1975) found that 40 clasts was a suitable size of sample for studying orientation of particles in recent gravels, although Johansson (1963) suggested that more than 50 clasts are required if orientation is diffuse. This study showed that larger samples are

desirable for a statistical treatment of fabric. The author and his assistant each measured half of the clasts in each sample to avoid bias, and since all clasts removed from the face were measured, the samples are considered representative of the variability of fabric within the units. While this method lacks the accuracy of laboratory procedures such as those of Krumbein (1939), it is rapid and useful in remote localities where clasts must be studied *in situ*. Data were analysed using computer programmes written by E.H. Koster, B. Jones, J.-M. Sempels, R. Hartree and the author.

In this study, size is represented by the *arithmetic mean size*:

$$\bar{d} = \frac{A + B + C}{3}$$

Koster (1977, Table 9) showed that this parameter is a more precise measure of clast volume than the B (intermediate) axis measurement, used for example in the Sedimentary Petrology Seminar (1965).

Sphericity expresses quantitatively the degree of departure of a clast from equidimensionality, and was calculated as the *maximum projection sphericity* (Sneed and Folk, 1958):

$$\Psi_p = \sqrt[3]{\frac{C^2}{AB}}$$

These authors noted that Ψp compares the maximum projection area of the particle — a critical factor in hydraulic performance — with that of the nominal sphere, and it is therefore superior to the commonly used Wadell sphericity.

Particles of the same sphericity may have very different ratios between the three axial dimensions, a characteristic known as "form" (Sneed and Folk, 1958, p. 123). To distinguish between elongate (prolate) and discoidal (oblate) clasts of the same sphericity, Dobkins and Folk (1970) devised the Oblate-Prolate Index as a measure of form:

$$\bar{O}\bar{P} = \left[\frac{10\left(\frac{A - B}{A - C} - 0.50\right)}{C/A} \right]$$

Perfect blade-shaped clasts with any value of sphericity give an $\bar{O}\bar{P}$ value of zero, while discoidal clasts give negative values and rod-like clasts positive values. The relationship of sphericity and form may be seen from the shape measurement triangle of Dobkins and Folk (1970, Fig. 19), reproduced in Figure 41, which shows clearly that both Ψp and $\bar{O}\bar{P}$ are needed to fully specify clast shape.

Roundness ($\bar{R}$) was estimated visually using the chart of Powers (1953, Fig. 1), with numerical values (as used by Folk, 1968, p. 11) assigned to each roundness class:

0-1 = very angular	3-4 = sub-rounded
1-2 = angular	4-5 = rounded
2-3 = sub-angular	5-6 = well-rounded

The clasts of the Peel Sound Formation show a narrow range of roundness, being mainly sub-rounded to well-rounded (see Photo 39), and estimation proved difficult, so that correlations involving roundness are less reliable.

Several workers have noted the influence of clast size on morphology and mechanism of transport (e.g. Sneed and Folk, 1958; Pittman and Ovenshine, 1968), and have grouped clasts into separate Ø classes for analysis. The size-frequency distribution of the clasts used in the present fabric studies is shown in Figure 42, with most clasts in the very large pebble to small cobble grades. Regression analysis was conducted on the clast samples as a whole.

Fabric and paleoflow conditions

Conglomerate fabric provides information on paleocurrent directions and on hydrodynamic conditions during flow (Chapter 4). Gravel fabric is a good indicator of flow direction since it forms at high stage when deflection of flow by large-scale bedforms is minimal (Bluck, 1974). Rust (1975), in a study of outwash gravels in Iceland and in the Donjek River, Yukon, observed that when data are grouped for a sufficiently large area, the vector means of AB dip directions agree closely

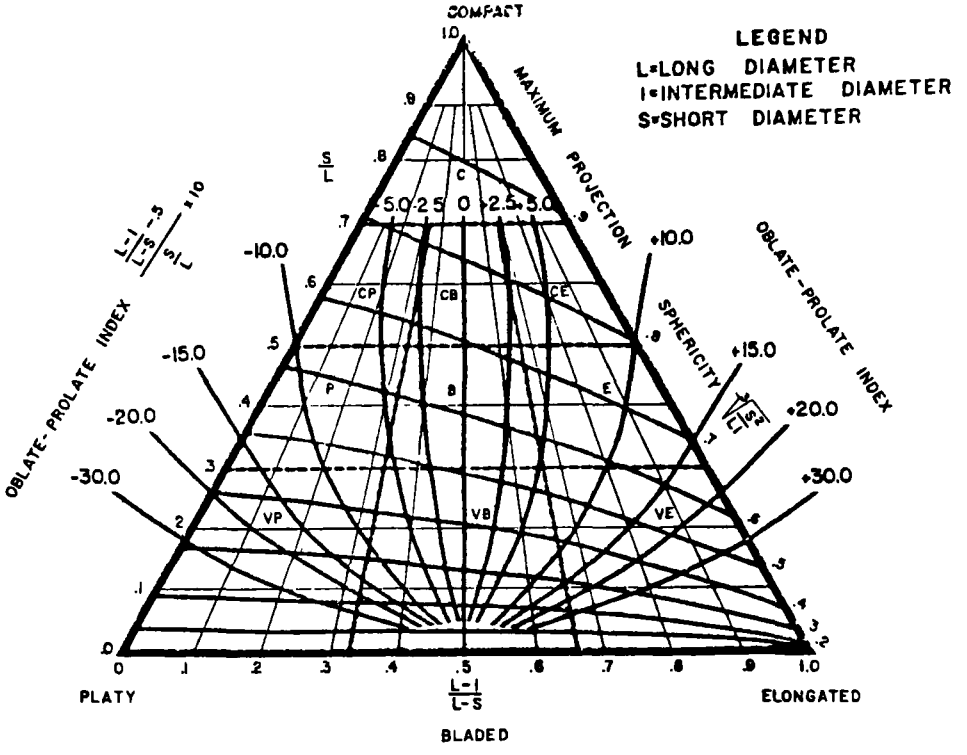

Fig. 41. Shape measurement triangle. Sphericity contours are lines sloping gently to right, form classes are enclosed by dashed lines (after Sneed and Folk, 1958); contours for $\overline{OP}$ index are concave-upward curves, with negative values indicating oblate pebbles and positive values indicating prolate pebbles. After Dobkins and Folk (1970), Fig. 19.

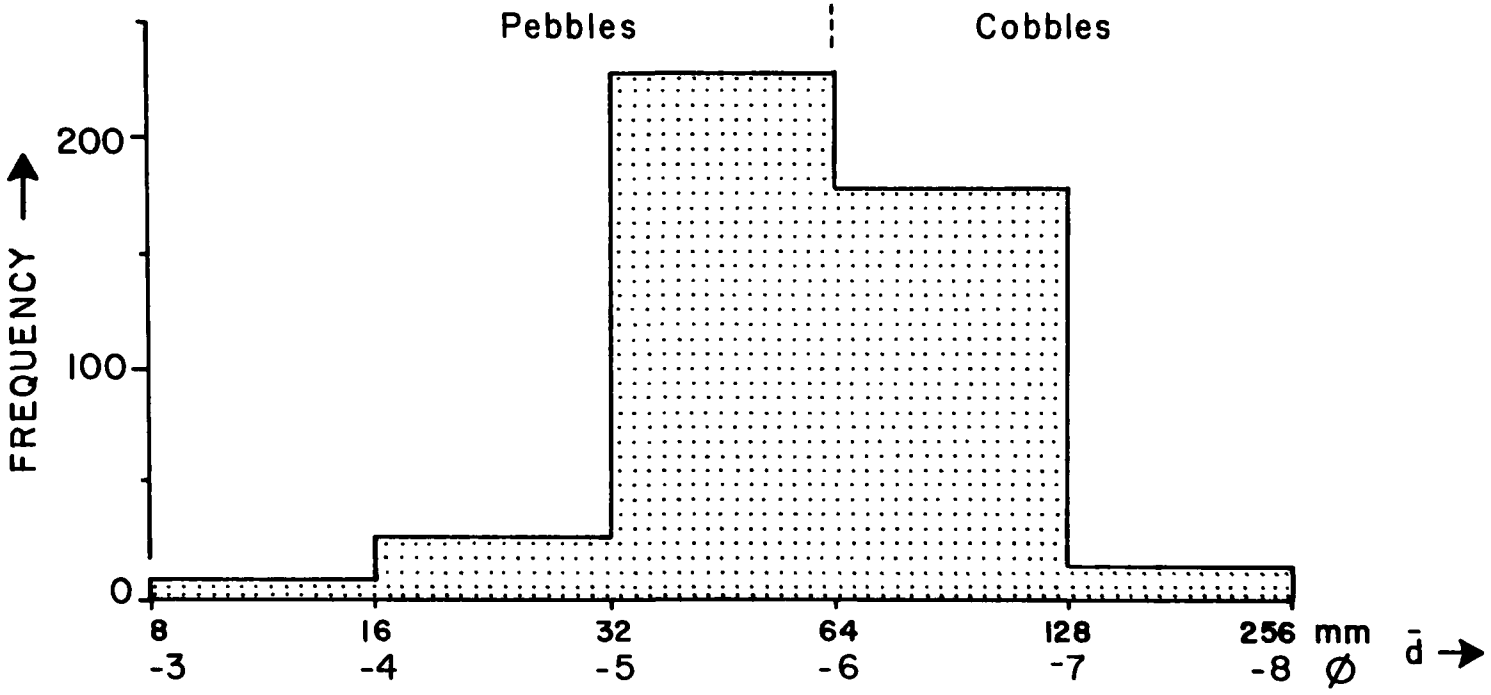

Fig. 42. Size-frequency distribution of clasts in fabric samples. n = 456.

with the orientation of surface channels and braid bars. A-axis orientation may also indicate flow direction, although AB dip direction is a better indicator in framework gravel showing contact imbrication (Sedimentary Petrology Seminar, 1965, p. 281; Johansson, 1965; Rust, 1972b, p. 387-8). Furthermore, the bipolar A-axis data are ambiguous as regards flow direction, unless coupled with data on the orientation of the AB plane. Local components of the flow system generate the observed fabric, so that a large amount of data will be necessary if fabric is to be used as a paleocurrent indicator. For example, Byrne (1963) observed considerable variation in AB dip direction due to highly divergent flow on a gravel bar in the Santiam River, Oregon,and similar variation was also noted by Folk and Ward (1957, p. 4) in the Brazos River, Texas. Teisseyre (1976), in a study of fabric in modern and Carboniferous fluvial sediments, noted that proximity to channel banks results in clasts dipping obliquely to the channel axis.

The comparison of vector means for AB dip direction (imbrication) with cross-bed data from the Peel Sound conglomerates (Fig. 37) confirms that the imbricated clasts are dipping predominantly upstream. In the rest of this study, the vector mean of each sample will be taken to indicate local upstream direction during formation of the fabric. Figure 43 shows a contoured equal area plot for an imbricate sample with good clast orientation. Of the eleven samples,

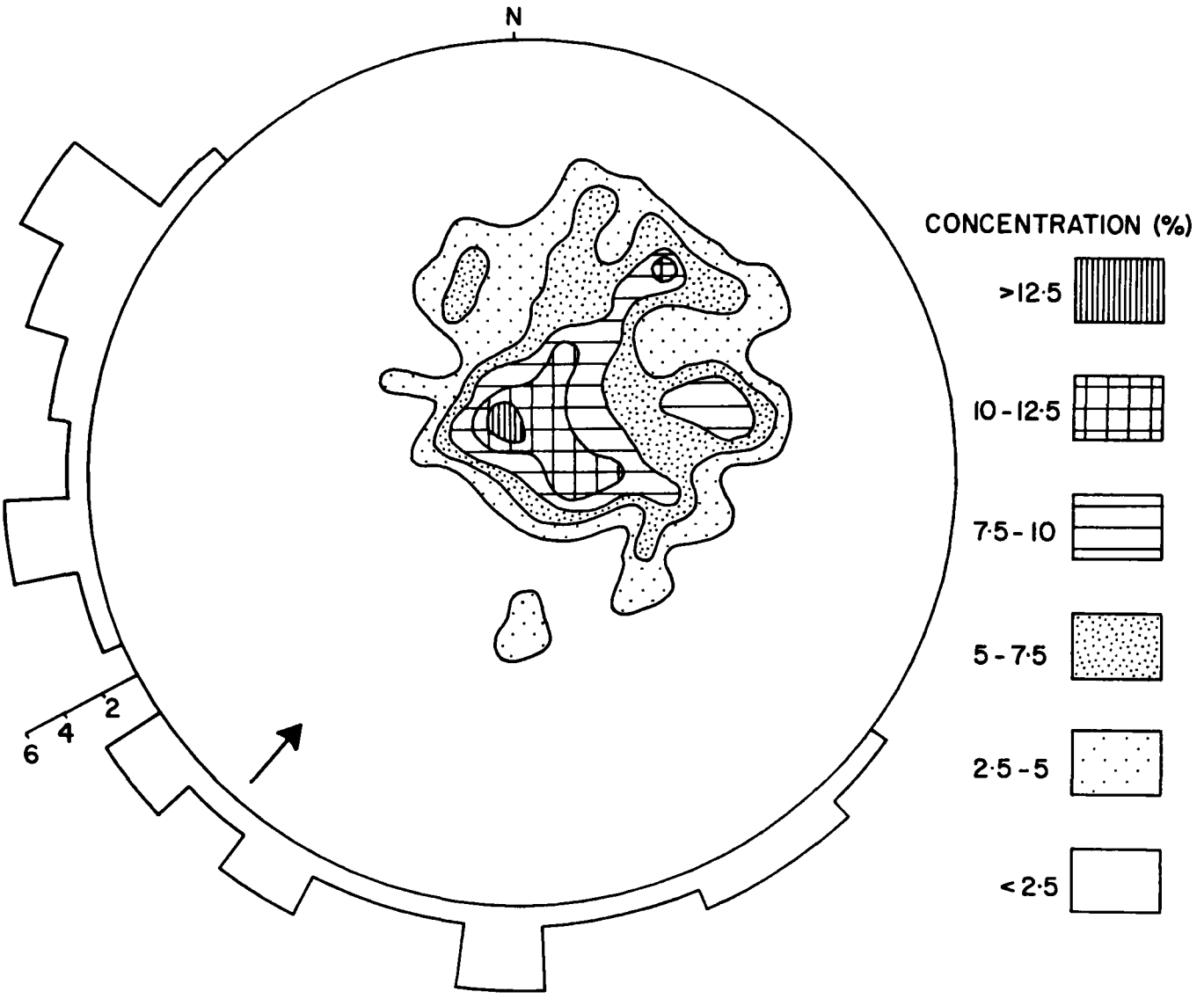

Fig. 43. Stereographic plot of conglomerate clast orientation (sample C5). Sample consists of 40 clasts, with $\bar{d}$ ranging from 36-160 mm. Equal area plot shows poles to AB planes. Arrow shows flow direction (opposite of vector mean for AB dip direction). The circular histogram shows sense of plunge of A-axes. Note consistency of AB dip direction (significance $< 10^{-5}$) and the asymmetric distribution of A-axis inclination with respect to flow direction.

six give vector means for AB dip direction that are significant at the 95% level and two more are significant at the 90% level (Appendix C1). In contrast, vector means for A-axis orientation are significant in only three samples, confirming Rust's (1972b) observation that AB dip direction is a better indicator of flow. Comparison with framework gravels of the Donjek (Rust, 1972b, Table 1) indicates a higher dispersion of A-axis orientation in the Peel Sound samples. Vector magnitudes are generally low for both fabric elements.

While the AB dip direction is a good indicator of the local flow direction, A-axis orientation is useful as an indicator of hydrodynamic conditions (see summaries in Walker, 1975a, and Koster, 1977, p. 21-26). The isolate or contact nature of the clasts (Laming, 1966, p. 946) exercises a major control on the orientation of the A-axis. Isolate clasts commonly show current-normal orientation, usually with AB planes dipping upstream (e.g. Donjek river gravels, Rust, 1972b), and experiments by Koster (1977, p. 86-92) showed that isolate clasts placed in an initially current-parallel orientation on the bed were reoriented to a transverse position under a variety of flow conditions. Contact fabrics commonly show more variable orientation due to collision between clasts, but current-normal orientation is common (e.g. Sedimentary Petrology Seminar, 1965; McDonald and Banerjee, 1971 — transverse ribs in outwash gravel; Rust, 1972b), with rolling of clasts about their long axes

during bedload transport (Lane and Carlson, 1954, p. 459). Indeed, Johansson (1963) believed this to be a stable arrangement for a contact load on a flat bed. Current-parallel orientation is also common, and usually results from saltation of clasts above the bed, whether during torrential river flooding (Krumbein, 1940, 1942) or by dispersion of clasts in submarine flows, as interpreted for the Lower Paleozoic Cap Enragé Formation of Gaspé by Davies and Walker (1974). Sliding of clasts down foreset surfaces can also produce a longitudinal orientation (Johansson, 1963; Sengupta, 1966). In general, smaller (and, commonly, prolate) clasts show a greater tendency to current-parallel orientation since a lower competency of flow is required for their suspension, and they also tend to be reoriented around larger particles. Under conditions of torrential flow, preferred orientation commonly is poorly defined, since "...distinction between bed and suspended load loses some of its sharpness.", (Krumbein, 1942, p. 1392). Comparison of vector means for AB dip direction and A-axis orientation in the eleven samples from the Peel Sound Formation ("whole samples" in Fig. 44; right hand column of Appendix C1) shows that three clast samples are oriented with A-axes parallel to AB dip direction (AB/A-axis $< 10°$), while two samples show transverse orientation (AB/A-axis $> 74°$). The remaining samples show oblique A-axis orientations. This implies that clasts were commonly in traction as a bedload with current-normal orientation, but that flow

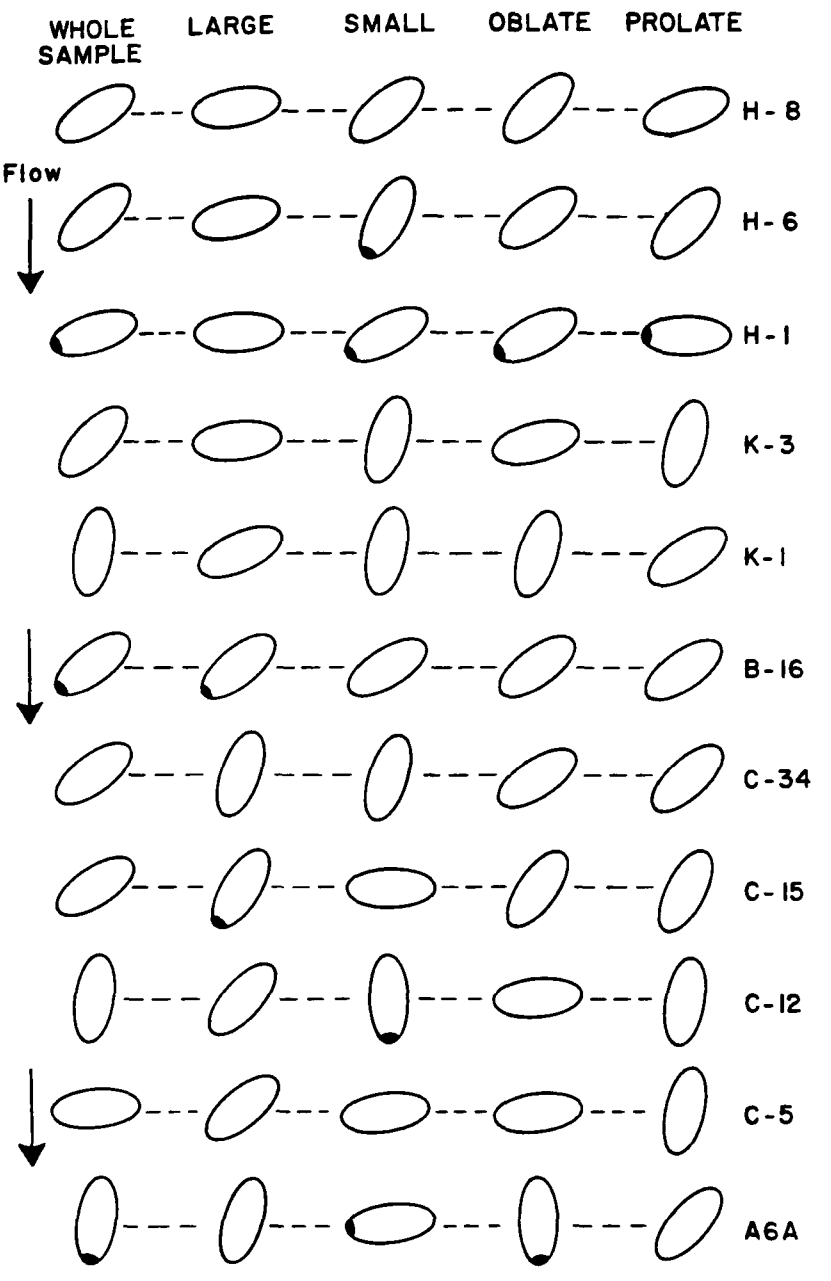

Fig. 44. A-axis orientation in eleven fabric samples. Sample numbers refer to units in sections G74B, C, K and H; sample A6A was collected just below the base of section G74A. Flow direction for each sample is derived from AB dip direction. Orientation of ellipsoid long axes indicates angular deviation of vector mean for A-axis orientation from the flow direction for the whole sample ($n \approx 40$), and split fractions ($n \approx 20$). Blackened tips indicate samples with vector magnitude significant at the 95% level. Orientations for sample B-16 are with respect to AB dip direction of large fraction (higher significance level).

was sometimes of sufficient energy to cause saltation of particles with final deposition in current-parallel orientation.

Koster (1977, p. 93-100) showed that inclination of the A-axis of isolate clasts is mainly a function of clast asymmetry. Although not considered empirically in this study, the sense of plunge of the A-axis was noted for each clast. In several samples with a strong transverse orientation, A-axes plunge consistently to one side rather than being symmetrically disposed about the AB dip direction (see the circular histogram of A-axis inclination in Fig. 43). This probably reflects stacking of clasts in a lateral as well as an upstream direction. In samples with a current-parallel tendency, A-axes plunge upstream, with a secondary transverse grouping often present. In these cases, sense of A-axis plunge is an additional indicator of flow direction.

The mean value of AB dip (α) for 306 Peel Sound clasts dipping upstream ($\gamma < 90°$) was 32.8°, with a standard deviation of 17.3°. Modern stream gravels show similar values of mean α — 20-25° modal class for Wolf Run gravel (Sedimentary Petrology Seminar, 1965), and means of 26.1° and 32.9° for samples from Iceland and the Yukon, respectively (Rust, 1975).

The general effect of size and shape on the nature of A-axis orientation was investigated, using the programme SPLIT. For each sample, the programme prints out clast parameters in a column of increasing $\bar{d}$ or $\bar{\bar{OP}}$, enabling the orien-

tation of relatively large and small or oblate and prolate fractions of equal size to be analysed separately. The median value at which the split is made differs from sample to sample; the small fraction is predominantly in the 16-64 mm range, and the large fraction in the 64-128 mm range (Fig. 42). The size and shape fractions do not consist of exactly the same clasts since there is no significant overall correlation between $\bar{d}$ and $\overline{OP}$ (Table 12). Results are shown pictorially in Figure 44. Orientation of the fractions varies but in general, there is a tendency for large and oblate fractions to be transverse, and for small and prolate fractions to be current-parallel. A good transverse orientation of all fractions is shown by sample G74H-1.

The fabric of the Peel Sound Formation conglomerates is comparable to that observed by Krumbein (1940, 1942) in Californian river gravels deposited from high-energy floods in restricted canyons. Both deposits show current-transverse and current-parallel A-axis orientations, with samples generally showing weak preferred orientation. The Peel Sound fabrics thus suggest periods of torrential stream flow.

Process-response model for fabric development

Numerous studies have attempted to relate fabric elements (especially AB dip and A-axis orientation) to aspects of clast morphology such as size, shape and roundness, to the concentration of clasts on the bed, and to hydrodynamic factors such as depth of water, velocity and slope. Some of the major studies have been those of Krumbein (1939), Cailleux

(1945), Schlee (1957), Unrug (1957), Johansson (1963, 1965) and Rust (1972b, 1975); for an excellent summary of the literature, see Koster (1977 , p. 15-26). The confusing results obtained indicate that although all these factors influence the development of particle orientation, none provides a complete explanation for the phenomenon. As Johansson (1965, p. 49) stated: "For certain conclusions about the dependance of particle dip in different conditions a thorough factor analysis is needed, including measurements of hydrodynamic parameters, sediment feed, sorting, particle sizes, shape and mass, and pressure distribution under controlled laboratory conditions".

During the last few years, flume studies conducted by E.H. Koster at the University of Ottawa have elucidated some of the principles governing the development of coarse clast fabric. Koster studied the fabric of clasts <u>isolate</u> on a sand bed, with imbrication (generally so termed, despite the absence of shingling) resulting from scouring at the upstream ends of the stationary clasts. A current crescent is formed (Peabody, 1947; Sengupta, 1966), and the particle slides into the scour hollow until it lies below the sediment surface, ceases to be an obstacle to flow, and eventually is buried in an upstream-dipping orientation. Johnston (1922, p. 388) noted, "The stones finally assume a position in which they offer the least possible resistance to the current. If the stones dipped downstream they would present their edges

to the current and therefore offer considerable resistance to the current." Many coarse bedload streams deposit framework gravel with contact imbrication, and in these cases, imbrication may be attained instantaneously with deposition by "shingling" of one clast against another. However, it is believed that the principles outlined by Koster (1977) are applicable to both types of imbrication, with the contact type representing a more complex response.

One outcome of Koster's study was the realisation that the projection area (A_p) of the clast is a much more meaningful parameter of response to flow conditions than any of the previously considered factors, a conclusion anticipated by Johansson (1963, p. 90-91), who referred to the "mantle area" of a clast as an important influence on imbrication. The concept of projection area is illustrated in Figure 45a. A flat-lying clast with its long axis parallel to flow will project to the flow the minimum area possible for that clast, while the same clast in transverse orientation with its surface of maximum area (AB plane) vertical will project the maximum possible area. Projection area thus takes into account the effect of size, shape and orientation of the clast, and is likely to provide a more complete explanation of fabric than any of these factors individually. It can be computed using equations developed by Koster (1977, p. 69-71 and Appendix 8.1), assuming the clasts to be triaxial ellipsoids. Koster showed that the area projected by the clast

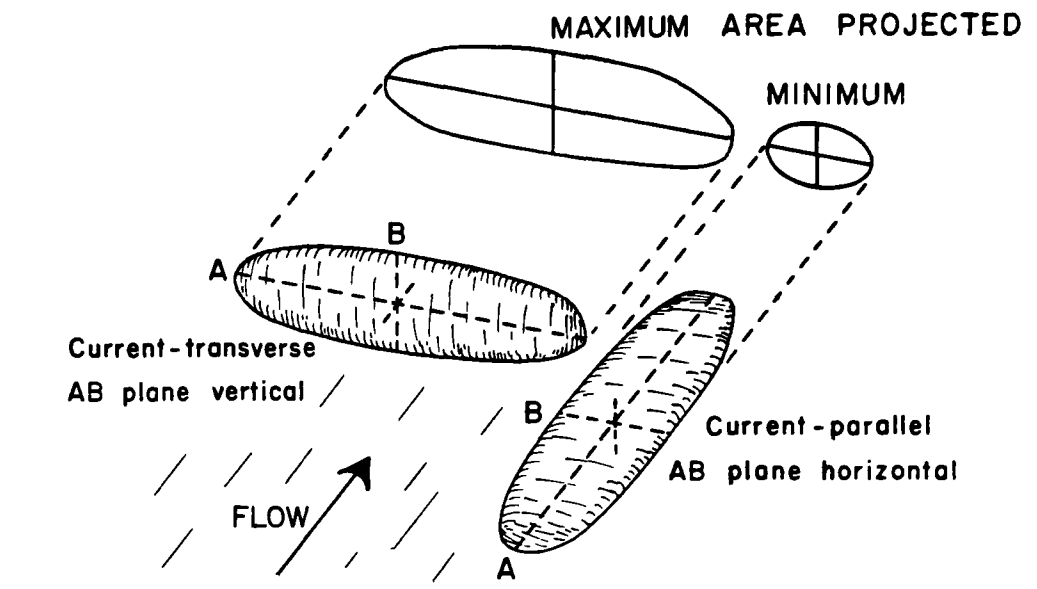

b

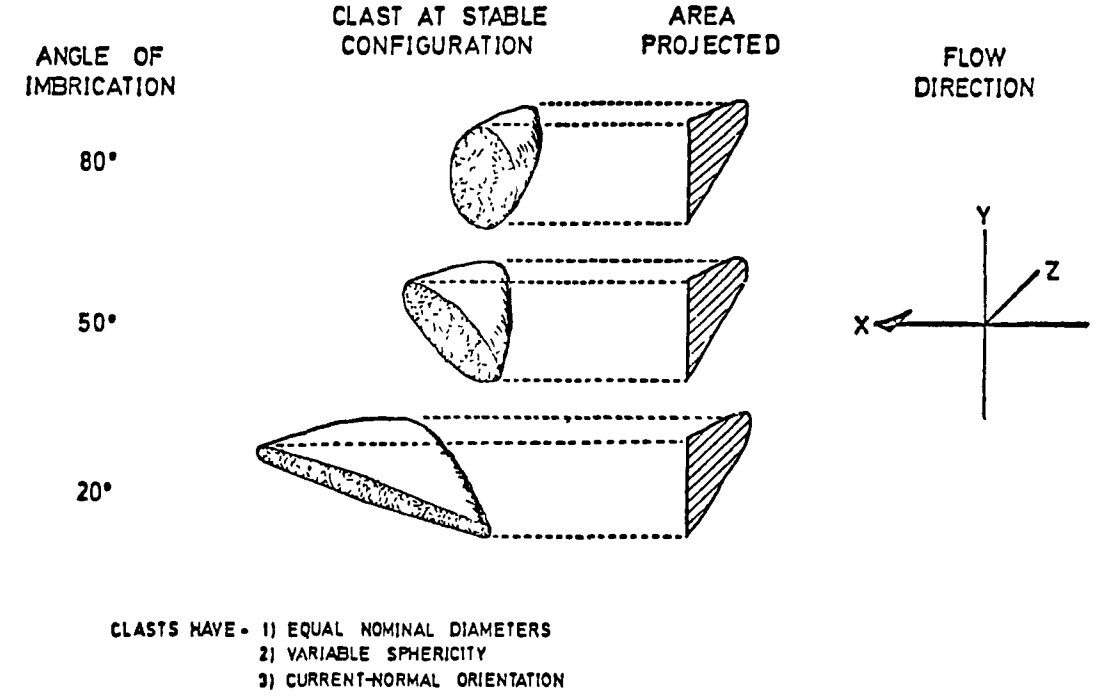

Fig. 45. Illustration of the concept of projection area.
a) Relationship between area projected and clast orientation.
b) Maintenance of equilibrium area for clasts of variable sphericity by adjustment of the angle of imbrication. From Koster (1977), Fig. 17.

to the flow during experimental runs bears a definite relationship to the volume (proportional to mass) of the clast: a clast of a given size and shape will tend to adjust its orientation in the flow so that its projection area will approximate the area projected by a sphere with the same volume as the clast ("nominal sphere"). The diameter of the nominal sphere is known as nominal diameter (Wadell, 1932), given by:

$$d_n = \sqrt[3]{a.b.c.}$$

for ellipsoidal clasts (Koster, 1977, p. 41). Thus, under equilibrium conditions, discoidal clasts with a relatively large potential projection area will tend to dip at low angles in order to approximate the projection area of the nominal sphere, while clasts of the same volume but higher sphericity will dip at higher angles (Fig. 45b). The projection area of the nominal sphere is known as the equilibrium area (A_p) for the clast (Koster, 1977, p. 78), and in the flume runs, A_p was found to be a power function of d_n:

$$A_p = c.\, d_n^{\,e}$$

where c is the coefficient and e is the exponent. Values of the coefficient and exponent were obtained experimentally over a range of Froude numbers and hence with a variety of

bedforms. For clasts on a plane bed at the transition between the lower and upper flow regimes, a more stable imbrication should be attained than on a bed affected by migrating bedforms of higher relief. Under these conditions, the relationship was found to approximate:

$$A_p = d_n^2$$

and hence this equation is considered to constitute an optimum relationship with dynamic significance. The degree to which a sample of clasts approaches this relationship is a measure of the hydrodynamic stability achieved during the formation of the imbricate fabric.

Koster's analysis enables the development of coarse clast fabric to be expressed in terms of a process-response model (Fig. 46). Material weathered from the source rocks is acted upon by processes of transport, resulting in the observed morphology of the clasts — expressed in terms of size, sphericity, shape and roundness (size is here considered as a "morphological" feature). During deposition from the flow, these clasts acquire a preferred orientation (fabric), defined by the AB dip (α) and dip direction (δ), and the A-axis orientation (β) and its plunge. The morphology and orientation of each clast determine its projection area, allowing an appraisal of the degree to which the imbricate clast approached hydrodynamic stability during the process

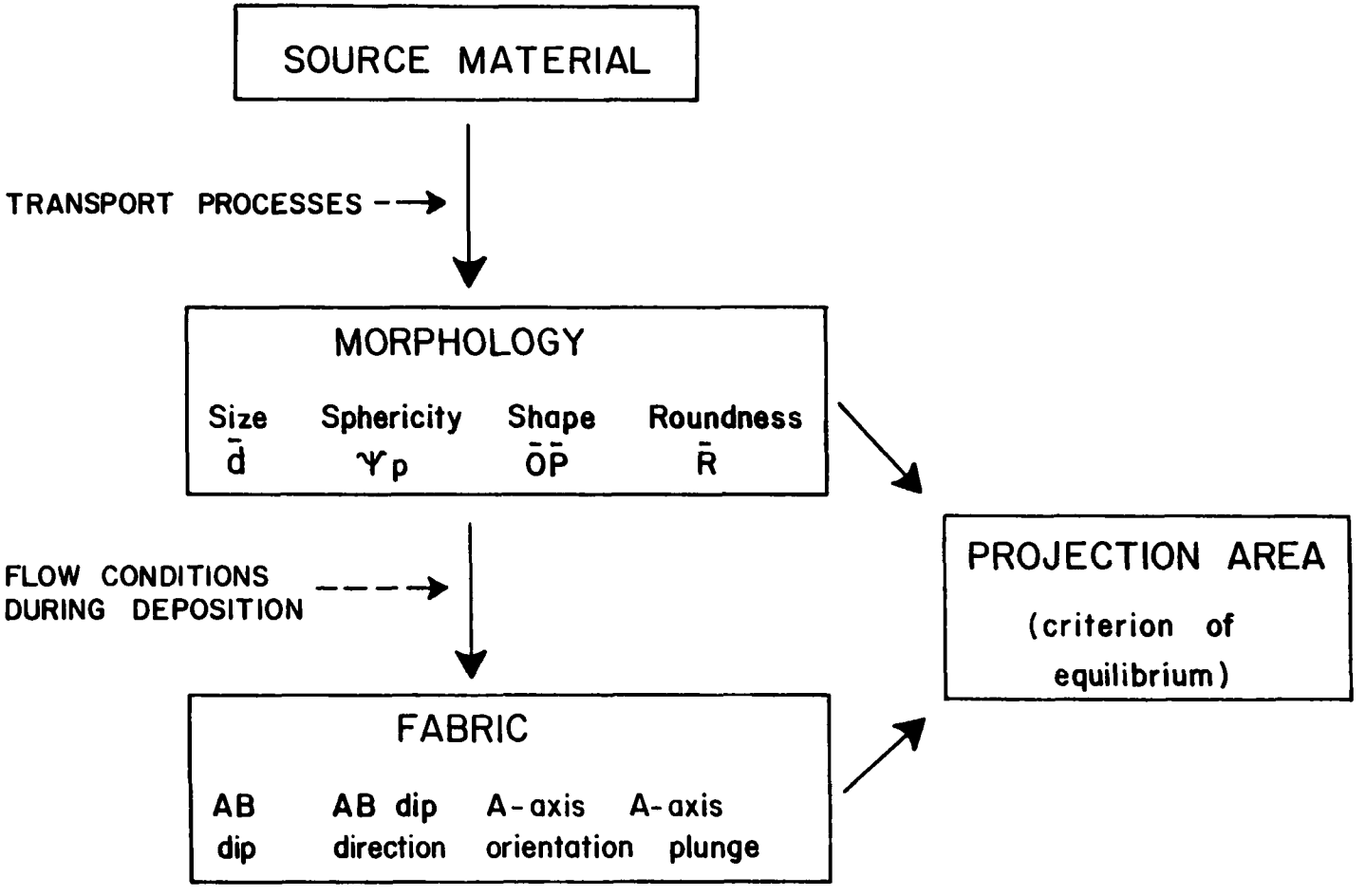

Fig. 46. Process-response model for the development of coarse clast fabric.

201

of orientation. The results contribute to the interpretation of depositional conditions.

The principles discussed by Koster (1977) can be applied to the coarse clast fabrics of ancient conglomerates. The analysis of factors influencing fabric in the Peel Sound conglomerates will consider the factors in the following stages (Fig. 46):

1) Evolution of clast morphology — the effect of source material and transport processes.
2) Development of clast fabric — the influence of clast morphology.
3) Attainment of fabric equilibrium, as indicated by the projection areas of the clasts (calculated from data on morphology and fabric).

Evolution of clast morphology

Effect of source material

The nature of the source material influences particle morphology by determining the internal lithological characteristics of the particle (e.g. hardness, and the presence of anisotropy due to bedding, schistosity and jointing) and the size and shape of the clast liberated from the parent rock (Sneed and Folk, 1958, p. 114-115). These authors found that "...the most important single factor governing pebble morphology is lithologic composition." (ibid., p. 115), with

each lithology differing in overall morphological characteristics. Clasts in the Peel Sound Formation comprise two main lithotypes: red quartzose sandstone derived from the Aston Formation, and buff-weathering dolostone from the Lower Paleozoic formations and the Proterozoic Hunting Formation. Both lithotypes appear isotropic in hand specimen, although weak layering is apparent in thin section. Of 558 clasts measured to the nearest mm, 367 (65.8%) were sandstone and 164 (29.4%) were dolostone, with the remaining 4.8% consisting of various sedimentary, igneous and metamorphic types (Chapter 4).

Comparison of the morphology of the measured sandstone and dolostone clasts gives the following results:

1) Mean size: dolostone $\bar{d} = 4.37 \pm 2.08$ cm

sandstone $\bar{d} = 5.99 \pm 2.55$ cm

Mean values for both lithotypes lie in the very large pebble grade, although the t-test shows that, at the 95% confidence level, the two sets of data give significantly different distributions.

2) Sphericity and form: The shape measurement triangle (Fig. 41) shows oblate and prolate spheroids and spheres as three end members of a shape continuum. Mean values of parameters have limited meaning, e.g. a mean $\bar{O}\bar{P}$ Index of zero may indicate a predominance of bladed clasts or a mixture of oblate and prolate forms, and hence Ψ_p and $\bar{O}\bar{P}$ for sandstone and dolostone are compared by means of

histograms in Figure 47. The histograms show a similar shape distribution for both lithotypes, with the modal class for Ψp at 0.60-0.65 and for $\bar{O}\bar{P}$ at -2.0 to +2.0. Both dolostone and sandstone clasts tend to be blade-shaped and of moderate sphericity.

3) Mean roundness for each lithology was estimated for the clasts used in fabric studies, and also for samples taken systematically through the measured sections (Appendix C3):

dolostone	$\bar{R}$	=	4.516 (1290 clasts)
sandstone	$\bar{R}$	=	4.812 (1230 clasts)
igneous and metamorphic types	$\bar{R}$	=	4.726 (240 clasts)

Clasts of all lithotypes tend to lie in the rounded class.

It is apparent that clast composition was not the major factor governing morphology, in view of the general similarity of values for both sandstone and dolostone. The formations from which both types of clast were derived are commonly medium to thick bedded and relatively massive in internal texture, and both sandstone and dolostone clasts appear isotropic, lacking any obvious internal fabric. This may account for the similarity in morphology, despite the action of weathering and transport. Mechanical breakage along planes of weakness was probably of major importance in the

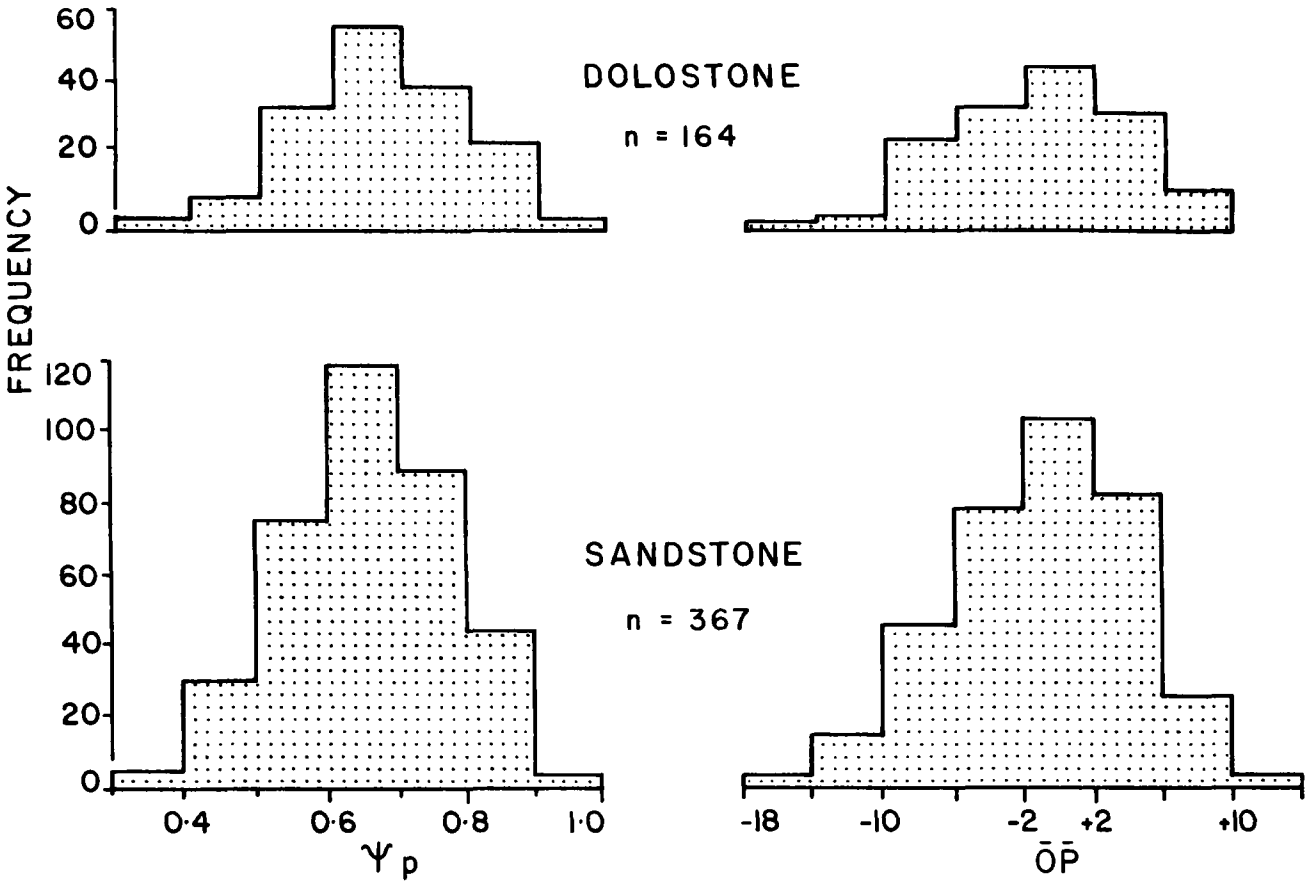

Fig. 47. Histograms of Ψp and $\bar{O}\bar{P}$ for sandstone and dolostone clasts.

205

degradation of clasts in the Peel Sound rivers, in view of the prevailing semi-arid climate (physical weathering dominant), and the high-energy transport of the clasts. Hence the size and shape of the initial clastic particles weathered from the source rocks may have exerted a major influence on the mean values and the range in values shown by the parameters of morphology, in the absence of an anisotropic internal fabric to control changes of morphology during transport.

Similar conclusions regarding the significance of the source rock in controlling clast morphology were drawn by Pittman and Ovenshine (1968) for gravels of the Merced River, California. They observed that relatively isotropic granitic source rocks produced talus fragments of high sphericity which underwent no obvious shape evolution during downstream transport.

Effect of transport processes

Clast samples from modern rivers commonly show correlation between morphological parameters, e.g. in the Sedimentary Petrology Seminar (1965), a correlation of +0.412 was observed between size and flatness. Such correlations can result from:

1) Clasts showing morphological correlation being weathered from outcrop, e.g. weathering of thin-bedded rocks would yield discs and blades of similar thickness,

and hence larger clasts would be flatter (negative correlation between $\bar{d}$ and $\bar{\bar{OP}}$).

2) Processes operative during transport, e.g. abrasion might simultaneously reduce size and increase roundness (negative correlation between $\bar{d}$ and $\bar{R}$).

3) Interdependence of parameters due to terms used in their formulation.

Processes of transport commonly produce such correlations. In a study of gravel over 270 miles of the lower Colorado River, Texas, Sneed and Folk (1958) were able to relate many aspects of morphology, especially sphericity and form, to the processes of transport of the different size fractions.

A correlation matrix for the four morphological parameters of the studied clasts is presented in Table 12. Values of the correlation coefficients are generally low, with only three of the six correlations significant at the 95% level (although the t-test is not very discriminating for samples as large as 558). Figure 48 illustrates the scattered distribution of the data, and correlations are not improved by treating sandstone and dolostone separately. The only parameters to show a visually apparent correlation are Ψp and $\bar{\bar{OP}}$ (Fig. 48b). It appears that clasts of higher sphericity tend to be more elongate (show positive values of $\bar{\bar{OP}}$). Dobkins and Folk (1970) observed a similar positive correlation in clast samples from Tahiti-Nui, and suggested that discoidal forms (negative $\bar{\bar{OP}}$) of low sphericity result from

TABLE 12. Correlation table for parameters of clast morphology. 558 clasts of all lithotypes; for correlations involving roundness, n = 229. Asterisk denotes correlations with significance levels in excess of 95%.

	$\bar{d}$	Ψ_p	$\bar{O}\bar{P}$	$\bar{R}$
$\bar{d}$	1.00	-0.13*	-0.00	+0.23*
Ψ_p		1.00	+0.47*	-0.07
$\bar{O}\bar{P}$			1.00	-0.12
$\bar{R}$				1.00

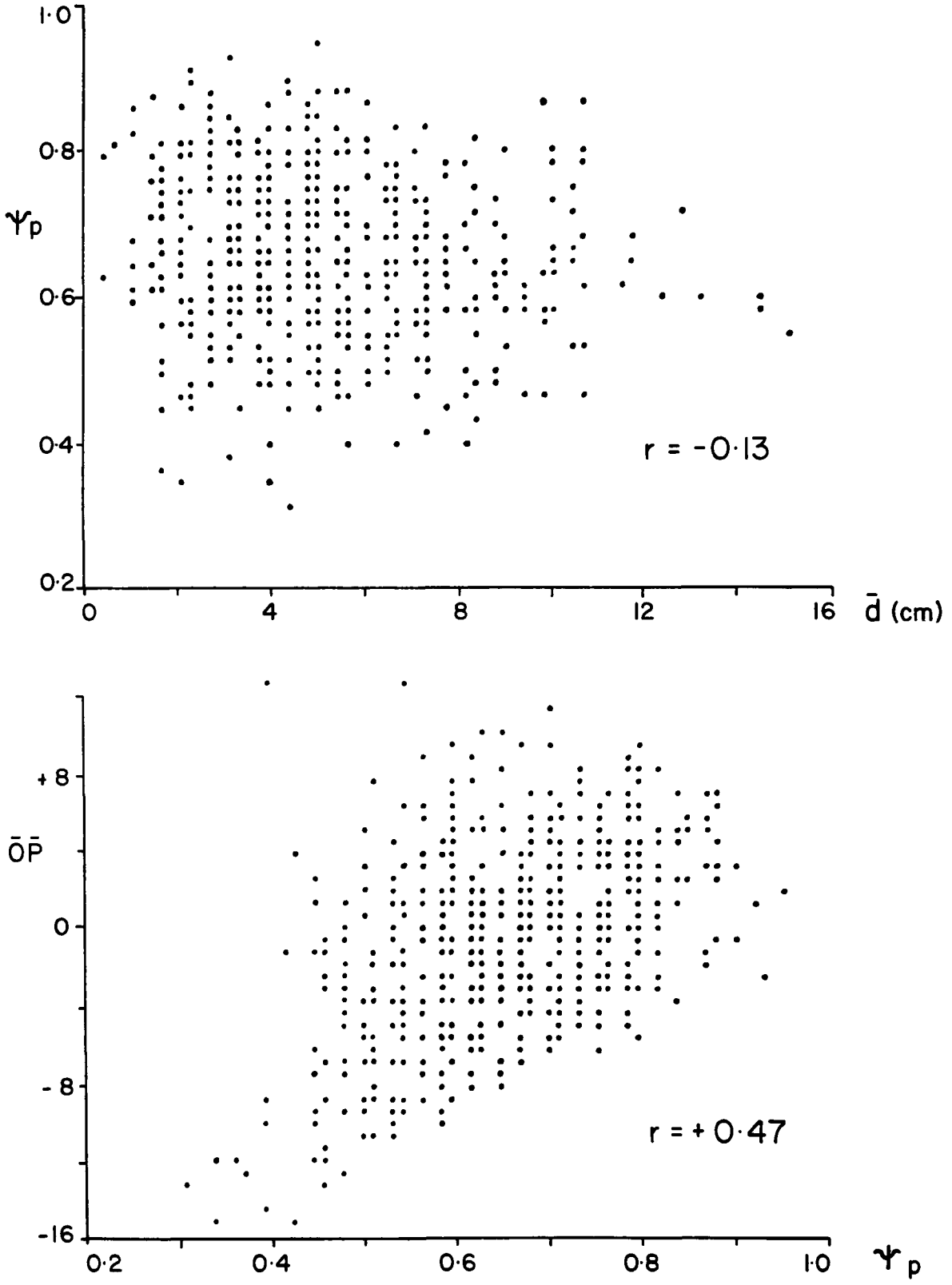

Fig. 48. a) Bivariant graph of $\bar{d}$ against Ψp. n = 558. Correlation coefficient is significant at the 95% level. Graph traced from computer print-out, with superimposed data points shown by one point.

b) Bivariant graph of Ψp against $\bar{O}\bar{P}$. n = 558.

abrasion of the clasts on beaches. However, it is probable that part of the correlation results from interdependence of the two parameters. Since Ψp compares the maximum projection area of the particle with that of a sphere of the same volume (Sneed and Folk, 1958, p. 118), the greater the projection area of the particle the lower will be the sphericity. A discoidal clast of low (negative) $\bar{O}\bar{P}$ will have a greater maximum projection area, and hence may show lower sphericity, than an elongate clast with an equal but positive $\bar{O}\bar{P}$ value. This is evident from Figure 41, in which the lines of equal Ψp slope to the right, resulting for example in a possible Ψp of up to 0.63 for a clast of +20.0 $\bar{O}\bar{P}$, but a maximum of only 0.40 for a clast with -20.0 $\bar{O}\bar{P}$. Thus, by definition, Ψp and $\bar{O}\bar{P}$ will show some measure of positive correlation.

It is possible that since the studied clasts comprise samples from different units, good correlation of parameters within the individual samples has been obscured by pooling the data. However, statistical analysis shows a high degree of variation within the samples but a low between-sample variation, features characteristic of fluvial gravels rather than beach gravels on Tahiti-Nui (Dobkins and Folk, 1970, p. 1181).

The lack of significant correlation for clasts of the Peel Sound Formation may be explained by two aspects of clast transport discussed in Chapter 4 and earlier in this chapter.

Clasts were deposited close to the source and have undergone relatively little transport in comparison to Sneed and Folk's 270 mile study section. Furthermore, during high energy transport in proximal settings, collision between clasts is frequent, resulting in discontinuous fragmentation rather than continuous abrasion, a process unlikely to produce correlation between the parameters. Similarly, Pittman and Ovenshine (1968) found little correlation in gravel along a 43 mile stretch of the Merced River. In their study, the shape of granitic pebbles showed no systematic downstream change in any of the size classes considered, while mean roundness varied considerably downstream, with local conditions of high-energy transport reducing mean roundness as a result of chipping and breakage in the high-gradient reaches. Broken clasts comprised up to 20% of clasts in some samples, and the authors concluded that a combination of high energy and short transport distance have prevented the progressive development of shape or roundness with transport. Dobkins and Folk (1970, p. 1180) commented: "In principle, a river is a very crude and inefficient shaper — presumably because of wide fluctuations in velocity — while a beach with relatively constant wave vigor is almost surgeon-like in picking out variously-sized pebbles to be shaped in diverse ways."

Fabric: influence of clast morphology

Clast morphology results partly from the nature of the

source material (weathered from the outcrop) and partly from processes operative during transport. Fabric is produced during deposition, and, as noted by Davies and Walker (1974, p. 1214), "Clast fabric...when measured carefully and systematically, is a clue to the final few seconds of clast movement before deposition takes place." In a framework gravel, it is unlikely that fabric will be substantially altered by reworking during waning flow (Rust, 1975, p. 245, in contrast to the view of Folk and Ward, 1957, p. 5), or by compactional effects after burial.

The three following elements (Fig. 36) will be considered for each clast:

1) Angle of dip of the AB plane (α).

2) Deviation of the dip direction of the AB plane from the true flow direction (δ). In studies of modern rivers, flow direction can be observed directly (Sedimentary Petrology Seminar, 1965), but in the present study, the vector mean for AB dip directions in each sample was assumed to indicate flow direction (clasts dipping upstream). For about 30% of the measured clasts, δ is $>90°$, i.e. the clasts were dipping downstream, but elimination of such clasts in trial samples did not consistently affect correlation with morphology.

3) Deviation of the A-axis orientation from a position transverse to flow direction (β).

Correlation of the three fabric elements with $\bar{d}$, Ψp and $\bar{O}\bar{P}$ for the eleven samples is shown in Table 13. The samples were analysed separately rather than being pooled, and the table indicates the general tendencies for all the samples. with the number of samples significant at the 95% level for each pair of parameters. Roundness was not considered further in view of its limited range, and the observation of Krumbein (1942) that roundness was not an important factor governing behaviour of clasts during tansport in the flume. Few samples show significant correlation and the tendencies noted must be considered tentative. AB dip direction (δ) shows the best adjustment to morphology, giving more significant correlations than the other fabric elements. AB dip (α) shows little apparent relationship to morphology. This contrasts with the results of Koster (1977, Table 11), who observed that α for isolate clasts gave a significant positive correlation with Ψp and $\bar{O}\bar{P}$ (higher dips characteristic of more spherical and elongate clasts), as indicated by a consideration of equilibrium area (Fig. 45b). Results from the Peel Sound conglomerates suggest high-energy conditions , preventing full equilibration during deposition of imbricate gravel; similarly, in a study of modern gravels, the Sedimentary Petrology Seminar (1965, p. 278) concluded that "The currents that orient gravel during floods in Wolf Run are evidently so intense that variation in size and flatness has virtually no influence on the hydrodynamic response of the particles."

TABLE 13. Correlation table plotting morphological parameters of clasts against fabric. Each description of correlation is compiled from 11 samples of about 40 clasts. Figures below indicate number of samples (out of 11) showing significant correlation at the 95% level.

	ANGLE OF AB DIP (α)	DEVIATION OF AB DIP DIRECTION FROM FLOW (γ)	DEVIATION OF A-AXIS ORIENTATION FROM TRANSVERSE (β)
$\bar{d}$	Small clasts show high dips 0	Large and small clasts show less deviation 5	Large clasts tend to be transverse 2
Ψ_p	High sphericity clasts show high dip 0	High sphericity clasts show less deviation 5	High sphericity clasts tend to be transverse 1
$\bar{O}\bar{P}$	Oblate clasts show high dip 1	Prolate clasts show less deviation 0	Oblate clasts tend to be transverse 1

Attainment of fabric equilibrium

The concept of equilibrium area (Fig. 45b) enables a statistical appraisal of the degree of hydrodynamic stability achieved by the fabric (Koster, 1977). As discussed above, samples of clasts showing stable imbrication should approximate the relationship $A_p = d_n^2$. For each clast, the following four values of projection area were calculated from the data A, B, C, α and β, using the programme FULLIMBRIC (Koster, 1977, Appendix 8.2):

1) The actual area projected to the paleoflow (vector mean for AB dip directions + 180°), using the observed values of α and β.

2) The maximum possible projection area, with $\alpha = 90°$ and $\beta = 0°$.

3) The minimum possible projection area, with $\alpha = 0°$ and $\beta = 90°$.

4) The projection area of a sphere with the same volume as the clast (nominal sphere), calculated simply by $A_p = \pi r^2$, where r is the nominal radius.

Clasts with $\delta > 90°$ (reversely dipping) were excluded, reducing sample size to 22-36. Thirty percent of the clasts showed reverse dips, whereas Rust (1972b) found that only 8-23% of clasts in contact fabrics of the Donjek river dipped outside a 60° upstream arc. For each sample, the values of actual, maximum, minimum and nominal projection areas were correlated

against nominal diameter using the programme FULLOGREG, to give four regression lines. These are plotted graphically in Figure 49 for the range of A_p and d_n observed in the samples. The shaded areas for each sample are bounded by the maximum and minimum lines which define the potential range in projection area for each sample, related to the range in size and shape of the clasts. The position and slope of the line for actual projection area can be compared visually with the position and slope of the theoretical lines, or the method of Imbrie (1956, p. 235-238) can be used to investigate whether the regression lines differ statistically in slope and position. If the fabric shows stability, with clasts projecting equilibrium areas, the actual line should not differ significantly from the line for nominal spheres but should be significantly different from the lines for maximum and minimum projection area.

It is apparent from Figure 49 that in several samples the line for observed A_p closely approximates the line for nominal spheres, indicating that the contact fabric was in equilibrium with the flow. For example, the actual line for sample A6A is not statistically different either in position or in slope from the line for nominal spheres. It is notable that two of the samples (G74C-12 and G74B-16) which show close approximation to the sphere line also show the largest number of significant correlations between fabric and morphology.

Consideration of projection area indicates that contact

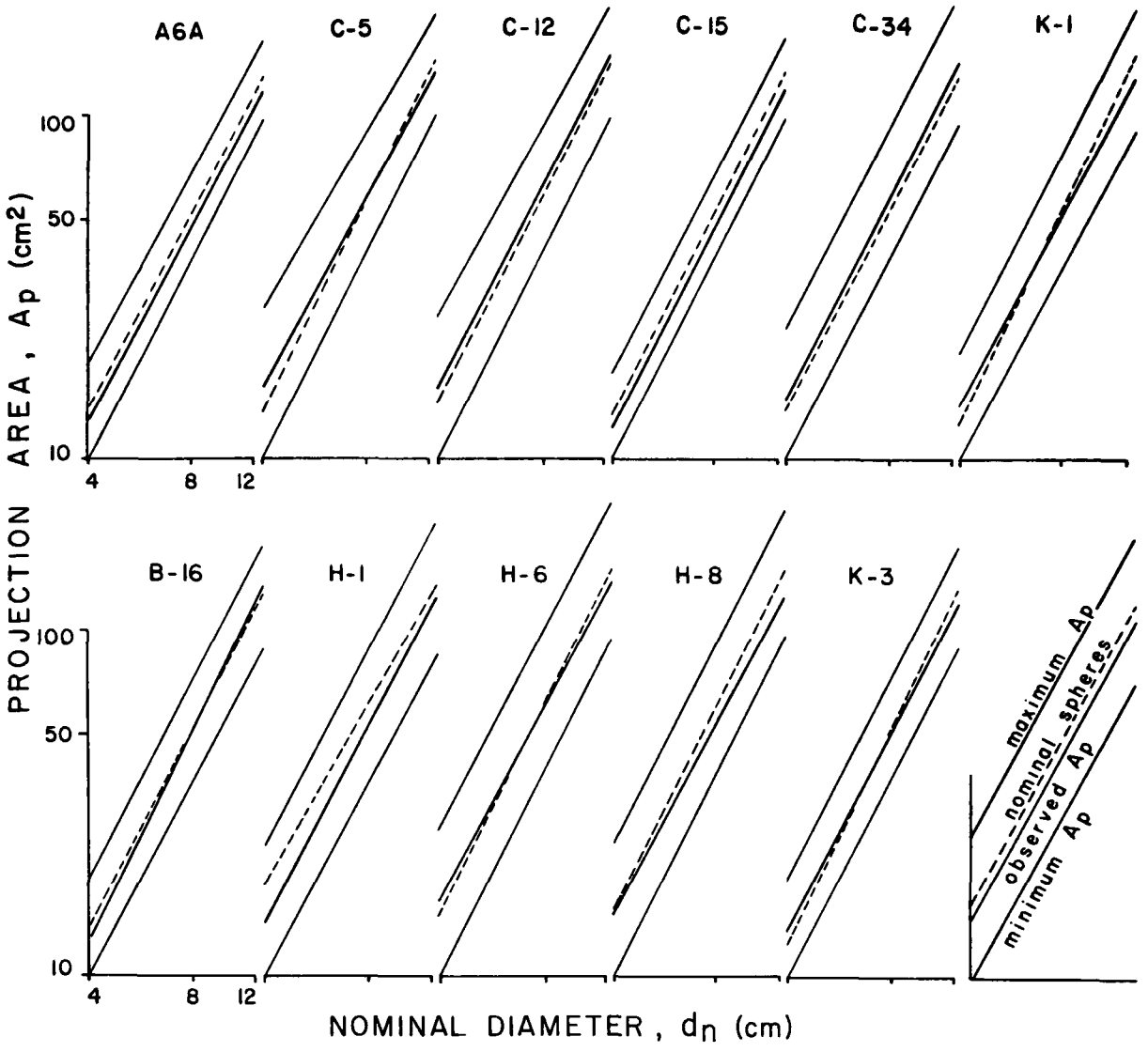

Fig. 49. Projection areas of eleven clast samples as a function of nominal diameter. Four regression lines are shown for each sample; the degree of approximation of the regression line for the observed clast orientation to that for the nominal spheres gives a measure of the degree of equilibrium attained.

imbrication in conglomerates of the Peel Sound Formation shows features characteristic of stable imbrication in isolate clast fabrics. This conclusion is surprising in view of the inevitable collisions between clasts during the deposition of a contact fabric; the clasts would be expected to adopt positions of convenience rather than hydrodynamic stability. Consideration of the depositional process provides a possible explanation. At peak flow in braided channels, bedload movement of clasts takes place in "diffuse gravel sheets", a few pebbles thick (Hein and Walker, 1977). As the flow wanes, the least transportable (commonly the largest) clasts cease to move, and achieve stable imbrication by sliding into upstream scour pockets. These essentially isolate clasts act as a "baffle" to trap particles still in motion. The trapped particles shingle against the stationary clasts, thus adopting an orientation approximating stability. An initial framework of isolate clasts may thus result in a stably imbricated contact fabric when the particles have ceased to move.

Summary

1) In framework conglomerate samples from the Peel Sound Formation, fabric shows a preferred orientation with imbricate clasts dipping predominantly upstream and A-axis orientation, although more dispersed, showing current-parallel, current-

normal and oblique tendencies. These features are consistent with sedimentological evidence of rapid transport, such as poor sorting and poorly developed horizontal stratification. The fabrics are comparable to those observed in fluvial gravels deposited from torrential flows in proximal settings, with clasts transported both as bedload and suspended load. Small and prolate clasts show more tendency to be oriented parallel to the flow.

2) The nature of the source rocks exerted a major control on clast morphology, with internal texture probably of greater importance than lithotype per se. Relatively little evolution of morphology occurred during downstream transport, reflecting the short distance of transport and the high-energy conditions characteristic of the proximal setting. The intensity of flow may also explain the limited influence exerted by size and shape of clasts on the depositional fabric.

3) Despite the apparent disorder shown by the fabric, study of the area projected to the flow by the clast indicates that the contact fabrics show features characteristic of stable imbrication for isolate fabrics (experiments of Koster, 1977). Clast projection area is a more comprehensive parameter of response to the flow than the fabric elements usually considered. It is suggested that contact fabric is a special case of isolate fabric, with the majority of particles achieving an orientation approximating hydrodynamic stability as a result of imbrication against stationary isolate clasts during waning flow.

CHAPTER 6. ORIGIN OF DOLOMITE IN THE CLASTIC WEDGE

Introduction

The origin of dolomite has long been a problem for stratigraphers, and the classic paper of Van Tuyl (1916) gives an exhaustive review of early work and ideas. Discussion has centered around the fact that while dolomite is abundant in the stratigraphic record, it was thought until recently to be absent from modern environments. Many theories sought to explain this apparent anomaly by advocating post-depositional alteration of calcareous sediment. In recent years, however, Holocene dolomite has been described from several areas, including Bonaire, Andros Island and the Persian Gulf (e.g. Illing et al., 1965; Shinn et al., 1965) , the Coorong lagoon of South Australia (Von der Borch, 1976), Baffin Bay, Texas (Behrens and Land, 1972), and Jamaica (Land, 1973). It is now generally accepted that dolomite forms at or near the sediment surface by several processes. Studies of ancient dolostones have also added to our understanding of the problem (see Friedman and Sanders, 1967). Dolomite is abundant in the Siluro-Devonian clastic wedge on Somerset Island, and its petrography and geochemistry will be discussed in the light of these recent studies.

Distribution of dolomite in the clastic wedge

Most studies of dolomite have used a descriptive classification implying an allogenic origin, with terms such as finely or coarsely crystalline (Folk, 1962), but in the present study, such a scheme was considered inappropriate in view of the petrographic evidence for abundant detrital dolomite outlined below, and the "clastic" field appearance of rocks containing both dolomitic material and siliceous grains. The dolomitic rocks are described in terms of grain size (Table 4).

The three following intergradational but distinctive size groupings of dolomite are characteristic of the clastic wedge:

1) Dolorudite (rock fragments larger than sand-size, composed of dolomite) is abundant in Peel Sound Formation members 2 and 4. Dolostone constitutes up to 100% of the clasts (Fig. 40). The clasts are composed of interlocking grains of dolarenite and dolosiltite.

2) Dolarenite to dolosiltite (sand- to silt-sized dolomite) is a major constituent of the Somerset Island and Peel Sound Formations. Fine dolarenite to fine dolosiltite (Table 4) is abundant in facies C_f, F_l and F_m; fine to medium dolarenite is common in the sandstone facies and in the matrix of the Peel Sound conglomerates.

3) Dololutite (very fine grained dolomite) is relatively

uncommon in the clastic wedge. It occurs as thin lenses and intraclasts (Chapter 2) in the Somerset Island Formation.

The stratigraphic distribution of these groups in the Cape Anne syncline is shown diagrammatically in Figure 50, which illustrates the general coarsening upward of the dolomite component in the clastic wedge. The origin of the dolomite is discussed below.

Detrital dolomite

Detrital dolomite is dolomite that has been transported prior to final deposition. Amsbury (1962, p. 5), in accordance with the suggestion of Rodgers (1954, p. 230-232), used the term "detrital" for dolomite eroded from old source rocks, as distinct from dolomite formed within the depositional basin and locally reworked. Sabins (1962, p. 1185), in a study of Cretaceous rocks of the U.S. Western Interior, defined detrital dolomite in a similar manner, and also noted that much of the locally formed dolomite ("primary") had been transported; detrital and transported "primary" dolomite were distinguishable on petrographic criteria. The present writer supports the view of Lindholm (1969, p. 1038) that both varieties of transported dolomite be called detrital, on the grounds that both have been deposited mechanically, and that they may not always be distinguishable in thin section.

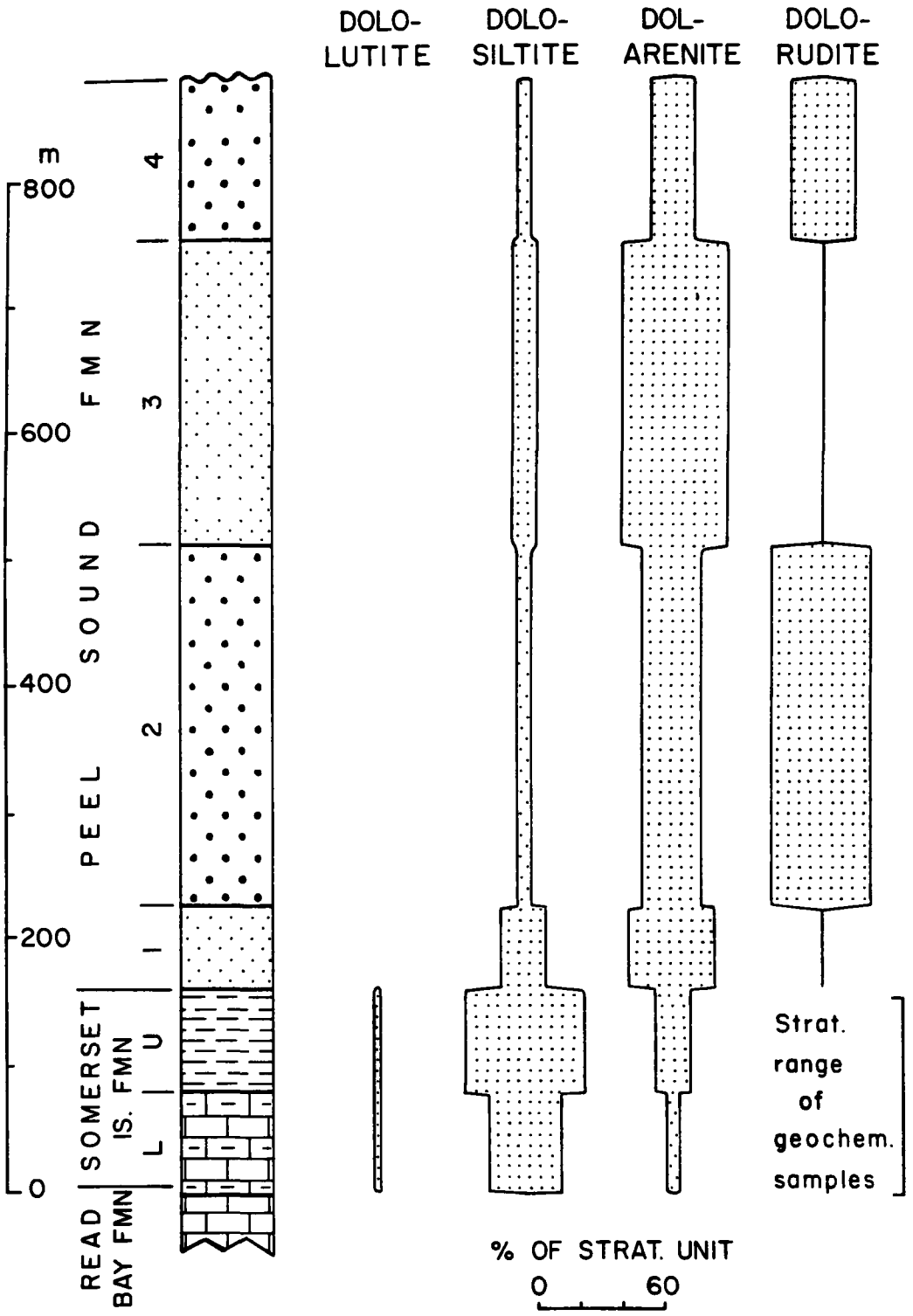

Fig. 50. Distribution of dolomite in the clastic wedge of the Cape Anne syncline. Proportions of the types in each unit are calculated from facies percentages and petrographic data.

The dolorudite in the clastic wedge is clearly detrital. The presence of derived fossils and stratigraphic studies of the percentage of clast types in the conglomerates (Chapter 4) show that the dolorudite was derived by erosion of Lower Paleozoic and Proterozoic rocks of the Boothia Uplift. Dolostone composed of crystals of dolarenite and dolosiltite grade is the major lithology of the Lang River and Allen Bay Formations (Dixon, 1973, p. 136) and of the Hunting Formation (Dixon, 1974), and available information on the Cape Storm Formation (Turner and Dixon, 1971; Kerr, 1975) suggests a similar lithology.

Detrital dolarenite and dolosiltite has seldom been described in the literature, although Van Tuyl (1916, p. 271-4, 329-334, 391) quoted several earlier workers who believed that some sand- and silt-sized dolomite was deposited mechanically as clastic grains. Most studies have tended to emphasise processes of penecontemporaneous and post-depositional dolomitisation. More recently, petrographic evidence for detrital dolomite in ancient sediments was presented by Sander (1951), Lemon and Blackadar (1963, p. 23), Amsbury (1962), Sabins (1962), Bluck (1965), Lindholm (1969) and Jones and Dixon (1975). Detrital dolomite was identified in Recent marine sediments from Florida by Deffeyes and Martin (1962), and reported from streams in central Texas by Amsbury (1962). Evidence for the detrital nature of dolarenite and dolosiltite in the clastic wedge on Somerset Island will be considered in

relation to sedimentation features, size, sorting and shape of grains, and the percentage of dolomite in the rocks.

Sedimentation features

The dolomite is associated commonly with clastic grains (mainly quartz) in primary sedimentary structures, especially in facies C_f and F_1 (Photos 5, 45 and 46). The well-defined parallel lamination is produced by comparable changes in grain size of both quartz and dolomite, with calcitic pellets contributing to the coarser laminae. Some laminae are graded, with fine dolarenite fining up to coarse or fine dolosiltite, the coarsest grains being concentrated in small-scale irregularities at the base of the laminae, in load casts, and in infilled desiccation cracks. The size of spaces between original framework grains and allochems (either void or filled with a calcareous matrix) may have determined the size of diagenetically formed dolomite; however, while pellets with minor quartz grains form a framework in some coarser laminae, there is no obvious framework to control the size of the dolomite in the finer laminae. Much of the lamination in facies F_1 is interpreted as cryptalgal, implying that original detrital sediment, including dolomite, was bound by algal filaments; a few domal stromatolites also consist of well-laminated fine dolarenite. Dolarenite in the sandstone facies is commonly "clastic textured" (Rodgers, 1954, p. 231), occurring in cross-beds.

While dolosiltite shows a clear relationship to primary sedimentary structures in facies C_f and F_l, such a relationship cannot be conclusively demonstrated for the thick structureless units of facies F_m. However, if detrital dolorudite and dolarenite is abundant in the clastic wedge, detrital dolosiltite should also be present. Facies F_m was deposited in a terrestrial environment (Chapter 2), a setting in which detrital dolosiltite is a more probable constituent than dolomite formed in situ.

Size and sorting

In confirmation of the apparent size relationship between quartz and dolomite noted above, the graph in Figure 51 shows that the maximum apparent size of dolomite is proportional to that of quartz in forty thin sections (correlation coefficient of 0.700, significant at $>99.99\%$ level). This suggests that the dolomite and quartz have been transported together, and that the dolomite is detrital. Quartz in most thin sections tends to be coarser than the dolomite, with most data points plotting above the 1:1 line of Figure 51; this may be explained by the elongate shape of some quartz grains in comparison to the more equant form of the dolomite, and by the lower density of quartz (hydraulically equivalent to smaller, denser grains of dolomite). Furthermore, the size disparity becomes greater with increasing size: in coarser sediments, quartz grains range up to more than 0.6 mm in

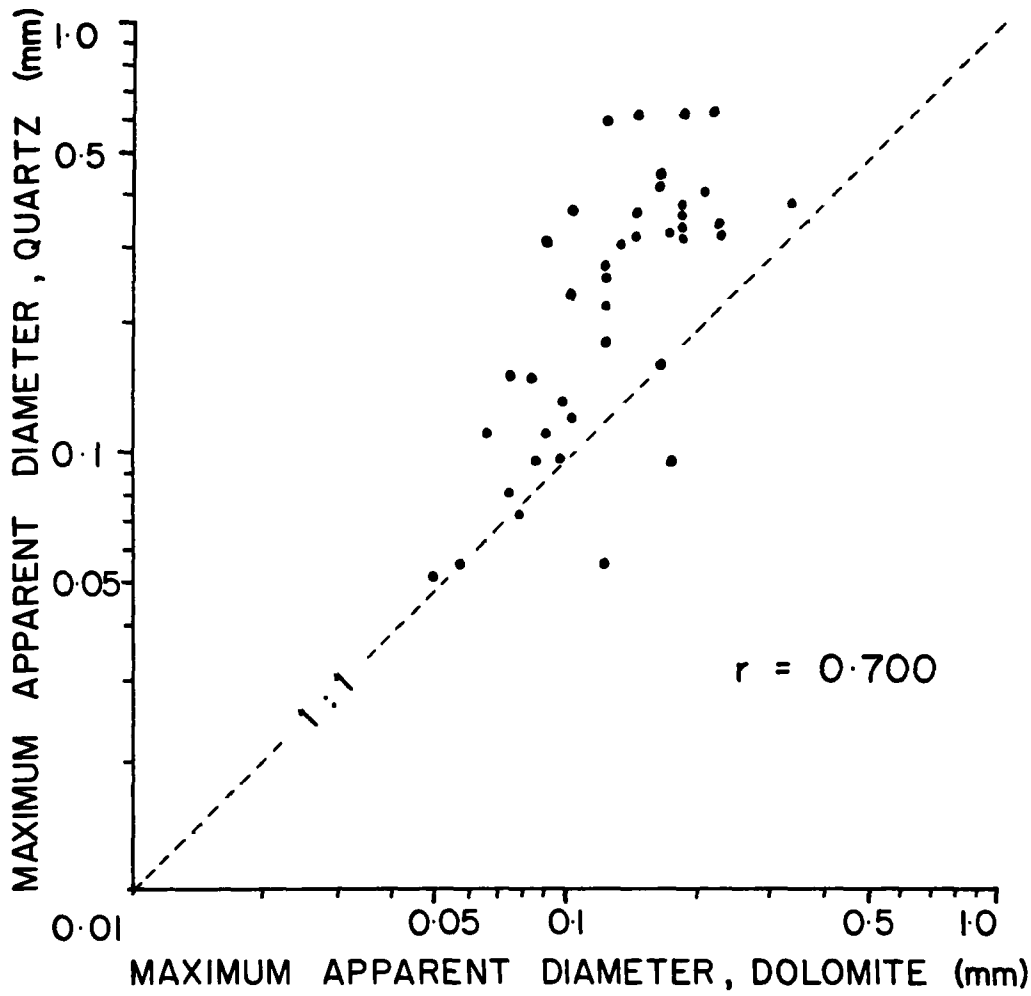

Fig. 51. Maximum apparent diameters of quartz and dolomite grains, in 40 thin sections of rocks from the clastic wedge on Somerset Island.

apparent diameter compared to 0.33 mm for dolomite, a function of the size distribution of grains supplied by the source; in finer sediments, a few euhedral rhombs (?secondary) increase the maximum size of dolomite relative to that of quartz. Sabins (1962, p. 1188 and Fig. 2) noted a similar size correlation in very fine- to medium-grained sandstones, and the consistently finer size of the dolomite was explained by the density contrast. Size correlation was also described by Bluck (1965) from the Middle Devonian of Indiana, by Lindholm (1969) from the Devonian Onondaga Formation of New York, and from the Upper Silurian Leopold Formation on Somerset Island by Jones and Dixon (1975).

The insoluble residue content of 49 limestone and dolostone samples from the clastic wedge shows a positive correlation with Mg% as determined by atomic absorption spectroscopy (see below), with a correlation coefficient of 0.527, significant at the 99.99% level. In contrast, 216 samples combined from the Lang River to Peel Sound Formations gave a correlation of -0.059. This may suggest that the correlation of Mg and insoluble residue in the clastic wedge is unusual for the Lower Paleozoic sequence, probably due to the presence of detrital dolomite in the clastic wedge. However, correlations between the abundance of silicate clastic material and dolomite content have commonly been noted (e.g. in dolomitic limestones from Pennsylvania by Lesley, 1879 , discussed by Fairbridge , 1957 , p. 154; Schmidt , 1965). Such correlations may result simply

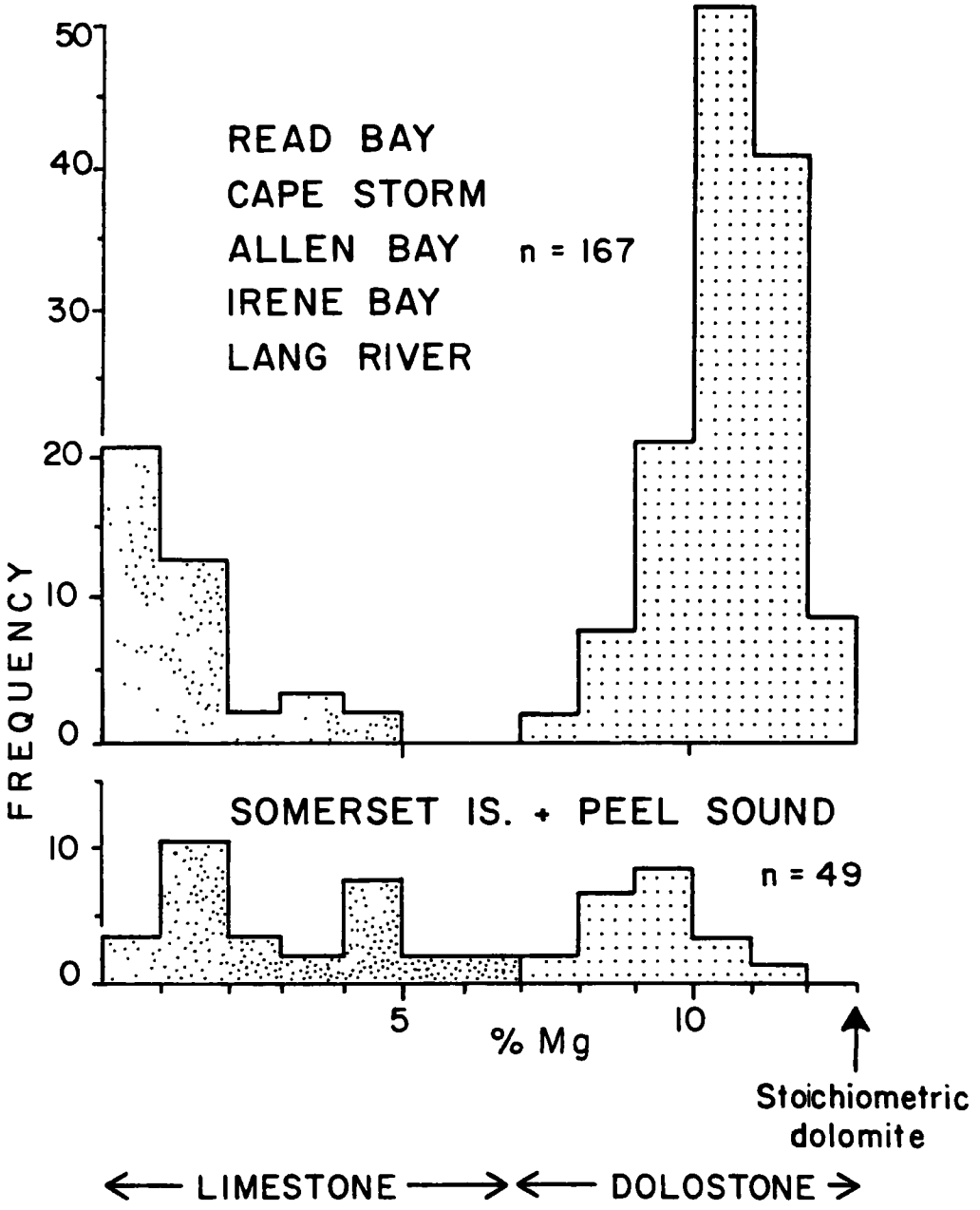

Fig. 52. Mg% of total carbonate in Lower Paleozoic carbonates of the Boothia Uplift region. Limestone and dolostone separated at 50% of molecular dolomite. Data from Veizer et al. (in press).

from environmental association due to the prevalence of dolomitisation in nearshore, terrigenous environments, or for chemical reasons (clays may act as "membranes" during dolomitisation: Kahle, 1965; Veizer, 1970). The grain size correlation is thus a more reliable indication that the dolarenite and dolosiltite are detrital.

Shape

Grain shape commonly is difficult to define, especially where the sediment is fine grained and particles are closely packed. Most dolomite grains appear subhedral, but some are euhedral or anhedral. The abundance of subhedral crystals in beds which also show evidence of detrital origin may be explained by limited transport and the fine grain-size. Kuenen (1960) observed that quartz grains of silt to fine sand grade undergo little rounding even after prolonged transport and abrasion under eolian conditions. In the clastic wedge, quartz silt associated with dolomite is also predominantly sub-angular.

In a few units, shape gives a clear indication of a detrital origin, as a result of late diagenetic overgrowth. Photo 47 shows euhedral dolomite crystals containing well-rounded dolarenite nuclei, stained brown (especially along cleavages), in optical continuity with the unstained dolomite overgrowths. The nuclei are evidently detrital, and resemble grains observed in the Cretaceous of Texas (Amsbury, 1962, Plates 5 and 7). Zoning is a common feature of dolomite crystals (Katz, 1971;

Folk and Siedlecka, 1974), but in this instance, the rounded nature of the nuclei and the contrast in shade with the exterior is strong evidence for overgrowth. Lindholm (1969) suggested that detrital grains of dolomite would greatly assist later dolomitisation by acting as nuclei. Such well-defined nuclei are exceptional, and should be distinguished from the apparent overgrowths observed in many coarse dolosiltite and very fine dolarenite grains in the two formations. These grains contain poorly defined, rounded "cores", noticeably darker than the exterior and probably consisting of fine inclusions of clastic or calcareous material. Taft (1961), Veizer (1970) and Folk and Siedlecka (1974) have observed similar inclusions in the central part of dolomite crystals.

Dolomite percentage

Dolarenite grains are abundant in fine- to medium-grained sandstones of the Peel Sound Formation (Fig. 50). The grains have interlocked during compaction so that the nature of the matrix is uncertain, although it probably consists of dolosiltite with some terrigenous fines. Point counts on five thin sections show that quartz and other silicate grains average 49%(range 12.6 - 63.5%),while dolarenite averages 51% (range 36.6 - 87.4%). Some of these rocks must contain detrital dolomite, unless the quartz grains were originally supported by a calcareous matrix that was later dolomitised. The absence

of both limestone clasts and micritic matrix in the sandstones and conglomerates suggests that calcareous material was not an original detrital component. A few dolarenite grains in the sandstones are polycrystalline and thus certainly detrital (Sabins, 1962, p. 1185).

The content of dolomite in the finer calcareous and dolomitic siltstones of the clastic wedge also supports a detrital origin. The Mg distribution (Fig. 52) contrasts with that of the other Lower Paleozoic formations on Somerset Island. X-Ray diffraction shows that the general departure of the dolostones from the Mg% expected for stoichiometric dolomite is due to admixture of calcite with the dolomite (Veizer et al., in prep.), but "limestones" and "dolostones" in most of the Lower Paleozoic sediments tend to be distinct. The formations of the clastic wedge, however, contain a particularly high proportion of Mg values intermediate between the end members, and this may readily be explained by the mixing of mechanically deposited dolomite with detrital calcareous material.

Penecontemporaneous dolomite

Penecontemporaneous dolomite ("syngenetic" group of Friedman and Sanders, 1967) is relatively fine grained dolomite formed in situ during or very shortly after deposition. Textural evidence for replacement is commonly lacking, although

there is as yet no indisputable evidence that dolomite precipitates from surface waters.

The dololutite of the Somerset Island Formation (Photos 48 and 49) shows good evidence for formation at or very close to the depositional surface. The top surfaces of the beds are fissured and irregular, indicating subaerial exposure and erosion, and dololutite intraclasts are locally abundant (Chapter 2 and Photo 11). Dololutite crusts very similar to those in the Somerset Island Formation have been described from modern supratidal flats by several authors (Deffeyes et al., 1965; Shinn et al., 1965; Shinn, 1968; Logan, 1974). At Abu Dhabi in the Persian Gulf, groundwaters under the tidal flats become increasingly saline landwards, with an increase in the Mg/Ca ratio of the brine as a result of the precipitation of aragonite and gypsum (Butler, 1969). The brines cause dolomitisation of the superficial carbonate, and salinity and Mg/Ca ratio decrease towards the landward limit of tidal flooding. Brines may rise by capillary action in fine sediment (Shinn et al., 1965), or by evaporative pumping in which evaporation of groundwater on the flats acts as a pump to draw marine water through the sediment (Hsü and Siegenthaler, 1969). The latter mechanism was considered more probable in flats of the Sinai area by Gavish (1974), since the coarse sediment precludes capillary action. Groundwater concentration may also result from the downward percolation of marine waters concentrated by evaporation during flooding of the supratidal flats

following spring tides or storms (Butler, 1969).

Secondary dolomite

Secondary dolomite ("diagenetic" group of Friedman and Sanders, 1967) is relatively coarse grained dolomite formed in situ by dolomitisation after deposition. Textural evidence indicates an origin by replacement of calcareous sediment. Penecontemporaneous and secondary dolomite form end members of a diagenetic continuum, and secondary dolomitisation as here defined may occur relatively soon after deposition. The terms indicate the sequence of dolomitisation events as judged from textural evidence, and imply no particular time after deposition or degree of consolidation and depth of burial during dolomitisation.

Secondary dolomite is common in the clastic wedge. Micritic limestones contain isolated euhedral rhombs of dolomite, uniformly of silt size. Coarser isolated rhombs replace sparite within paired ostracod valves, and diagenetic gypsum crystals (enclosing ostracod fragments and now composed of ferroan calcite microspar) are also replaced by rhombs. Secondary overgrowths on detrital dolarenite grains have been described in the previous section.

Dolomite of similar type is now known to precipitate from groundwaters of relatively low salinity in modern environments. Land (1973) observed euhedral 8-25μ rhombs dispersed in micrite,

replacing allochems and lining cavities in Jamaican Pleistocene limestones; coring showed that the presence of dolomite was related to the level of the present-day water table. Folk and Siedlecka (1974) interpreted 50-100μ rhombs replacing sparry calcite in the Upper Paleozoic of Bear Island, Svalbard, as the product of hyposaline dolomitisation. The theory behind such dolomitisation has been discussed by Badiozamani (1973) and Folk and Land (1975), and although preliminary, the following points are especially pertinent:

1) The dolomite is relatively coarse (e.g. 50-100μ), clear and euhedral. It commonly replaces secondary calcite void fillings, and original sediment.

2) Dolomitisation is promoted by mixing of fresh and saline groundwaters. Marine waters with a relatively high Mg/Ca ratio ($\geq$1:1) are the source of Mg^{2+} ions; dolomite precipitates when mixing with freshwater reduces salinity (see discussion and Fig. 1 in Folk and Land, 1975). When the groundwaters are mixed in suitable proportions, the non-linearity of the $CaCO_3$ solubility curve may cause oversaturation with respect to dolomite but undersaturation with respect to calcite, resulting in dolomitisation (Badiozamani, 1973, Fig. 4). Such dolomitisation was termed "Dorag" by Badiozamani.

3) Any surface or sub-surface environment where sediments are affected alternately by waters of high Mg/Ca ratio (especially hypersaline brines) and low salinity may be a locus of dolomitisation. In Jamaica, dolomitisation occurs in the

"mixing zone" at the interface of marine and fresh phreatic waters (Land, 1973). Such a zone of mixing is present at the meteoric-tidal groundwater interface beneath tidal flats, and progradation of the flats would result in the seaward migration of the mixing zone, with relatively early dolomitisation of the near-surface sediment.

An unusual occurrence of groundwater dolomitisation has recently been documented by Von der Borch (1976). In the area of Coorong lagoon, South Australia, very fine (10-20μ) dolomite apparently forms in surface sediments through evaporation of fresh groundwater. The Mg^{2+} ions may be derived from weathering of basic volcanics inland from the zone of dolomitisation. The dolomite in this case forms from low salinity groundwater but petrographically resembles dololutite of hypersaline type.

Secondary dolomite in the clastic wedge on Somerset Island may be of Dorag type. The clear euhedral rhombs are relatively coarse, and commonly replace secondary void fillings. The tidal flat environment discussed in Chapter 2 would have provided an ideal location for the mixing of groundwaters both in the surface and sub-surface; evidence suggests that meteoric flooding occurred commonly on the flats (Chapter 2), generating the "schizohaline" environment of Folk and Siedlecka (1974) characterised by rapid changes of salinity from hypersaline to dilute. Finally, progradation of the tidal flats which produced the cyclicity would have enabled the mixing zone to migrate

through extensive volumes of sediment shortly after deposition.

Trace element geochemistry and facies analysis

Trace elements in carbonate rocks may provide useful information about depositional environments and early diagenetic history. Sr^{2+} is one of the main trace elements substituting for Ca^{2+} in the lattices of carbonate minerals, and as such is a potential tool in facies analysis. The predicted Sr content of phases precipitated from sea water is about 8200 ppm for aragonite and 1200 ppm for calcite (Kinsman, 1969), and the Sr content of present day limestones shows a roughly bimodal distribution. A high-Sr group with about 7500-10,000 ppm Sr comprises inorganically precipitated aragonite and most skeletal aragonite; and a low-Sr group with about 800-4500 ppm Sr comprises inorganic and organic calcite and molluscan aragonite (Bathurst, 1975, Fig. 225). The bimodal distribution of Sr in modern sediments is thus largely a function of the mineralogy of the sediment, and if mineralogy is facies related, the distribution of Sr may be useful as a facies indicator. Aragonite is the predominant carbonate mineral of many tidal flat environments (e.g. Shinn et al., 1969; Illing et al., 1965), resulting from inorganic and biochemical precipitation (Bathurst, 1975, p. 204-5 and 276-292). High-magnesium calcite tends to be more prevalent in open sea neritic and shallow bathyal environments (Veizer and Demović, 1974. p. 105-107). Sr content

is thus facies related, and in tidal flat environments, increased Sr may also correlate with increased salinity.

It might be expected that such an original facies-related distribution of trace elements would be destroyed during redistribution of the elements in diagenesis. However, Veizer and Demovič (1974) and Veizer (1977) showed that Phanerozoic limestones in the Carpathians and Australia give a bimodal distribution of Sr similar to that described above for modern environments. Rocks from hypersaline environments, for example, are relatively rich in Sr as compared to rocks from open marine environments. Most redistribution of trace elements probably occurs during transformation from a metastable to a stable mineral assemblage in a partially closed wet chemical system. This was deduced independently by Pingitore (1976) from a consideration of the fabric and trace element content of originally aragonitic corals after vadose and phreatic diagenesis on Barbados, and by Veizer (1977) from a study of Sr content and oxygen isotope distribution in samples of Archaean to Recent age. Hence the nature of the original sediment may exert greater control on the resulting rock chemistry than the diagenetic fluids, despite an order of magnitude reduction in Sr content.

The Sr content of dolostones may depend largely upon the original mineralogy of the dolomitised material, with high-Sr dolomite resulting from dolomitisation of inorganic aragonite and low-Sr dolomite from dolomitisation of calcite. If the

original aragonite inverted to calcite before dolomitisation, the dolomite will be poor in Sr. The trace element distribution of dolostones, while likely to be facies related, may be more usefully considered to depend on the timing of dolomitisation, with "early diagenetic" dolostone formed from aragonite and "late diagenetic" dolostone formed from calcite (Veizer et al., in press).

The distribution of Na in modern carbonates is poorly known. Fritz and Katz (1972) showed that in Middle Devonian sediments at Pine Point, N.W.T., Na is enriched in supratidal fine-grained dolostone with respect to coarser dolostone of later origin, so that Na content may also be facies and time related.

A geochemical hypothesis may be formulated to investigate the origin of dolarenite and dolosiltite, the predominant size of dolomite, in the clastic wedge. If the dolostones are relatively rich in Sr and Na, they may be interpreted as early diagenetic in type and the dolomite probably originated by dolomitisation of aragonite under hypersaline or hyposaline conditions. If Sr and Na contents are relatively low, a late diagenetic origin is indicated, and the dolomite probably originated by dolomitisation of calcite under conditions of low salinity. The dolomite may subsequently have been transported as detrital grains. It is often instructive to compare trace element distributions in formations from the same depositional basin, and the Somerset Island and

Peel Sound Formations will be considered in the context of the entire Lower Paleozoic succession.

Geochemical analysis of the Lower Paleozoic dolostones of the Boothia Uplift region

The Lower Paleozoic formations on Somerset Island (Table 1) form an excellent succession for investigating dolomitisation and the facies control of trace element distribution, since limestones and dolostones from subtidal to supratidal environments are represented. After preliminary analysis of samples from the Read Bay Formation by Jim Savelle and from the Somerset Island and Peel Sound Formations by the author, a more comprehensive project was undertaken by Dr. J. Veizer, with sampling of the older formations by B. Jones. J. Lemieux analysed the samples for Ca, Mg, Sr, Na, Fe and Mn by atomic absorption spectroscopy (Appendix D). Sample locations, methods and precision of analysis and results are fully described by Veizer et al. (1977 and in press), so that only certain aspects of the project relevant to the origin of the dolomite will be discussed. The Read Bay and Irene Bay Formations did not yield dolostone samples. Forty-nine samples of limestone and dolostone (facies C, C_f, F_l and F_m) were collected from the Somerset Island Formation in the Creswell Bay area, and from the upper member of the Peel Sound Formation (Sandstone-

Carbonate facies of Miall, 1970b) at Baring Channel, Prince of Wales Island. The samples came from the following stratigraphic intervals:

1) Peel Sound Formation at Baring Channel

2) lower member of the Somerset Island Formation at Creswell Bay

3) upper member of the Somerset Island Formation (basal strata) at Creswell Bay

4) higher strata of the upper member at Creswell Bay

Samples in the first three intervals were collected from progradational coastal sequences (Chapter 2), and those in the fourth interval from clastic-carbonate cycles of the alluvial plain (facies association 3, Chapter 3). The dolostones consist mainly of dolarenite and dolosiltite, with only two samples containing dololutite. No dolomitic conglomerates or sandstones of fluvial origin were analysed.

The Sr and Na distribution for the dolostone samples from the Lower Paleozoic formations shows that two geochemical groups are present (Fig. 53). Dolostones from the Lang River and Allen Bay Formations and from interval 4 of the clastic wedge are relatively poor in both Sr and Na. Dolostones of the Cape Storm Formation and from intervals 1 to 3 of the clastic wedge are relatively rich in Sr and Na. The remarkably high range of values for Sr in the Cape Storm Formation reflects the presence in one section of celestite ($SrSO_4$), confirmed by X-Ray diffraction, and the samples from this section were

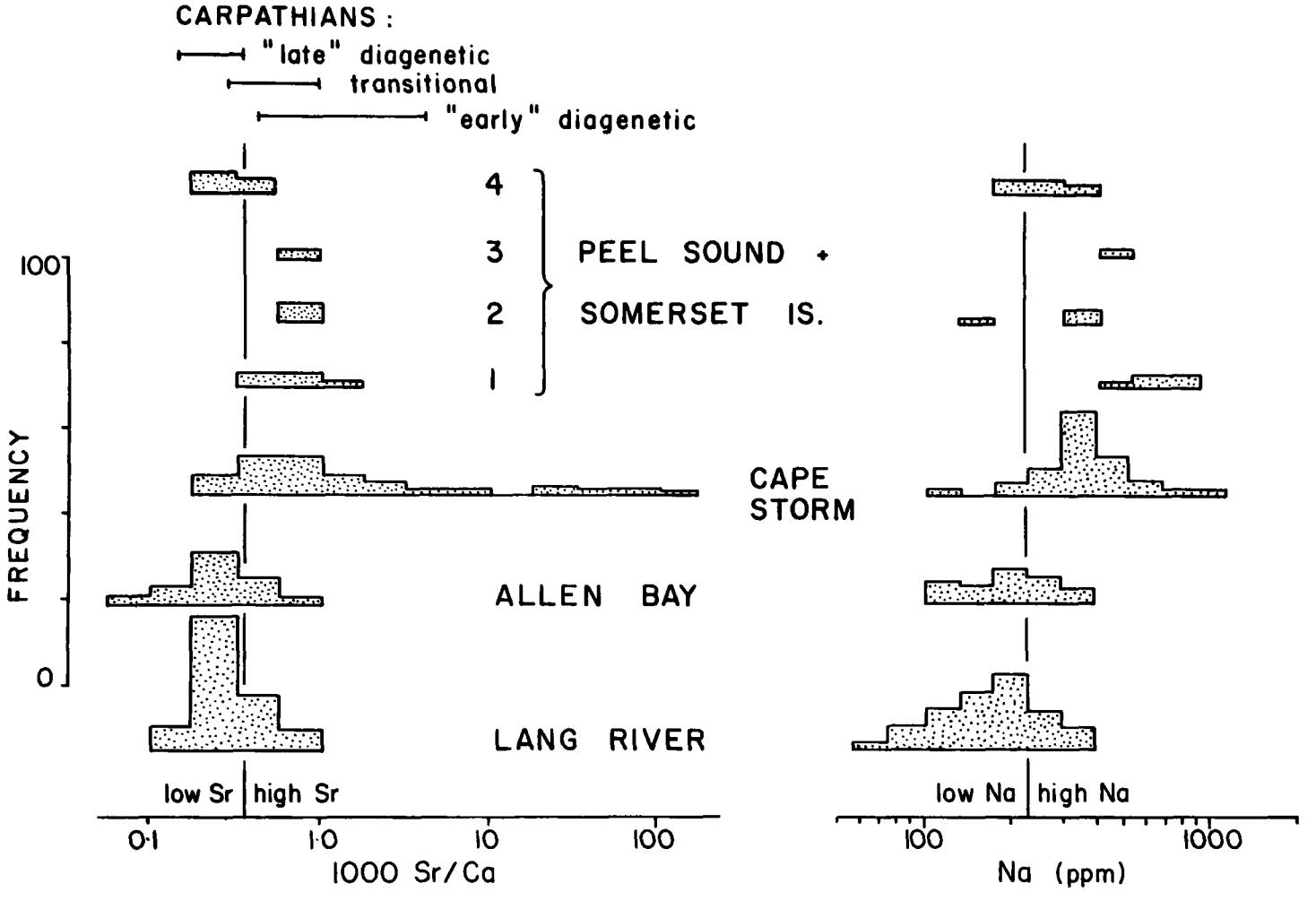

Fig. 53. Sr and Na in dolostones from the Lower Paleozoic of the Boothia Uplift region. Numbers 1 to 4 indicate stratigraphic intervals in the clastic wedge (see text). Sr calculated as 1000 Sr/Ca in the soluble fraction. Carpathians data from Veizer and Demovič (1974). Data from Veizer et al. (in press).

242

omitted from statistical comparison. Application of the t-test to the Na and Sr distributions of the dolostone samples shows that stratigraphic units within each geochemical group do not differ significantly at the 95% confidence level, while units in different geochemical groups differ significantly in these parameters. For comparison, the range of values of 1000 Sr/Ca encountered in early and late diagenetic dolostones (terms used in a general sense from petrography) from the Mesozoic of the Carpathians (Veizer and Demovič, 1974) is also shown in Figure 53. The low-Sr, low-Na group of the Arctic succession lies in the range of late diagenetic dolostones, and the high-Sr, high-Na group compares well with the early diagenetic dolostones of the Carpathians.

Discussion

Petrographic study of dolostones in the clastic wedge indicates that the dolomite is predominantly detrital, with *in situ* secondary dolomite and some penecontemporaneous dolomite present in the Somerset Island Formation. The geochemical data suggest that dolomite of early diagenetic type (high-Sr, high-Na) characterises the lower part of the clastic wedge (intervals 1 to 3) and that dolomite of late diagenetic type (low-Sr, low-Na) is present in the upper part (interval 4). The geochemistry of the dolostones does not provide a unique solution for their origin, but it imposes

some constraints on interpretation. The high-Sr, high-Na groups of the clastic wedge could have been derived largely from erosion of the Cape Storm Formation. The Proterozoic Hunting Formation which underlies the Paleozoic sequence on Somerset Island could also have been a source of detrital dolomite; it was not analysed geochemically, but was interpreted as a tidal flat sequence by Tuke et al. (1966) and Dixon (1974), and is likely to fall in the high- Sr and -Na group. The low-Sr, low-Na group could have been derived from erosion of the Lang River and Allen Bay Formations. Alternatively, the two geochemical groups could reflect dolomitisation of aragonite and calcite, respectively, during deposition of the clastic wedge, with subsequent erosion and transport of the dolomite as detrital grains. The following interpretation is suggested for integration of the petrographic and geochemical data.

During deposition of the lower part of the Somerset Island Formation, the tidal flats were evidently environments of hypersalinity: evaporites are common and the Sr and Na distribution of the associated limestones suggests a highly saline depositional and early diagenetic environment (Veizer et al., 1977 and in press). In this setting, dololutite beds (early diagenetic dolomite, rich in Sr and Na) formed from hypersaline brines in superficial sediments. At the same time, Dorag dolomitisation may have occurred through mixing of fresh and saline groundwaters at the landward

margin of the flats. The dolarenite and dolosiltite thus formed would also have been rich in Sr and Na if dolomitisation took place relatively early, before inversion of aragonite to calcite. As the flats prograded seaward producing cyclic sequences (Chapter 2), seaward migration of the zone of groundwater mixing would have resulted in secondary dolomitisation.

Semi-arid supratidal flats suffer frequent subaerial erosion, following torrential rains for example, and on the Somerset Island flats, such events could have reworked the relatively coarse grained Dorag dolomite and distributed it seaward across the flats. Reworking of Recent dolomite is known from modern environments. Aivar Depers (pers. comm., 1977) noted rounded to sub-rounded dolomite grains on tidal flats at Spencer Gulf, South Australia, and suggested that they may have been reworked from algal and/or supratidal facies, with rounding taking place during the extensive phases of sheet erosion associated with shallow tidal flow. Bluck (1965) attributed detrital dolomite on Middle Devonian tidal flats to reworking of early-formed dolomite on landward parts of the flats. A local source of this nature for the detrital dolomite in the lower part of the Somerset Island Formation readily explains the presence of both secondary and detrital dolarenite and dolosiltite in the sediments; a local source is also consistent with the relatively low relief and limited source potential of the Boothia Uplift at that time.

As the Boothia Uplift rose, detrital dolomite from bedrock sources would have become increasingly important, contributing to the dolomitic conglomerates and sandstones of the Peel Sound Formation.

The speculative nature of the proposed sequence of events, and in particular the application of the Dorag model, must be emphasised. Analysis of the dolostone clasts and dolomitic sandstones of the Peel Sound Formation would enable comparison with possible bedrock sources of dolostone, and the dolomite size grades in the Somerset Island Formation should also be characterised by analysis of selected specimens. The sections in the West Creswell area are discontinuous, and systematic sampling of a continuous section through the clastic wedge is recommended.

45. Detrital dolomite in graded laminae. Laminae (facies F_1) composed mainly of subhedral fine dolarenite passing up into dolosiltite. with ostracod fragments and minor quartz and muscovite. Plane polarised light. Unit G74J-9f (Photo 5).

46. Detrital dolomite in a desiccation crack. Crack infilled by medium-grained quartz (q) and fine dolarenite (d). Plane polarised light. Unit G74J-9f (Photo 5).

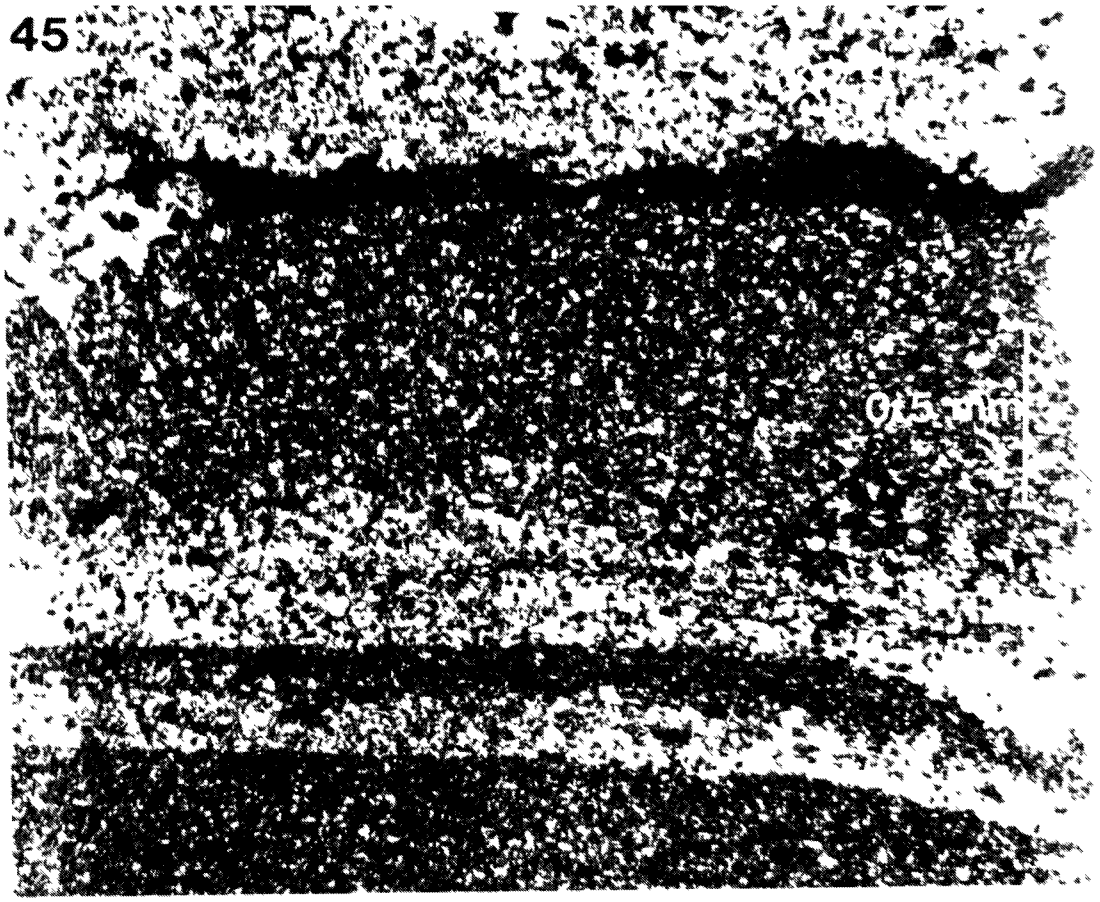
45
0.5 mm

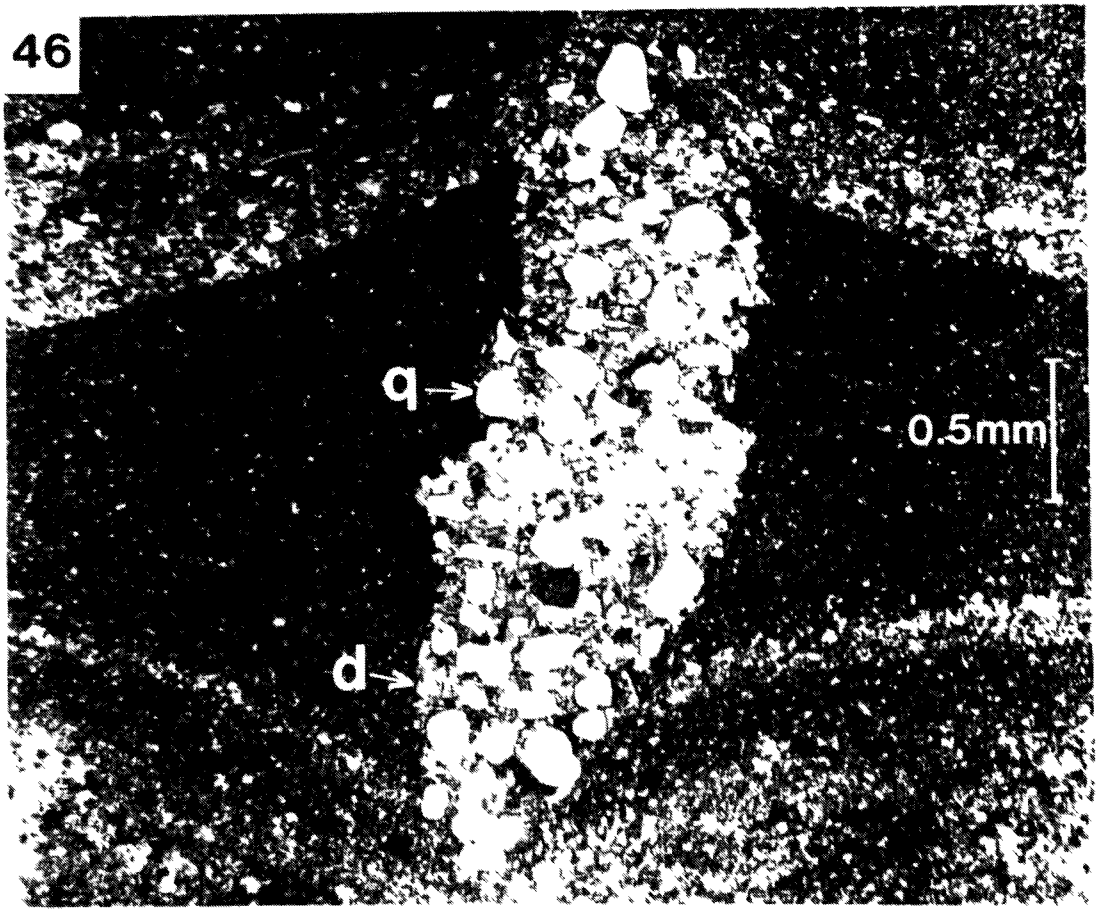
46
q
d
0.5mm

47. Overgrowths on detrital dolomite grains. Overgrowths of clear euhedral dolomite, rounded cores of dark dolomite. Surrounding grains mainly quartz. Plane polarised light. Unit G73L-15a, Loc. 11.


47
0.1mm

48. Dololutite containing ostracod valves and indistinct pellets. Plane polarised light. Unit G73K-28, Loc. 12.

49. Dololutite containing medium-grained quartz. Small vugs infilled by sparite. Plane polarised light. Unit G73J-22, Loc. 9.

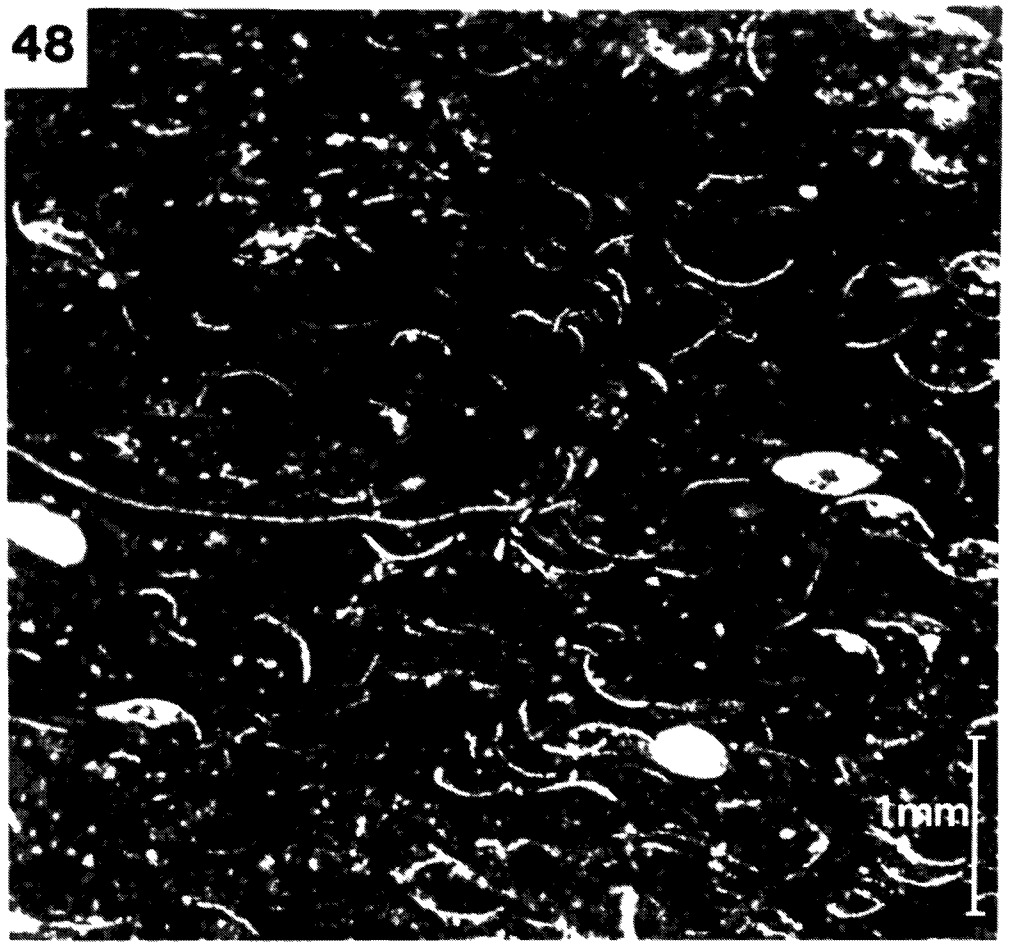
48
1mm

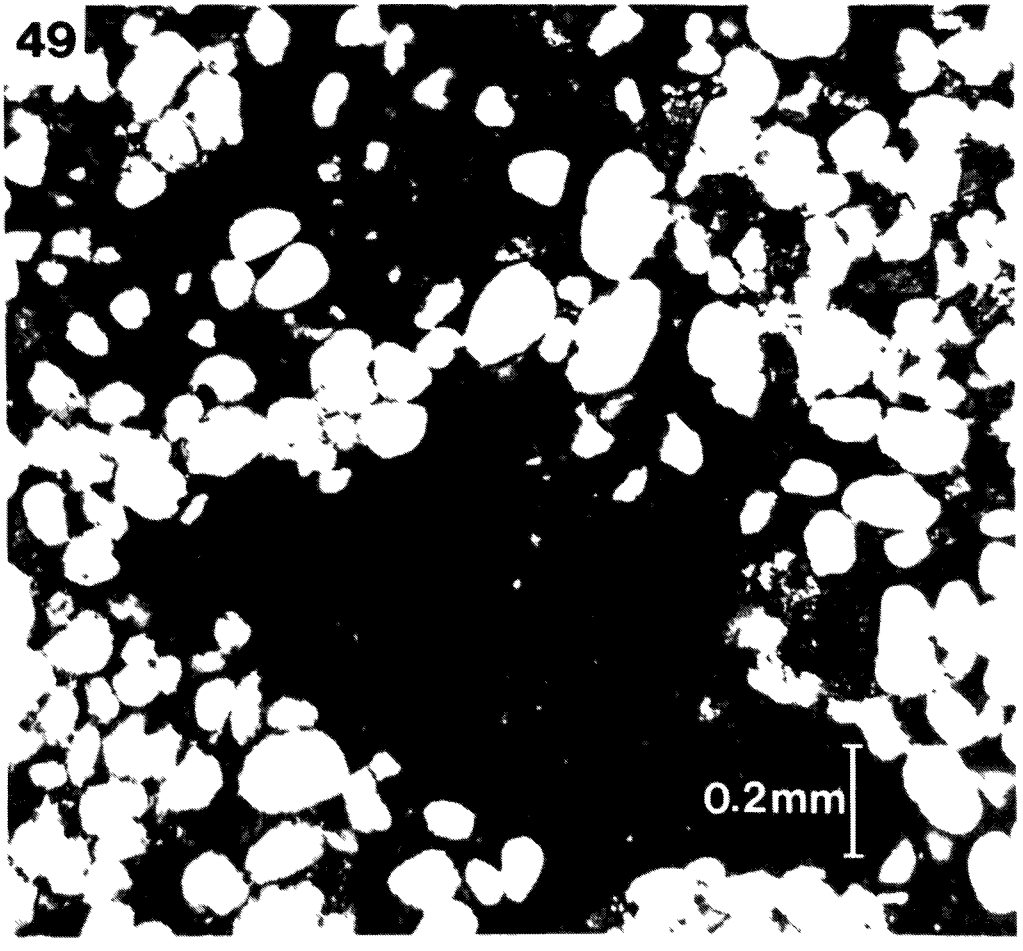
49
0.2mm

CHAPTER 7. SEDIMENTATION OF THE CLASTIC WEDGE IN THE BOOTHIA UPLIFT REGION

Introduction

Silurian rocks of the south-central Arctic Islands are divided by a major facies boundary that passes through central Cornwallis Island (Thorsteinsson and Tozer , 1970), (Fig. 54). North of this boundary, graptolitic limestones and shales of the Cape Phillips Formation were deposited in a deep water miogeosynclinal basin. Shallow water platform carbonates, such as the Allen Bay, Cape Storm and Read Bay Formations, accumulated south of the boundary. In Late Silurian-Early Devonian times, local uplift resulted in widespread deposits containing coarse clastic sediments. The clastic wedge which developed adjacent to the Boothia Uplift was the result of diachronous tectonism that varied in age and style locally and gave rise to sediments with strong lateral facies changes. Like all regressive sequences, it is inherently complex, and most stratigraphic terminology has proved applicable only locally.

This chapter presents a correlation for stratigraphic units at several localities in the Boothia Uplift region, and an outline of the sedimentary history of the area in Upper Silurian to Lower Devonian times. Previous studies dealing with the tectonic history and regional sedimentation

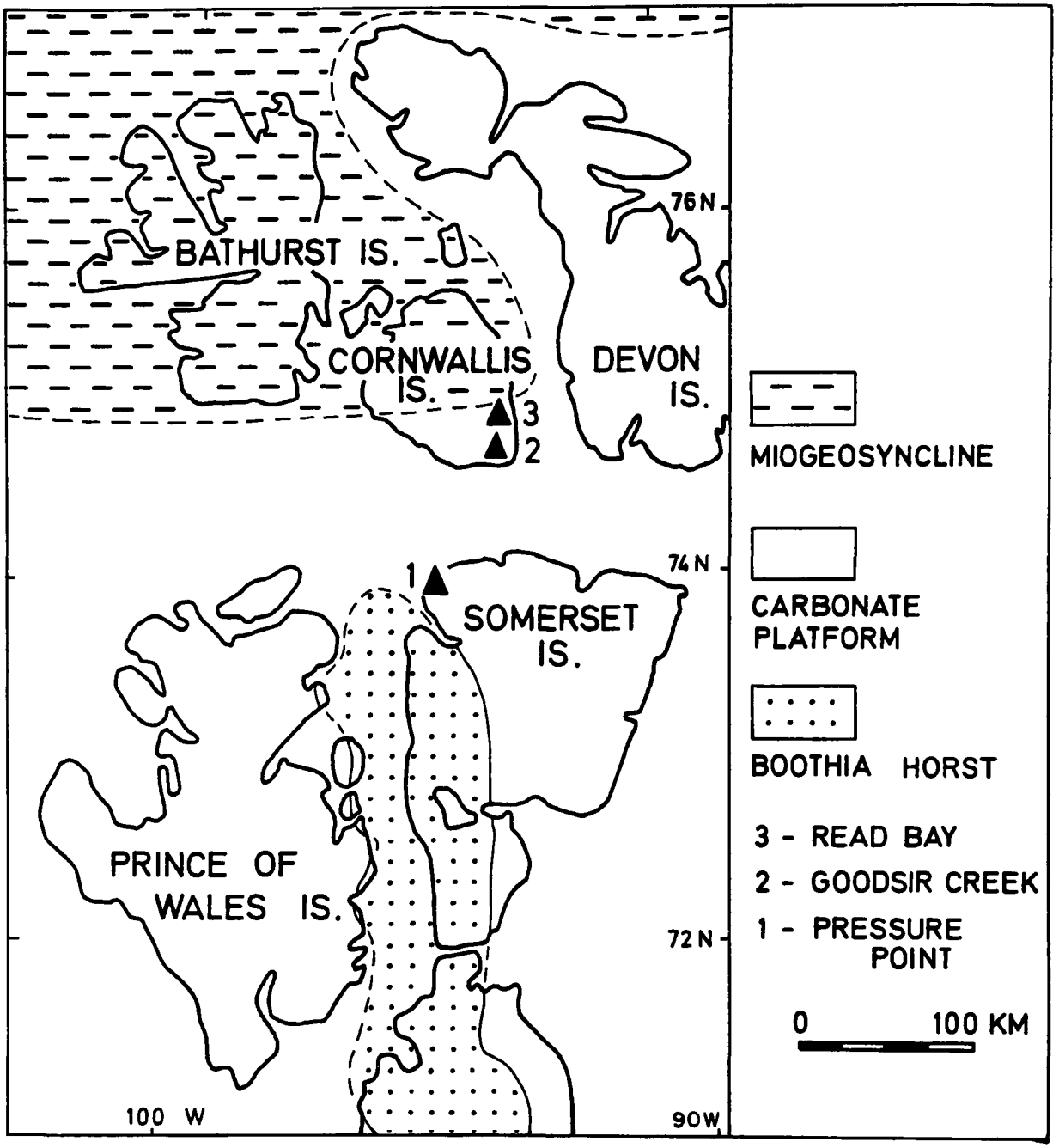

Fig. 54. Upper Silurian paleogeography of the south-central Arctic Islands. Data from Blackadar and Christie (1963) and Mayr (1973). After Gibling and Narbonne (1977), Fig. 1.

of the area include those of Kerr and Christie (1965), Brown et al. (1969), Walcott (1970), Dineley (1971), Daae and Rutgers (1975) and Kerr and deVries (1977); Kerr (1977) provided a particularly good summary of the relationship between tectonism and sedimentation in the area. Some aspects of the present study are also presented in Gibling and Narbonne (1977), Miall, Gibling and Kerr (1978), and Miall and Gibling (in press).

Terminology for the Boothia Uplift has recently been redefined by Kerr (1977, p. 1378). In the south-central Arctic Islands, the Uplift consists of the Boothia Horst, an elongate northward extension of crystalline basement rocks of the Precambrian Canadian Shield, and the overlying Cornwallis Fold Belt (Thorsteinsson, 1958, p. 116), a north-plunging anticlinorium containing mainly Proterozoic to Upper Devonian sedimentary rocks. The present-day structure results largely from a series of tectonic events (pulses) known collectively as the Cornwallis Disturbance, and the Late Silurian-Early Devonian tectonism described in this study formed Pulse 2, the major tectonic episode of the Disturbance.

Stratigraphic successions

Strata examined by the author on Somerset, Prince of Wales and Cornwallis Islands show a conformable upward

gradation from marine to continental sedimentation, (Fig. 55). On Somerset Island, the predominantly subtidal Read Bay Formation is composed of nodular and wavy-bedded mottled and argillaceous limestones with an abundant invertebrate fauna (Jones and Dixon, 1977). The overlying inter-supratidal Somerset Island Formation passes up into the sandstones and conglomerates of the Peel Sound Formation, largely of alluvial fan and braided stream origin (Chapters 2 to 4).

The corresponding stratigraphic units on Prince of Wales Island were described by Miall (1969, 1970a and b) and examined by the author at Transition Bay and Baring Channel. The upper part of the Read Bay Formation contains numerous sandstone beds (?littoral, Miall, 1969, p. 33), domal stromatolites, and a coral-brachiopod fauna. The lower member of the Peel Sound Formation contains thick beds of grey-yellow pebble conglomerate interbedded with red sandstone, siltstone, and argillaceous limestone containing marine fossils. Depositional environments ranged from sub/intertidal to distal fluvial. The lower member probably passes laterally westward into finer grained sediments (Miall et al., 1978). The upper member of the Peel Sound Formation near the Boothia Uplift comprises red cobble and boulder conglomerate with minor sandstone, and was deposited on a series of alluvial fans (Miall, 1970a). This Conglomerate Facies passes westward through a Sandstone and Sandstone-Carbonate to a Carbonate Facies (Miall, 1970b), the latter two facies now being

included in the newly defined Drake Bay Formation (Mayr, in press).

The lower member of the Peel Sound Formation and the Somerset Island Formation occupy a similar position in the regressive sequences on the two islands. The two units, however, are strikingly different, with the Prince of Wales succession containing abundant pebble conglomerate and sandstone — very rare rock types in the carbonate and siltstone succession on Somerset Island. Furthermore, the conglomerates of the upper member of Prince of Wales Island contain clasts up to 150 cm in diameter (Miall, 1970a, p. 569), while the conglomerate members in the Peel Sound Formation on Somerset Island contain clasts no larger than 35 cm. The succession on Prince of Wales Island is thus consistently coarser than that on Somerset Island.

The Cornwallis Island succession was originally described by Thorsteinsson (1958), and the sedimentology of strata at Goodsir Creek and Read Bay was outlined by Gibling and Narbonne (1977). Member A of the Read Bay Formation is generally similar to the Read Bay Formation on Somerset Island, but Members B and C have no lithological equivalents south of Barrow Strait. Member B is composed largely of black shale, probably deposited under protected shallow subtidal conditions. The lower part of Member C, shallow subtidal in origin, consists of massive recrystallised dolostone and limestone with a rich coral-stromatoporoid fauna. The upper part

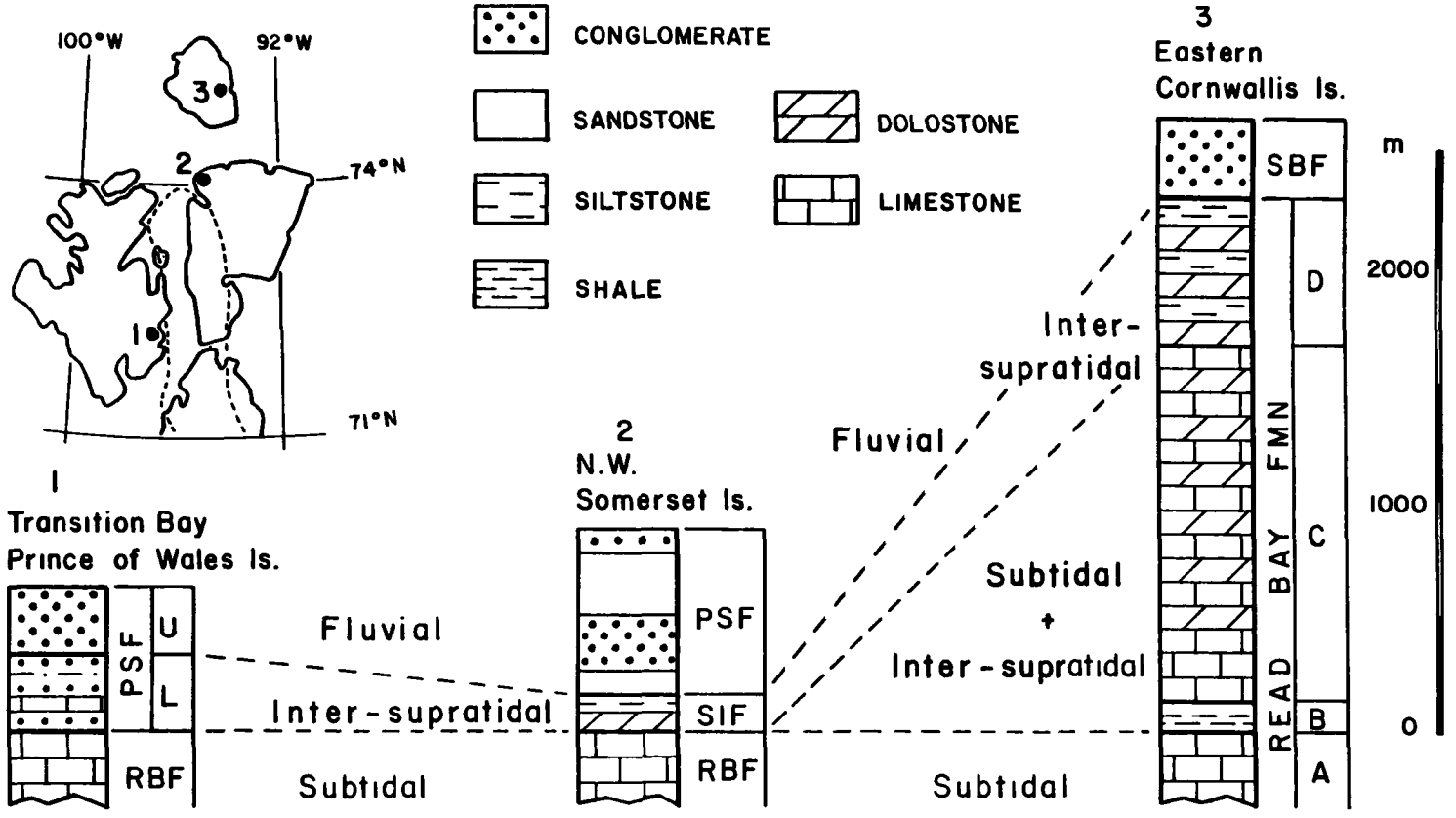

Fig. 55. Lithological correlation of Upper Silurian-Lower Devonian strata in the Boothia Uplift region. The contact between the Read Bay Formation (Member A) and the overlying stratigraphic unit is used as a datum. Data from Prince of Wales and Cornwallis Islands from reconnaissance by the author. RBF, SIF, PSF and SBF = Read Bay, Somerset Island, Peel Sound and Snowblind Bay Formations.

255

consists of alternate units of silty dolostone with algal lamination, desiccation cracks and a restricted ostracod-gastropod fauna (intertidal), and coral-stromatoporoid biostromes (shallow subtidal). Member D contains carbonate-clastic cycles similar to those of the upper member of the Somerset Island Formation (Chapter 2). The red sandstones and conglomerates of the overlying Snowblind Bay Formation, fluvial in origin, are broadly similar to those of the Peel Sound Formation on Somerset Island.

Regressive sequences are also present elsewhere in the Boothia Uplift region: on the Boothia Peninsula (Miall et al., 1978) , on Lowther Island (Thorsteinsson and Kerr, 1973), on other parts of Cornwallis Island (Thorsteinsson and Kerr, 1968; Kerr, 1977), on western Devon Island (Thorsteinsson and Tozer, 1963, p. 125; Uyeno, 1977), and on Bathurst Island (Kerr, 1974). These strata have not been examined by the author.

Age correlation

Table 14 shows a probable age correlation for the three successions based on identification of ostracoderms, conodonts and graptolites. On Somerset Island, the base of the Somerset Island Formation is dated as late Ludlovian or Pridolian on the basis of conodonts, and the Peel Sound Formation may extend into the Gedinnian (see section on age in Chapter 1).

The lower member of the Peel Sound Formation on Prince of Wales Island is believed to be of similar age to the Somerset Island Formation because the two units contain similar vertebrate assemblages (e.g. Broad, 1973; Broad and Dineley, 1973), and show a similar succession of faunas (D.K. Elliott, unpublished data). The upper member in the Sandstone-Carbonate Facies at Baring Channel has yielded conodonts found in Upper Lochkovian and Early to Mid Pragian (late Gedinnian-Siegenian) strata elsewhere in the Arctic Islands (Uyeno, in Gibling and Narbonne, 1977).

The succession on Cornwallis Island has been dated by means of conodonts (Uyeno, 1977), the results generally confirming earlier work summarised in Berdan et al. (1969). The base of Member D is dated as Lochkovian (approximately Gedinnian). The basal beds of the Snowblind Bay Formation contain a distinctive vertebrate fauna including Ctenaspis, Anglaspis, pteraspidids, osteostracans, porolepids, arthrodires, psammosteids and acanthodians, very similar to a vertebrate fauna obtained from the previously noted strata at Baring Channel (D.K. Elliott, in Gibling and Narbonne, 1977) . This suggests a late Gedinnian or younger age for the Snowblind Bay Formation.

In general as seen in Table 14, clastic sedimentation south of Barrow Strait commenced in the Late Silurian (Ludlovian). but did not affect Cornwallis Island until the Early Devonian (Gedinnian).

Table 14. Age and correlation of Siluro-Devonian strata in the Boothia Uplift region. Time lines are all approximate as biostratigraphic control is limited, and many of the formational contacts are diachronous. After Fig. 7 of Miall *et al.* (1978).

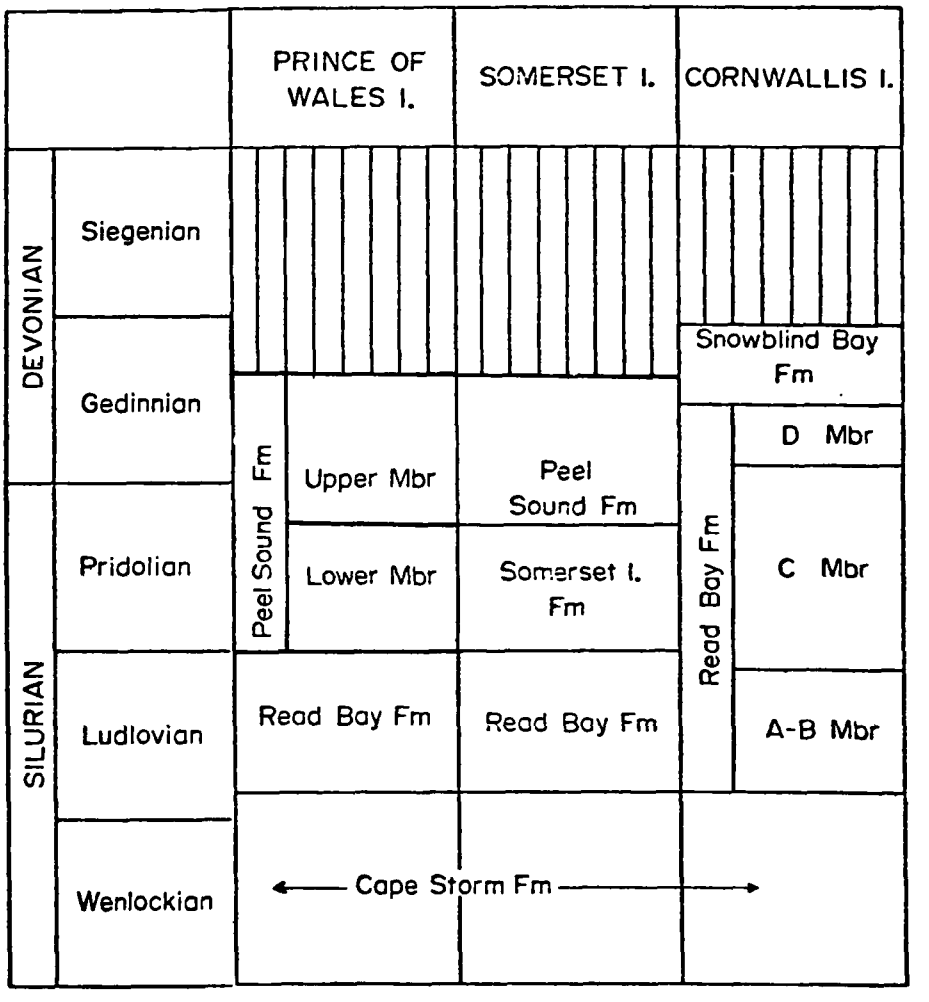

Development of the clastic wedge to the south of Barrow Strait

Several lines of evidence show that the Boothia Uplift was the source of the detrital sediment on Somerset and Prince of Wales Islands:

1) Lateral facies changes on Somerset Island (Figs. 4 and 5) and on Prince of Wales Island (described above) reflect the deposition of progressively finer detritus away from the Uplift (Fig. 56). In particular, coarse conglomerates are present only near the Uplift.

2) Most types of clasts in the conglomerates correspond to rock types presently exposed in the area of the Uplift (Chapter 4; Miall, 1970a, Table 1). Alternative source areas for these rock types are either far distant (Thorsteinsson and Tozer, 1963, p. 124) or unknown. The conglomerates show "reverse stratigraphy" (Fig. 40; Miall, 1970a, Fig. 4), with the oldest beds containing lithotypes present in formations at high levels in the Cornwallis Fold Belt, and younger beds containing lithotypes occurring in the lower levels of the Fold Belt and in the underlying crystalline basement of the Boothia Horst. The inverse relationship between the sequence of rock types in the Boothia Uplift and the adjacent clastic wedge further supports identification of the Uplift as the source area.

3) Paleocurrent data from both sandstone and conglomerate members of the Peel Sound Formation on Somerset Island

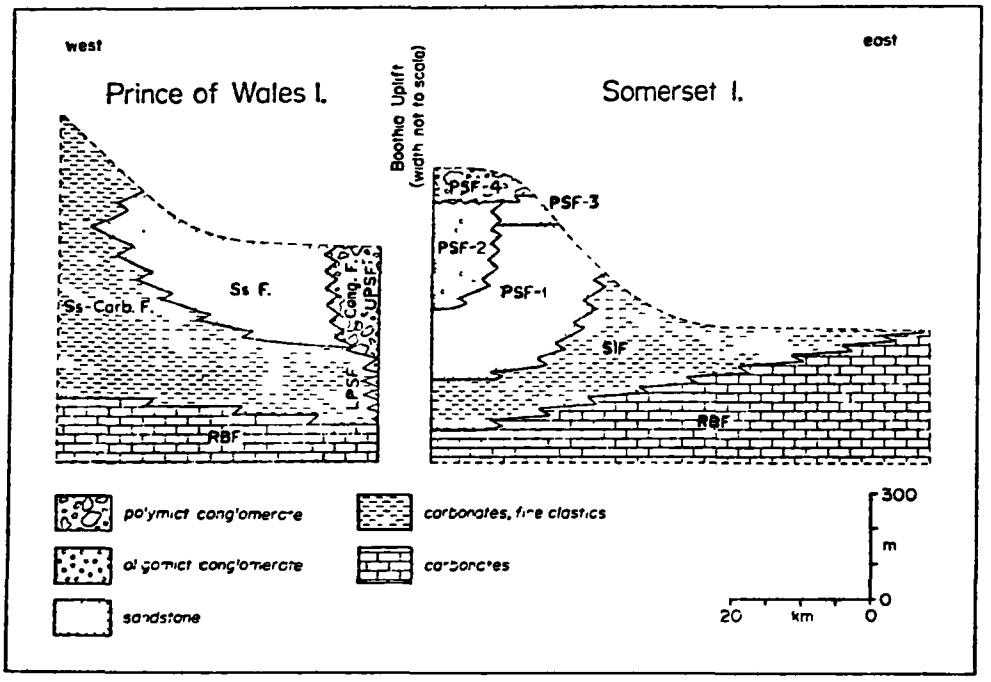

Fig. 56. Comparison of the clastic wedges flanking the Boothia Uplift. RBF, SIF and PSF = Read Bay, Somerset Island and Peel Sound Formations, respectively. Cong. F., Ss. F. and Ss.-Carb. F. = Conglomerate, Sandstone and Sandstone-Carbonate Facies of the Peel Sound Formation. After Miall and Gibling (in press), Fig. 17.

indicate transport to the east (Figs. 28 and 37; Appendix B); only facies S_g shows an anomalous northwesterly transport direction. Paleocurrent data from the upper member of the Peel Sound Formation on Prince of Wales Island show transport to the west (Miall, 1970b, Fig. 3, data summarised in Appendix B), also indicated by contours of maximum clast size and lithotype percentage in the Conglomerate Facies (Miall, 1970a). Flow was thus away from the Uplift in both directions.

Tentative paleogeographic reconstructions are shown in Figure 57. In Ludlovian times, the sea probably occupied the entire area, since the Read Bay Formation adjacent to the Boothia Horst shows no evidence of detritus derived from the Uplift (Jones and Dixon, 1977, bottom of p. 1450 — contrary statement in first paragraph incorrect, pers. comm. B. Jones, 1977). The abrupt onset of clastic sedimentation in late Ludlovian/Pridolian times resulted in the gradual outward progradation of tidal flat and alluvial zones on both islands (Fig. 57a), with a narrow zone of alluvial fans adjacent to the Uplift on Prince of Wales Island. These sediments constitute the Somerset Island and basal Peel Sound Formations on Somerset Island, and the lower member of the Peel Sound Formation on Prince of Wales Island. During the late Pridolian and early Gedinnian, relief on the Uplift increased steadily, and large quantities of gravel derived from the mountain belt were deposited as alluvial fans on both sides of the Uplift

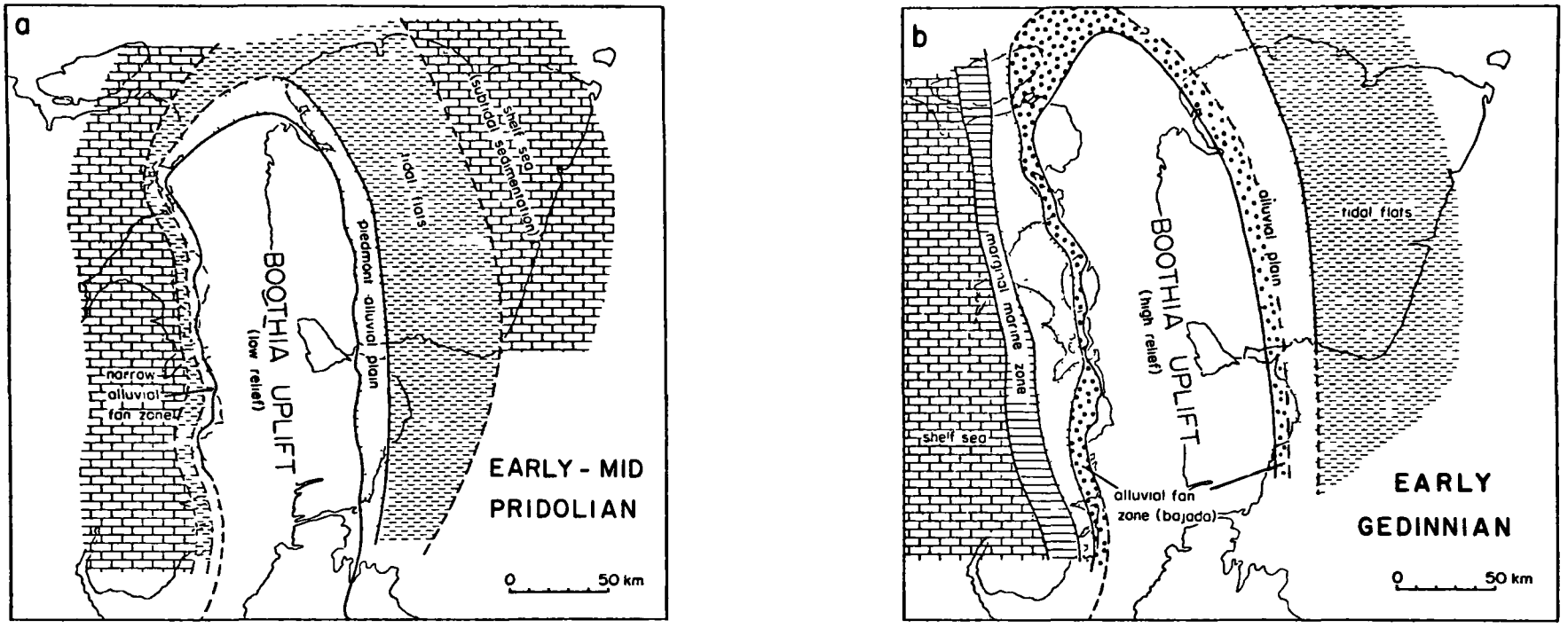

Fig. 57. Paleogeographic interpretations of the Boothia Uplift region.
a) During deposition of the lower member of the Somerset Island Formation.
b) During deposition of Peel Sound member 2. Modified from Miall and Gibling (in press), Figs. 18 and 19.

(Fig. 57b). These constitute Peel Sound Formation members 2 and 4 on Somerset Island, and the Conglomerate Facies on Prince of Wales Island. As continental conditions spread progressively westward from the Uplift on Prince of Wales Island, a terrestrial-marine transitional zone containing sand and carbonate was established (marginal marine zone of Fig. 57b).

The giant cross-beds of member 3 are interpreted as eolian dune deposits (Chapter 3) and show transport from the southeast (Fig. 28). Paleogeographic reconstructions by Woodrow et al. (1973, Fig. 1) show the Boothia Uplift located at approximately 20°N during the Middle and Late Devonian; latitude lines are oriented northeast-southwest with respect to present-day co-ordinates. Assuming a similar trade-wind pattern to the present, the prevailing wind direction would have been from the Devonian northeast, the present-day north. The orientation of cross-beds in facies Sg, however, indicates winds from the present-day southeast. This apparently anomalous orientation possibly reflects the influence of the mountainous Boothia Uplift on local weather patterns. Detailed interpretation of the paleocurrent trend will not be attempted since the paleogeographic reconstructions may not be precisely correct (a difference of a few degrees of latitude could be significant) and Devonian patterns of atmospheric circulation may not have been the same as those of today. The paleogeographic

implications of a fluvial interpretation for the giant cross-beds (Miall and Kerr, 1977) are discussed by Miall and Gibling (in press).

Corresponding sedimentation zones are much narrower on Prince of Wales than on Somerset Island, and while the clastic wedge on Prince of Wales Island has a maximum width of only 40 km, it is at least 70 km wide on Somerset Island. The present-day structure of the Boothia Uplift also exhibits asymmetry, with a narrow folded and faulted zone west of the Uplift and a broad area of block faulting and relatively gentle folding to the east (Kerr and Christie, 1965, p. 917; Kerr, 1977, Fig. 7A). Tectonism was concurrent with sedimentation, as shown by a probable syndepositional fold at Cape Brodie (Miall, 1970a, Fig. 5), and by the uplift and erosion of member 2 in the Cape Anne syncline before deposition of member 4 (Figs. 5 and 56). The asymmetry in structure may have influenced contemporaneous sedimentation as follows: rapid uplift to the west, commonly along reverse faults (Kerr, 1977, p. 1391), resulted in a steep depositional slope with coarse clastic sediment building out directly into the sea; gentle uplift to the east resulted in a broad, low-energy alluvial plain and tidal flat complex. Climatic factors, especially rain shadow effects causing higher rainfall and runoff on the west of the Uplift, may have contributed to the sedimentary asymmetry. However, the northwesterly orientation of the presumed eolian cross-beds of member 3 (Fig. 28)

indicates southerly rather than westerly prevailing winds for at least part of the time on the Somerset Island side.

Development of the clastic wedge to the north of Barrow Strait

The source of Read Bay Formation Member D and the Snowblind Bay Formation on Cornwallis Island has not previously been positively identified because of the isolated nature of the outcrop, although derivation from the Boothia Uplift has commonly been assumed (e.g. Kerr and Christie, 1965, p. 921; Thorsteinsson and Tozer, 1970, p. 561; Miall, 1973, Fig. 1; Kerr, 1977, p. 1387). In the summer of 1976, paleocurrent data was collected from the basal beds of the Snowblind Bay Formation at Read Bay during a reconnaissance of the two stratigraphic units with G.M. Narbonne. Results are shown in Figure 58 and Appendix B. Large-scale cross-stratification, generally as isolate sets, gave a vector mean of 059°, roughly parallel to the vector mean of 067°/247° for bipolar structures (primary current lineation and groove casts) in interbedded sandstones with horizontal stratification. The orientation of both groups is statistically highly significant (probability of random orientation $<10^{-3}$). Orientation of ripple crests gave a vector mean of 155°, not statistically significant. Transport towards the east and northeast strongly suggests that the sediment was derived from the Cornwallis Fold Belt. The probable northward extent

of the Boothia Uplift during the Early Devonian is shown in Figure 59.

Little data is available concerning lateral facies changes or clast compositions in the Snowblind Bay Formation. Clasts in the lowermost conglomerate beds at Read Bay consist mainly of pink or buff dolostone, limestone, red and green siltstone, and chert, with fragments of fossils (especially favositid corals and crinoids), suggesting derivation from Lower Paleozoic formations. R. Thorsteinsson (in Gibling and Narbonne, 1977) reported that graptolite-bearing concretions derived from the Cape Phillips Formation occur in the highest beds of the Snowblind Bay Formation, indicating that uplift and erosion extended north of the facies boundary shown in Figure 54.

The clastic succession on eastern Cornwallis Island shows strong similarity to the regressive sequence on Somerset Island, as noted above. The paleocurrent and clast lithotype data support derivation from the Cornwallis Fold Belt on the eastern flank of the Boothia Uplift. Clastic sedimentation commenced to the south of Barrow Strait in the Late Silurian, and by Early Devonian times (Table 14), extensive tidal flats (Member D) and alluvial plains (basal Snowblind Bay Formation) covered eastern Cornwallis Island as the Uplift advanced northward. These were succeeded by the outbuilding of coarse-grained alluvium (conglomerates of the Snowblind Bay Formation) as relief on the Uplift increased.

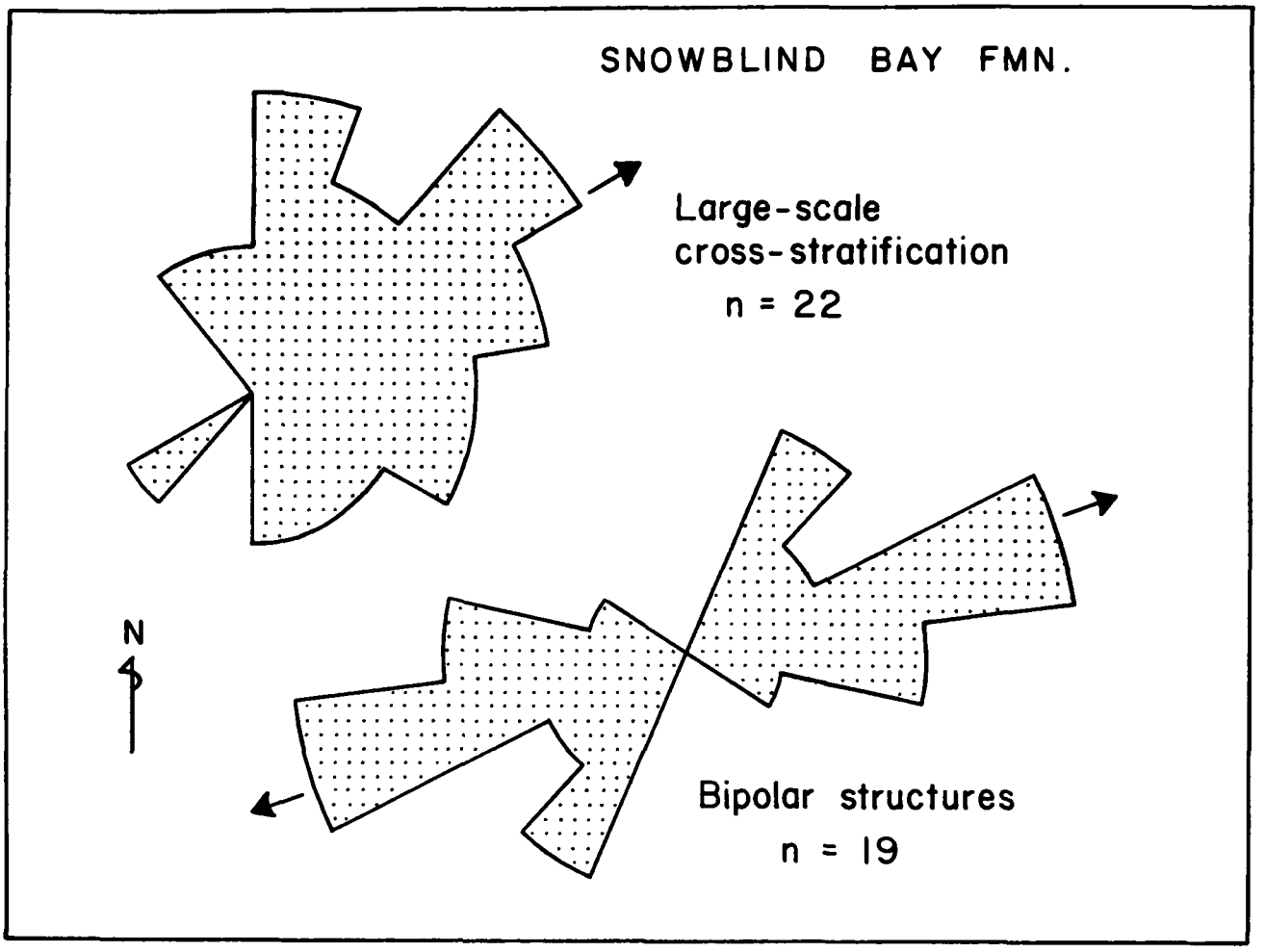

Fig. 58. Paleocurrent data from the Snowblind Bay Formation. Measurements from the basal 35 m at Read Bay, Cornwallis Island. Arrows indicate statistical vector means. Cross-stratification (planar and trough) measured in sandstone and conglomerate. Bipolar structures comprise primary current lineation (n=11) and groove casts (n=7).

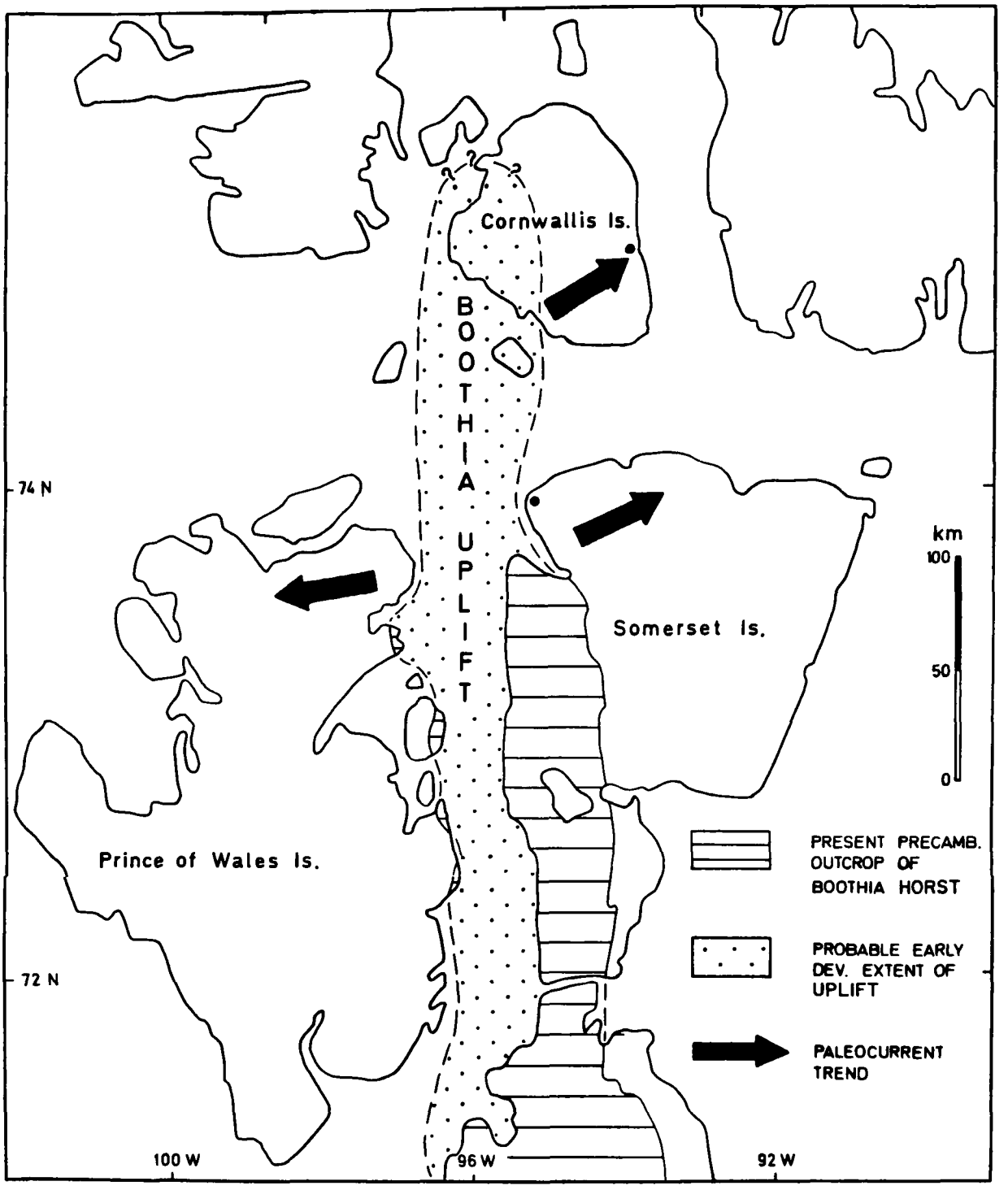

Fig. 59. Paleocurrent trends in the Peel Sound and Snowblind Bay Formations. Details in Appendix B. After Gibling and Narbonne (1977), Fig. 5.

Siluro-Devonian topography and climate of the Boothia Uplift region

The abundance of coarse clastic sediment derived from the Uplift suggests that considerable topographic relief was achieved. Calculation of the thickness of sediment removed during uplift allows estimation of the amount of uplift and possibly of the original elevation.

On eastern Cornwallis Island, outcrops of the Snowblind Bay Formation rest unconformably on the Middle Ordovician Thumb Mountain Formation west of Snowblind Bay (map in Thorsteinsson and Kerr, 1968); the Irene Bay, Allen Bay and Read Bay Formations, probably totalling about 4140 m (Kerr, 1977, p. 1387), have been removed by pre-Snowblind Bay erosion. To the south of Barrow Strait, small outliers of the Peel Sound Formation rest on Precambrian basement west of Stanwell-Fletcher Lake (Miall and Kerr, 1977), indicating that Lower Paleozoic and Proterozoic rocks on the Boothia Horst were removed by pre-Peel Sound erosion. The Lower Paleozoic column adjacent to the Horst totals between 800 and 1500 m (Table 1), although most of the formations probably thinned considerably across the Uplift (Brown et al., 1969). The Proterozoic Aston and Hunting Formations, both of which contributed abundant detritus to the clastic wedge on both flanks of the Uplift (Miall, 1970a; Chapter 4) reach maximum thicknesses, respectively, of at least 800 m (Dixon et al.,

1971) and 1370 m (Dixon, 1974) where they outcrop against the Boothia Horst. The Aston Formation rests unconformably on the crystalline basement and is unlikely to have maintained a constant thickness across the Uplift (Brown et al., 1969, p. 538). while the Hunting Formation was probably also variable in thickness since it rests unconformably on the Aston Formation (Reinson et al., 1976). Sedimentary rocks on the west side of the Uplift were mainly removed by erosion by Gedinnian times, since clasts derived from the crystalline basement comprise 60% of the total at the top of the upper member in some sections (Miall, 1970a, Fig. 4). The amount of crystalline basement eroded cannot be estimated. Hence up to 3700 m of sedimentary rock (although probably much less), with an unknown thickness of Precambrian basement, might have been removed by pre-Peel Sound erosion in this area.

Elevation of the Boothia Uplift was probably rapid and episodic. Abrupt contacts between members characterise the Somerset Island and Peel Sound Formations. In particular, the abrupt basal contacts of the conglomerate members on Somerset Island and the abrupt coarsening from pebble to cobble and boulder conglomerate at the base of the Peel Sound upper member on Prince of Wales Island suggest that a considerable elevation was achieved rapidly during each phase of uplift. The above calculations indicate that if uplift was rapid, with phases occurring within a relatively short

time period, a relief of more than 4000 m (about 13,000 feet) could have been attained locally on the Boothia Uplift. An estimate of 2-3000 m (6500-10,000 feet) for the elevation of the Uplift is probably a more reasonable figure.

A paleomagnetic reconstruction by Woodrow et al. (1973, Fig. 1) showed the Boothia Uplift at approximately 20°N during the Middle and Late Devonian. At this latitude, a tropical climate probably would have prevailed during the Late Silurian to Early Devonian. Periodic aridity is indicated by gypsum beds and halite casts in the Somerset Island Formation; in addition, the presence of diagenetic gypsum and penecontemporaneous dolomite suggest intense evaporation,producing hypersaline groundwaters. The probable eolian deposits of Peel Sound Formation member 3 indicate prolonged periods of aridity. Calcrete deposits, resulting from soil-forming processes, are commonly observed in modern semi-arid environments, but were not observed in the Boothia Uplift region; however, calcrete formation requires a slow rate of alluvial accretion (Leeder, 1975), and its absence cannot be used as an indicator of climate. Periodic precipitation in the source area is indicated by the abundance of fluvial deposits in the Peel Sound Formation. This need not imply a humid climate since braided rivers occur in regions both of arid and humid climate where discharge fluctuates strongly (Miall, 1977, p. 6-7).

The distribution of plant remains in the clastic wedge may reflect climatic conditions. Megascopic plants are very rare. Possible vascular plant material (Photo 50) was obtained from the upper member of the Somerset Island Formation, and is probably Pridolian in age. Plant material (Photo 51) occurs in the Sandstone-Carbonate Facies of the Peel Sound Formation (Drake Bay Formation) on Prince of Wales Island, and is dated as late Gedinnian to Siegenian (see above). Trilete spores and probable vascular plant material were extracted from samples of Read Bay Member B on Cornwallis Island (D.C. McGregor, unpublished report), and are dated as late Ludlovian (Uyeno, 1977); the presence of material of this type suggests, but does not prove, the existence of a terrestrial flora (Banks, 1975; Gray and Boucot, 1977) in the Boothia Uplift region. Samples from the clastic wedge on Somerset Island did not yield such material on dissolution. Rootlet beds were not observed in the clastic wedge. Since vascular plants (identified by the presence of tracheids) occur in strata of uppermost Ludlovian age in Wales (Edwards and Davies, 1976), and probable plant material is present in late Ludlovian strata on Cornwallis Island, the extreme rarity of plant material in the clastic wedge south of Barrow Strait suggests unfavourable conditions, probably aridity.

The sedimentary evidence and plant distribution indicate that the Boothia Uplift region experienced an arid or semi-

arid climate during the Late Silurian to Early Devonian. The abundance of fluvial sediments suggests either that a more humid climate prevailed in the mountainous source area, or that torrential rainfall occurred periodically. At Laguna Madre, Texas, the annual rainfall is relatively high, averaging 69 cm, but intense evaporation results in a semi-arid climate (Rusnak, 1960, Table 1).

Summary

Siluro-Devonian sequences on Somerset, Prince of Wales and Cornwallis Islands comprise marine carbonate sediments overlain by terrestrial clastic sediments. Lateral facies changes. paleocurrent and clast lithotype data indicate that the Boothia Uplift was the source area for the clastic sediments on all three islands. Clastic sedimentation commenced in the Late Silurian south of Barrow Strait and in the Early Devonian north of Barrow Strait, and hence uplift advanced northward with time. Siluro-Devonian elevation of the Boothia Uplift totalled 4000 m locally. On the western flank, rapid uplift resulted in alluvial sediment building out directly into the sea, while on the eastern flank, gentle uplift resulted in a broad alluvial plain and tidal flat complex. A prevailing semi-arid climate is suggested by the sedimentary evidence and the plant distribution.

50. Probable plant material (p) from the upper member of the Somerset Island Formation at Loc. 13.

51. Plant material from the Peel Sound Formation at Baring Channel, Prince of Wales Island.

50

51

CHAPTER 8. CONCLUSIONS

1) The Siluro-Devonian clastic wedge of Somerset Island is a regressive sequence divided into mappable stratigraphic units (members of the Somerset Island and Peel Sound Formations) with contacts defined by distinctive changes in lithology, stratification and fauna. The succession of stratigraphic units reflects a transition from open marine to terrestrial conditions during regression.

2) The Boothia Uplift was the main source of detrital sediment in the clastic wedge on Somerset Island. Most clast lithotypes in the Peel Sound conglomerates can be matched in the presently exposed area of the Uplift. The conglomerates show "reverse stratigraphy", the succession of lithotypes being consistent with progressive erosion of the Boothia Uplift. Paleocurrent data indicate easterly to northeasterly transport, and lateral facies changes reflect the deposition of progressively finer sediment eastward. Uplift, rapid and episodic, totalled 4000 m locally.

3) The Somerset Island Formation is mainly of tidal flat origin, and contains carbonate-clastic cycles. Several types of stromatolitic lamination, closely comparable to types of Recent algal mat at Shark Bay, Western Australia, occur in the cycles, and their distribution suggests a

succession of environments from shallow subtidal to terrestrial during the deposition of each cycle. The cyclicity reflects repeated tidal flat progradation which probably resulted from tectonism during elevation of the Boothia Uplift.

4) The Peel Sound Formation and parts of the Somerset Island Formation upper member represent terrestrial, mainly fluvial, deposition. The conglomerates are of framework type, with imbrication, horizontal stratification and rare cross-stratification, and are interpreted as braided river deposits. The sandstones of Peel Sound member 1 are associated with a low proportion (0-20%) of primary fines, and are predominantly trough and planar cross-stratified with fining-upward cycles; they are interpreted also as braided river deposits. Two types of gravelly and of sandy braided deposits were distinguished on the basis of facies assemblages, lateral continuity of units, and the presence of cyclicity. The types can be related to proximity to the source, which acts through factors such as slope, channel sinuosity and availability of sediment grades. Conglomerates of proximal type pass laterally into sandstones of distal type away from the Boothia Uplift in the Cape Anne syncline, and these two types constitute the bulk of the clastic wedge on Somerset Island.

5) Clast morphology and fabric can be related by a process-response model to the source rocks and processes operative

during transport and deposition. In the Peel Sound framework conglomerates, the nature of the source rocks, especially the internal texture, largely determined clast size, shape and roundness, with transport processes producing relatively little evolution of morphology. Clast size and shape exerted only a limited influence on the depositional fabric. These conclusions reflect a combination of the short transport distance and the intensity of flow in a proximal fluvial setting. Analysis of clast projection area suggests that the contact fabrics, despite their apparent disorder, fulfill the criteria proposed by Koster (1977) for hydrodynamic stability in isolate fabrics. Contact fabric may be a special case of isolate fabric, with both fabrics reflecting a similar response to the flow.

6) Detrital, penecontemporaneous and secondary dolomite is present in the clastic wedge. Detrital dolomite is abundant in the Peel Sound conglomerates, and is common in finer grained sediments, as indicated by the relationship of the dolarenite and dolosiltite grains to primary sedimentary structures. Analysis of trace elements in the carbonates, especially Sr and Na, can impose constraints on the interpretation of dolomite origin. The dolomite in the lower part of the clastic wedge is mainly of early diagenetic type, and its detrital condition probably reflects erosion of penecontemporaneous and secondary dolomite formed on the tidal flats.

Dolomite higher in the clastic wedge was derived mainly from sedimentary formations of the Boothia Uplift.

7) Siluro-Devonian sedimentation in the Boothia Uplift region was examined in conjunction with G.M. Narbonne, A.D. Miall and J. Wm. Kerr. Regressive sequences containing clastic sediment derived from the Boothia Uplift occur on Somerset, Prince of Wales and Cornwallis Islands. Uplift advanced northward with time. The asymmetry in facies distribution east and west of the Uplift reflects local differences in tectonic style during uplift.

ACKNOWLEDGEMENTS

I am deeply grateful to B.R. Rust and O.A. Dixon for their willing assistance throughout the project, and for their painstaking and thoughtful criticism of the manuscript, and to J. Veizer for helpful advice and critical reading. A.J. Baer, F.H.A. Campbell and H.M. French made valuable comments on the final version. I am indebted to G.M. Narbonne for extensive discussion on many aspects of Arctic geology, and to E.H. Koster and B. Jones for patient help in statistical analysis. Assistance and enjoyable companionship in the field was given by J.-M. Sempels and D.K. Elliott. M.J. Jackson and members of the Polar Continental Shelf Project provided help in expedition organisation. M.J. Copeland, O.A. Dixon, D.K. Elliott, P. Hoffman, B. Jones and T.T. Uyeno identified some of the fossils. Thanks go to E.W. Hearn for photography and to V. Griese for making thin sections. A postgraduate scholarship from the National Research Council of Canada and a grant from the Department of Indian and Northern Affairs financed the research; to these organisations, I extend grateful thanks.

Many friends at the Department of Geology and in the Christian community of Ottawa gave me encouragement and support; and especially, thankfulness is expressed to Sonia Williams for her warm interest and for her typing of the thesis.

REFERENCES CITED

ALLEN, J.R.L. 1963. The classification of cross-stratified units, with notes on their origin. Sedimentology 2: 93-114.

———————— 1964a. Studies in fluviatile sedimentation: six cyclothems from the lower Old Red Sandstone, Anglo-Welsh Basin. Sedimentology 3: 163-198.

———————— 1964b. Primary current lineation in the lower Old Red Sandstone (Devonian), Anglo-Welsh Basin. Sedimentology 3: 89-108.

———————— 1965. Fining-upwards cycles in alluvial successions. Geol. J. 4: 229-246.

———————— 1970a. Studies in fluviatile sedimentation: a comparison of fining-upwards cyclothems, with special reference to coarse-member composition and interpretation. J. Sediment. Petrol. 40: 298-323.

———————— 1970b. A quantitative model of grain size and sedimentary structures in lateral deposits. Geol. J. 7: 129-146.

———————— 1974. Sedimentology of the Old Red Sandstone (Siluro-Devonian) in the Clee Hills area, Shropshire, England. Sediment. Geol. 12: 73-167.

AMSBURY, D.L. 1962. Detrital dolomite in central Texas. J. Sediment. Petrol. 32: 5-14.

ASHLEY, G.M. and DUNCAN, I.J. 1977. The Hawkesbury Sandstone: a critical review of proposed environmental models.

J. Geol. Soc. Aust. 24: 117-119.

AUGUSTINUS, P.G.E.F. and RIEZEBOS, H.Th. 1971. Some sedimentological aspects of the fluvioglacial outwash plain near Soesterberg (the Netherlands). Geol. Mijnbouw 50: 341-348.

BADIOZAMANI, K. 1973. The Dorag dolomitization model — application to the Middle Ordovician of Wisconsin. J. Sediment. Petrol. 43: 965-984.

BANKS, H.P. 1975. The oldest vascular land plants: a note of caution. Rev. Palaeobot. Palynol. 20: 13-25.

BATHURST, R.G.C. 1966. Boring algae, micrite envelopes and lithification of molluscan biosparites. Geol. J. 5: 15-32.

_____ 1975. Carbonate sediments and their diagenesis. Elsevier Publ. Co., Amsterdam, 2nd edition, 658 pp.

BECKER, G.F. 1893. Finite homogeneous strain, flow and rupture of rocks. Geol. Soc. Am., Bull. 4: 13-90.

BEHRENS, E.W. and LAND, L.S. 1972. Subtidal Holocene dolomite, Baffin Bay, Texas. J. Sediment. Petrol. 42: 155-161.

BERDAN, J.M. 1968. Possible paleoecologic significance of leperditiid ostracods. Geol. Soc. Am., Spec. Pap. 121: 337 (abstract).

_____ et al. 1969. Siluro-Devonian boundary in North America. Geol. Soc. Am., Bull. 80: 2165-2174.

BERRY, W.B.N. and BOUCOT, A.J. 1973. Glacio-eustatic control of Late Ordovician-Early Silurian platform sedimentation and faunal changes. Geol. Soc. Am., Bull. 84: 275-284.

BEUTNER, E.C., FLUECKINGER, L.A. and GARD, T.M. 1967. Bedding geometry in a Pennsylvanian channel sandstone. Geol. Soc. Am., Bull. 78: 911-916.

BLACKADAR, R.G. 1963. Somerset Island between Aston Bay and Creswell Bay. In Y.O. Fortier et al. (eds.), Geol. Surv. Can., Mem. 320: 143-150.

———————— and Christie, R.L. 1963. Geological reconnaissance, Boothia Peninsula, and Somerset, King William, and Prince of Wales Islands, District of Franklin. Geol. Surv. Can., Pap. 63-19, 15 pp.

BLATT, H., MIDDLETON, G. and MURRAY, R. 1972. Origin of sedimentary rocks. Prentice-Hall Publ. Co., Eaglewood Cliffs, New Jersey, 634 pp.

BLISSENBACH, E. 1954. Geology of alluvial fans in semiarid regions. Geol. Soc. Am., Bull. 65: 175-190.

BLUCK, B.J. 1964. Sedimentation of an alluvial fan in southern Nevada. J. Sediment. Petrol. 34: 395-400.

———————— 1965. Sedimentation of Middle Devonian carbonates, southeastern Indiana. J. Sediment. Petrol. 35: 656-682.

———————— 1967. Sedimentation of beach gravels: examples from South Wales. J. Sediment. Petrol. 37: 128-156.

———————— 1974. Structure and directional properties of

some valley sandur deposits in southern Iceland. Sedimentology 21: 533-554.

BOOTHROYD, J.C. and ASHLEY, G.M. 1975. Processes, bar morphology, and sedimentary structures on braided outwash fans, northeastern Gulf of Alaska. In A.V. Jopling and B.C. McDonald (eds.), Glaciofluvial and glaciolacustrine sedimentation. Soc. Econ. Paleontol. Mineral., Spec. Publ. 23: 193-222.

BOSELLINI, A. and HARDIE, L.A. 1973. Depositional theme of a marginal marine evaporite. Sedimentology 20: 5-27.

BROAD, D.S. 1973. Amphiaspidiformes (Heterostraci) from the Silurian of the Canadian Arctic Archipelago. Geol. Surv. Can., Bull. 222: 35-50.

———— and DINELEY, D.L. 1973. Torpedaspis, a new Upper Silurian and Lower Devonian genus of Cyathaspididae (Ostracodermi) from Arctic Canada. Geol. Surv. Can., Bull. 222: 53-90.

BROWN, R.L., DALZIEL, I.W.D. and RUST, B.R. 1969. The structure, metamorphism, and development of the Boothia Arch, Arctic Canada. Can. J. Earth. Sci. 6: 525-543.

BULL, W.B. 1964. Geomorphology of segmented alluvial fans in western Fresno County, California. U.S. Geol. Surv., Prof. Pap. 352E: 89-129.

———— 1972. Recognition of alluvial-fan deposits in the stratigraphic record. In J.K. Rigby and W.K. Hamblin (eds.), Recognition of ancient sedimentary environments. Soc. Econ. Paleontol. Mineral., Spec. Publ. 16: 63-83.

BUTLER, G.P. 1969. Modern evaporite deposition and geochemistry of coexisting brines, the sabkha, Trucial Coast, Arabian Gulf. J. Sediment. Petrol. 39: 70-89.

BUURMAN, P. 1975. Possibilities of palaeopedology. Sedimentology 22: 289-298.

BYRNE, J.V. 1963. Variations in fluvial gravel imbrication. J. Sediment. Petrol. 33: 467-469.

CAILLEUX, A. 1945. Distinction des galets marins et fluviatiles. Soc. Geol. Fr., Bull. 15: 375-404.

CANT, D.J. 1975. Sandy braided stream deposits in the South Saskatchewan River. Geol. Soc. Am., Abstr. 7(6): 731.

———— 1977. A comparison of recent and ancient sandy braided river sedimentation. Geol. Assoc. Can., Abstr. 2: 10.

———— and WALKER, R.G. 1976. Development of a braided-fluvial facies model for the Devonian Battery Point Sandstone, Québec. Can. J. Earth Sci. 13: 102-119.

CHIEN, N. 1961. The braided stream of the lower Yellow River. Scientia Sinica 10: 734-754.

CHUBER, S. and PUSEY, W.C. 1972. Cyclic San Andreas facies and their relationship to diagenesis, porosity and permeability in the Reeves field, Yoakum County, Texas. In J.G. Elam and S. Chuber (eds.), Cyclic sedimentation in the Permian Basin. 2nd edition, West Texas Geol. Soc., Midland, Texas: 135-150.

COLEMAN, J.M. 1969. Brahmaputra River: channel processes and sedimentation. Sediment. Geol. 3: 129-239.

COLLINSON, J.D. 1970. Bedforms of the Tana River, Norway. Geogr. Ann., Ser. A 52: 31-56.

CONAGHAN, P.J. and JONES, J.G. 1975. The Hawkesbury Sandstone and the Brahmaputra: a depositional model for continental sheet sandstones. J. Geol. Soc. Aust. 22: 275-283.

COTTER, E. 1971. Paleoflow characteristics of a Late Cretaceous river in Utah from analysis of sedimentary structures in the Ferron Sandstone. J. Sediment. Petrol. 41: 129-138.

CURRAY, J.R. 1956. The analysis of two-dimensional orientation data. J. Geol. 64: 117-131.

CURRY, R.R. 1966. Observation of alpine mudflows in the Tenmile Range, central Colorado. Geol. Soc. Am., Bull. 77: 771-776.

DAAE, H.D. and RUTGERS, A.T.C. 1975. Geological history of the Northwest Passage. Bull. Can. Pet. Geol. 23: 84-108.

DALEY, B. 1973. Fluvio-lacustrine cyclothems from the Oligocene of Hampshire. Geol. Mag. 110: 235-242.

DAVIES, G.R. 1970. Algal-laminated sediments, Gladstone Embayment, Shark Bay, Western Australia. In B.W. Logan et al., Carbonate sedimentation and environments, Shark Bay, Western Australia. Am. Assoc. Pet. Geol., Mem. 13: 169-205.

DAVIES, I.C. and WALKER, R.G. 1974. Transport and deposition of resedimented conglomerates: the Cap Enragé formation,

Cambro-Ordovician, Gaspé, Québec. J. Sediment. Petrol. 44: 1200-1216.

DEFFEYES, K.S., LUCIA, F.J. and WEYL, P.K. 1965. Dolomitization of Recent and Plio-Pleistocene sediments by marine evaporite waters on Bonaire, Netherlands Antilles. In L.C. Pray and R.C. Murray (eds.), Dolomitization and limestone diagenesis. Soc. Econ. Paleontol. Mineral., Spec. Publ. 13: 71-88.

———————— and MARTIN, E.L. 1962. Absence of Carbon-14 activity in dolomite from Florida Bay. Science (AAAS) 136: 782.

DENISON, R.H. 1956. A review of the habitat of the earliest vertebrates. Fieldiana; Geol. 11: 359-457.

DENNY, C.S. 1965. Alluvial fans in the Death Valley region, California and Nevada. U.S. Geol. Surv., Prof. Pap. 466, 62pp.

DeWINDT, J.T. 1972. Vertebrate fossils as paleocurrent indicators in the Upper Silurian of the central Appalachians. Compass 49: 125-137.

DICKSON, J.A.D. 1966. Carbonate identification and genesis as revealed by staining. J. Sediment. Petrol. 36: 491-505.

DINELEY, D.L. 1966. Geological studies in Somerset Island, University of Ottawa Expedition, 1965. Arctic 19: 270-277.

———————— 1968. Osteostraci from Somerset Island. Geol. Surv. Can., Bull. 165: 49-63.

———————— 1971. Arches and basins of the southern Arctic Islands of Canada. Geol. Assoc. (Lond.), Proc. 82: 411-444.

DIXON, J. 1973. Stratigraphy and invertebrate paleontology of early Paleozoic rocks, Somerset and Prince of Wales Islands, N.W.T. Unpubl. Ph.D. thesis, Univ. of Ottawa, 246 pp.

———— 1974. Revised stratigraphy of the Hunting Formation (Proterozoic), Somerset Island, Northwest Territories. Can. J. Earth Sci. 11: 635-642.

DIXON, O.A., WILLIAMS, S.R. and DIXON, J. 1971. The Aston Formation (?Proterozoic) on Prince of Wales Island, Arctic Canada. Can.J. Earth Sci. 8: 732-742.

DOBKINS, J.E.Jr. and FOLK, R.L. 1970. Shape development on Tahiti-Nui. J. Sediment. Petrol. 40: 1167-1203.

DUNHAM, R.J. 1962. Classification of carbonate rocks according to depositional texture. In W.E. Ham (ed.), Classification of carbonate rocks — a symposium. Am. Assoc. Pet. Geol., Mem. 1: 33-61.

DYER, K.R. 1970. Grain-size parameters for sandy-gravels. J. Sediment. Petrol. 40: 616-620.

DZULYNSKI, S. and WALTON, E.K. 1965. Sedimentary features of flysch and greywackes. Elsevier Publ. Co., Amsterdam, 274 pp.

EARLEY, C.F. and GOODELL, H.G. 1968. The sediments of Card Sound, Florida. J. Sediment. Petrol. 38: 985-999.

EDHORN, A.-S. 1977. Early Cambrian algae croppers. Can. J. Earth Sci. 14: 1014-1020.

EDWARDS, D. and DAVIES, E.C.W. 1976. Oldest recorded in situ tracheids. Nature 263: 494-495.

EINSTEIN, H.A. 1968. Deposition of suspended particles in a gravel bed. Am. Soc. Civ. Eng., Proc., J. Hydraul. Div. 94: 1197-1205.

EMERY, K.O. 1956. Sediments and water of Persian Gulf. Am. Assoc. Pet. Geol., Bull. 40: 2354-2383.

ENOS, P. 1977. Flow regimes in debris flow. Sedimentology 24: 133-142.

EVANS, G., SCHMIDT, V., BUSH, P., and NELSON, H. 1969. Stratigraphy and geologic history of the sabkha, Abu Dhabi, Persian Gulf. Sedimentology 12: 145-159.

EYNON, G. and WALKER, R.G. 1974. Facies relationships in Pleistocene outwash gravels, southern Ontario: a model for bar growth in braided rivers. Sedimentology 21: 43-70.

FAHNESTOCK, R.K. 1969. Morphology of the Slims River. In V.C. Bushnell and R.H. Ragle (eds.), Scientific results of Icefield Ranges Research Project. Am. Geogr. Soc. and Arctic Inst. North America, 1: 161-172.

FAIRBRIDGE, R.W. 1957. The dolomite question. In R.J. Le Blanc and J.G. Breeding (eds.), Regional aspects of carbonate deposition. Soc. Econ. Paleontol. Mineral., Spec. Publ. 5: 125-178.

FISHER, R.V. 1971. Features of coarse-grained, high-concentration fluids and their deposits. J. Sediment. Petrol. 41: 916-927.

FOLK, R.L. 1959. Practical petrographic classification of limestones. Am. Assoc. Pet. Geol., Bull. 43: 1-38.

———— 1962. Spectral subdivision of limestone types. In W.E. Ham (ed.), Classification of carbonate rocks — a symposium. Am. Assoc. Pet. Geol., Mem. 1: 62-84.

———— 1968. Petrology of sedimentary rocks. Hemphill Publ. Co., Austin, Texas, 182 pp.

———— and LAND, L.S. 1975. Mg/Ca ratio and salinity: two controls over crystallization of dolomite. Am. Assoc. Pet. Geol., Bull. 59: 60-68.

———— and SIEDLECKA, A. 1974. The "schizohaline" environment: its sedimentary and diagenetic fabrics as exemplified by Late Paleozoic rocks of Bear Island, Svalbard. Sediment. Geol. 11: 1-15.

———— and WARD, W.C. 1957. Brazos River bar: a study in the significance of grain size parameters. J. Sediment. Petrol. 27: 3-26.

FRIEDMAN, G.M. 1959. Identification of carbonate minerals by staining methods. J. Sediment. Petrol. 29: 87-97.

———— and SANDERS, J.E. 1967. Origin and occurrence of dolostones. In G.V. Chilingar, H.J. Bissell and R.W. Fairbridge (eds.), Carbonate rocks. Origin, occurrence and classification. Elsevier Publ. Co., Amsterdam: 267-348.

FRIEND, P.F. and MOODY-STUART, M. 1970. Carbonate deposition on the river floodplains of the Wood Bay Formation (Devonian) of Spitsbergen. Geol. Mag. 107: 181-195.

FRITZ, P. and KATZ, A. 1972. The sodium distribution of dolomite crystals. Chem. Geol. 10: 237-244.

GARRETT, P. 1970. Phanerozoic stromatolites: non-competitive ecologic restriction by grazing and burrowing animals. Science (AAAS) 169: 171-173.

GAVISH, E. 1974. Geochemistry and mineralogy of a recent sabkha along the coast of Sinai, Gulf of Suez. Sedimentology 21: 397-414.

GEBELEIN, C.D. 1974. Biologic control of stromatolite microstructure: implications for Precambrian time stratigraphy. Am. J. Sci. 274: 575-598.

———— and HOFFMAN, P. 1973. Algal origin of dolomite laminations in stromatolitic limestone. J. Sediment. Petrol. 43: 603-613.

GERMANN, K. 1969. Reworked dolomite crusts in the Wettersteinkalk (Ladinian, Alpine Triassic) as indicators of early supratidal dolomitization and lithification. Sedimentology 12: 257-277.

GIBLING, M.R. 1977. Cyclic sedimentation in the Upper Silurian of Somerset Island, Arctic Canada. Geol. Soc. Am., Abstr. 9(3): 268.

———— and NARBONNE, G.M. 1977. Siluro-Devonian sedimentation on Somerset and Cornwallis Islands, Arctic Canada. Bull. Can. Pet. Geol. 25: 1145-1146.

———— and RUST, B.R. 1977. Proximal and distal sandy braided alluvium in Devonian successions of the Arctic and Gaspé. Geol. Assoc. Can., Abstr. 2: 20.

GINGERICH, P.D. 1969. Markov analysis of cyclic alluvial sediments. J. Sediment. Petrol. 39: 330-332.

GLENNIE, K.W. 1970. Desert sedimentary environments. Elsevier Publ. Co., Amsterdam,222 pp.

GRABAU, A.W. 1904. On the classification of sedimentary rocks. Am.Geologist 33: 228-247.

GRAMANN, F. 1971. Brackish or hyperhaline ? Notes on paleoecology based on ostracoda. In H.J. Oertli (ed.), Colloquium on the paleoecology of ostracodes. Bull. du Centre de Recherches, Pau, France: 93-99.

GRAY, J. and BOUCOT, A.J. 1977. Early vascular land plants: proof and conjecture. Lethaia 10: 145-174.

GUSTAVSON, T.C. 1974. Sedimentation on gravel outwash fans, Malaspina Glacier Foreland, Alaska. J. Sediment Petrol. 44: 374-389.

HAGAN, G.M. and LOGAN, B.W. 1974. History of Hutchison Embayment tidal flat, Shark Bay, Western Australia. In B.W. Logan et al., Evolution and diagenesis of Quaternary carbonate sequences, Shark Bay, Western Australia. Am. Assoc. Pet. Geol., Mem. 22: 283-315.

HARBAUGH, J. and BONHAM-CARTER, G. 1970. Computer simulation in geology. Wiley-Interscience Publ. Co., New York.

HARDIE, L.A. 1968. The origin of the Recent non-marine evaporite deposit of Saline Valley, Inyo County, California. Geochim. Cosmochim. Acta 32: 1279-1301.

HARMS, J.C. and FAHNESTOCK, R.K. 1965. Stratification, bed forms, and flow phenomena (with an example from the Rio Grande). In G.V. Middleton (ed.), Primary sedimentary structures and their hydrodynamic interpretation. Soc. Econ. Paleontol. Mineral., Spec. Publ. 12: 84-115

———————, MacKENZIE, D.B. and McCUBBIN, D.G. 1963. Stratification in modern sands of the Red River, Louisiana. J. Geol. 71: 566-580.

HATCH, F.H. and RASTALL, R.H. 1965. Petrology of the sedimentary rocks. Murby Publ. Co., London, 4th edition, 408 pp.

HEIN, F.J. and WALKER, R.G. 1977. Bar evolution and development of stratification in the gravelly, braided, Kicking Horse River, British Columbia. Can. J. Earth Sci. 14: 562-570.

HOFFMAN, P. 1974. Shallow and deepwater stromatolites in Lower Proterozoic platform-to-basin facies change, Great Slave Lake, Canada. Am. Assoc. Pet. Geol., Bull. 58: 856-867.

HOOKE, R. LeB. 1967. Processes on arid-region alluvial fans. J. Geol. 75: 438-460

HORNE, R.R. 1975. The association of alluvial fans, aeolian and fluviatile facies in the Caherbla Group (Devonian), Dingle Peninsula, Ireland. J. Sediment. Petrol. 45: 535-540.

HORODYSKI, R.J. and VONDER HAAR, S.P. 1975. Recent calcareous stromatolites from Laguna Mormona (Baja California) Mexico. J. Sediment. Petrol. 45: 894-906.

HSÜ, K.J. and SIEGENTHALER, C. 1969. Preliminary experiments on hydrodynamic movement induced by evaporation and their bearing on the dolomite problem. Sedimentology 12: 11-25.

HUNT, C.B. 1972. Geology of soils. Their evolution, classification, and uses. W.H. Freeman, San Francisco, 344 pp.

HUNTER, R.E. 1976. Comparison of eolian and subaqueous sandflow cross-strata. Am. Assoc. Pet. Geol. 60: 683 (abstract).

ILLING, L.V., WELLS, A.J. and TAYLOR, J.C.M. 1965. Penecontemporary dolomite in the Persian Gulf. In L.C. Pray and R.C. Murray (eds.). Dolomitization and limestone diagenesis. Soc. Econ. Paleontol. Mineral., Spec. Publ. 13: 89-111.

IMBRIE, J. 1956. Biometrical methods in the study of invertebrate fossils. Am. Mus. Nat. Hist., Bull. 108: 215-252.

JACKSON, R.G. II. 1975. Velocity-bed-form-texture patterns of meander bends in the lower Wabash River of Illinois and Indiana. Geol. Soc. Am., Bull. 86: 1511-1522.

———————— 1976 a. Largescale ripples of the lower Wabash River. Sedimentology 23: 593-623.

———————— 1976 b. Depositional model of point bars in the lower Wabash River. J. Sediment. Petrol. 46: 579-594.

JAMIESON, T.F. 1860. On the drift and rolled gravel of the north of Scotland. J. Geol. Soc. Lond. 16: 347-371.

JOHANSSON, C.E. 1963. Orientation of pebbles in running water. A laboratory study. Geogr. Ann., Ser. A 45: 85-112.

———————— 1965. Structural studies of sedimentary deposits. Geol. Foeren. Stockh., Foerh. 87: 3-61.

JOHNSON, A.M. 1970. Physical processes in geology. W.H. Freeman, San Francisco, 577 pp.

JOHNSTON, W.A. 1922. Imbricated structure in river-gravels. Am. J. Sci. 4: 387-390.

JONES, B. and DIXON, O.A. 1975. The Leopold Formation: an Upper Silurian intertidal/supratidal carbonate succession on north-eastern Somerset Island, Arctic Canada. Can. J. Earth Sci. 12: 395-411.

———— and ———— 1976. Storm deposits in the Read Bay Formation (Upper Silurian), Somerset Island, Arctic Canada (an application of Markov chain analysis). J. Sediment. Petrol. 46: 393-401.

———— and ———— 1977. Stratigraphy and sedimentology of Upper Silurian rocks, northern Somerset Island, Arctic Canada. Can. J. Earth Sci. 14: 1427-1452.

JONES, B.F. 1965. The hydrology and mineralogy of Deep Springs Lake, Inyo County, California. U.S. Geol. Surv., Prof. Pap. 502A, 56 pp.

KAHLE, C.F. 1965. Possible roles of clay minerals in the formation of dolomite. J. Sediment. Petrol. 35: 448-453.

KARCZ, I. 1972. Sedimentary structures formed by flash floods in southern Israel. Sediment. Geol. 7: 161-182.

KATZ, A. 1971. Zoned dolomite crystals. J. Geol. 79: 38-51.

KENNEDY, W.J. 1975. Trace fossils in carbonate rocks. In R.W. Frey (ed.), The study of trace fossils. Springer-Verlag Publ. Co., New York: 377-398.

KERR, J. Wm. 1974. Geology of Bathurst Island Group and Byam Martin Island, Arctic Canada. Geol. Surv. Can., Mem. 378, 152 pp.

———————— 1975. Cape Storm Formation — a new Silurian unit in the Canadian Arctic. Bull. Can. Pet. Geol. 23: 67-83.

———————— 1977. Cornwallis Fold Belt and the mechanism of basement uplift. Can. J. Earth Sci. 14: 1374-1401.

———————— and CHRISTIE, R.L. 1965. Tectonic history of Boothia Uplift and Cornwallis Fold Belt, Arctic Canada. Am. Assoc. Pet. Geol., Bull. 49: 905-926.

———————— and deVRIES, C.D.S. 1977. Structural geology of Somerset Island and Boothia Peninsula, District of Franklin. Geol. Surv. Can., Pap. 77-1A: 107-111.

KILENYI, T.I. 1971. Some basic questions in the palaeoecology of ostracods. In H.J. Oertli (ed.), Colloquium on the paleoecology of ostracodes. Bull. du Centre de Recherches, Pau, France: 31-44.

KINSMAN, D.J.J. 1969. Interpretation of Sr^{+2} concentrations in carbonate minerals and rocks. J. Sediment. Petrol. 39: 486-508.

KLAPPER, G. and MURPHY, M.A. 1975. Silurian-Lower Devonian conodont sequence in the Roberts Mountains Formation of central Nevada. Univ. Calif. Publ. Geol. Sci. 111, 62 pp.

KLEIN, G. deV. and SANDERS, J.E. 1964. Comparison of sediments from Bay of Fundy and Dutch Wadden Sea tidal flats. J. Sediment. Petrol. 34: 18-24.

KOSTER, E.H. 1977. Experimental studies of coarse-grained sedimentation. Unpubl. Ph.D. thesis, Univ. of Ottawa, 221 pp.

KRUMBEIN, W.C. 1939. Preferred orientation of pebbles in sedimentary deposits. J. Geol. 47: 673-706.

———————— 1940. Flood gravel of San Gabriel Canyon, California. Geol. Soc. Am., Bull. 51: 639-676.

———————— 1941. Measurement and geological significance of shape and roundness of sedimentary particles. J. Sediment. Petrol. 11: 64-72.

———————— 1942. Flood deposits of Arroyo Seco, Los Angeles County, California. Geol. Soc. Am., Bull. 53: 1355-1402.

———————— and DACEY, M.F. 1969. Markov chains and embedded chains in geology. J. Int. Ass. Mathl. Geol. 1: 79-96.

KUENEN, Ph.H. 1960. Experimental abrasion. 4. Eolian action: Jour. Geol. 68: 427-449.

KUMAR, N. and SANDERS, J.E. 1974. Inlet sequence: a vertical succession of sedimentary structures and textures created by the lateral migration of tidal inlets. Sedimentology 21: 491-532.

LAMING, D.J.C. 1966. Imbrication, paleocurrents and other sedimentary features in the Lower New Red Sandstone, Devonshire, England. J. Sediment. Petrol. 36: 940-959.

LAND, L.S. 1973. Holocene meteoric dolomitization of Pleistocene limestones, north Jamaica. Sedimentology 20: 411-424.

LANE, E.W. and CARLSON, E.J. 1954. Some observations on the effect of particle shape on the movement of coarse sediments. Am. Geophys. Union, Trans. 35: 453-462.

LEEDER, M.R. 1973a. Sedimentology and palaeogeography of the Upper Old Red Sandstone in the Scottish Border Basin. Scot. J. Geol. 9: 117-144.

———————— 1973b. Fluviatile fining-upwards cycles and the magnitude of palaeochannels. Geol. Mag. 110: 265-276.

———————— 1975. Pedogenic carbonates and flood sediment accretion rates: a quantitative model for alluvial arid-zone lithofacies. Geol. Mag. 112: 257-270.

LEFLEF, D. 1973. Significant relations between textural and structural features of the rocks in the Churchbay-Templebreedy Members of the uppermost Old Red Sandstone complex, south of Cork, Ireland. Geol. Mijnbouw 52: 257-276.

LEIGHTON, M.W. and PENDEXTER, C. 1962. Carbonate rock types. In W.E. Ham (ed.), Classification of carbonate rocks — a symposium. Am. Assoc. Pet. Geol., Mem. 1: 33-61.

LEMON, R.R.H. and BLACKADAR, R.G. 1963. Admiralty Inlet area, Baffin Island, District of Franklin. Geol. Surv. Can., Mem. 328, 84 pp.

LEOPOLD, L.B. and WOLMAN, M.G. 1957. River channel patterns: braided, meandering, and straight. U.S. Geol. Surv., Prof. Pap. 282B: 39-85.

———————— , ———————— and MILLER, J.P. 1964. Fluvial processes in geomorphology. W.H. Freeman, San Francisco, 522 pp.

LINDHOLM, R.C. 1969. Detrital dolomite in Onondaga Limestone (Middle Devonian) of New York: its implications to the "dolomite question". Am. Assoc. Pet. Geol., Bull. 53: 1035-1042.

LOGAN, B.W. 1974. Inventory of diagenesis in Holocene - Recent carbonate sediments, Shark Bay, Western Australia. In B.W. Logan et al., Evolution and diagenesis of Quaternary carbonate sequences, Shark Bay, Western Australia. Am. Assoc. Pet. Geol., Mem. 22: 195-249.

———— and CEBULSKI, D. 1970. Sedimentary environments of Shark Bay, Western Australia. In B.W. Logan et al., Carbonate sedimentation and environments, Shark Bay, Western Australia. Am. Assoc. Pet. Geol., Mem. 13: 1-37.

———— , HOFFMAN, P. and GEBELEIN, C.D. 1974. Algal mats, cryptalgal fabrics, and structures, Hamelin Pool, Western Australia. In B.W. Logan et al., Evolution and diagenesis of Quaternary carbonate sequences, Shark Bay, Western Australia. Am. Assoc. Pet. Geol., Mem. 22: 140-194.

———— , REZAK, R. and GINSBURG, R.N. 1964. Classification and environmental significance of algal stromatolites. J. Geol. 72: 68-83.

LUCIA, F.J. 1972. Recognition of evaporite-carbonate shoreline sedimentation. In J.K. Rigby and W.K. Hamblin (eds.). Recognition of ancient sedimentary environments. Soc. Econ. Paleontol. Mineral., Spec. Publ. 16: 160-191.

MARTINI, I.P. and OSTLER, J. 1973. Ostler lenses: possible environmental indicators in fluvial gravels and conglomerates. J. Sediment. Petrol. 43: 418-422.

MAYR, U. 1973. Lithologies and depositional environments of the Allen Bay — Read Bay Formations (Ordovician-Silurian) on Svendsen Peninsula, central Ellesmere Island. In J.D. Aitken and D.J. Glass (eds.). Proceedings of the symposium on the geology of the Canadian Arctic. Geol. Assoc. Can. and Can. Soc. Pet. Geol.: 143-157.

———— in press. Stratigraphy and correlation of Lower Paleozoic subsurface sections, Cornwallis, Devon, Somerset, and Russell Islands, Canadian Arctic Archipelago. Geol. Surv. Can., Bull.

McBRIDE, E.F., SHEPHERD, R.G. and CRAWLEY, R.A. 1975. Origin of parallel, near-horizontal laminae by migration of bed forms in a small flume. J. Sediment. Petrol. 45: 132-139.

McCABE, P.J. 1977. Deep distributary channels and giant bedforms in the Upper Carboniferous of the central Pennines, northern England. Sedimentology 24: 271-290.

McDONALD, B.C. and BANERJEE, I. 1971. Sediments and bedforms on a braided outwash plain. Can. J. Earth Sci. 8: 1282-1301.

McKEE, E.D. 1966. Structures of dunes at White Sands National Monument, New Mexico (and a comparison with structures of dunes from other selected areas). Sedimentology 7: 1-69.

———— and BIGARELLA, J.J. 1972. Deformational structures in Brazilian coastal dunes. J. Sediment. Petrol. 42: 670-681.

MIALL, A.D. 1969. The sedimentary history of the Peel Sound Formation, Prince of Wales Island, Northwest Territories. Unpubl. Ph. D. thesis, Univ. of Ottawa, 279 pp.

———— 1970a. Devonian alluvial fans, Prince of Wales Island, Arctic Canada. J. Sediment. Petrol. 40: 556-571.

———— 1970b. Continental marine transition in the Devonian of Prince of Wales Island, Northwest Territories. Can. J. Earth Sci. 7: 125-144.

———— 1973. Markov chain analysis applied to an ancient alluvial plain succession. Sedimentology 20: 347-364.

———— 1974. Paleocurrent analysis of alluvial sediments: a discussion of directional variance and vector magnitude. J. Sediment. Petrol. 44: 1174-1185.

———— 1977. A review of the braided-river depositional environment. Earth-Sci. Rev. 13: 1-62.

———— and GIBLING, M.R. in press. The Siluro-Devonian clastic wedge of Somerset Island, Arctic Canada, and some regional paleogeographic implications. Sediment. Geol.

————, KERR, J.Wm., GIBLING, M.R. 1978. The Somerset Island Formation: an Upper Silurian to ?Lower Devonian intertidal/supratidal succession, Boothia Uplift region, Arctic Canada. Can. J. Earth Sci. 15: 181-189.

———————— and KERR, J. Wm. 1977. Phanerozoic stratigraphy and sedimentology of Somerset Island and northeastern Boothia Peninsula. Geol. Surv. Can., Pap. 77-1A: 99-106.

MIDDLETON, G.V. and HAMPTON, M.A. 1973. Sediment gravity flows: mechanics of flow and deposition. In G.V. Middleton and A.H. Bouma (eds.), Turbidites and deep-water sedimentation. Soc. Econ. Paleontol. Mineral., short course No. 1: 1-38.

MONTY, C.L.V. 1967. Distribution and structure of Recent stromatolitic algal mats, eastern Andros Island, Bahamas. Soc. Geol. Belg., Ann. 90: 55-100.

MOODY-STUART, M. 1966. High- and low-sinuosity stream deposits. with examples from the Devonian of Spitsbergen. J. Sediment. Petrol. 36: 1102-1117.

NORRIS. R.M. and NORRIS, K.S. 1961. Algodones dunes of southeastern California. Geol. Soc. Am., Bull. 72: 605-620.

PEABODY, F.E. 1947. Current crescents in the Triassic Moenkopi Formation. J. Sediment. Petrol. 17: 73-76.

PETTIJOHN, F.J. 1975. Sedimentary rocks. Harper and Row Publ.Co., New York, 3rd edition, 628 pp.

PINGITORE, N.E. Jr. 1976. Vadose and phreatic diagenesis: processes, products and their recognition in corals. J. Sediment. Petrol. 46: 985-1006

PITTMAN, E.D. and OVENSHINE, A.T. 1968. Pebble morphology in the Merced River (California). Sediment. Geol. 2: 125-140.

PLUMLEY, W.J. 1948. Black Hills terrace gravels: a study in sediment transport. J. Geol. 56: 526-577.

POTTER, P.E. 1955. The petrology and origin of the Lafayette Gravel. Part 1. Mineralogy and petrology. J. Geol. 63: 1-38.

———————— and BLAKELY, R.F. 1968. Random processes and lithologic transitions. J. Geol. 76: 154-170.

POWERS, M.C. 1953. A new roundness scale for sedimentary particles. J. Sediment. Petrol. 23: 117-119.

READ, J.F. 1973. Carbonate cycles, Pillara Formation (Devonian), Canning Basin, Western Australia. Bull. Can. Pet. Geol. 21: 38-51.

REINECK, H.-E. and SINGH, I.B. 1975. Depositional sedimentary environments. Springer-Verlag Publ. Co., New York, 439 pp.

REINSON, G.E., KERR, J.Wm. and STEWART, W.D. 1976. Stratigraphic field studies, Somerset Island, District of Franklin (58B to F). Geol. Surv. Can., Pap. 76-1A: 497-499.

RODGERS, J. 1954. Terminology of limestone and related rocks: an interim report. J. Sediment. Petrol. 24: 225-234.

RUSNAK, G.A. 1960. Sediments of Laguna Madre, Texas. In F.P. Shepherd et al. (eds.), Recent sediments, northwest Gulf of Mexico. Am. Assoc. Pet. Geol. : 153-196.

RUST, B.R. 1972a. Structure and process in a braided river. Sedimentology 18: 221-245.

———— 1972b. Pebble orientation in fluvial sediments. J. Sediment. Petrol. 42: 384-388.

———— 1975. Fabric and structure in glaciofluvial gravels. In A.V. Jopling and B.C. McDonald (eds.), Glaciofluvial and glaciolacustrine sedimentation. Soc. Econ. Paleontol. Mineral., Spec. Publ. 23: 238-248.

———— in press. The interpretation of ancient alluvial successions in the light of modern investigations. Proc. Guelph Symposium on Geomorphology.

RYDER, J.M. 1971. The stratigraphy and morphology of para-glacial alluvial fans in south-central British Columbia. Can. J. Earth Sci. 8: 279-298.

SABINS, F.F.Jr. 1962. Grains of detrital, secondary, and primary dolomite, from Cretaceous strata of the Western Interior. Geol. Soc. Am., Bull. 73: 1183-1196.

SANDER, B. 1951. Contributions to the study of depositional fabrics (rhythmically deposited Triassic limestones and dolomites). Am. Assoc. Pet. Geol., 207 pp., translated by E.B. Knopf.

SCHENK, P.E. 1969. Carbonate-sulfate-redbed facies and cyclic sedimentation of the Windsorian Stage (Middle Carboniferous), Maritime Provinces. Can. J. Earth Sci. 6: 1037-1066.

SCHLEE, J. 1957. Fluvial gravel fabric. J. Sediment. Petrol. 27: 162-176.

SCHMIDT, V. 1965. Facies, diagenesis, and related reservoir properties in the Gigas Beds (Upper Jurassic), northwestern Germany. In L.C. Pray and R.C. Murray (eds.), Dolomitization and limestone diagenesis. Soc. Econ. Paleontol. Mineral., Spec. Publ. 13: 124-168.

SCHUMM, S.A. 1968. River adjustment to altered hydrologic regimen — Murrumbidgee River and paleochannels, Australia. U.S. Geol. Surv., Prof. Pap. 598, 65 pp.

———————— 1972. Fluvial paleochannels. In J.K. Rigby and W.K. Hamblin (eds.), Recognition of ancient sedimentary environments. Soc. Econ. Paleontol. Mineral., Spec. Publ. 16: 98-107.

SCHWARZ, H.-U., EINSELE, G. and HERM, D. 1975. Quartz-sandy, grazing-contoured stromatolites from coastal embayments of Mauritania, West Africa. Sedimentology 22: 539-561.

SEDIMENTARY PETROLOGY SEMINAR, 1965. Gravel fabric in Wolf Run. Sedimentology 4: 273-283.

SELLARDS, E.H. 1923. Geologic and soil studies on the alluvial lands of the Red River valley. Texas Univ., Bull. 2327: 27-87.

SENGUPTA, S. 1966. Studies on orientation and imbrication of pebbles with respect to cross-stratification. J. Sediment. Petrol. 36: 362-369.

SHARP, R.P. 1966. Kelso dunes, Mojave Desert, California. Geol. Soc. Am., Bull. 77: 1045-1074.

SHINN, E.A. 1968. Selective dolomitization of recent sedimentary structures. J. Sediment. Petrol. 38: 612-616.

———————, GINSBURG, R.N. and LLOYD, R.M. 1965. Recent supratidal dolomite from Andros Island, Bahamas. In L.C. Pray and R.C. Murray (eds.), Dolomitization and limestone diagenesis. Soc. Econ. Paleontol. Mineral., Spec. Publ. 13: 112-123.

———————, LLOYD, R.M. and GINSBURG, R.N. 1969. Anatomy of a modern carbonate tidal-flat, Andros Island, Bahamas. J. Sediment. Petrol. 39: 1202-1228.

SMITH, H.M. 1945. The fresh-water fishes of Siam, or Thailand. U.S. Natl. Mus., Bull. 188, 622 pp.

SMITH, N.D. 1968. Cyclic sedimentation in a Silurian intertidal sequence in eastern Pennsylvania. J. Sediment. Petrol. 38: 1301-1304.

———————— 1970. The braided stream depositional environment: comparison of the Platte River with some Silurian clastic rocks, north-central Appalachians. Geol. Soc. Am., Bull. 81: 2993-3014.

———————— 1971a. Pseudo-planar stratification produced by very low amplitude sand waves. J. Sediment. Petrol. 41: 69-73.

———————— 1971b. Transverse bars and braiding in the lower Platte River, Nebraska. Geol. Soc. Am., Bull. 82: 3407-3420.

———————— 1972. Some sedimentologic aspects of planar cross-stratification in a sandy braided river. J. Sediment. Petrol. 42: 624-634.

———————— 1974. Sedimentology and bar formation in the upper Kicking Horse River, a braided outwash stream. J. Geol. 82: 205-223.

SNEED, E.D. and FOLK, R.L. 1958. Pebbles in the lower Colorado River, Texas — a study in particle morphogenesis. J. Geol. 66: 114-150.

STEIDTMANN, J.R. 1974. Evidence for eolian origin of cross-stratification in sandstone of the Casper Formation, southernmost Laramie Basin, Wyoming. Geol. Soc. Am., Bull. 85: 1835-1842.

STRIDE, A.H. 1970. Shape and size trends for sand waves in a depositional zone of the North Sea. Geol. Mag. 107: 469-477.

SUGDEN, W. 1963. Some aspects of sedimentation in the Persian Gulf. J. Sediment. Petrol. 33: 355-364.

TAFT, W.H. 1961. Authigenic dolomite in modern carbonate sediments along the southern coast of Florida. Science (AAAS) 134: 561-562.

TEISSEYRE, A.K. 1976. Pebble fabric in braided stream deposits with examples from recent and "frozen" Carboniferous channels (Intrasudetic Basin, central Sudetes). Geol. Sudetica 10: 7-56.

THOMPSON, R.W. 1968. Tidal flat sedimentation on the Colorado River delta, northwestern Gulf of California. Geol. Soc. Am., Mem. 107, 133 pp.

THORSTEINSSON, R. 1958. Cornwallis and Little Cornwallis Islands District of Franklin Northwest Territories. Geol. Surv. Can., Mem. 294, 134 pp.

———————— and KERR, J.Wm. 1968. Cornwallis Island and adjacent smaller islands, Canadian Arctic Archipelago. Geol. Surv. Can., Pap. 67-64, 16 pp.

———————— and ———————— 1973. Geology of Lowther Island. Geol. Surv. Can., Open File 139.

———————— and TOZER, E.T. 1963. Geology of northern Prince of Wales Island and northwestern Somerset Island. In Y.O. Fortier et al. (eds.), Geol. Surv. Can., Mem. 320: 117-129.

———————— and ———————— 1970. Geology of the Arctic Archipelago. In R.J.W. Douglas (ed.), Geology and economic minerals of Canada. Dept. of Energy, Mines and Resources, Ottawa: 547-590.

TUKE, M.F., DINELEY, D.L. and RUST, B.R. 1966. The basal sedimentary rocks in Somerset Island, N.W.T. Can. J. Earth Sci. 3: 697-711.

TURNER, P. 1974. Lithostratigraphy and facies analysis of the Ringerike Group of the Oslo region. Norg. Geol. Unders. 314: 101-131.

TURNER, S. and DIXON, J. 1971. Lower Silurian thelodonts from Prince of Wales Island, Northwest Territories. Lethaia 4: 385-392.

TWIDALE, C.R. 1971. Hillslopes and pediments in the Flinders Ranges, South Australia. In J.N. Jennings and J.A. Mabbutt (eds.), Landform studies from Australia and New Guinea. Australia Natl. Univ. Press., Canberra: 95-117.

UNRUG, R. 1957. Recent transport and sedimentation of gravels in the Dunajec valley (Western Carpathians). Acta Geol. Pol. 7: 217-257.

UYENO, T.T. 1977. Summary of conodont biostratigraphy of the Read Bay Formation at its type sections and adjacent areas, eastern Cornwallis Island, District of Franklin. Geol. Surv. Can., Pap. 77-1B: 211-216.

VAN TUYL, F.M. 1916. The origin of dolomite. Iowa Geol. Surv., Ann. Rep. 25: 251-422.

VEIZER, J. 1970. Zonal arrangement of the Triassic rocks of the western Carpathians: a contribution to the dolomite problem. J. Sediment. Petrol. 40: 1287-1301.

———— 1977. Diagenesis of pre-Quaternary carbonates as indicated by tracer studies. J. Sediment. Petrol. 47: 565-581.

———— and DEMOVIČ, R. 1974. Strontium as a tool in facies analysis. J. Sediment. Petrol. 44: 93-115.

————, LEMIEUX, J., JONES, B., GIBLING, M.R. and SAVELLE, J. 1977. Sodium: paleosalinity indicator in ancient carbonate rocks. Geology (Boulder) 5: 177-179.

————, ————, ————, ———— and ———— in press. Paleosalinity and dolomitization of a Lower Paleozoic carbonate sequence, Somerset and Prince of Wales Islands, Arctic Canada. Can. J. Earth Sci.

VON DER BORCH, C.C. 1976. Stratigraphy and formation of Holocene dolomitic carbonate deposits of the Coorong area, South Australia. J. Sediment. Petrol. 46: 952-966.

WADELL, H. 1932. Volume, shape and roundness of rock particles. J. Geol. 40: 443-451.

WALCOTT, R.I. 1970. An isostatic origin for basement uplifts. Can. J. Earth Sci. 7: 931-937.

WALKER, R.G. 1971. Nondeltaic depositional environments in the Catskill clastic wedge (Upper Devonian) of central Pennsylvania. Geol. Soc. Am., Bull. 82: 1305-1326.

———— 1975a. Conglomerate: sedimentary structures and facies models. In J.C. Harms et al., Depositional environments as interpreted from primary sedimentary structures and stratification sequences. Soc. Econ. Paleontol. Mineral., short course No. 2: 133-161.

———— 1975b. Generalized facies models for resedimented conglomerates of turbidite association. Geol. Soc. Am., Bull. 86: 737-748.

———— 1976. Facies models 3. Sandy fluvial systems. Geoscience Canada 3: 101-109.

WALKER, T.R. and HARMS, J.C. 1976. Eolian origin of Flagstone Beds, Lyons Sandstone (Permian) type area, Boulder County, Colorado. In R.C. Epis and R.J. Weimer (eds.), Studies in Colorado field geology. Colorado Sch. Mines, Prof. Contr. 8: 110-122.

WALTHER, J. 1893-1894. Einleitung in die Geologie als historische Wissenschaft. Fischer Verlag Publ. Co., Jena, 3 vols.

WENTWORTH, C.K. 1922. A scale of grade and class terms for clastic sediments. J. Geol. 30: 377-392.

WILLIAMS, G.E. 1968. Formation of large-scale trough cross-stratification in a fluvial environment. J. Sediment. Petrol. 38: 136-140.

———————— 1971. Flood deposits of the sand-bed ephemeral streams of central Australia. Sedimentology 17: 1-40.

WILLIAMS, P.F. and RUST, B.R. 1969. The sedimentology of a braided river. J. Sediment. Petrol. 39: 649-679.

WILSON, J.L. 1967. Carbonate-evaporite cycles in the lower Duperow Formation of Williston Basin. Bull. Can. Pet. Geol. 15: 230-312.

———————— 1975. Carbonate facies in geologic history. Springer-Verlag Publ. Co., New York, 471 pp.

WINDER, C.G. 1965. Alluvial cone construction by alpine mudflow in a humid temperate region. Can. J. Earth Sci. 2: 270-277.

WOOD. G.V. and WOLFE, M.J. 1969. Sabkha cycles in the Arab/ Darb Formations off the Trucial Coast of Arabia. Sedimentology 12: 165-191.

WOODROW, D.L., FLETCHER, F.W. and AHRNSBRAK, W.F. 1973. Paleogeography and paleoclimate at the deposition sites of the Devonian Catskill and Old Red facies. Geol. Soc. Am., Bull. 84: 3051-3064.

APPENDIX A. LOCATION OF SECTIONS, AND GEOLOGICAL STRUCTURE

North coast of Somerset Island (Fig. A1; map A of Fig. A2)

The Somerset Island and Peel Sound Formations are poorly exposed except in river gorges and sea cliffs. The Cape Anne syncline (Photo 2) is the dominant structural feature of the northwestern corner of the island (Thorsteinsson and Tozer, 1963, p. 127); the structure is asymmetric, with dips of up to 26° on the western limb (ibid.), commonly 5-10° in the sections measured, and 5-10° on the eastern limb. The syncline plunges northward. Deformation occurred mainly during the Upper Silurian to Upper Devonian Cornwallis Disturbance (Kerr, 1977).

Gibling (in Miall et al., 1978) noted a good reference section of the Somerset Island Formation south of Pressure Point (section G74G). A steep canyon cut into the Read Bay Formation passes upstream into a gentle valley exposing the Somerset Island Formation, with eastward dips of less than 10° along the north bank. The formation is 66% exposed, but is usually snow-covered early in the season. The lower member, 57 m thick, is composed mainly of thick-bedded grey-green dolomitic siltstones with ostracods and gastropods. Interbedded bioclastic limestones contain a fauna of brachiopods, corals, stromatoporoids and crinoids. In the upper member, 72 m thick, massive and laminated red dolomitic

siltstones predominate, and limestone is uncommon. Ostracods and ostracoderms are common throughout; gastropods are rare. The Peel Sound Formation outcrops above.

The eastern limb of the Cape Anne syncline constitutes the type area of the Peel Sound Formation (Thorsteinsson and Tozer, 1963, p. 121). Strata were examined in sections G76A-C.

The complex NW-SE trending graben 8 km west of Cunningham Inlet resulted from the Cretaceous-Tertiary Eurekan Rifting Episode (Kerr, 1977, p. 1398). The graben contains outcrops of the Somerset Island Formation, including deformed bodies of gypsum, and overlying the Read Bay Formation. A valley 5 km northeast of Pressure Point, with a similar trend, is the site of a second graben (Fig. 5) identified by the author in 1974; member 4 of the Peel Sound Formation outcrops in the valley bottom (section G74K) and is clearly downthrown in comparison with member 2 in cliffs adjacent to the graben (sections G74A-C).

Creswell Bay area, Somerset Island (Fig. A1; maps B-D of Fig. A2)

Much of the area to the north of Creswell Bay is covered by Quaternary sediments, but river gorges with good exposure of the Somerset Island and Peel Sound Formations cut through an escarpment underlain by Lower Paleozoic strata at the eastern margin of the Boothia Horst (sections G73J-M). To

the north of Cape Garry on the western shore of Creswell Bay, a series of comparable but discontinuous sections (G73A-I) are exposed in gorges over a distance of 11 km.

The strata are deformed into the asymmetric Creswell Bay syncline (Blackadar, 1963, p. 150), which plunges gently southward. The western limb consists essentially of broad belts of flat-lying or gently folded strata separated by narrow zones of steeply dipping to vertical strata, parallel to strike faults (Kerr and Christie, 1965, p. 917). In the area examined to the north of Creswell Bay, the structure is essentially monoclinal. The strata dip gently eastward in the Lower Paleozoic carbonates, steepen to 70° at the incoming of the Somerset Island Formation (in association with strike faults), and show dips of a few degrees in the upper member of the formation further east. A photographic section of part of the monocline is shown in Photo 52. The strike faults trend N-S and can be traced for up to 25 km (e.g. forming the scarp to the west of the measured sections, Fig. A2, map C). A dip fault displaces the N-S scarp by about 600 m to the west of section G73N (Fig. A2, map C).

The type section of the Somerset Island Formation was measured by Miall (in Miall et al., 1978) along a tributary of the Creswell River, 45 km north of Creswell Bay (73 11'N, 93 35'W; location shown with a triangle in Fig. 2). The beds dip at 13 to 20° towards the east, and exposure along the south bank of the stream is virtually continuous.

In July 1976 there was little snow cover, although semi-permanent snowdrifts cover most of the north bank of the stream. At this locality the lower member is 98 m thick and the upper member 193 m. The lower member consists mainly of laminated, platy-weathering, cream to pale grey dolomitic siltstone and limestone with ostracods and gastropods. Lumpy weathering limy beds also are present, containing bioclastic lenses, stromatoporoids and colonial corals. The upper member is composed mainly of alternate beds of grey micrite and red siltite. The former commonly have sharp lower contacts and gradational upper contacts. Ostracoderm fragments and ostracods occur mainly near the top of the formation, and are the only fossil remains evident in the upper member at the type section.

On the eastern limb of the syncline, the strata dip westwards at less than 3°. Individual beds of the Somerset Island Formation can be traced over long distances (map D of Fig. A2), and higher strata outcrop progressively to the northwest in gorges cutting the low escarpment bordering the Creswell River flood plain. Good sections of the Somerset Island Formation are present near Fury Point (Miall et al., 1978) . The lower member is well exposed in stream valleys that descend across the sea cliffs (e.g. section shown with a triangle in map D of Fig. A2). It consists predominantly of fine-grained laminated dolostone and limestone but contains several thick units of nodular, bioclastic limestone with

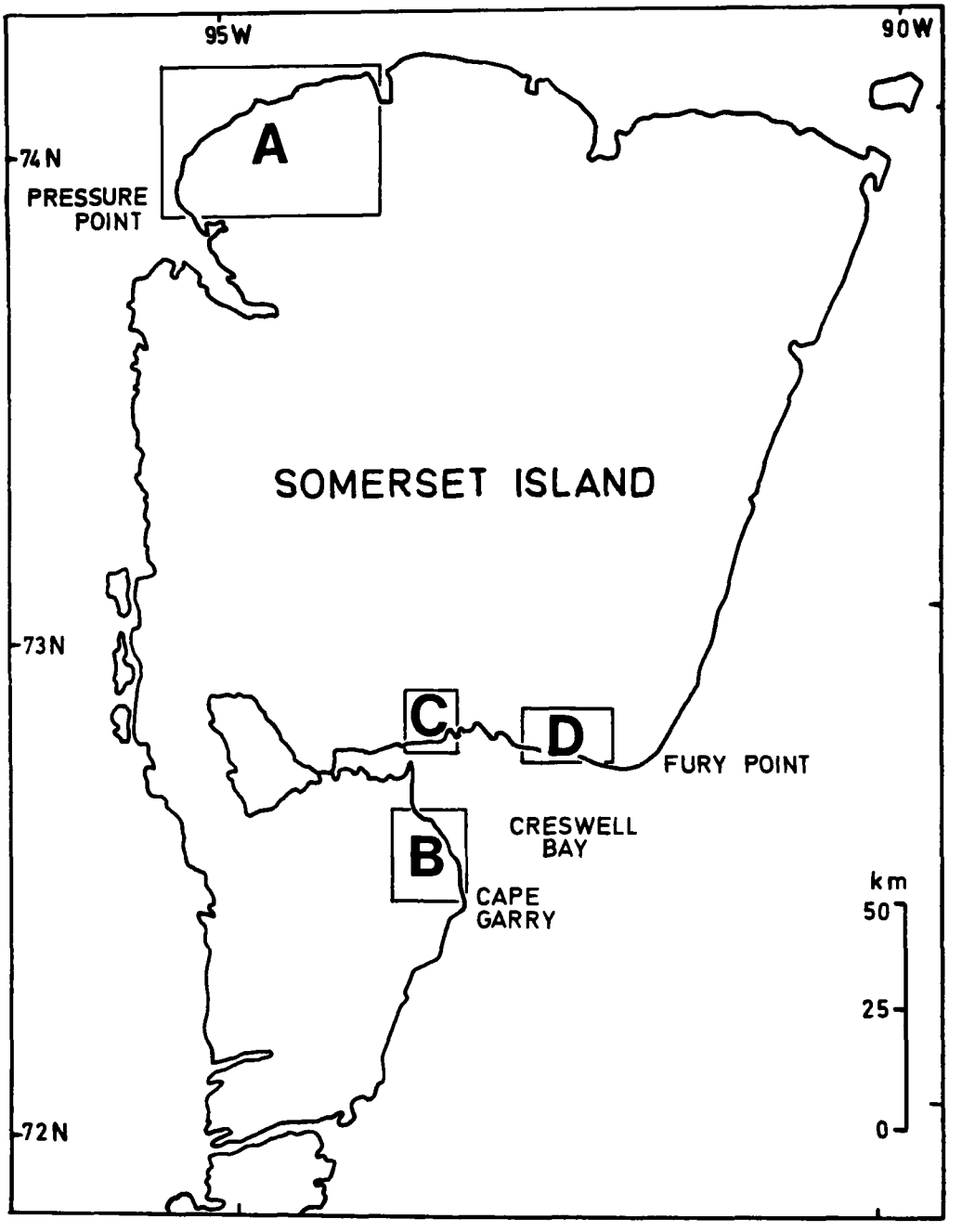

Fig. A1. Location of detailed section maps shown in Figure A2.

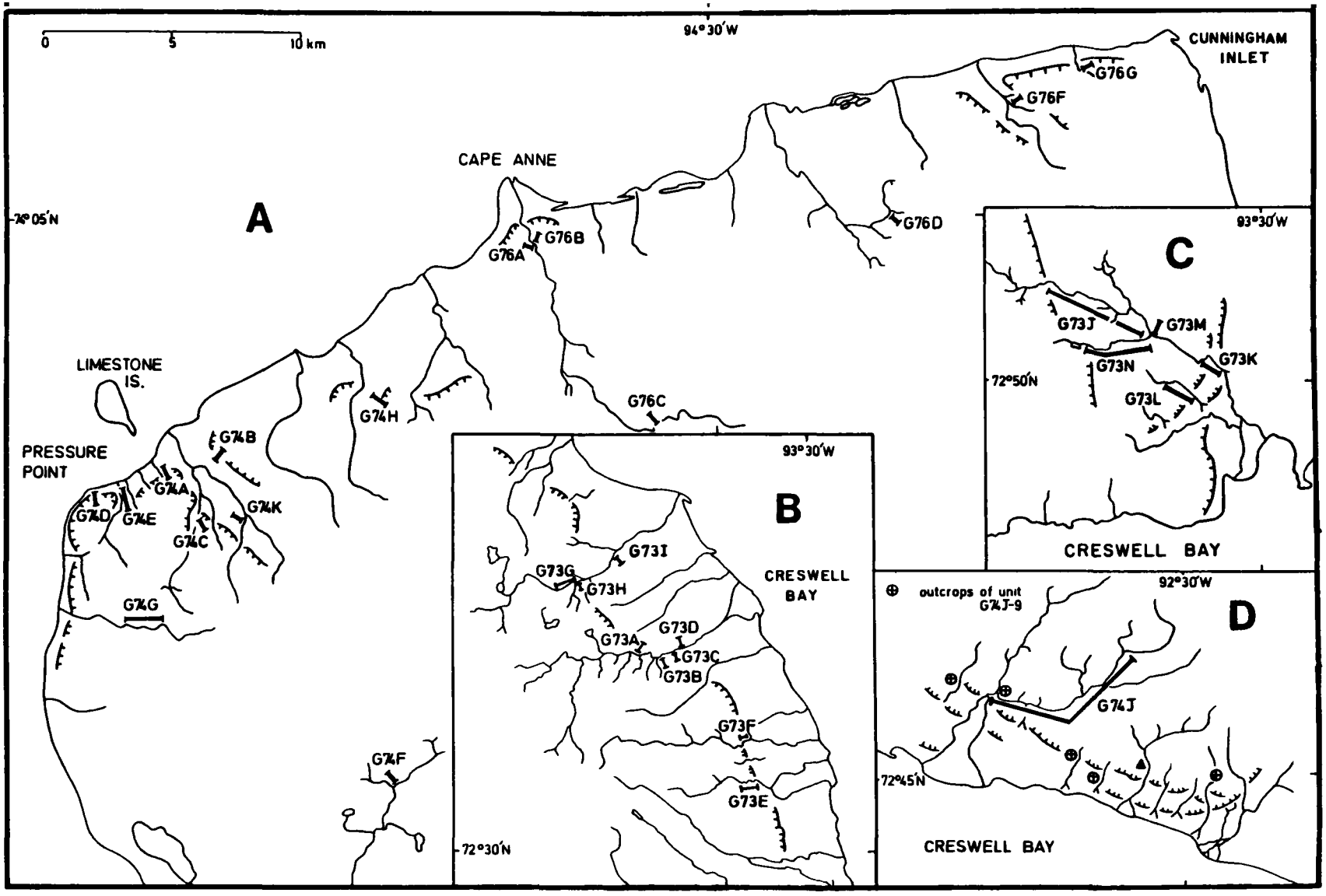

Fig. A2. Location of measured sections on Somerset Island. Prominent escarpments shown by ticked lines.

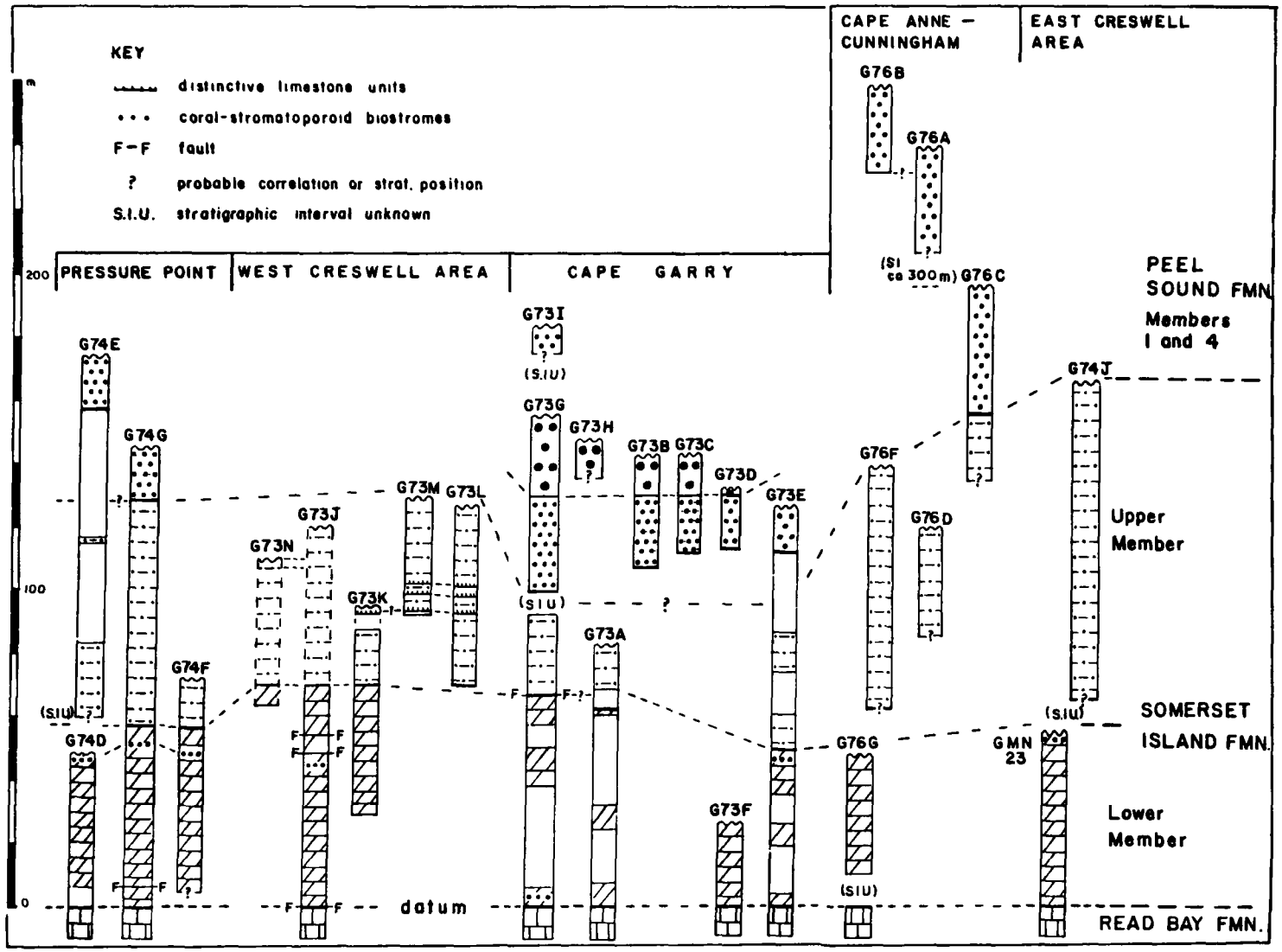

Fig. A3. Correlation of measured sections in the Somerset Island and basal Peel Sound Formations on Somerset Island. Section GMN 23 measured by G.M. Narbonne. Sections G74A, B, C, H and K (Peel Sound members 2 and 4) in the Cape Anne syncline are omitted.

abundant brachiopods, gastropods and ostracods similar to the typical Read Bay lithofacies. The upper member of the formation is also well exposed (section G74J).

A suggested correlation for the sections measured is shown in Figure A3, and a detailed locality register for each section follows. Bed-by-bed section logs are available at the Department of Geology, University of Ottawa.

Detailed location of sections (Localities 1 to 16 shown in Fig. 2)

North coast

Section G74A (Locality 4)

74°00'N, 95°11'W. Crags behind beach, 3.5 km NE of Pressure Point, and just west of large river valley.
Peel Sound Formation member 2: 97.1 m
(Base not seen but section commences close to base of member; section consists of pebble conglomerate with minor sandstone, not recorded in detail.)

Section G74B (Locality 4)

74°01'N, 95°07'W. Crags on E margin of large river valley, 5.5 km NE of Pressure Point.
Peel Sound Formation member 2: 76.1 m
(Base not seen, section consists of pebble conglomerate with minor sandstone, not recorded in detail. Probably overlies G74A, from which it is separated by a graben.)

Section G74C (Locality 4)

73°59'N, 95°09'W. Crags on E side of tributary, 4.5 km SE of Pressure Point.

Peel Sound Formation member 2: 95.1 m

(Base not seen, lithology as in previous sections. Overlies G74A, may be in part equivalent to G74B.)

Section G74D (Locality 1)

73°59'30"N, 95°17'W. Sea cliffs 0.25 km east of Pressure Point. Section commences ca. 100 m above sea level, and continues in low scarps on cliff top.

Somerset Island Formation lower member: 48.4 m

(Base of formation)

Section G74E (Locality 1)

73°59'30"N, 95°14'W. Crags of river gorge, 2 km E of Pressure Point, section commences at mouth of gorge, close to sea level.

Peel Sound Formation member 1: 17.5 m

Somerset Island Formation upper member: 102.7 m

(Base not seen. Section overlies G74D with probable covered interval between.)

Section G74F (Locality 3)

73°53'N, 94°55'W. Crags on NE side of tributary stream, 16 km SE of Pressure Point. Section measured upstream from confluence.

Somerset Island Formation upper member: 15.5 m

lower member: 52.3 m

(Base not seen)

Section G74G (Locality 2)

73°57'30"N, 95°16'W. Crags on NE side of stream, 4 km SSE of Pressure Point. Section commences in gentle valley upstream from canyon, just above waterfall.

Peel Sound Formation member 1: 16.2 m

Somerset Island Formation upper member: 71.9 m

lower member: 56.9 m

(Contact seen with Read Bay Formation)

Section G74H (Locality 5)

74°02'N, 94°55'W. Crags on north face of mountain (ca. 300 m elevation), 12.5 km NE of Pressure Point.

Peel Sound Formation member 4: 92.0 m

(Base not seen)

Section G74K (Locality 4)

73°59'N, 95°06'W. Bluff at confluence of tributary stream with NW flowing river, 6 km ESE of Pressure Point.

Peel Sound Formation member 4: 41.8 m

(Base not seen; strata lie in graben, downthrown)

Section G76A (Locality 6)

74°05'N, 94°43'W. Crags on NE bank of stream in incised meander bend, 2.5 km S of Cape Anne.

Peel Sound Formation member 1: 33.0 m

(Base not seen)

Section G76B (Locality 6)

Same locality as G76A, but on opposite bank and slightly farther south.

Peel Sound Formation member 1: 26.5 m

(Base not seen, probably overlies most of G76A).

Section G76C (Locality 7)

74°01'N, 94°35'W. Crags on north bank of stream, 11 km SE of Cape Anne. Locality G of Thorsteinsson and Tozer (1963, p. 122).

Peel Sound Formation member 1: 35.0 m

Somerset Island Formation upper member: 21.0 m

(Base not seen)

Section G76D (Locality 8)

74°05'N, 94°16'W. Crags in southern angle of stream confluence, 15 km ESE of Cape Anne.

Somerset Island Formation upper member: 35.0 m

(Base not seen)

Section G76F (Locality 8)

74°07'30"N, 94°06'W. SW-facing cliff at NE margin of Cunningham graben. Poor exposure, with scree weathering red/green. Section commences at stream level.

Somerset Island Formation upper member: 76.6 m

(Base not seen)

Section G76G (Locality 8)

74°08'N, 94°04'W. Crags on east side of river gorge, 5 km SSW of northwestern corner of Cunningham Inlet. Section commences about 50 m above stream (locality of section CF of Jones, 1974).

Somerset Island Formation lower member: 36.8 m

(Base not observed, but section may be close to base of member.)

West Creswell area

Section G73J (Locality 9)

Section commences at 72°52'N, 93°45'W, continues to 72°51'N, 93°35'W. Base of section in crags on north side of river 9.5 km north of Creswell Bay, strata dipping eastwards at 55°. Discontinuous outcrops continue 6 km downstream. Localities on A.P. A16080-104.

Somerset Island Formation upper member: 50.0 m (estim.)

lower member: 70.8 m

(Base seen; thicknesses uncertain due to discontinuous outcrop and faulting.)

Section G73K (Locality 12)

72°51'N, 93°34'W. Section commences at mouth of narrow canyon with large waterfall, 6 km N of Creswell Bay, continues upstream until valley broadens and runs NW. Strata measured on both sides, where accessible.

Somerset Island Formation upper member: 18.0 m+
lower member: 41.1 m

(Base not seen; discontinuous outcrop in upper member)

Section G73L (Locality 11)

72°50'N, 93°37'W. Section commences at mouth of narrow valley; measured on S side until exposure ceases at hill top. 5.5 km north of Creswell Bay.

Somerset Island Formation upper member: 58.0 m

(Base not seen)

Section G73M (Locality 10)

72°51'N, 93°38'W. Bluff on NE side of river, opposite junction with tributary, 7.5 km N of Creswell Bay.

Somerset Island Formation upper member: 36.3 m

(Base not seen; partly correlative with G73L)

Section G73N (Locality 10)

72°51'N, 93°43'W to 72°51'N, 93°38'W. Discontinuous outcrops in river valley, commencing at outflow from small lake, 4.5 km N of Creswell Bay, terminating opposite to section G73M.

Somerset Island Formation upper member: 40.0 m +

lower member: 6.0 m

(Base not seen)

N.B. Sections G73J, K, L, M and N contain red, cross-bedded sandstone which, by definition, should be the Peel Sound Formation; however, the sandstones are impersistent vertically, and the strata overlie sediments typical of the lower member of the Somerset Island Formation. They are thus placed in the upper member of that formation.

East Creswell area

Section G74J (Locality 13)

From 92°44'W, 72°46'30"N, (base) to 72°47'30"N, 92°35'W (top). Crags of river gorge, section commencing at mouth of gorge. 17.5 km NW of Fury Point.

Somerset Island Formation upper member: 98.3 m

(Base not seen, probably close to base of member.)

Correlative strata also examined along margin of plateau for 13 km to the SE and 14 km to the NW. Strata exposed young progressively NW. Total thickness of strata in upper member estimated at >160 m.

Cape Garry area

Section G73A (Locality 15)

72°34'N, 93°42'W. Steep buttress on N side of stream, section continued NE in small scarps along hilltop. 13.5 km NW of Cape Garry.

Somerset Island Formation upper member: 17.7 m
lower member: 68.8 m

(From basal contact, top not seen.)

Section G73B (Locality 15)

72°34'N, 93°40'W. Cliff on S side of stream, just E of small tributary, 1 km SE of section G73A. Commences at stream level. 13.5 km NW of Cape Garry.

Peel Sound Formation member 4: 12.3 m
member 1: 23.2 m

(Base not seen)

Section G73C (Locality 15)

72°34'N, 93°38'W. Cliff on south side of stream, 0.75 km E of section G73B. Commences at stream level. 13.5 km NW of Cape Garry.

Peel Sound Formation member 4: 13.3 m
member 1: 19.3 m

(Base not seen; partly correlative with G73B.)

Section G73D (Locality 15)

72°34'N, 93°38'W. Cliff on N side of stream, slightly E of section G73C. Commences at stream level. 13.5 km NW of Cape Garry.

Peel Sound Formation member 4: 2.0 m
member 1: 16.7 m

Base not seen; partly correlative with G73B and C.

Section G73E (Locality 16)

72°32'N, 93°36'W. Section commences on S side of stream where straight gorge becomes winding, strata measured on both sides until banks become gentle and exposure is poor. 7.5 km NW of Cape Garry.

Somerset Island Formation upper member: 77.5 m
lower member: 50.4 m

(Base seen)

Section G73F (Locality 16)

72°33'N, 93°35'W. N side of stream close to mouth of gorge. 8.5 km NW of Cape Garry.

Somerset Island Formation lower member: 25.5 m

(Base seen)

Section G73G (Locality 14)

From 72°36'N,93°47'30"W to 72 36'N, 93 46'W. Section commences in poorly exposed strata on N side of stream

where flow swings from E to NE, and continues downstream with discontinuous outcrops. Locality numbers on A.P. A16080-100. 18 km NW of Cape Garry.

Peel Sound Formation	member 4:	24.3 m
	member 1:	31.9 m
Somerset Island Formation	upper member:	25.6 m+
	lower member:	66.7 m

(Position of base of formation uncertain due to poor exposure.)

Section G73H (Locality 14)

72°36'N, 93°46'W. Cliff on S bank of stream E of tributary, opposite and partly correlative with uppermost strata of G73G. 18 km NW of Cape Garry.

Peel Sound Formation member 4: 12.5 m

(Base not seen)

Section G73I (Locality 14)

72°37'N, 93°43'W. Cliff on S bank of stream, where valley starts to flatten out. 18 km NW of Cape Garry.

Peel Sound Formation: 8.0 m

52. Panoramic view of the structure on the western limb of the Creswell Bay syncline (section G73J, Loc. 9). RB = Read Bay Formation, Sl(lr) and (ur) = Somerset Island Formation, lower and upper members. F = line of strike fault. Courtesy of J.-M. Sempels.

52

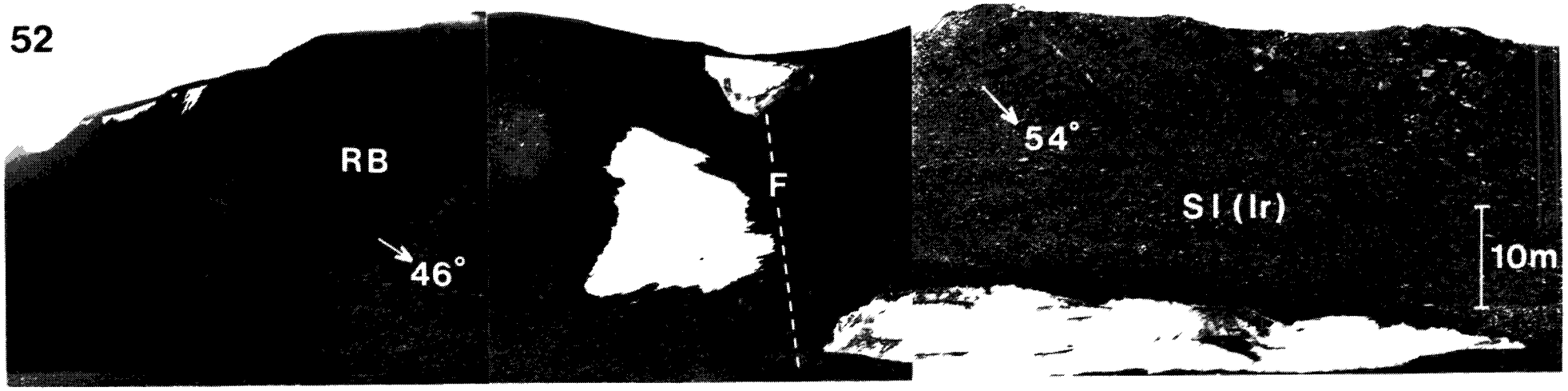

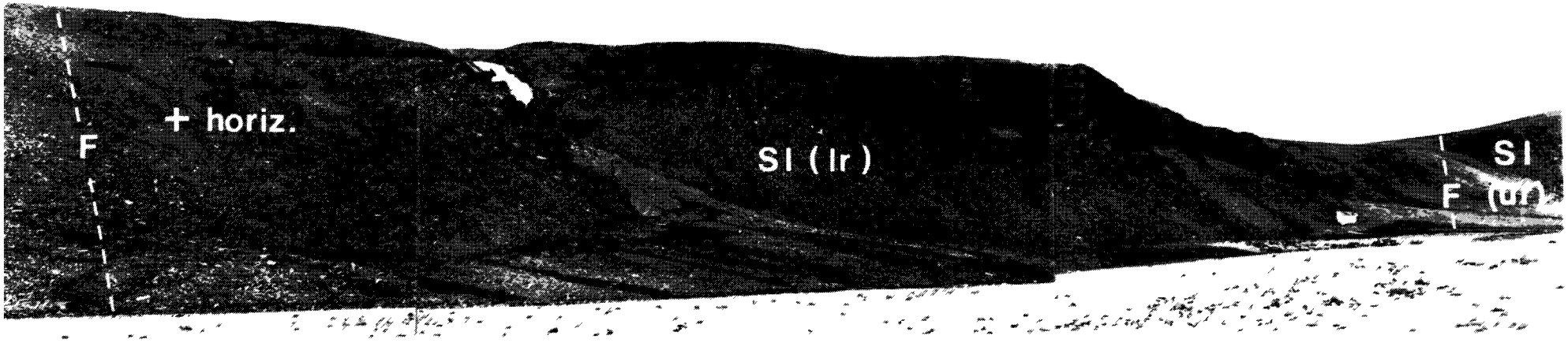

APPENDIX B. PALEOCURRENT DATA

FORMATION AND LOCATION	DIRECTIONAL SEDIMENTARY STRUCTURES	VECTOR MEAN (degrees)	NUMBER OF READINGS	VECTOR MAGNITUDE (%)	SIGNIFICANCE LEVEL
SOMERSET ISLAND, Peel Sound Fmn. member 1, Loc. 6	Large-scale trough and planar cross-strata	031	25(34)[1]	48	< .01
member 3, Loc. 5	Large-scale trough cross-strata (S_{pt})	089	12(41)[1]	63	< .01
	Giant cross-strata (S_g)	317	15	78	$< 10^{-4}$
members 2 and 4, Locs. 4 and 5	Large-scale cross-strata	062	21	43	< .02
	Imbrication	219	16	80	$< 10^{-4}$
CORNWALLIS ISLAND, Snowblind Bay Fmn. at Read Bay (75°04'N, 93°32'W)	Large-scale planar and trough cross-strata	059	23	62	$< 10^{-3}$
	Primary current lineation and groove casts	067/247	18	72	$< 10^{-4}$
	Strike of ripple crests	155/333	18	18	> .50
PRINCE OF WALES ISLAND Peel Sound Fmn. upper member	Large-scale planar and trough cross-strata	260 (grand mean)	148	—	—

(data from Miall, 1969, 1970b)

1 Total number of measurements in cosets

APPENDIX C1. ORIENTATION DATA FOR SAMPLES OF CLASTS USED IN FABRIC STUDIES

Sample numbers refer to units in sections G74B, C, K and H; sample A6A was collected just below the base of section G74A. Samples were divided into two equal sub-samples at the median value of $\bar{d}$ and $\bar{O}\bar{P}$ Index (large/small, oblate/prolate sub-samples). Each sub-sample was analysed for AB dip direction and A-axis orientation. Vector mean (degrees), vector magnitude (%) and significance level are given for each analysis (asterisk denotes significance at greater than 95% level). AB/A-axis indicates angle between vector means for AB dip direction and A-axis orientation for entire sample. Large sub-sample of B-16 was used for AB dip direction due to greatly improved significance level.

APPENDIX C2. MORPHOLOGY AND IMBRICATION ANGLE OF SAMPLES OF CLASTS USED IN FABRIC STUDIES

"1" indicates clasts measured to the nearest half cm. "2" includes all axial measurement data to the nearest mm. For sample locations, see caption to Appendix C1.

APPENDIX C3. CLAST/MATRIX %, CLAST TYPES, AND ROUNDNESS OF CLAST SAMPLES USED FOR STRATIGRAPHIC STUDIES

Stratigraphic height: sections considered consecutive in the order shown, with covered intervals between sections and the thickness of member 3 omitted. Clast counts: about 100 points (clasts and matrix) at 10 cm spacing. Roundness: mean of 30 clasts for each lithology. For sample locations, see caption to Appendix C1.

C1

SAMPLE NUMBER	AB DIP DIRECTION					A-AXIS ORIENTATION					AB/ A-AXIS
	All Clasts	Large	Small	Oblate	Prolate	All Clasts	Large	Small	Oblate	Prolate	
	189.4	125.4	209.0	228.5	168.1	128.9	108.1	138.5	141.9	115.7	
H-8	26.2	17.6	47.3			18.3	13.7	27.8			61
	.05	.50	.01*	.30	.20	.20	.70	.20	.20	.70	
	321.7	338.7	313.3	273.3	034.5	092.7	064.4	113.9	087.2	099.9	
H-6	12.4	8.5	16.8			23.3	31.9	39.4			49
	.50	.80	.60	.20	.40	.10	.10	.05*	.20	.40	
	352.8	353.6	351.4	348.3	002.8	067.1	083.5	056.3	058.2	083.9	
H-1	67.4	86.4	48.4			36.9	33.3	49.2			74
	$<10^{-5}$*	$<10^{-5}$*	.01*	$<10^{-5}$*	.01*	.01*	.10	.01*	.02*	.05*	
	220.1	247.4	204.4	222.9	210.7	085.8	136.5	055.9	115.7	023.8	
K-3	41.1	32.7	55.3			3.6	19.6	22.2			46
	10^{-3}*	.10	.01*	.01*	.30	.95	.50	.30	.40	.70	
	220.8	221.3	217.3	230.7	225.2	031.4	109.4	028.4	058.1	098.2	
K-1	34.0	55.2	10.6			11.5	7.6	31.0			9
	.01*	.01*	.80	.20	.01*	.50	.90	.10	.60	.40	
	092.5	340.5	103.1	345.6	008.9	106.1	108.5	101.0	106.6	105.4	
B-16	17.6	41.0	15.6			29.5	40.2	19.3			54
	0.30	.04*	.60	.70	.30	.03*	.04*	.50	.05	.30	
C-34	333.9	348.5	320.5	327.8	345.1	097.3	133.6	172.7	096.0	107.4	
	42.0	44.0	43.0			13.2	13.2	25.7			57
	10^{-3}*	.02*	.03*	.02	.04*	.40	.70	.20	.40	.95	
C-15	019.7	289.9	043.9	090.9	041.3	078.3	052.1	111.2	055.0	173.6	
	10.6	9.5	23.2			17.0	37.9	35.7			59
	.60	.80	.40	.70	.80	.30	.05*	.05	.80	.20	
C-12	272.8	250.2	292.7	290.2	251.9	100.7	136.5	092.9	178.6	103.0	
	48.7	47.8	56.9			19.9	10.8	37.9			8
	10^{-4}*	.01*	.01*	.01*	.01*	.10	.70	.03*	.80	.10	
C-5	332.7	355.3	314.2	346.0	306.9	057.5	100.9	070.2	057.4	164.7	
	56.9	54.9	66.5			14.4	14.1	32.7			85
	$<10^{-5}$*	.01*	10^{-3}*	$<10^{-3}$*	.02*	.40	.60	.10	.30	.60	
A6A	085.8	081.8	180.0	089.5	091.8	095.8	104.5	000	087.4	127.0	
	25.0	50.5	3.51			32.2	25.8	41.0			10
	.05	.01*	.95	.80	.03*	.02*	.20	.04*	.01*	.30	

C2

SAMPLE NUMBER	NO. OF CLASTS	SAMPLE MEANS				
		$\bar{d}$(cm)	Ψ_p	$\bar{O}\bar{P}$	$\bar{R}$	α(degrees)
H-8	40	6.14	0.633	-0.16		26.0
H-6	40	6.55	0.625	-1.60		30.0
H-1	40	7.35	0.618	-2.49		42.9
K-3	40	7.84	0.694	-1.02		34.0
K-1	41	6.67	0.651	-1.80		35.4
B-16	40	5.16	0.708	1.03		21.7
C-34	44	6.08	0.594	-3.19		28.1
C-15	40	5.22	0.742	1.08		23.7
C-12	100	5.28	0.671	-0.83	4.76	43.0
C-5[1]	115	5.93	0.677	-1.87	4.72	29.9
C-4[1]	98	4.20	0.651	-0.20	4.70	
C-1	92	3.47	0.682	-0.49	4.60	
A6A	41	3.86	0.691	-0.47	4.17	38.6
GRAND MEANS	771	5.41	0.666	-0.94		
	558[2]	5.51	0.666	-0.87		
	446				4.65	
	437					32.6

C3

UNIT NO.	STRAT. HEIGHT (m)	CLAST %	DOLOSTONE %	SANDSTONE %	IGNEOUS %	METAMORPHIC %	OTHER %	ROUNDNESS DOLOSTONE	ROUNDNESS SANDSTONE	ROUNDNESS IGNEOUS & MET.
		CLAST COUNTS						ROUNDNESS		
H-8	417	66	34.7	45.3	4.0	13.3	2.7	4.53	4.7	4.83
H-7b	385	63	6.3	74.6	4.8	7.9	6.4	4.87	4.77	4.7
H-7a	381	65	32.3	52.2	6.1	10.8		4.33	4.87	4.63
H-6	375	64	25	60.9	4.7	6.3	3.1	4.33	4.93	4.63
H-1	329	65	40	35.3	13.8	9.2	1.7	4.57	4.7	4.83
K-3	305	67	34.3	61.1			4.6	4.73	4.87	
K-1	292	57	14	85.9					4.83	
B-23	282	61	49.2	50.8				4.54	4.83	
B-22	278	65	50.8	49.2				4.33	4.87	
B-21	276	67	62.7	35.8			1.5	4.4	4.83	
B-20	272	70	62.8	37.2				4.36	4.8	
B-19	270	69	46.4	50.7			2.9	4.57	4.87	
B-17	266	63	68.3	27			4.7	4.63	4.8	
B-16	256	65	52.3	47.6				4.7	4.87	
B-15	255	68	58.8	38.2			3.0	4.4	4.83	
B-14	243							4.4	4.9	
B-13	242	44	86.4	13.6				4.3	4.8	
B-10	237	62	45.2	54.8				4.33	4.83	
B-7	232	66	62.1	37.8				4.13	4.72	
B-5	221	60	73.3	23.3			3.4	4.64	4.85	
B-2	217	46	73.9	21.7			4.4	4.4	4.8	
C-35	204	52	77	21.2			1.1	4.43	4.85	
C-34	202	68	63.2	29.4			7.4	4.7	4.83	
C-32	200	60	86.7	13.3				4.67	4.87	
C-31	196	57	98.3	1.7				4.5		
C-30b	191	63	76.2	22.2			1.6	4.7	4.8	
C-30a	186	60	61.7	38.3				4.79	4.93	
C-24	182	58	91.4	6.9			1.7			
C-23	179	62	59.7	33.9			6.4			
C-21	176	60	51.7	43.3			5	4.2	4.8	
C-19	174	64.5	56.8	41.3			1.9	4.43	4.83	
C-18	173	69	92.8	7.2				4.2	4.8	
C-17	173	55	70.9	27.1			2	4.33	4.67	
C-16	172	56	89.3	10.7				4.23	4.76	
C-15	171	62	37.1	59.7			3.2	4.37	4.83	
C-14	169	61	45.9	47.5			6.6			
C-12	163	68	41.2	57.4			1.4	4.47	4.82	
C-11	155	73	94.5	5.5						
C-10	154	63	63.5	33.4			3.1			
C-9	149	47	95.8	4.2						
C-8	147	64	75	25						
C-6	143	62	85.5	14.5						
C-5	139	64	32.8	65.6			1.6	4.57	4.78	
C-4	132	67	50.8	49.2				4.6	4.81	
C-2	113	60	90	10						
C-1b	112	59	76.3	22			1.7	4.69	4.49	
C-1a	109	62	81.5	16			2.5			
A-24b	87	61	95	5				4.77	4.8	
A-24a	73	72	87.5	12.5				4.83	4.9	
A-21	51	70	97	3				4.83		
A-18	41	60	81.5	16.5			2	4.83	4.83	
A-17	34	59	90	8.5			1.5	4.87	4.8	
A-10	24	51	88	10			2	4.67	4.83	
A-5	15	40	95	5						
A-1	10	42	100	0						
A6A	9	68	100	0				4.17		

APPENDIX D. GEOCHEMICAL DATA

Sections G73P and G73R are at Baring Channel, Prince of Wales Island (details in bed-by-bed section log at Department of Geology). Locations of the other sections are described in Appendix A. Analysis was by J. Lemieux, following preliminary analysis for all elements except Na by M.R.G. Soluble fraction data recalculated on 100% carbonate basis.

	SAMPLE	INSOLUBLE RESIDUE %	SOLUBLE FRACTION Mg%	Sr ppm	Na ppm	Fe ppm	Mn ppm
SOMERSET ISLAND FMN.(UPPER MEMBER)							
1	G73J-50a	18.5	10.73	70	242	844	536
2	-50c	30.8	9.31	65	230	967	646
3	-50b	24.1	10.17	72	260	1186	613
4	-43a	31.9	10.65	68	369	1370	559
5	-47c	25.8	9.19	98	260	1906	681
6	-47b	24.8	8.55	77	218	1608	702
7	-45	25.1	9.64	119	370	1290	399
8	-47a	15.8	11.03	83	249	796	588
9	G73K-28	13.5	4.92	265	403	805	236
10	-22	10.9	0.77	365	212	370	164
11	-23	57.1	2.42	310	315	909	240
12	-24	28.3	5.50	322	365	813	225
13	G73L-6	19.1	4.36	272	335	922	248
14	-7b	12.9	1.02	325	264	398	204
15	-8a	12.5	0.32	326	305	536	123
16	-8b	15.6	6.11	314	387	1024	148
17	-9a	17.6	9.47	249	501	1246	246
18	-9b	17.4	8.67	211	436	1052	255
19	-15a	23.4	3.90	171	252	685	239
PEEL SOUND FMN.(UPPER MEMBER)							
20	G73R-1a	16.7	2.98	228	236	2563	382
21	-1c	26.3	4.80	223	142	5075	474
22	-1e	38.8	4.85	201	386	5415	376
23	-2	45.6	9.49	199	483	8813	555
24	-7	70.7	9.69	92	788	7686	686
25	G73P-1a	11.9	1.25	768	254	2213	257
26	-1b	11.5	1.04	728	288	1634	252
27	-2	21.7	1.75	447	570	2206	244
28	-3	34.3	7.78	300	610	6189	376
29	-4	63.5	9.21	121	825	11586	614
30	-7	65.1	9.03	163	756	10854	605
31	-10	65.3	8.41	161	951	12182	493
32	-12	69.4	8.82	127	690	10918	595
33	-16	46.1	4.43	360	440	6699	447
SOMERSET ISLAND FMN.(LOWER MEMBER)							
34	G73J-3	29.7	6.80	215	334	3674	203
35	-5	16.9	2.82	442	284	1519	36
36	-6	15.6	3.14	385	359	1514	70
37	-7	30.4	8.82	181	351	4007	170
38	-8	19.2	1.11	589	281	1199	123
39	-9	16.1	1.17	530	247	1054	124
40	-10	30.2	1.78	431	348	1719	72
41	-11	50.4	4.48	220	500	3210	175
42	-15	47.1	1.57	238	301	1977	204
43	-16	19.9	7.82	154	217	3147	157
44	-17	37.4	8.42	147	364	2970	155
45	-18	12.9	1.50	197	289	873	56
46	-22	15.5	5.96	156	312	1572	160
47	-23	32.0	4.07	293	406	896	101
48	-29	11.4	0.87	491	270	468	44
49	-36	14.6	1.24	463	299	488	59